CHEMICAL REVIEWS

pubs.acs.org/CR Review

The Mutually Inspiring Biological and Chemical Synthesis of Fungal Bicyclo[2.2.2]diazaoctane Indole Alkaloids

Lei Du,[†] Longyang Dian,[†] Sean A. Newmister, Yuwei Xia, Guanzhong Luo, David H. Sherman,* and Shengying Li*

Cite This: https://doi.org/10.1021/acs.chemrev.4c00250 Read Online

ABSTRACT: Fungal indole alkaloids bearing a bicyclo[2.2.2]diazaoctane (BCDO) core structure are a fascinating family of natural products that exhibit a wide spectrum of biological activities. These compounds also display remarkable structural diversity, with many different diastereomers and enantiomers produced by specific fungal strains. The biogenesis of the unique BCDO moiety has long been proposed to involve an intramolecular [4+2] *hetero*-Diels−Alder (IMDA) reaction, but the exact mechanisms for this hypothetical transformation have remained elusive until recently. This review aims to summarize the whole history of synthetic and biosynthetic studies of fungal BCDO indole alkaloids, by covering the discovery, biomimetic syntheses, total syntheses, biosynthetic pathway elucidation, and biological activities of representative compounds. We highlight the mutual inspiration and corroboration between biological and synthetic chemists in exploring the intriguing biosynthetic mysteries of this family of natural products. We also provide perspectives and clues for the remaining biosynthetic problems.

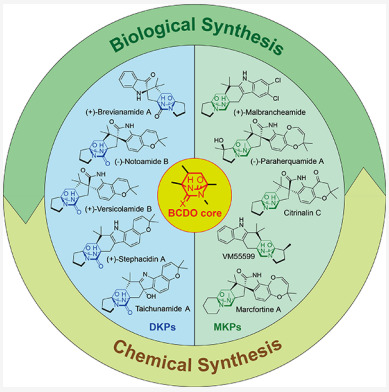

CONTENTS

Received: April 2, 2024
Revised: December 3, 2024
Accepted: December 10, 2024

1. INTRODUCTION

The fungal indole alkaloids bearing a unique bicyclo[2.2.2]-diazaoctane (BCDO) core structure have continuously been isolated from various marine and terrestrial strains of *Aspergillus*, *Penicillium* and *Malbranchea* genera, showing anthelmintic, insecticidal, antitumor, antiviral, antibacterial, calmodulin-inhibitory and other activities. Although indole alkaloids are widely produced by many bacteria, fungi, and plants, interestingly, the subfamily of BCDO-bearing alkaloids have only been discovered from the kingdom of fungi to date. For decades, these fungi specific, bioactivity diverse, and structurally intriguing natural products have been attracting broad interest from natural product, biological, synthetic, medicinal, and theoretical chemists. A wealth of studies on derivatives discovery, biological activities, biosynthetic mechanisms, and organic synthesis have been conducted.

The most fascinating issues related to these natural products include: 1) the biogenesis of the central BCDO structure, which has long been proposed to be formed biosynthetically through an intramolecular [4+2] *hetero*-Diels−Alder (IMDA) reaction; 2) the mechanisms for the diversified biosynthesis of distinct diastereomers and enantiomers by specific producer fungi; and 3) other specific structural variations on the skeletons, e.g., prenylation, hydroxylation, desaturation, isomerization, cyclization, and dimerization. To address these intriguing issues, both synthetic and biological chemists have been making great research efforts and mutually inspiring contributions.

This review covers the literature of the whole history for biosynthetic and chemical synthetic explorations of fungal BCDO indole alkaloids since the discovery of the first family member, brevianamide A, in 1969.

2. DISCOVERY OF BICYCLO[2.2.2]DIAZAOCTANE INDOLE ALKALOIDS FROM NATURE

Since the isolation of the family-founding member brevianamide A from *Penicillium brevicompactum* in 1969, hundreds of fungal BCDO indole alkaloid family members have been reported (Table 1). According to our count through March 2024, there have been a total number of 182 BCDO indole alkaloids discovered from nature, which are uniformly produced by filamentous fungi. Representative structures (Figure 1) include the insecticidal (+)-brevianamides from *Penicillium* spp., the anticancer agents (−)-notoamides from *Aspergillus protuberus* (previously named *Aspergillus* sp. MF297-2) and (+)-notoamides (the enantiomers of corresponding (−)-notoamides) from *Aspergillus amoenus* (previously *A. versicolor* NRRL 35600), the antitumor stephacidins from *Aspergillus ochraceus*, the versicolamides, the anti-inflammatory taichunamides, the insecticidal and antimicrobial sclerotiamides, the anti-biofilm waikialoids, the antimicrobial amoenamide B, the asperversiamides, aspergamide, the antiproliferative waikikiamides, the antiparasitic paraherquamides from *Penicillium* spp., the calmodulin-inhibiting malbrancheamides, the cytotoxic marcfortines, VM55599, the paralytic asperparaline (also named aspergillimide or M55598), the neurocyte protective and antifungal chrysogenamide, the anti-acetylcholinesterase mangrovamides, citrinalin, the penicimutamides, penioxamide, and spiromalbramide.

The BCDO indole alkaloids with complex structural diversity can be categorized into diketopiperazine (DKP) and monoketopiperazine (MKP) subfamilies according to the number of keto group(s) on the BCDO moiety. Comparatively, the current amount of DKPs (111 members) is higher than that of MKPs (71 members). According to the three stereocenters in the BCDO core structure, all known DKPs and MKPs fall into four groups, covering all theoretically possible diastereomers (Figure 2). In the DKP subfamily, the [*S*,*S*,*S*] and [*S*,*R*,*S*] groups comprise the majority of members (51 and 36, respectively), while the [*R*,*S*,*R*] and [*R*,*R*,*R*] configurations are adopted by a smaller number of members (12 and 12, respectively). In the MKP subfamily, most members (57) have the [*S*,*S*,*S*] configuration. There are only 1, 3 and 10 members belonging to the [*R*,*S*,*R*], [*R*,*R*,*R*] and [*S*,*R*,*S*] groups, respectively. It is intriguing to understand how these biased stereoselectivity patterns are formed in nature.

The biogenetic mechanisms of these stereospecific BCDO cores have been attracting continuing interest since the discovery of the first family member brevianamide A. Porter and Sammes first proposed a plausible biosynthetic hypothesis of the [4+2] IMDA process.[1] During the long pursuit of the enzyme (i.e., Diels−Alderase, *abbr.*, DAase) to mediate the putative [4+2] IMDA cycloaddition (Scheme 1), our laboratories and others have proposed and then confirmed that DKPs and MKPs adopt distinct biosynthetic strategies for construction of their respective core scaffolds. In brief, the core structure of DKP brevianamide A is formed through a spontaneous IMDA cycloaddition,[2] while those of MKPs are assembled to generate the *syn* (malbrancheamide and paraherquamide A) or *anti* (precitrinadin A) products by different bifunctional reductases/DAases.[3,4] It appears that fungi have evolved different enzymatic and nonenzymatic strategies to achieve the common [4+2] IMDA reactions, but there remain unknown mechanisms to be explored.

Moreover, diastereomerically distinct and enantiomerically antipodal BCDO alkaloids continue to be discovered (Figure 1), suggesting that specific producer fungi may deploy diversified biosynthetic mechanisms for construction of various diastereomers and enantiomers. One of the most fascinating examples is the marine-derived fungus *A. protuberus*, which produces (+)-stephacidin A and (−)-notoamide B, while the terrestrial-derived fungus *A. amoenus* generates their corresponding enantiomers (−)-stephacidin A and (+)-notoamide B.[5]

Structurally, the backbone of all DKP BCDO alkaloids originates from the nonribosomal peptide synthetase (NRPS)-based condensation of L-tryptophan and L-proline. By contrast, the backbone of MKPs consists of the unchanged tryptophan and a variable second amino acid (Figure 1), such as L-proline (e.g., malbrancheamide, citrinalin C, penicimutamide D, and cycloexpansamine A), L-isoleucine (oxidatively cyclized to β-methylproline, e.g., paraherquamide A, VM55599, penicimutamide D, aculeaquamide A, peniciherquamide A, and cycloexpansamine A), L-leucine (oxidatively cyclized to γ-methylproline, e.g., mangrovamide A, and paraherquamide J-2), and L-lysine (e.g., marcfortine A, penioxamide A, penioxalamine A, and probably chrysogenamide A).

It is worth noting that many, but not all BCDO alkaloids contain a chiral *spiro*-substructure, for instance, the *spiro*-2-oxindole moiety in DKPs notoamides, versicolamides, sclerotiamides and MKPs spiromalbramides and paraherquamides; and the 3-*spiro*-ψ-indoxyl group in brevianamides. These *spiro*-substructures are considered (confirmed in some cases) to be formed via initial indole 2,3-epoxidation with subsequent ring-opening and semipinacol rearrangement

https://doi.org/10.1021/acs.chemrev.4c00250
Chem. Rev. XXXX, XXX, XXX−XXX

Table 1. Structures, Bioactivities and Sources of BCDO Indole Alkaloids[a]

Compound	Source	Bioactivity
Diketopiperazines		
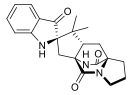 (+)-Brevianamide A	*P. brevicompactum*[2,7,9,30,105,155-165] *P. viridicatum*[10,160,166-169] *P. ochraceum*[11] *P. duclauxii*[170] *Penicillium* sp.[171]	Insecticidal activity[131,132]
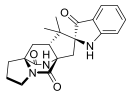 (-)-Brevianamide A	Chemical synthesis[26,31]	ND
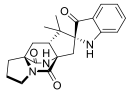 (+)-Brevianamide B	*P. brevicompactum*[2,7,9,30,161,168] *P. viridicatum*[10]	ND
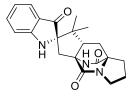 (-)-Brevianamide B	Chemical synthesis[22,23,26,31]	ND
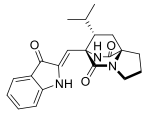 Brevianamide C	*P. brevicompactum*[7,9,105,162,168]	Cytotoxic activity (IC_{50}, 15.6 μM against HCT116 cell line)[105]
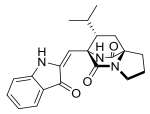 Brevianamide D	*P. brevicompactum*[7,9]	Insecticidal activity[131]
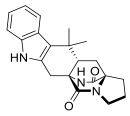 Deoxybrevianamide A	Chemical synthesis[7,161]	ND
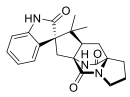 Brevianamide X	*P. brevicompactum*[2,105]	ND
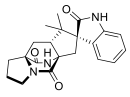 Brevianamide Y	*P. brevicompactum*[2,105]	ND
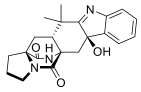 **9**	*P. brevicompactum*[2]	ND

https://doi.org/10.1021/acs.chemrev.4c00250
Chem. Rev. XXXX, XXX, XXX−XXX

Table 1. continued

Compound	Source	Bioactivity
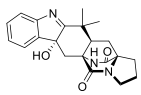 **38**	*P. brevicompactum*[2]	ND
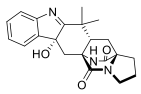 **8**	*P. brevicompactum*[2]	ND
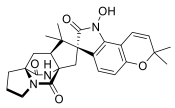 (-)-Notoamide A	*Aspergillus* sp.[172] *Annulohypoxylon cf. stygium*[173] *A. protuberus*[35] *A. versicolor*[64]	Cytotoxic activity (IC_{50}, 27 and 29 μM against HeLa and L1210 cell lines, respectively)[35] Inhibition of RANKL-induced osteoclastogenic differentiation[135]
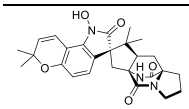 (+)-Notoamide A	*A. amoenus*[135,174]	ND
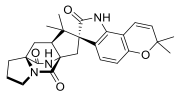 (-)-Notoamide B	*A. sulphureus and Isaria felina co-culture*[134] *Fusarium sambucinum*[136] *A. ochraceus*[133,175] *Aspergillus* sp.[139,176] *A. cf. stygium*[173] *A. protuberus*[35] *A. versicolor*[64]	Anticancer activity (~64% inhibition ratio of the colony formation of 22Rv1 prostate cancer cells at 100 μM)[134] Anti-inflammatory activity (36.8% and 40.6% inhibition ratios of cytokines IL-1β and TNF-α at the concentration of 20 μM, respectively)[133] Cytotoxic activity (IC_{50}, 52 and 36 μM against HeLa and L1210 cell lines, respectively)[35] Inhibition of RANKL-induced osteoclastogenic differentiation[135]
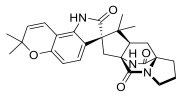 (+)-Notoamide B	*A. taichungensis*[65] *A. amoenus*[37,174]	ND
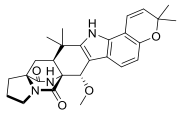 (-)-Notoamide F	*A. amoenus*[174]	ND
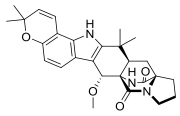 (+)-Notoamide F	*A. sulphureus and I. felina co-culture*[134] *Aspergillus* sp.[36,172,176] *A. ochraceus*[137] *A. ostianus*[137] *A. versicolor*[137]	ND
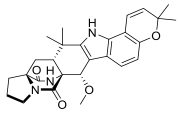 6-*epi*-Notoamide F	*A. taichungensis*[65]	ND

https://doi.org/10.1021/acs.chemrev.4c00250
Chem. Rev. XXXX, XXX, XXX−XXX

Table 1. continued

Compound	Source	Bioactivity
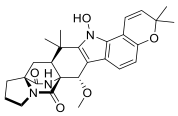 Notoamide G	*Aspergillus* sp.[36] *A. ochraceus*[137]	Antitumor (IC_{50}, 244, 87, 219, and 279 nM against SMMC-7721, HCT-8, MCF-7, and HUVEC cell lines, respectively; IC_{50}, 0.66-2.70 μM against various liver cancer cell lines)[137]
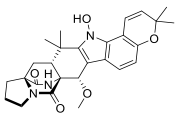 6-*epi*-Notoamide G	Photoinduced product[177]	ND
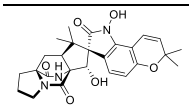 Notoamide H	*Aspergillus* sp.[36,138]	Antifungal activity (MIC, 25 μg/mL against *R. solani*)[138] Anti-inflammatory activity (IC_{50}, 46.2 μM against *P. acnes*-induced THP-1 cells)[138]
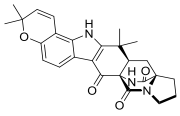 (-)-Notoamide I	*A. amoenus*[174]	ND
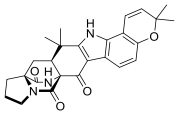 (+)-Notoamide I	*Aspergillus* sp.[36] *A. ochraceus*[137]	Cytotoxic activity (IC_{50}, 21 μg/mL against HeLa cell line)[36]
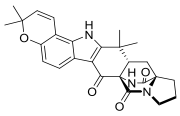 (-)-6-*epi*-Notoamide I	*A. amoenus*[174] *Aspergillus* sp.[138]	ND
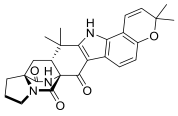 (+)-6-*epi*-Notoamide I	*A. protuberus*[63]	ND
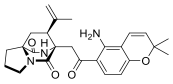 (-)-Notoamide L	*Aspergillus* sp.[38,178]	ND
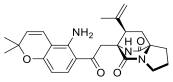 (+)-Notoamide L	*A. amoenus*[174]	ND
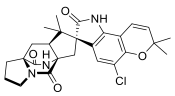 (-)-Notoamide N	*Aspergillus* sp.[38]	ND

https://doi.org/10.1021/acs.chemrev.4c00250
Chem. Rev. XXXX, XXX, XXX−XXX

Table 1. continued

Compound	Source	Bioactivity
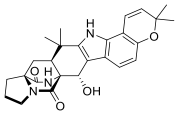 Notoamide R 21-Hydroxystephacidin A	*Aspergillus* sp.[40,138,176] *A. ostianus*[137]	Anti-inflammatory activity (IC_{50}, 34.3 μM against *P. acnes*-induced THP-1 cells)[138]
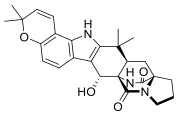 (-)-Notoamide R	*A. amoenus*[174]	ND
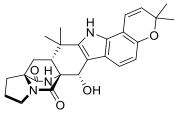 6-*epi*-Notoamide R	*Aspergillus sp* [138]	ND
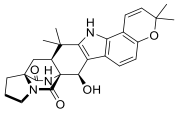 19-*epi*-Notoamide R	*A. ochraceus*[137]	ND
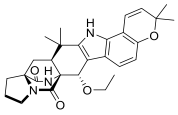 10-*O*-Ethylnotoamide R	*A. sulphureus and I. felina co-culture*[134]	ND
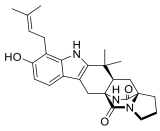 (-)-Notoamide T	Chemical synthesis[62]	ND
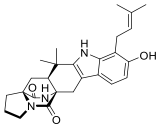 (+)-Notoamide T	Chemical synthesis[62]	ND
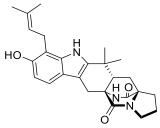 (-)-6-*epi*-Notoamide T	Chemical synthesis[62]	Inhibition of RANKL-induced osteoclastogenic differentiation (IC_{50}, 1.7 μM against murine RAW264 cells)[135]
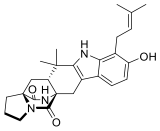 (+)-6-*epi*-Notoamide T	Chemical synthesis[62]	Inhibition of RANKL-induced osteoclastogenic differentiation (IC_{50}, 4.4 μM against murine RAW264 cells)[135]

https://doi.org/10.1021/acs.chemrev.4c00250
Chem. Rev. XXXX, XXX, XXX−XXX

Table 1. continued

Compound	Source	Bioactivity
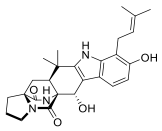 Notoamide T2	*A. protuberus*[62]	ND
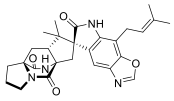 (±)-6-*epi*-Notoamide T3	*A. protuberus*[63]	ND
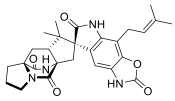 (±)-6-*epi*-Notoamide T4	*A. protuberus*[63]	ND
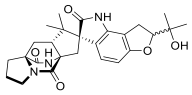 (±)-6-*epi*-Notoamide T5	*A. protuberus*[63]	ND
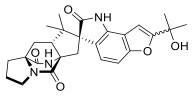 (±)-6-*epi*-Notoamide T6	*A. protuberus*[63]	ND
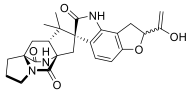 (±)-6-*epi*-Notoamide T7 (±)-6-*epi*-Notoamide T8	*A. protuberus*[63]	ND
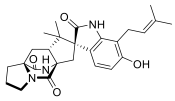 (±)-6-*epi*-Notoamide T9	*A. protuberus*[63]	ND
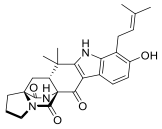 (±)-6-*epi*-Notoamide T10	*A. protuberus*[63]	ND
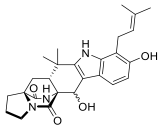 (±)-6-*epi*-Notoamide T11 (±)-6-*epi*-Notoamide T12	*A. protuberus*[63]	ND
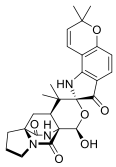 (+)-Notoamide O	*Aspergillus* sp.[40]	ND

https://doi.org/10.1021/acs.chemrev.4c00250
Chem. Rev. XXXX, XXX, XXX−XXX

Table 1. continued

Compound	Source	Bioactivity
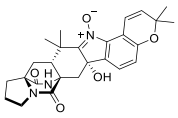 Notoamide U	*A. taichungensis*[65]	ND
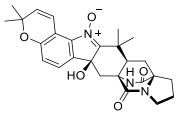 (-)-Notoamide U	*A. amoenus*[174]	ND
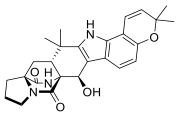 Notoamide V	*A. taichungensis*[65]	ND
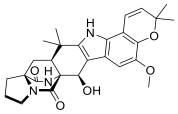 Notoamide W	*A. ochraceus*[137]	ND
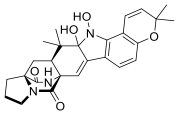 Notoamide W-2	Photoinduced product[177]	ND
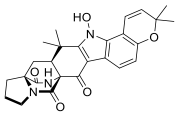 Notoamide X	*A. ochraceus*[137]	ND
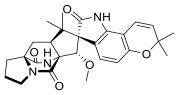 Notoamide Y	*A. ochraceus*[137]	ND
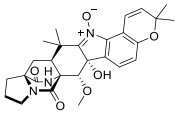 Notoamide Z Asperthrin D	*A. ochraceus*[137] *Aspergillus* sp.[138]	ND
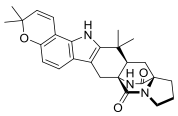 (-)-Stephacidin A	*A. taichungensis*[65] *A. amoenus*[37] *Aspergillus* sp.[139] *A. ochraceus*[140]	Inhibition of RANKL-induced osteoclastogenic differentiation[135] Antibacterial activity (MIC, 14.5 μM against *S. epidermidis*)[139] Mitochondrial respiratory inhibitor (IC_{50}, 34.6 μM against NADH oxidase)[140]

https://doi.org/10.1021/acs.chemrev.4c00250
Chem. Rev. XXXX, XXX, XXX−XXX

Table 1. continued

Compound	Source	Bioactivity
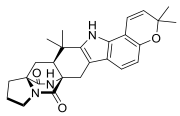 (+)-Stephacidin A	*A. ochraceus*[44,133,137,179] *Aspergillus* sp.[176,178] *A. tennesseensis*[180] *A. versicolor*[67,137] *A. cf. stygium*[173] *A. protuberus*[35]	Cytotoxic activity (IC_{50}, 1.0-13.1 μM against various human tumor cell lines)[44] Anti-inflammatory activity (46.5% and 32.6% inhibition ratios of cytokines IL-1β and TNF-α at the concentration of 20 μM, respectively)[133]
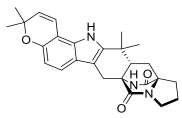 (-)-6-*epi*-Stephacidin A	*A. amoenus*[61]	ND
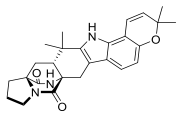 (+)-6-*epi*-Stephacidin A	*A. taichungensis*[65,177] *Aspergillus* sp.[63] *A. amoenus*[61]	Inhibition of RANKL-induced osteoclastogenic differentiation[135]
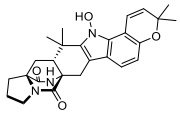 *N*-Hydroxy-6-*epi*-stephacidin A	*A. taichungensis*[177]	ND
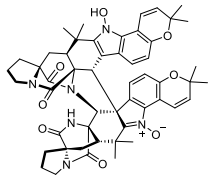 (-)-Stephacidin B	*A. ochraceus*[44,181] *A. westerdijkiae*[182]	Cytotoxic activity (IC_{50}, 0.06-0.46 μM against various human tumor cell lines; GI_{50}, 135, 346, 91, and 289 nM against LNCap, βT-549, T-47D, and MALME-3M cell lines, respectively)[44,183] Antitumor activity (IC_{50}, 0.091, 0.194, 0.403, and 0.268 μM against SMMC-7721, HCT-8, MCF-7, and HUVEC cell lines, respectively; IC_{50}, 0.42-3.19 μM against various liver cancer cell lines)[137]
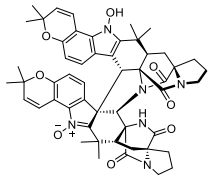 (+)-Stephacidin B	Chemical synthesis[112]	ND
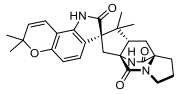 (-)-Versicolamide B	*Aspergillus* sp.[38] *A. versicolor*[137]	ND
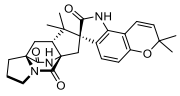 (+)-Versicolamide B	*A. taichungensis*[65] *A. amoenus*[37] *Aspergillus* sp.[38,63] *A. versicolor*[63,64,137]	ND

https://doi.org/10.1021/acs.chemrev.4c00250
Chem. Rev. XXXX, XXX, XXX−XXX

Table 1. continued

Compound	Source	Bioactivity
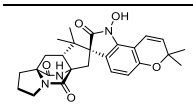 (+)-Versicolamide C	*A. taichungensis*[65]	ND
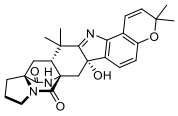 Taichunamide A	*A. taichungensis*[65]	ND
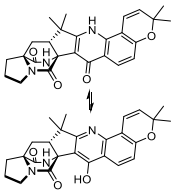 Taichunamide B	*A. taichungensis*[65]	ND
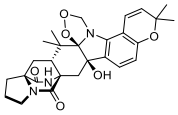 Taichunamide C	*A. taichungensis*[65]	ND
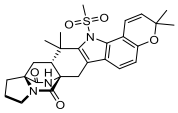 Taichunamide D	*A. ochraceus*[133] *A. taichungensis*[65]	Anti-inflammatory activity (38.9% and 34.5% inhibition ratios of cytokines IL-1β and TNF-α at the concentration of 20 μM, respectively)[133]
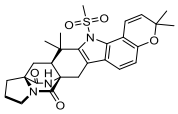 21-*epi*-Taichunamide D	*A. versicolor*[67]	ND
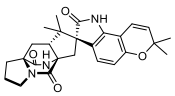 (-)-Taichunamide E	*A. taichungensis*[65] *A. cf. stygium*[173]	ND
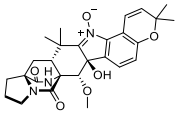 Taichunamide F	*A. taichungensis*[65]	ND
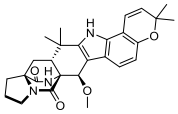 Taichunamide G	*A. taichungensis*[65]	ND
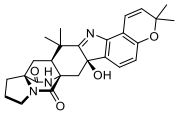 Taichunamide H Speramide A	*A. versicolor*[66] *F. sambucinum*[136] *A. ochraceus*[66,141]	Antimicrobial activity (MIC, 4-32 μg/mL against multiple bacteria and fungi; MIC of 0.8 μM against *Pseudomonas aeruginosa*)[136,141]

https://doi.org/10.1021/acs.chemrev.4c00250
Chem. Rev. XXXX, XXX, XXX−XXX

Table 1. continued

Compound	Source	Bioactivity
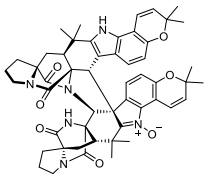 Waikialoid A	*Aspergillus* sp.[176]	Anti-biofilm formation activity (IC_{50}, 1.4 μM against *Candida albicans*)[176]
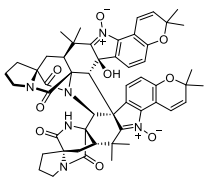 Waikialoid B	*Aspergillus* sp.[176]	ND
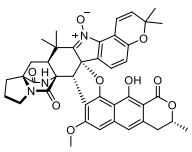 Waikikiamide A	*Aspergillus* sp.[172]	Antiproliferative activity (IC_{50}, 0.519, 1.855, 0.62, and 0.78 μM against HT1080, PC3, Jurkat, and A2780S cell lines, respectively)[172]
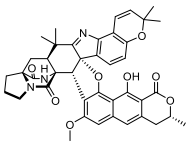 Waikikiamide B	*Aspergillus* sp.[172]	ND
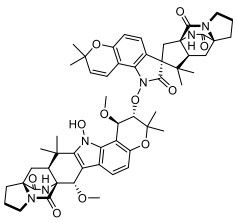 Waikikiamide C	*Aspergillus* sp.[172]	Antiproliferative activity (IC_{50}, 1.135, 1.805, 1.79 and 1.127 μM against HT1080, PC3, Jurkat, and A2780S cell lines, respectively)[172]
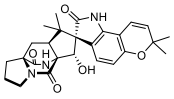 (-)-Sclerotiamide (-)-Sclerotamide	*F. sambucinum*[136] *Aspergillus* sp.[138,176] *A. sclerotiorum*[184] *A. ochraceus*[133,175,179] *A. protuberus*[35] *A. sulphureus and I. felina co-culture*[134]	Insecticidal activity (83.2% mortality rate under diet at 500 *ppm* against *Helicoverpa armigera*; 46% mortality rate under diet at 200 *ppm* against *Helicoverpa zea*)[136,184] Antimicrobial activity (MIC, 4-16 μg/mL against multiple bacteria and fungi; MIC of 25 μg/mL against *R. solani*)[136,138] Anti-inflammatory activity (IC_{50}, 41.6 μM against *P. acnes*-induced THP-1 cells)[138] Caseinolytic protease P (ClpP) activator (EC_{50}, 39.6, 87.5, and 2.6 μM for decapeptide (DFAP), FITC-casein, and Hill slope, respectively)[185] Anticancer activity (~65% inhibition ratio of the colony formation of 22Rv1 prostate cancer cells at 100 μM)[134]

https://doi.org/10.1021/acs.chemrev.4c00250
Chem. Rev. XXXX, XXX, XXX−XXX

Table 1. continued

Compound	Source	Bioactivity
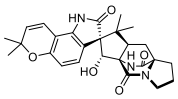 (+)-Sclerotiamide	*A. amoenus*[56]	ND
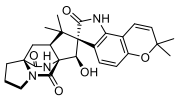 (-)-10-*epi*-Sclerotiamide	*A. westerdijkiae*[186]	ND
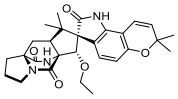 10-*O*-ethylsclerotiamide	*A. sulphureus and I. felina co-culture*[134]	ND
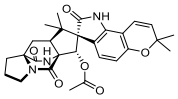 10-*O*-acetylsclerotiamide	*A. sulphureus and I. felina co-culture*[134]	ND
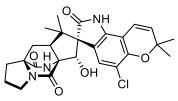 5-Chlorosclerotiamide	*A. westerdijkiae*[186,187]	ND
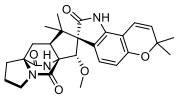 Sclerotiamide B	*F. sambucinum*[136]	Insecticidal activity (70.2% mortality rate under diet at 500 *ppm* against *H. armigera*)[136] Antimicrobial activity (MIC, 8-32 μg/mL against multiple bacteria and fungi)[136]
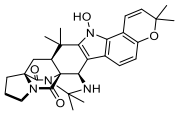 Sclerotiamide C	*A. sclerotiorum*[188]	Cytotoxic activity (IC_{50}, 1.7, 1.6, 1.8, and 1.5 μM against HeLa, A549, HepG2, and SMMC-7721 cell lines, respectively)[188]
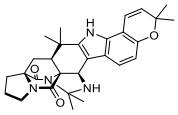 Sclerotiamide D	*A. sclerotiorum*[188]	Cytotoxic activity (IC_{50} >10 μM against HeLa, A549, HepG2, and SMMC-7721 cell lines)[188]
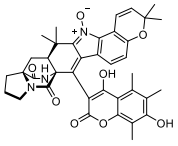 Sclerotiamide E	*A. sclerotiorum*[188]	Cytotoxic activity (IC_{50} >10 μM against HeLa, A549, HepG2, and SMMC-7721 cell lines)[188]
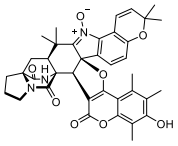 Sclerotiamide F	*A. sclerotiorum*[188]	Cytotoxic activity (IC_{50}, 7.9, 7.8, 8.1, and 6.7 μM against HeLa, A549, HepG2, and SMMC-7721 cell lines, respectively)[188]

https://doi.org/10.1021/acs.chemrev.4c00250
Chem. Rev. XXXX, XXX, XXX−XXX

Table 1. continued

Compound	Source	Bioactivity
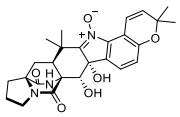 Sclerotiamide G	*A. sclerotiorum*[188]	Cytotoxic activity (IC_{50} >10 μM against HeLa, A549, HepG2, and SMMC-7721 cell lines)[188]
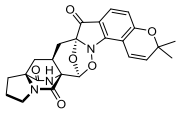 Sclerotiamide H	*A. sclerotiorum*[188]	Cytotoxic activity (IC_{50} >10 μM against HeLa, A549, HepG2, and SMMC-7721 cell lines)[188]
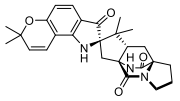 Amoenamide B	*A. amoenus*[189]	ND
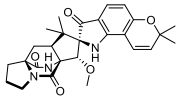 Amoenamide C	*F. sambucinum*[136]	Antimicrobial activity (MIC, 1-32 μg/mL against multiple bacteria and fungi)[136]
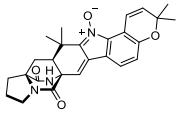 Avrainvillamide CJ-17665	*A. ochraceus*[137,190,191] *Aspergillus* sp.[176,192] *A. westerdijkiae*[182]	Antitumor activity (IC_{50}, 0.059, 0.209, 2.443, and 1.225 μM against SMMC-7721, HCT-8, MCF-7, and HUVEC cell lines, respectively; IC_{50}, 0.63-3.39 μM against various liver cancer cell lines; IC_{50}, 1100, 643, 116, 112 and 78 nM against NB4, HL-60, MV4-11, OCI-AML3, and Molm-13 acute myeloid leukemia (AML) cell lines, respectively; GI_{50} (growth-inhibitory potencies), 0.33 and 0.42 μM against T-47D and LNCap cell lines, respectively; IC_{90}, 1.1 μg/mL against HeLa cell line; GI_{50}, 0.24, 0.62, 0.20, and 0.41 μM against LNCap, βT-549, T-47D, and MALME-3M cell lines, respectively)[137,183,190,191,193] Antibacterial activity (MIC, 12.5, 12.5, and 25 μg/mL against *Staphylococcus aureus*, *Streptococcus pyogenes*, and *Enterococcus faecalis*, respectively)[191]
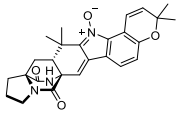 (+)-6-*epi*-Avrainvillamide	*A. taichungensis*[65,177]	ND
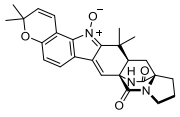 (-)-Avrainvillamide	Chemical synthesis[112]	ND

https://doi.org/10.1021/acs.chemrev.4c00250
Chem. Rev. XXXX, XXX, XXX−XXX

Table 1. continued

Compound	Source	Bioactivity
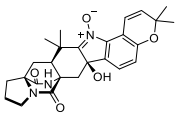 Aspergamide A	*A. ochraceus*[117,194]	ND
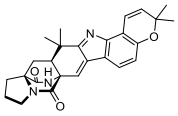 Aspergamide B	*A. ochraceus*[117,194]	ND
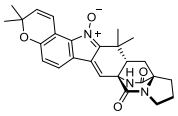 Asperthrin A	*Aspergillus* sp.[138]	Antimicrobial activity (MIC, 8-100 μg/mL against multiple bacteria and fungi) [138] Anti-inflammatory activity (IC_{50}, 30.5 μM against *P. acnes*-induced THP-1 cells)[138]
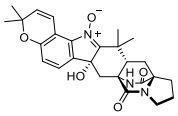 Asperthrin B	*Aspergillus* sp.[138]	ND
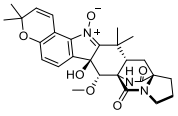 Asperthrin C	*Aspergillus* sp.[138]	ND
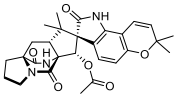 Asperthrin E	*Aspergillus* sp.[138]	Antifungal activity (MIC, 25 μg/mL against *R. solani*)[138] Anti-inflammatory activity (IC_{50}, 30.5 μM against *P. acnes*-induced THP-1 cells)[138]
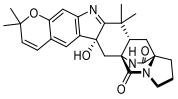 Asperversiamide A	*A. versicolor*[195]	ND
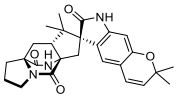 Asperversiamide B	*A. versicolor*[195]	ND
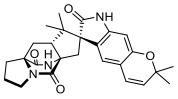 Asperversiamide C	*A. versicolor*[195]	ND
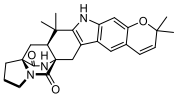 Asperversiamide D	*A. versicolor*[195]	ND
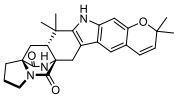 Asperversiamide E	*A. versicolor*[195]	ND

https://doi.org/10.1021/acs.chemrev.4c00250
Chem. Rev. XXXX, XXX, XXX−XXX

Table 1. continued

Compound	Source	Bioactivity
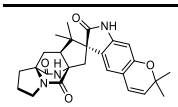 (+)-Isonotoamide B	*Paecilomyces variotii*[195,196]	Cytotoxic activity (IC_{50}, 55.9 μM against NCI-H460 cell line)[196]
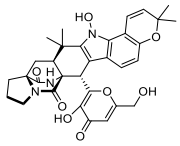 (+)-Versicoamide F	*A. tennesseensis*[180]	Antiproliferative activity (IC_{50}, 83.4 μM against H460 cells)[180]
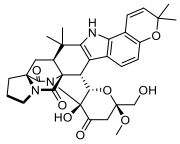 (+)-Versicoamide G	*A. tennesseensis*[180]	Antiproliferative activity (IC_{50}, 95.5 μM against H460 cells)[180]
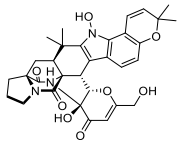 (+)-Versicoamide H	*A. tennesseensis*[180]	ND
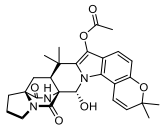 Asperinamide A	*Aspergillus* sp. TE-65L[197]	Anti-inflammatory activity[197]
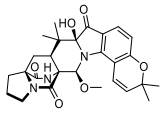 Aspertaichamide A	*A. taichungensis* 299[198]	Cytotoxic activity (IC_{50}, 19.2, 23.4, 48.5, and 1.7 μM against A549, HeLa, HepG2, and AGS cell lines, respectively)[198]
Monoketopiperazines		
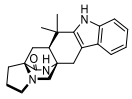 (+)-Premalbrancheamide	*P. purpurogenum*[199] *Malbranchea graminicola*[70] *M. aurantiaca*[144]	Calmodulin inhibitory activity (IC_{50}, 35.73 μM)[144]
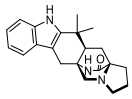 (-)- Premalbrancheamide	*P. purpurogenum*[199] *M. aurantiaca*[144]	ND

https://doi.org/10.1021/acs.chemrev.4c00250
Chem. Rev. XXXX, XXX, XXX−XXX

Table 1. continued

Compound	Source	Bioactivity
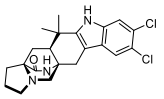 (+)-Malbrancheamide	*M. circinate*[145] *M. aurantiaca*[68,69,144,146] *M. graminicola*[70]	Calmodulin inhibitory activity (IC_{50}, 3.65 μM[68,143]; IC_{50}, 19.33 μM[142]) Vasorelaxant activity (EC_{50}, 2.7 μM)[146] α-Glucosidase (αGHY) inhibitory activity (IC_{50}, 71.3 and 458.7 μM for yeast and rat, respectively)[145] Protein Tyrosine Phosphatase 1B (PTP-1B) inhibitory activity (IC_{50}, 14.5 μM)[145] Inhibition of radicle growth of *Amaranthus hypochondriacus* (IC_{50}, 0.37 μM)[68]
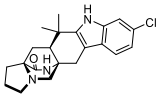 (+)-Malbrancheamide B	*M. aurantiaca*[69,144,146] *M. graminicola*[70]	Calmodulin inhibitory activity (IC_{50}, 183.28 μM)[144] Vasorelaxant activity (EC_{50}, 33.3 μM)[146]
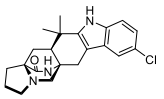 (+)-Isomalbrancheamide B	*M. graminicola*[70] *M. aurantiaca*[144,146]	Calmodulin inhibitory activity (IC_{50}, 41.56 μM)[144] Vasorelaxant activity (EC_{50}, 25.5 μM)[146]
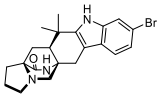 (+)-Malbrancheamide C	*M. graminicola*[70]	ND
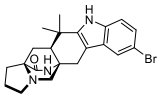 (+)-Isomalbrancheamide C	*M. graminicola*[70]	ND
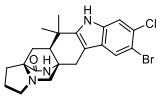 (+)-Malbrancheamide D	Enzymatic product[94]	ND
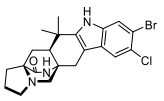 (+)-Isomalbrancheamide D	Enzymatic product[94]	ND
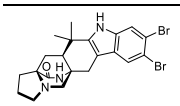 (+)-Malbrancheamide E	Enzymatic product[200]	ND
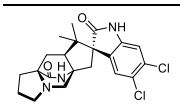 (-)-Spiromalbramide	*M. graminicola*[70,81]	ND
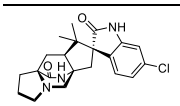 Spiromalbrancheamide B	Enzymatic product[81]	ND

https://doi.org/10.1021/acs.chemrev.4c00250
Chem. Rev. XXXX, XXX, XXX−XXX

Table 1. continued

Compound	Source	Bioactivity
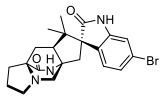 Spiromalbrancheamide C	Enzymatic product[81]	ND
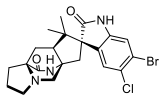 Spiroisomalbrancheamide D	Enzymatic product[81]	ND
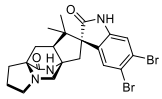 Spiromalbrancheamide E	Enzymatic product[81]	ND
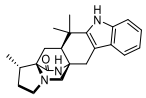 Preparaherquamide	*P. herquei*[201] *P. fellutanum*[77] *A. japonicus*[77] *A. aculeatinus*[80]	ND
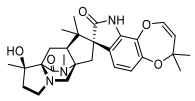 Paraherquamide A VM29919	*Aspergillus* sp.[82] *P. janthinellum*[79] *Penicillium* spp.[73] *P. fellutanum*[77] *A. japonicus*[77] *Penicillium* sp.[74] *P. cluniae*[78] *P. charlesii*[75]	Anthelmintic activity (100% reduction in faecal egg count with dose at 2.0 mg/kg; MIC_{50} of 31.2 μg/ml *in vitro*; 98% effective against *T. colubriformis* infection at an oral dose of 1.56 mg/kg)[73,74,148,202] Insecticidal activity (LD_{50}, 2.5 μg/ml against *Caenorhabditis elegans*; LD_{50}, 0.32 μg/nymph against *O. fasciatus*)[75,78]
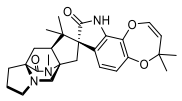 Paraherquamide B	*P. charlesii*[75] *P. cluniae*[78]	Insecticidal activity (LD_{50}, 100 μg/ml against *C. elegans*; LD_{50}, 16.54 μg/nymph against *O. fasciatus*)[75,78]
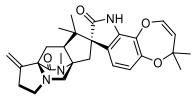 Paraherquamide C	*P. charlesii*[75]	Insecticidal activity (LD_{50}, 40 μg/ml against *C. elegans*)[75]
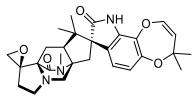 Paraherquamide D	*P. charlesii*[75]	Insecticidal activity (LD_{50}, 160 μg/ml against *C. elegans*)[75]
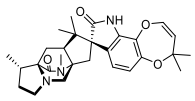 Paraherquamide E VM 54159	*Aspergillus* sp.[82] *A. aculeatinus*[80] *A. aculeatus*[203] *P. janthinellum*[79] *P. charlesii*[75] *P. cluniae*[78]	Anthelmintic activity (88, 96, and 99% reductions in faecal egg counts at the doses of 0.5, 1.0, and 2.0 mg/kg against adult *T. colubriformis* infection, respectively)[82] Cytotoxic activity (IC50, 1.9 μM against Bel-7402 cell line)[80] Insecticidal activity (LD_{50}, 6 μg/ml against *C. elegans*; LD_{50}, 0.089 μg/nymph against *O. fasciatus*)[75,78]

https://doi.org/10.1021/acs.chemrev.4c00250
Chem. Rev. XXXX, XXX, XXX−XXX

Table 1. continued

Compound	Source	Bioactivity
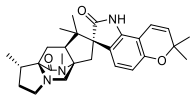 Paraherquamide F VM55594	*Penicillium* sp.[74] *P. charlesii*[75]	Insecticidal Activity (LD_{50}, 65 μg/ml against *C. elegans*)[75] Anthelmintic activity (MIC_{50} >500 μg/ml *in vitro*)[74]
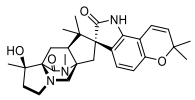 Paraherquamide G VM 54158	*Penicillium* sp.[74] *P. charlesii*[75]	Insecticidal activity (LD_{50}, 20 μg/ml against *C. elegans*)[75] Anthelmintic activity (MIC_{50} >500 μg/ml *in vitro*)[74]
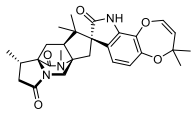 Paraherquamide H	*P. cluniae*[78]	ND
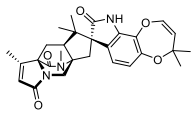 Paraherquamide I	*P. cluniae*[78]	ND
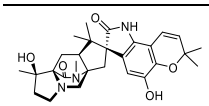 Paraherquamide J	*P. janthinellum*[79]	ND
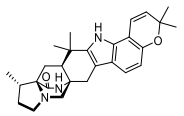 Paraherquamide K	*A. aculeatinus*[80] *P. simplicissimum* Δ*phqK*[81]	ND
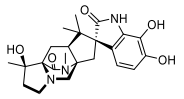 Paraherquamide K-2	*P. janthinellum*[79]	ND
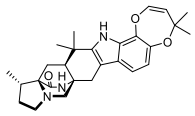 Paraherquamide L	*P. simplicissimum* Δ*phqK*[81]	ND
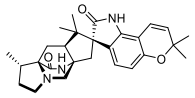 Paraherquamide M VM 55595	*A. aculeatinus*[80] *Penicillium* spp.[73] Enzymatic product[81]	ND
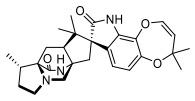 Paraherquamide N SB200437 UK 109692	*Aspergillus* sp.[82] *A. aculeatinus*[80] *P. janthinellum*[79] Enzymatic product[81]	ND

https://doi.org/10.1021/acs.chemrev.4c00250
Chem. Rev. XXXX, XXX, XXX−XXX

Table 1. continued

Compound	Source	Bioactivity
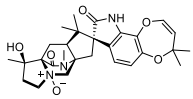 VM55596	*Penicillium* spp. [73] *P. cluniae*[78]	Anthelmintic activity (94% reduction in faecal egg count with a dose at 2.0 mg/kg)[73] Insecticidal activity (LD_{50}, 7.01 μg/nymph against *O. fasciatus*)[78]
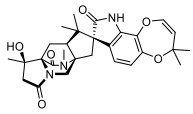 VM55597	*Penicillium* spp.[73] *P. cluniae*[78]	Insecticidal activity (LD_{50}, 0.91 μg/nymph against *O. fasciatus*)[78]
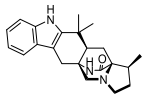 (-)-VM55599	*P. fellutanum*[77] *Penicillium* spp.[73,89]	ND
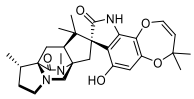 SB203105 VM54159	*Aspergillus* sp.[74,82]	Anthelmintic activity (MIC_{50}, 15.6 μg/ml *in vitro*)[74]
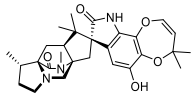 Aculeaquamide A	*A. aculeatinus*[80]	Cytotoxic activity (IC_{50}, 3.3 μM against Bel-7402 cell line)[80]
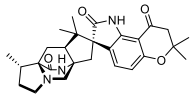 Peniciherquamide A	*P. herquei*[201]	ND
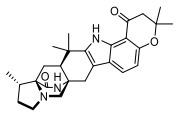 Peniciherquamide C	*P. herquei*[201]	Anti-HCV activity (IC_{50}, 5.1 μM)[201]
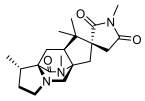 Asperparaline A Aspergillimide VM55598	*Aspergillus* sp.[82] *A. japonicus*[204,205]	Paralytic activity (against silkworms at a dose of 10 μg/g of diet and 3 μg/g of body weight with injection method)[204,205]
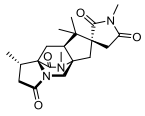 16-Keto aspergillimide SB202327	*Aspergillus* sp.[82]	Anthelmintic activity (*in vitro*)[82]
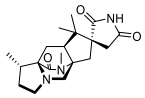 Asperparaline B	*A. japonicus*[205]	Paralytic activity (against silkworms at a dose of 10 μg/g of diet and 3 μg/g of body weight with injection method)[205]

https://doi.org/10.1021/acs.chemrev.4c00250
Chem. Rev. XXXX, XXX, XXX−XXX

Table 1. continued

Compound	Source	Bioactivity
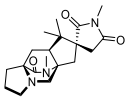 Asperparaline C	*A. japonicus*[205]	Paralytic activity (against silkworms at a dose of 10 μg/g of diet and 3 μg/g of body weight with injection method)[205]
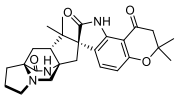 Citrinalin C	*P. citrinum*[206]	ND
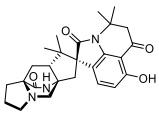 Cycloexpansamine A	*Penicillium* sp.[207]	Protein tyrosine phosphatase 1B (PTP-1B) inhibitory activity (IC_{50}, 27.6 μM)[207]
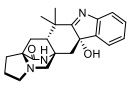 Penicimutamide D	*P. purpurogenum*[199]	ND
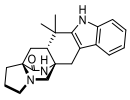 Penicimutamide E	*P. purpurogenum*[199]	ND
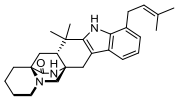 Penioxamide A	*P. oxalicum*[208]	Brine shrimp (*A. salina*) lethality (LD_{50}, 5.6 μM)[208]
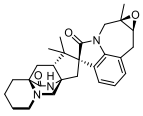 (+)-Penioxalamine A	*P. oxalicum*[209]	Cytotoxic activity (IC_{50}, 28.12 μM against HL-60 cell line)[209]
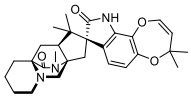 Marcfortine A	*P. paneum*[210,211] *P. roqueforti*[212-214] *A. carneus*[215]	Cytotoxic activity[211]
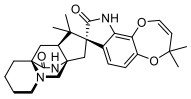 Marcfortine B	*P. paneum*[210,211] *P. roqueforti*[212-214]	Cytotoxic activity[211]
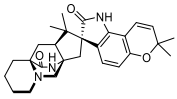 Marcfortine C	*P. paneum*[211] *P. roqueforti*[212-214]	Cytotoxic activity[211]
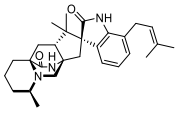 Chrysogenamide A	*P. chrysogenum*[216] *P. citrinum*[217]	Neurocyte protection activity (improving cells viability by 59.6% at the concentration of 1×10^{-4} μM)[216] Antifungal activity (reduced 61% of *P. digitatum* radial growth at 400 μg/mL)[217]

https://doi.org/10.1021/acs.chemrev.4c00250
Chem. Rev. XXXX, XXX, XXX−XXX

Table 1. continued

Compound	Source	Bioactivity
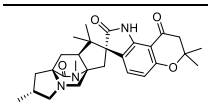 Mangrovamide A	*Penicillium* sp.[218,219] *P. herquei*[201]	ND
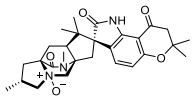 (-)-Mangrovamide B	*Penicillium* sp.[218]	ND
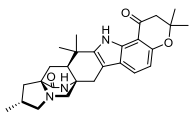 Mangrovamide C	*Penicillium* sp.[218,219] *P. herquei*[201]	Anti-acetylcholinesterase activity (IC_{50}, 58.0 μM)[218]
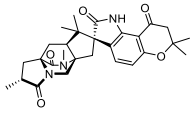 Mangrovamide D	*Penicillium* sp.[219]	ND
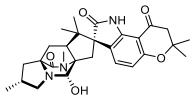 Mangrovamide E	*Penicillium* sp.[219]	ND
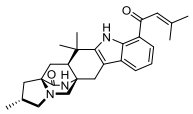 Mangrovamide F	*Penicillium* sp.[219]	ND
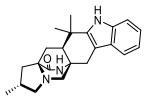 Mangrovamide G	*Penicillium* sp.[219]	ND
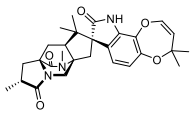 Paraherquamide J-2	*A. duricaulis*[220]	ND
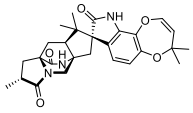 29-*N*-Demethylparaherquamide J	*A. duricaulis*[220]	ND
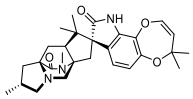 16-Deoxo-paraherquamide J	*A. duricaulis*[220]	Inhibitory effect on Aβ aggregation (IC_{50}, 269.5 μM)[220]
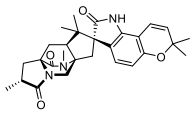 Paraherquamide K-3	*A. duricaulis*[220]	ND

https://doi.org/10.1021/acs.chemrev.4c00250
Chem. Rev. XXXX, XXX, XXX−XXX

Table 1. continued

Compound	Source	Bioactivity
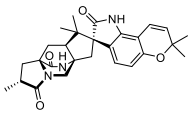 29-*N*-Demethylparaherquamide K	*A. duricaulis*[220]	Inhibitory effect on Aβ aggregation (IC_{50}, 244.3 μM)[220]
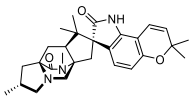 16-Deoxo-paraherquamide K	*A. duricaulis*[220]	ND
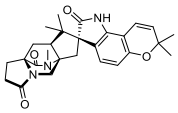 16-Oxo-paraherquamide B	*A. duricaulis*[220]	Protecting cells against Aβ aggregate-induced toxicity (EC_{50}, 149.6 μM), and inhibiting Aβ aggregation (IC_{50}, 186.6 μM)[220]
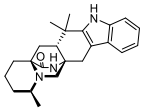 (+)-Precitrinadin A	*P. citrinum*[4,98]	ND
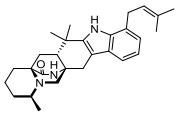 **59** Citrinadin-2	*P. citrinum*[98]	ND
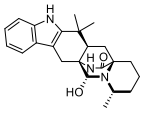 Citrinadin-3	*P. citrinum*[4]	ND
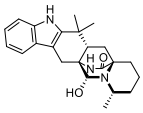 Citrinadin-4	*P. citrinum*[4]	ND
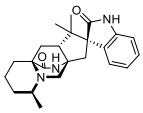 **60** Citrinadin-5	*P. citrinum*[98]	ND

https://doi.org/10.1021/acs.chemrev.4c00250
Chem. Rev. XXXX, XXX, XXX−XXX

Table 1. continued

Compound	Source	Bioactivity
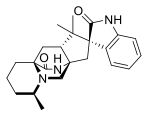 **60** Citrinadin-5	*P. citrinum*[98]	

[a]ND: Not determined. IC_{50}: half maximal inhibitory concentration. EC_{50}: half maximal effective concentration. LD_{50}: half of the lethal dose. MIC: minimum inhibitory concentration.

(Scheme 2). The stereochemical selectivity of this epoxidation is one of the major reasons for the highly diversified structures of BCDO alkaloids. Interestingly, this process can also generate another stable form, 3-hydroxyindolenine, which appears in some components of brevianamides, taichunamides and penicimutamides, *etc.*

Most BCDO indole alkaloids have post-modifications on the 6-membered aromatic ring originated from tryptophan, including hydroxylation, prenylation, cyclization, oxidation, and halogenation (Figure 1). The representative substructures include the pyran and dioxepin rings. The pyran moiety is widely present in a large number of DKPs (e.g., notoamides, stephacidins, versicolamides, and taichunamides) and MKPs (e.g., paraherquamides and mangrovamides). The dioxepin ring mainly exists in MKPs, such as paraherquamides, marcfortines, and aculeaquamide A. Halogenation modifications (chlorination and bromination) only exist in malbrancheamides. Intriguingly, there have been five reported dimers of BCDO indole alkaloids, including (+)-stephacidin B, (−)-stephacidin B, waikialoids A and B, and waikikiamide C. Some BCDO indole alkaloids can also condense with other structures to form more complex products. For instance, waikikiamides and versicoamides are formed by such a condensation with semivioxanthin and kojic acid (Scheme 3), respectively.

It is anticipated that more congeners of this family will be isolated from both marine and terrestrial fungi by natural product chemists worldwide, as these natural products have so far been exclusively found in fungi. A fascinating question is whether any family members could be found from Monera and/or Plantae in the future. The added new structures, bioactivities, as well as biogenetic mechanisms associated with BCDO indole alkaloids will continue to attract broad interest from scientists in diverse research areas.

3. BIOMIMETIC SYNTHESES BASED ON EARLY PROPOSAL/HYPOTHESIS FOR BIOGENESIS

The proposals for BCDO biogenesis in the DKP brevianamides and the MKP paraherquamides and malbrancheamides were mainly derived from continual biomimetic syntheses. With firm belief in the hypothetical IMDA-based assembly of the BCDO core, synthetic chemists courageously initiated explorations of BCDO biogenesis without any genetic knowledge and tools. They started to focus on the "biomimetic" syntheses of various compounds related to different BCDO indole alkaloid family members. These synthetic efforts have led to diverse isotopically labeled biosynthetic precursors for isotope incorporation studies. A wealth of key information about the reactivity of proposed biosynthetic intermediates was acquired, allowing for the refinement of different biosynthetic proposals. These efforts have driven the evolution of the long-standing IMDA hypothesis for biogenesis of fungal BCDO indole alkaloids.

3.1. Diketopiperazines

In this section, we will review in detail the exploration of DKPs' biogenesis, which is mainly based on the biosynthetic and related chemical principles, and isotopically labeled precursor feeding experiments. The representative fungal DKP alkaloids include brevianamides, notoamides, and stephacidins. In addition, the biogenesis of other DKPs including versicolamides and taichunamides is also discussed.

3.1.1. Brevianamides. Brevianamides (A−D) are the earliest discovered BCDO indole alkaloids, which were isolated by Birch and Wright from the culture extract of a *Penicillium brevicompactum* strain.[6−9] Since then, brevianamides A−D, along with related derivatives brevianamides E and F, were isolated from different *Penicillium* species including *Penicillium viridicatum*[10] and *Penicillium ochraceum*.[11]

Brevianamide A (i.e., (+)-brevianamide A) is a major metabolite of *P. brevicompactum*. The initial structural elucidation of this founding member of the BCDO indole alkaloid family relied primarily on chemical reduction and spectroscopic analysis, especially via its chemical derivative deoxybrevianamide A.[9] The presence of an indole substructure in brevianamide A naturally suggested L-tryptophan as a biosynthetic precursor.[8] The structure of its DKP core also indicated the other amino acid precursor, which was later confirmed to be L-proline.[6,8] Additionally, the loss of C_5H_9 in the mass spectrum implicated the possible presence of an isopentenyl group. Later, single crystal X-ray analysis of 5-bromo-brevianamide A enabled full determination of the absolute configuration of brevianamide A (Figure 3A).[12]

In the early 1970s, the absolute configuration of naturally occurring brevianamide B (i.e., (+)-brevianamide B) had not been assigned, which was thought to be the same as that of brevianamide A with regard to the BCDO core, but diastereomeric at the spiro-indoxyl stereogenic center.[7] This inference was mainly due to the experimental results showing that (−)-brevianamide B, the mirror-image isomer of natural (+)-brevianamide B, was generated in trace amounts during the photolysis of brevianamide A (Figure 3B). Additionally, (−)-brevianamide B was semisynthesized through several chemical procedures consisting of reduction to deoxybrevianamide A and stereoselective reoxidation (Figure 3C). In 1989 the correct absolute configuration of natural (+)-brevianamide B was elucidated by the Williams group through chemical total synthesis[13,14] and careful comparison of the chiroptical properties of the naturally occurring,[9] synthetic[15] and semisynthetic brevianamide B[7] (Figure 3A). They concluded that

https://doi.org/10.1021/acs.chemrev.4c00250
Chem. Rev. XXXX, XXX, XXX−XXX

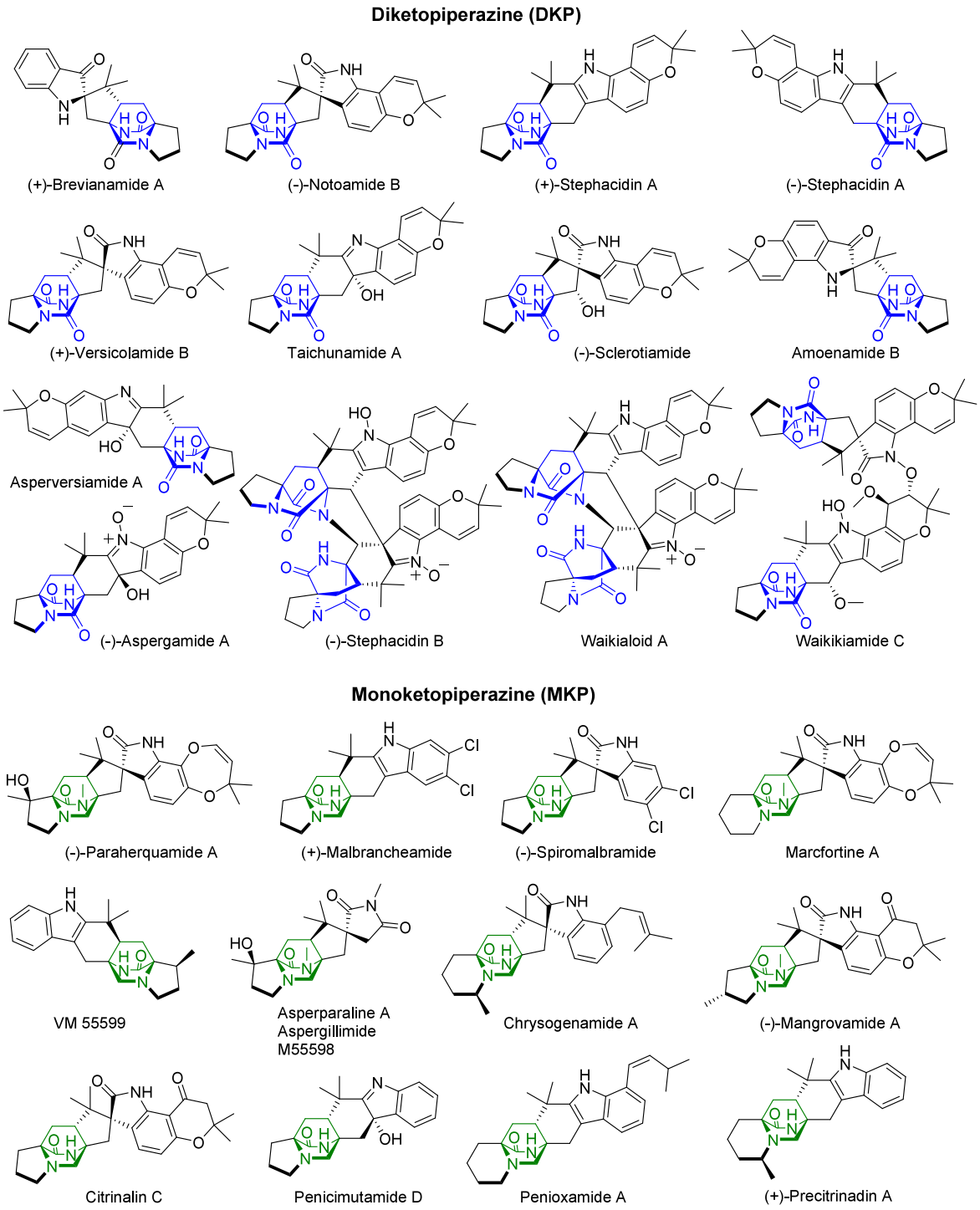

Figure 1. Representative diketopiperazine and monoketopiperazine BCDO indole alkaloids.

the natural (+)-brevianamide B is enantiomorphic to brevianamide A with respect to the BCDO core and has the same chiral configuration in the *spiro*-indoxyl substructure.

Brevianamides C and D were shown to be artifacts derived from irradiation of brevianamide A.[7] An almost quantitative, rapid conversion into the isomers brevianamides C and D was observed upon irradiation of the solution of brevianamide A in mixture with benzene and methanol or other methanolic solutions with visible light. When the producer *P. brevicompactum* was cultured in the dark and extracted under low light intensity, no sign of brevianamides C or D could be observed from thin layer chromatography, while brevianamides A and B were present in the neutral fraction. Thus, (−)-brevianamide B and brevianamides C and D are all photochemical artifacts rather than fungal metabolites.

Birch and Wright not only discovered the family of BCDO indole alkaloids but also first proposed the biogenetic hypothesis for brevianamides.[8] Accordingly, isotopic precursor feeding experiments were conducted for the brevianamides producing *P. brevicompactum* strain.[6,8] As expected, L-[methylene-^{14}C]-tryptophan, [1-^{14}C]-acetate, [2-^{14}C]-mevalonolactone, L-[U-^{14}C]-proline, and L-[5-^{3}H]-proline could be

https://doi.org/10.1021/acs.chemrev.4c00250
Chem. Rev. XXXX, XXX, XXX−XXX

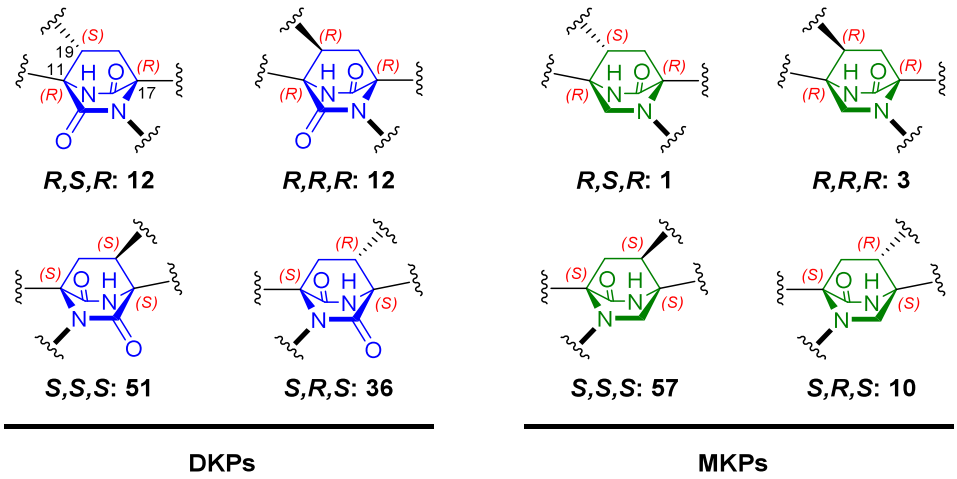

Figure 2. Stereoselectivity patterns of BCDO indole alkaloids. The numbers of each group member discovered from nature are displayed.

Scheme 1. Model Reaction of [4+2] *Hetero*-Diels–Alder (DA) Cycloaddition (*Upper Panel*) and Putative Biogenesis of Enantiomeric and Diastereomeric BCDO Structures through Intramolecular [4+2] *Hetero*-DA (IMDA) Cycloaddition (*Lower Panel*)[a]

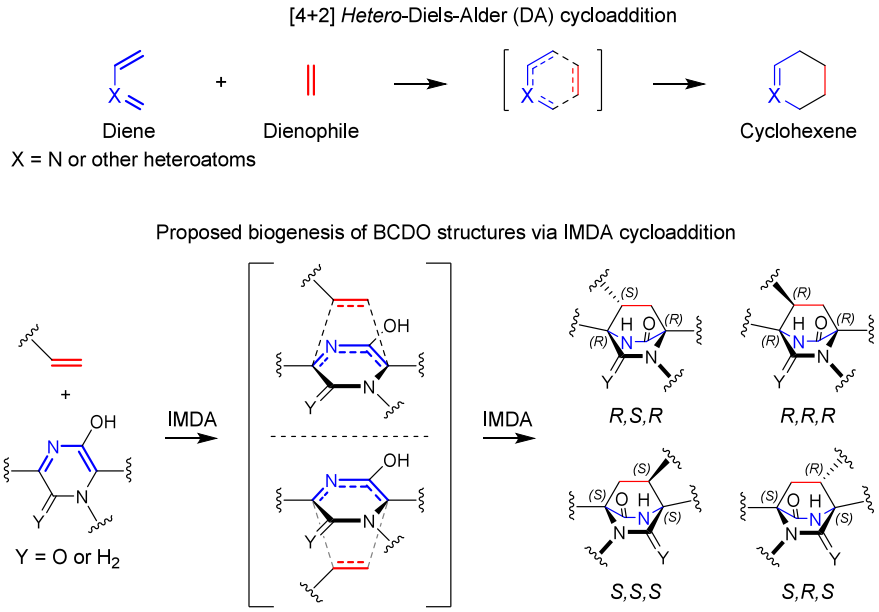

[a]The diene and dienophile groups are shown in blue and red, respectively.

Scheme 2. Biogenesis of *Spiro*-Substructures and 3-Hydroxyindolenine in BCDO Alkaloids

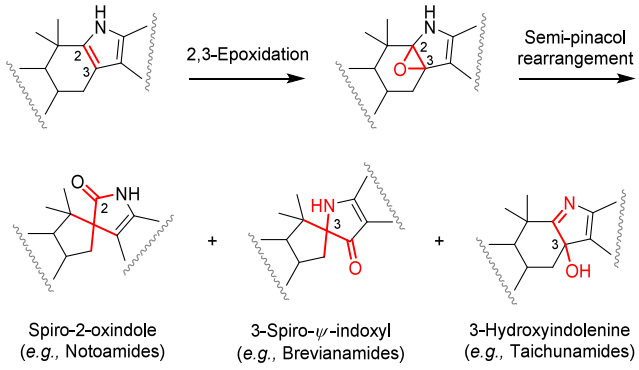

incorporated into brevianamide A (Scheme 4). Moreover, mevalonic acid was shown to be a virtually irreversible intermediate in fungal terpenoid biosynthesis.[16] Therefore, its incorporation is significant in terms of the presence of a terpene unit, and based on mass spectrometric analysis, it was inferred to be an isopentenyl group. Taken together, a reasonable biosynthetic intermediate deoxybrevianamide E, which was isolated from another fungus *Aspergillus ustus*, was tentatively proposed.[17]

Based on the putative chemical structure of brevianamide A,[9] Porter and Sammes proposed that the BCDO core structure might result from a [4+2] IMDA reaction between the isopentenyl unit (as dienophile) and the pyrazine moiety (as diene)[1] (Scheme 5A). To test this hypothesis, a pyrazine analogue **1** was chosen to react with dimethyl acetylenedicarboxylate in dimethylformamide at room temperature, which yielded the expected BCDO product (**2**) (Scheme 5B). The

https://doi.org/10.1021/acs.chemrev.4c00250
Chem. Rev. XXXX, XXX, XXX−XXX

Scheme 3. Condensation Reactions of BCDO Indole Alkaloids with Semivioxanthin and Kojic Acid Leading to Waikikiamides and Versicoamides, Respectively

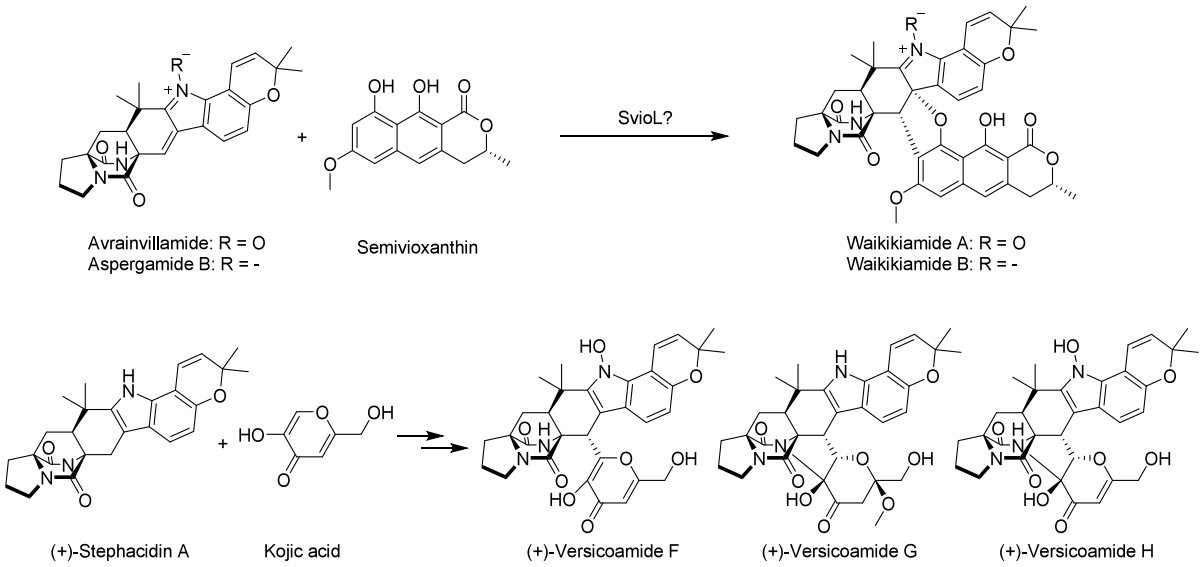

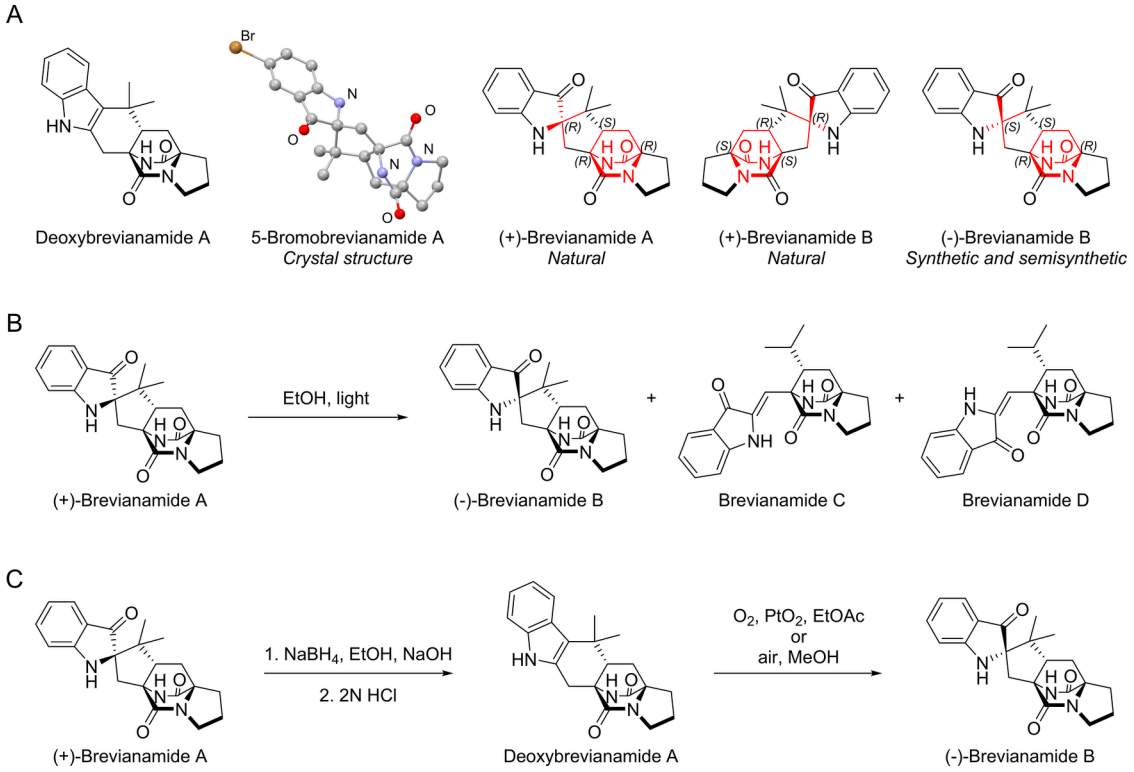

Figure 3. Structures of Brevianamide Derivatives (A), Photolysis of Brevianamide A (B), and Semisynthesis of (−)-Brevianamide B (C).

pyrazine analogue **3** was also able to undergo a DA reaction with norbornadiene to give the corresponding [4+2] adduct **4** (Scheme 5C). These results showed that the [4+2] IMDA reactions were favored in the cycloaddition equilibrium, as the formation of two amide groups partly compensated the resonance energy associated with the dihydroxypyrazine systems. In addition, more analogues similar to the structure of brevianamide A were prepared by following the same IMDA strategy.[1]

Further investigation by Birch and Russell for additional indole precursors from the metabolites of *P. brevicompactum* led to the discovery of brevianamide F in 1972.[7] Notably, only 1 mg of the crystalline brevianamide F was obtained from 40 L of fungal culture. Due to the small amount and technical limitation at that time, it was challenging to determine the stereochemistry of this compound. Analysis of its ultraviolet and mass spectra indicated that brevianamide F should be a derivative of tryptophan. The predominant occurrence of L-amino acids prompted the comparison of the natural product with a sample of chemically synthesized *cyclo*-L-tryptophanyl-L-proline, thereby confirming the identity of these two structures. It is evident that brevianamide F should be a common

https://doi.org/10.1021/acs.chemrev.4c00250
Chem. Rev. XXXX, XXX, XXX−XXX

Scheme 4. Isotopic Incorporations into Brevianamides by *P. brevicompactum*[a]

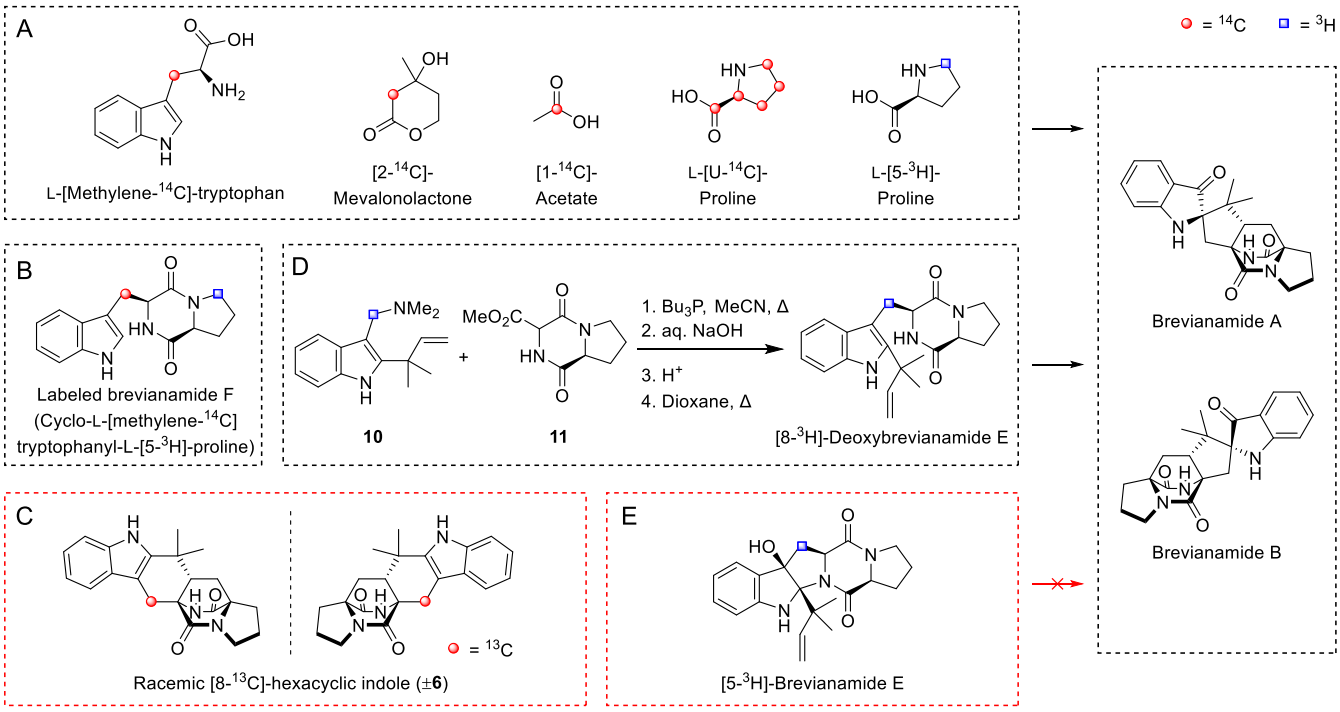

[a]Compounds in black dashed boxes could be incorporated into brevianamides, while those in red dashed boxes could not.

Scheme 5. Initial IMDA Proposal (A) for the BCDO Core and Related Chemical Tests (B, C)[a]

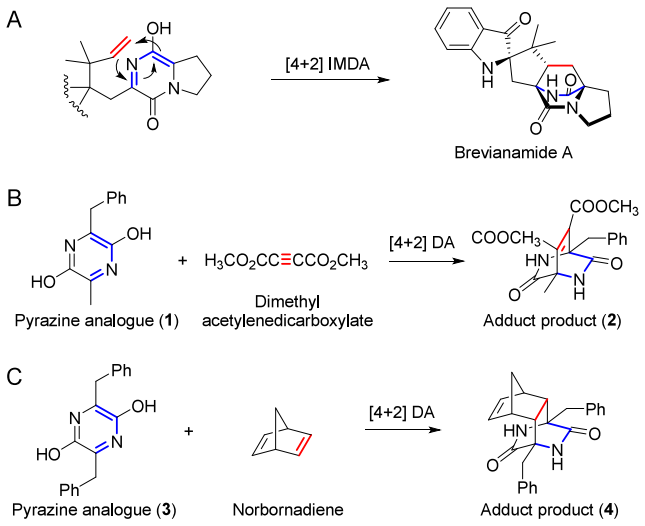

[a]The diene and dienophile groups are shown in blue and red, respectively.

biogenetic precursor for brevianamides. Although another postulated precursor deoxybrevianamide E (isolated from *A. ustus*[17]) was not detected in any cultures of *P. brevicompactum*, Birch and co-workers proposed an insightful biosynthetic route from brevianamide F to brevianamide A (Scheme 6A), which was confirmed to be essentially correct after almost half a century.[2]

To verify that brevianamide F is a building block of brevianamide A, the radioactive brevianamide F (i.e., *cyclo*-L-[methylene-^{14}C]tryptophanyl-L-[5-^{3}H]proline) was synthesized.[6] The feeding study showed that the intact, doubly labeled material was incorporated into brevianamide A (Scheme 4B). The highly specific incorporation of "hot" brevianamide F and the fact that deoxybreviamide E is the adduct of an isoprene unit and brevianamide F strongly supported the early biosynthetic steps leading to brevianamide A (Scheme 6A).

Next, the remaining biosynthetic steps of brevianamide A featuring the IMDA transformation were proposed[13] (Scheme 6B). Hypothetically, deoxybrevianamide E could act as a key intermediate leading to a hexacyclic indole **6** via oxidative [4+2] IMDA cycloaddition of the prenyl moiety across the piperazinedione nucleus, through an azadiene intermediate **5** derived from C−N bond desaturation. Further oxidation of the hexacyclic indole **6** followed by ring-contractive rearrangement (semipinacol rearrangement) would furnish brevianamide A.

After Williams and co-workers elucidated the correct absolute configuration of natural (+)-brevianamide B through total synthesis,[13,14,18] a modified biosynthetic pathway was suggested (Scheme 6C). The achiral azadiene intermediate **5** was postulated to undertake the [4+2] IMDA cycloaddition to furnish the enantiomeric hexacyclic indoles **6** and **7**. Oxidation of the hexacyclic indoles and subsequent pinacol-type rearrangement would afford the two spiroindoxyl diastereomers brevianamides A and B. Williams insightfully speculated that if this biosynthetic scheme was correct, the hydroxyindolenines **8** and **9** should not be enantiomeric but diastereomeric in order to generate the diastereomeric brevianamides A and B. Specifically, the major metabolite brevianamide A produced by *P. brevicompactum* should result from oxidation on the more hindered face of the hexacyclic indole **6** (providing the α-face hydroxyindolenine **8**), and the minor metabolite brevianamide B would derive from oxidation on the less hindered face of **7** (*via* β-face hydroxyindolenine **9**). This inference led to a hypothesis that *P. brevicompactum* probably had evolved different genes responsible for enantio-

https://doi.org/10.1021/acs.chemrev.4c00250
Chem. Rev. XXXX, XXX, XXX−XXX

Scheme 6. Early Proposed Brevianamides Biosynthetic Pathways. (A) The Biosynthetic Route from Brevianamide F to Brevianamide A Proposed by Birch.[7] (B) Hypothetical Biogenesis of Brevianamide A Featuring a Hexacyclic Indole Intermediate.[13] (C) Early Proposal for the Biogenesis of Brevianamides by Williams.[13,14,18] (D) The Revised Biosynthetic Pathway for Brevianamides A and B by Williams[19a]

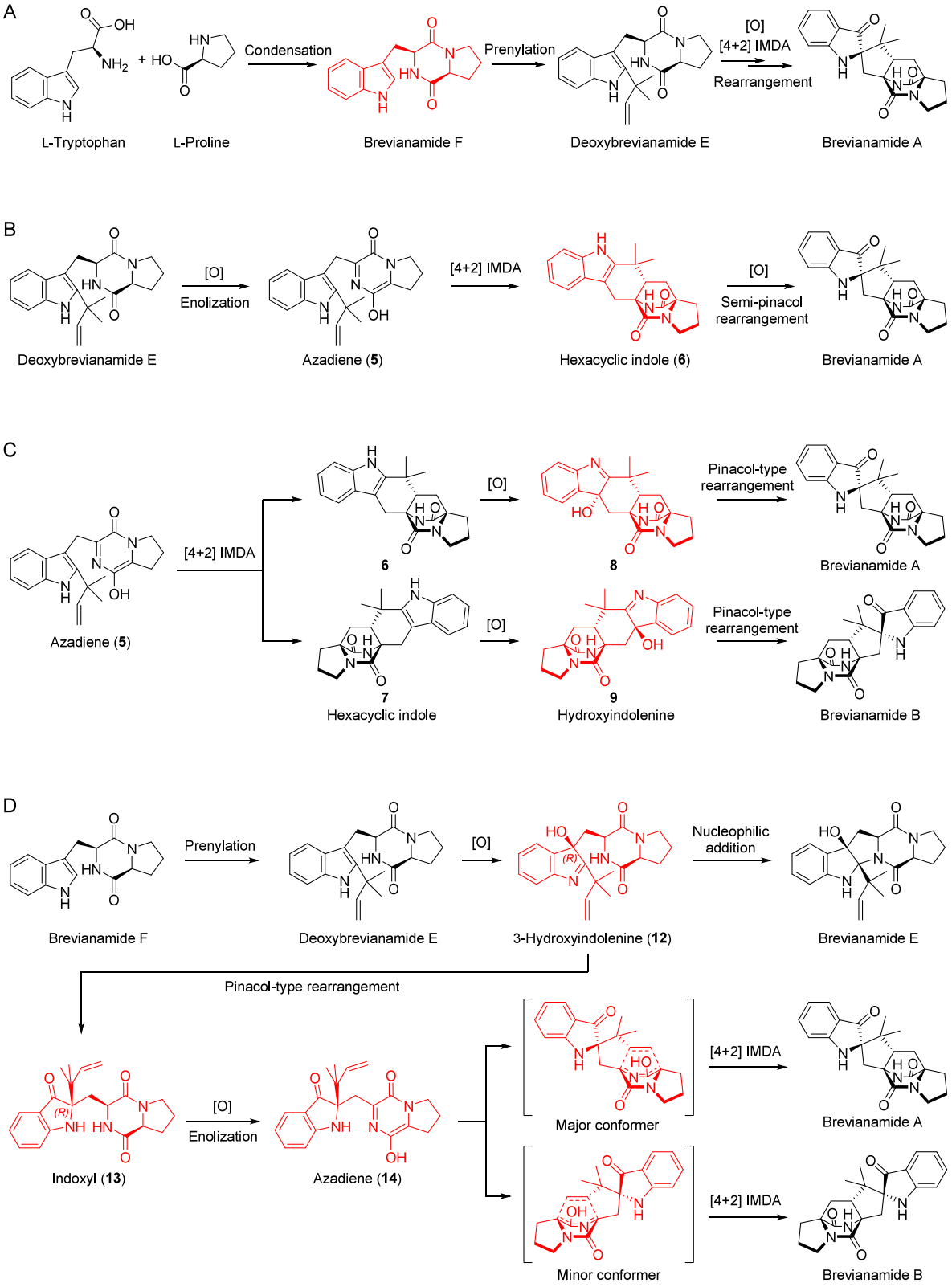

[a]Putative key intermediates are highlighted in red.

https://doi.org/10.1021/acs.chemrev.4c00250
Chem. Rev. XXXX, XXX, XXX−XXX

and diastereodivergent pathways for production of brevianamides A and B.

Since the putative hexacyclic indole **6** was considered to be a crucial biosynthetic precursor to the brevianamides, the fermentation extracts of *P. brevicompactum* were carefully examined at varying growth intervals in order to capture this hypothetical intermediate.[14,18] Despite intense efforts, the attempts to identify even trace amounts of the hexacyclic indoles were unsuccessful. Although this did not rule out the possibility that the hexacyclic indoles might be short-lived or tightly enzyme-associated (e.g., not being secreted into the fermentation media), the failure to trap hexacyclic indoles raised some new proposed routes to the brevianamides.

Thus, Williams et al. chemically synthesized the hypothetical biosynthetic precursor hexacyclic indole **6**.[18] Simply allowing this compound to remain in ethyl acetate solution in the air led to a variety of unidentified oxidative products. However, neither brevianamide A nor B could be detected in the final mixture. Additionally, chemical oxidation of the hexacyclic indole **6** with m-CPBA in CH_2Cl_2 followed by the treatment with NaOMe in MeOH gave (−)-brevianamide B in a good yield, but brevianamide A remained undetected. As brevianamide A could not have resulted from autoxidation or chemical manipulation of the hexacyclic indole **6**, the authors proposed that the indoxyl brevianamides should result from a specific enzymatic transformation.

To validate this proposal, the racemic [8-^{13}C]-hexacyclic indole (±**6**) was chemically synthesized for the isotopic incorporation experiment[19,20] (Scheme 4C). Feeding of this ^{13}C-labeled compound to cultures of the brevianamides A and B producing fungus failed to show significant enhancement of the C-8 signal in their ^{13}C NMR analysis and the $(M+1)^+/M^+$ intensity ratio in the mass spectra, indicating no incorporation of the hexacyclic indole. This result motivated more investigations of alternative biosynthetic pathways.

To ascertain the intermediacy of deoxybrevianamide E, the [8-^{3}H] labeled substance was synthesized from the gramine derivative [^{3}H]-**10** and the dioxopiperazine **11** through condensation, hydrolyzation, and decarboxylation[19,20] (Scheme 4D). Feeding experiments with the synthetic [8-^{3}H]-deoxybrevianamide E showed significant incorporation of the radioactivity into both brevianamides A and B, thus confirming their common biosynthetic origin. It is noteworthy that the incorporation of [8-^{3}H]-deoxybrevianamide E into brevianamide E was also highly efficient. These results confirmed that deoxybrevianamide E is indeed a biosynthetic precursor to brevianamides A, B, and E.

Furthermore, [5-^{3}H]-brevianamide E (prepared from [8-^{3}H]-deoxybrevianamide E by photooxidation and reduction) was also subject to the precursor feeding experiment.[19,20] However, no significant radioactivity incorporation was observed in both brevianamides A and B (Scheme 4E). Of note, the labeled brevianamide E seemed quite stable under the culture conditions with a high extraction recovery ratio. Brevianamide E was always present in a fairly constant proportion relative to brevianamide A in *P. brevicompactum* cultures, but it was not detected even in trace amount in the culture of another deoxybrevianamide E producing fungus *A. ustus*, strongly suggesting this product should not be an artifact. In consideration of these facts, brevianamide E was believed to be a shunt metabolite that would not be transformed to brevianamide A or B, representing a dead-end product in a side biosynthetic pathway.

Through a series of biomimetic syntheses of isotopically labeled brevianamide-related intermediates and corresponding feeding experiments, Williams and co-workers depicted a more detailed biosynthetic scheme to explain the stereochemical outcomes in the biosynthesis of brevianamides A and B[19] (Scheme 6D). Specifically, brevianamide F is converted into deoxybrevianamide E via a reverse prenylation step. This is followed by an *R*-selective hydroxylation at the 3-position of the indole, furnishing the 3-hydroxyindolenine **12**. Nucleophilic addition of the DKP secondary amide N to the C═N bond results in an N−C ring closure, giving rise to the shunt metabolite brevianamide E. Alternatively, a semipinacol rearrangement of the 3-hydroxyindolenine **12** affords the *R*-absolute stereochemistry at the quaternary center to give the indoxyl species **13**. Following oxidation and enolization of the DKP subunit to form an azadiene **14**, in the final step, an enzyme catalyzed [4+2] IMDA cyclization from the major conformer leads to brevianamide A, and from the other minor conformer results in brevianamide B. Hence, this proposal supports the existence of two enantiomorphic BCDO core systems.

Without genetic and biochemical evidence, it was difficult to explain why both brevianamides A and B are coproduced by *P. brevicompactum*. A central question was whether the hypothetical [4+2] IMDA cycloaddition is enzyme catalyzed or not. If the IMDA reaction is catalyzed by an enzyme, the preponderance of the major azadiene conformer over the minor one could result from either the relative activities of two different DAases or the differential affinity of a single enzyme toward each individual conformer. For the previous hypothesis, considering that DAases are rare in nature, it is unlikely that a biosynthetic system harbors two distinct DAases to recognize a common substrate. With regard to the latter hypothesis, it is also difficult to imagine that the intermediate could adopt two opposite conformations within a common active site. Thus, Williams proposed another possibility that the hypothetical "DAase" might just catalyze the oxidative process, converting indoxyl **13** into azadiene **14**, and the subsequent Diels−Alder cycloaddition reactions could occur spontaneously through substrate anchimeric assistance.[21]

To explore this hypothesis, Domingo and co-workers performed *ab initio* calculations for the four possible transition-state structures of the IMDA cycloaddition of the azadiene intermediate to give brevianamides A and B and the other two presumed isomers[21] (Scheme 7). Interestingly, the transition state 1 (TS1) that would lead to brevianamide A has the lowest relative energy, and TS2 corresponding to brevianamide B has a relative energy of 6.35 kcal/mol. This energy difference results from the favorable H-bond between the indoxyl N−H and the DKP carbonyl oxygen. The calculated energies of the other two epimers TS3 and TS4 (11.02 and 12.73 kcal/mol, respectively) are considerably higher. The calculation results are consistent with the experimental ratio of approximately 10−20:1 between brevianamides A and B, and no other isomers have ever been detected in fermentation cultures.

Although the hypothetical azadiene intermediate **14** is essential for the IMDA cycloaddition, there was no direct evidence for the existence of such an azadienic compound. Thus, Williams and co-workers carried out further total syntheses of brevianamides with different biomimetic strategies (see section 5.1 Total Synthesis of Brevianamides").[22−24] These studies to a large extent demonstrated that the core

https://doi.org/10.1021/acs.chemrev.4c00250
Chem. Rev. XXXX, XXX, XXX−XXX

Scheme 7. Transition State Structures for the Spontaneous IMDA Reactions Leading to Brevianamides A and B[a]

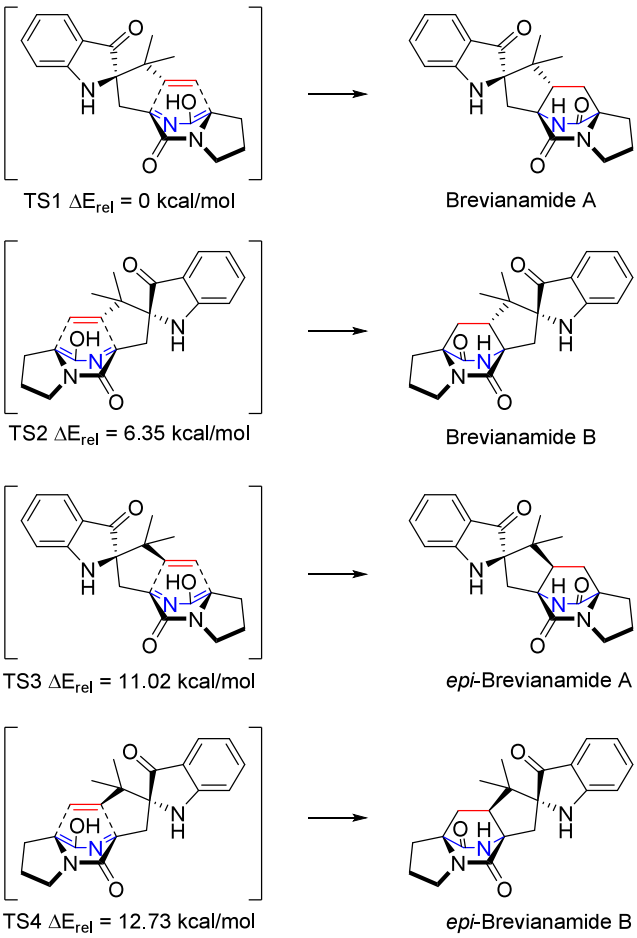

[a]The calculation was performed with the Gaussian 92 suite of programs and fully optimized at the restricted Hartree−Fock (RHF) level with the 3-21G and 6-31G* basis set.[21]

BCDO structure should likely arise from an IMDA cyclization between the isoprene-derived dienophile and the azadiene. It is noteworthy that the diastereofacial bias of the IMDA cyclization was not strongly affected by solvents, indicating that the proposed biosynthetic process is possible in aqueous solution under ambient conditions. The chemical cyclization in the laboratory favored the formation of the *syn*-configuration product (i.e., C19-*epi*-brevianamide A). This is different from the stereoselectivity in the natural biosynthetic case, which exclusively favors formation of the *anti* product (brevianamide A). This fact raises the possibility of enzyme-involved organization of the transition state structures or the existence of some unknown natural precursor.

Stocking et al. further investigated the attachment mode of dimethylallyl pyrophosphate (DMAPP) in the biosynthesis of brevianamide A by [$^{13}C_2$]-acetate feeding experiments[25] (Scheme 8). The isotopic enrichment results indicated that the isoprene unit in brevianamide A should arise via the canonical mevalonate pathway since both carbons of the dimethyl groups in brevianamide A were derived from the labeled acetate. Interestingly, one carbon of the two methyl groups showed a higher percentage of specifically incorporated ^{13}C than the other. This observation suggested that, although there was a loss of stereochemical integrity of the dimethyl groups originated from DMAPP in the biosynthesis of brevianamide A, the putative "reverse" prenyltransferase still maintained some degree of stereofacial bias during the reverse prenylation of brevianamide F to deoxybrevianamide E.

Recently, the Lawrence group achieved the chemical synthesis of brevianamide A and proposed a modified biosynthetic pathway[26] (Scheme 9). Their total synthesis involved a bioinspired cascade transformation of the linearly fused dehydrodeoxybrevianamide E, a natural product isolated from various *Penicillium* and *Aspergillus* species.[27−29] Essentially, the DKP ring was already at the redox state for the late-stage IMDA cyclization. The authors presumed this known natural product as a biosynthetic intermediate in brevianamides biosynthesis. Dehydrodeoxybrevianamide E was first diastereoselectively oxidized into dehydrobrevianamide E, which is not yet a known natural product. Retro-5-exo-trig ring opening followed by stereospecific 1,2-shift pinacol rearrangement gave the indoxyl species **15**. Subsequent tautomerization yielded the key enantiopure azadiene intermediate **14**, followed by the final spontaneous *anti*-selective

Scheme 8. Uneven ^{13}C Isotopic Incorporation Resulting from Reverse Prenylation

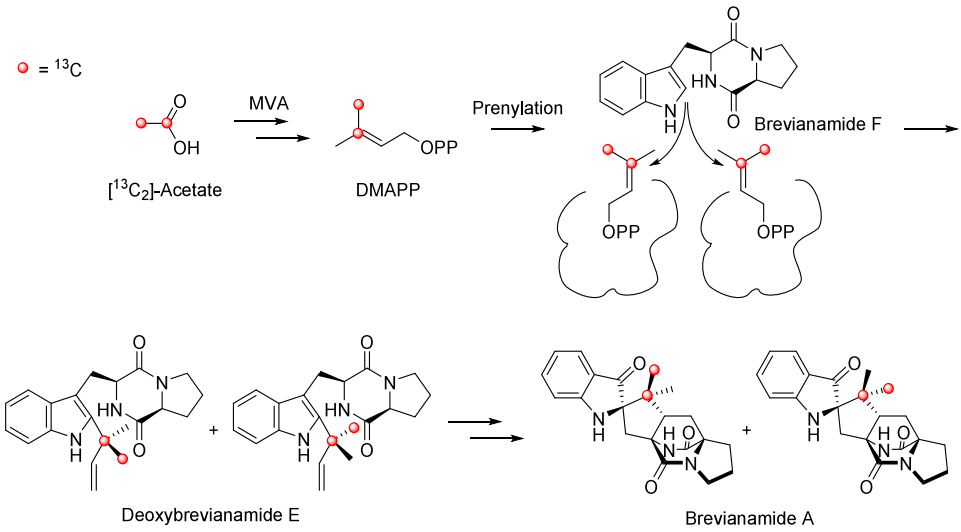

https://doi.org/10.1021/acs.chemrev.4c00250
Chem. Rev. XXXX, XXX, XXX−XXX

Scheme 9. Biosynthetic Routes for Brevianamides A, B, X and Y Proposed by Godfrey *et al.*[26a]

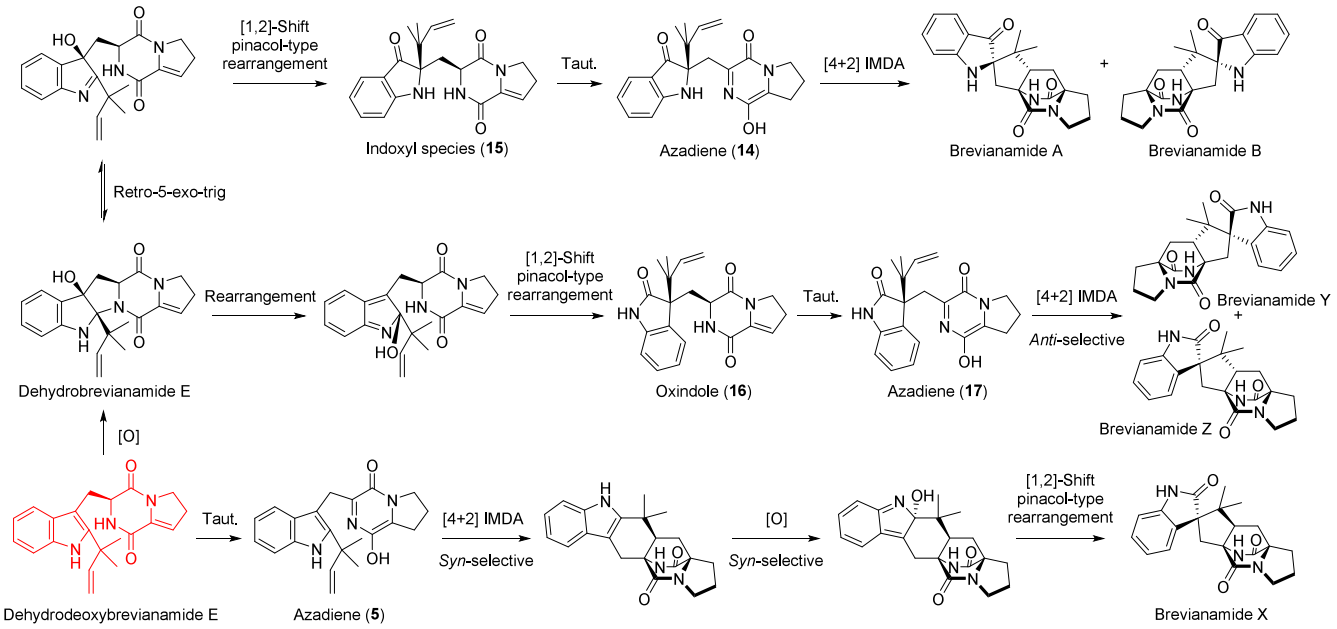

[a]The putative key intermediate is highlighted in red.

IMDA cycloaddition to generate brevianamides A and B in a 93:7 diastereomeric ratio, which is closely consistent with their ratio (∼10:1) in *P. brevicompactum* fermentation.[30] Thus, it was speculated that the IMDA reactions to generate brevianamides in natural producers might also be a spontaneous process without participation of a long-proposed DAase.

Furthermore, the successful chemical synthesis of brevianamides A and B led to an extension of the biosynthetic speculation to account for the formation of other known BCDO-containing brevianamide derivatives, namely, brevianamides X and Y.[31] It is worth mentioning that the Sun and Rateb groups independently designated two different natural products as brevianamide X,[32,33] which are not discussed in this review, as they do not belong structurally to BCDO brevianamides. Putative biosynthetic pathways following the hypothetical intermediate dehydrodeoxybrevianamide E to brevianamides X and Y were proposed accordingly (Scheme 9). Briefly, dehydrobrevianamide E could undergo an alternative pinacol-type rearrangement, via a transient epoxide intermediate, to give a thermodynamically more favorable oxindole species **16**. Subsequent tautomerization of the oxindole gave an enantiopure azadiene intermediate **17**, which would undergo similar IMDA cycloaddition to generate brevianamide Y. Moreover, a minor diastereomer named (+)-brevianamide Z was formed along with (+)-brevianamide Y in the chemical synthesis.[31] The diastereomeric relationship between brevianamides Y and Z is similar to that between brevianamide A and B, as they share a common spiro-stereogenic center and have enantiomeric bicyclo[2.2.2]diazaoctane cores. This suggests that (+)-brevianamide Z might be a potential natural product worth further investigation. It is worth mentioning that in 2022, Liu and co-workers isolated a natural product and also named it brevianamide Z.[34] This compound, however, is distinct from the one discussed in this review. For brevianamide X with a *syn*-configured BCDO core, the proposed pathway was different from that of brevianamide Y in that the BCDO core was considered to be formed through an early IMDA cycloaddition via a key intermediate azadiene followed by oxidation and pinacol rearrangement to generate brevianamide X.

3.1.2. Notoamides and Stephacidins. The BCDO-containing DKPs notoamides (i.e., notoamides A−D) were first isolated by the Tsukamoto group in 2007 from a marine-derived fungus *A. protuberus* that was isolated from the mussel *Mytilus edulis* collected off Noto Peninsula in the Sea of Japan.[35] The key structural difference between the notoamides and the brevianamides is the substitution of a dimethylpyranyl ring on the indole moiety of former structures (Figure 1). Since the original discovery, a fast-growing number of the notoamide family members have been reported, including notoamides A to Z.[36−43] The first isolation of stephacidins A and B, which were believed to be biosynthetically related to notoamide A, from the solid fermentation of *Aspergillus ochraceus* WC76466 was reported by Gao et al. in 2002.[44] Since then, stephacidins A and B, together with 6-*epi*-stephacidin A, have been isolated from various *Aspergillus* spp.; for example, stephacidins A and B were found to be coproduced with notoamides A−D by *A. protuberus*.[35]

Based on the structural relationship between notoamides and stephacidins[35] and biomimetic total syntheses,[45−48] their biogeneses were proposed (Scheme 10A). In the putative biosynthetic pathway, notoamide E is derived from deoxybrevianamide E upon installation of a dimethylpyran ring through sequential hydroxylation, prenylation and oxidative cyclization. Epoxidation of the indole C2═C3 bond of notoamide E with following pinacol-rearrangement or C−N ring closure gives notoamide C and D, respectively. Oxidative C−N desaturation of notoamide E generates the key azadiene intermediate **18**, followed by [4+2] IMDA reaction giving rise to stephacidin A containing the BCDO core. Subsequent epoxidation and pinacol-rearrangement lead to notoamide B, which further undergoes *N*-hydroxylation to produce the final product notoamide A.

https://doi.org/10.1021/acs.chemrev.4c00250
Chem. Rev. XXXX, XXX, XXX−XXX

Scheme 10. Variant Biosynthetic Proposals for Stephacidins and Notoamides. (A) Initial Proposal for Biogenesis of Stephacidin A and Notoamides A and B. (B) Proposed Biogenesis of Enantiomers of Notoamides and Stephacidins. (C) Alternative Biogenesis of the Enantiomeric Pair of Notoamides. (D) The Proposed Biosynthetic Pathway of Notoamides by Sherman and Co-workers. (E) The Proposed Stereochemically Parallel Pathways from Notoamide S in *A. protuberus* and *A. amoenus*

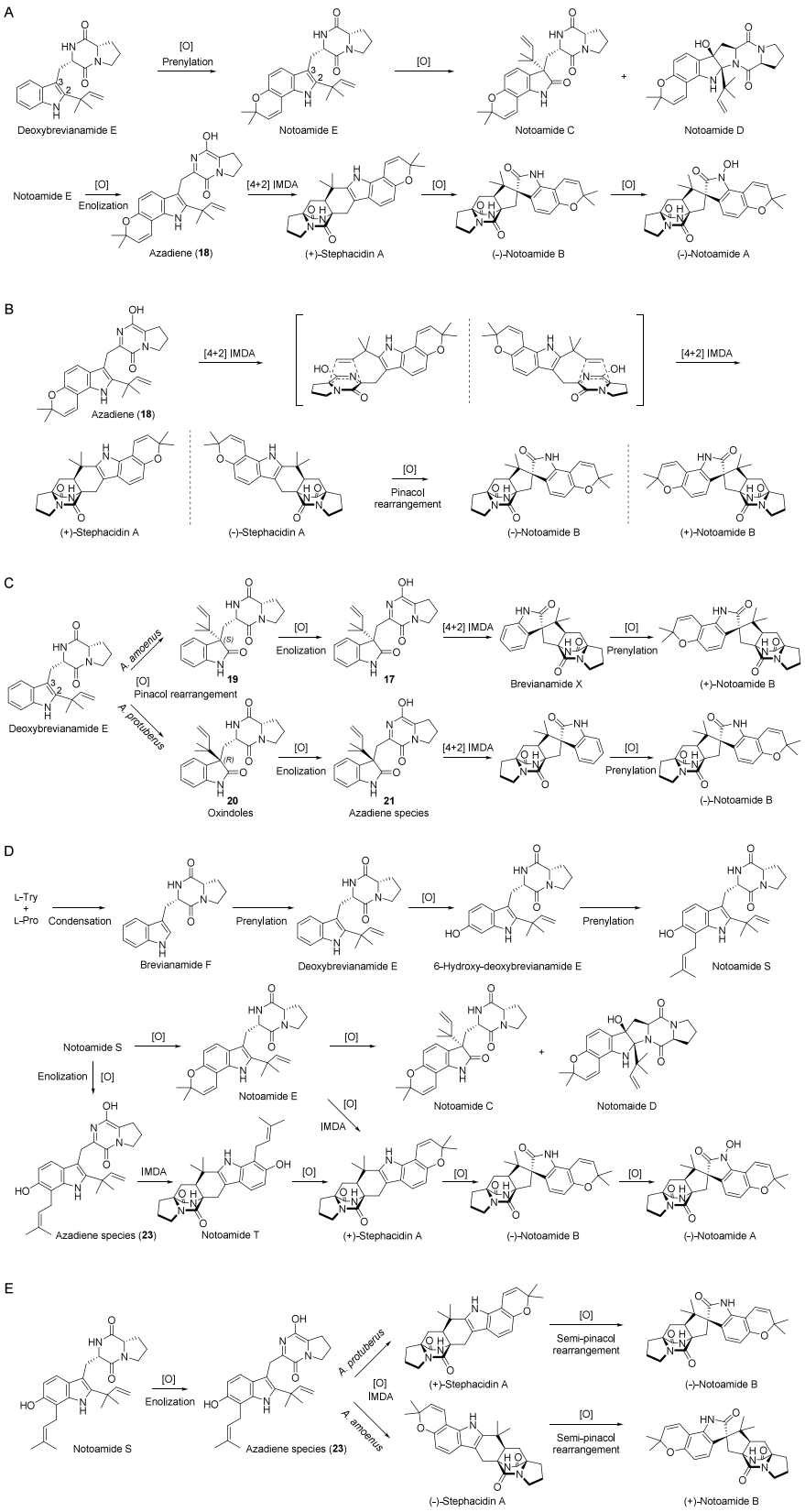

https://doi.org/10.1021/acs.chemrev.4c00250
Chem. Rev. XXXX, XXX, XXX−XXX

Scheme 11. A Putative Biosynthetic Route to the BCDO Core

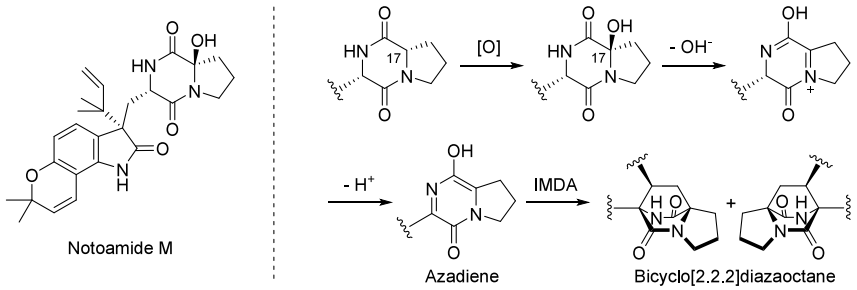

Intriguingly, multiple enantiomers of notoamides and stephacidins can be produced by different *Aspergillus* strains. For example, (−)-stephacidin A and (+)-notoamide B isolated from the terrestrial-derived fungus *A. amoenus* are the corresponding enantiomers of (+)-stephacidin A and (−)-notoamide B produced by the marine-derived fungus *A. protuberus*.[37] These enantiomeric compounds raised an enigmatic question on how these enantiomers containing multiple stereogenic centers are biosynthesized. This enigma led researchers to suspect that these distinct enantiomers might be assembled either via stereochemically parallel pathways or by stereoselective enzymes in different fungal species[37] (Scheme 10B).

Notoamide M was isolated in 2009, and it contains a hydroxy group at C-17[38] and thus is proposed to be a potential precursor to the azadiene species for the putative [4+2] IMDA cyclization (Scheme 11). Oxidation at C-17 of the DKP ring followed by dehydration seemed to occur prior to the formation of the azadiene species. This finding provided an indirect support to a potential mechanism for the IMDA-based construction of the BCDO core in notoamides.

An alternative biosynthetic pathway that explains the biogenesis of the two antipodes of notoamide B in different producing fungi was also proposed[38] (Scheme 10C). An *R*-selective indole oxidase in the marine-derived *A. protuberus* and an *S*-selective enzyme in terrestrial *A. amoenus* might catalyze the stereo-opposite epoxidation of deoxybrevianamide E, followed by pinacol rearrangement of the isoprenyl group from C-2 to C-3, thereby affording the distinct oxindole species **19** and **20**, the corresponding 3-*epi* diastereomers. Further oxidation and tautomerization of the oxindole species would generate the azadiene intermediates **17** and **21**, which undergo [4+2] IMDA to form the BCDO core. Subsequently, oxidation and prenylation reactions construct the pyran ring to yield (+)- or (−)-notoamide B. In the postulated biosynthetic pathway, the enantio-divergence comes from the consequence of incipient *R*- or *S*-selective epoxidation of indole instead of the enantioselective IMDA cyclization.

To test this hypothesis, $[^{13}C]_2$-$[^{15}N]$-deoxybrevianamide E was chemically synthesized for the precursor feeding experiments of *A. protuberus*[49] (Scheme 12A). Purification of the fungal metabolites afforded a mixture of the $[^{13}C]_2$-$[^{15}N]$-labeled compounds, whose structures were first elucidated to be the proposed oxindoles but later corrected to be brevinamide E and its epimer **22**.[50] However, no labeled bridged BCDO-containing alkaloids such as notoamide B were isolated. To further explore the downstream metabolites, the synthetic $[^{13}C]_2$-$[^{15}N]$-brevinamide E and the corresponding epimer were fed individually to the same strain. The results showed that no labeled downstream product was detected, indicating that these two compounds were shunt metabolites in the biosynthesis of notoamides.

According to the initially proposed notoamide biosynthetic pathway, notoamide E was postulated to be a key biosynthetic intermediate. To confirm the existence of notoamide E, the Tsukamoto group sought to detect and isolate this compound from *A. protuberus* fermentation cultures.[39] It was revealed that notoamide E existed only in the 5-day culture and then disappeared, which confirmed that this intermediate was indeed produced in the early phase of growth and rapidly converted into other downstream metabolites.

Subsequently, $[^{13}C]_2$-notoamide E was chemically synthesized by following the reported approach with the ^{13}C-labeled starting marterials.[51,52] The isotope incorporation experiment in *A. protuberus*[39] (Scheme 12B) showed that the ^{13}C isotopes from synthetic $[^{13}C]_2$-notoamide E were incorporated into notoamides C and D, along with 3-*epi*-notoamide C and three new minor alkaloids, notoamides E2−E4. Surprisingly, the BCDO-containing alkaloids, the ^{13}C-labeled notoamides A and B as well as stephacidin A, were not isolated from the feeding experiment. Of note, the yield of 3-*epi*-notoamide C, which was not isolated from the culture under unlabeled conditions in a normal medium, was higher than that of notoamide C. Feeding experiments in *A. amoenus*[53] showed similar results but only produced a trace amount of 3-*epi*-notoamide C. The authors reasoned that the presence of excess notoamide E in the feeding experiment might have changed the expression levels of some downstream enzymes, thereby altering the metabolite profile. These results also allowed the researchers to speculate that the timing of BCDO ring assembly precedes that of the pyran moiety.

After identification of notoamide gene clusters (Figure 7B) in *A. protuberus*[54] and *A. amoenus*,[5] as well as characterization and prediction of related enzyme functions, Sherman and coworkers proposed a plausible notoamide biosynthetic pathway[54] (Scheme 10D), in which notoamide S without the BCDO and pyran moieties was proposed as a key intermediate, potentially leading to the achiral azadiene **23**.[5] To explore the intermediacy of notoamide S to the distinct natural notoamide enantiomers produced by different fungi, the Williams group accomplished the total synthesis of notoamide S.[55]

Considering the observation that distinct enantiomers of stephacidin A and notoamide B were isolated from the marine-derived *A. protuberus*[54] and terrestrial-derived *A. amoenus*,[37] a stereochemically parallel pathway downstream of the precursor notoamide S was proposed[56] (Scheme 10E). The [4+2] IMDA cycloaddition and following oxidative ring closure would produce the (+)- and (−)-enantiomers of stephacidin A in the respective producing microorganisms. Opposite face-selective epoxidations followed by semipinacol rearrangement of the

https://doi.org/10.1021/acs.chemrev.4c00250
Chem. Rev. XXXX, XXX, XXX−XXX

Scheme 12. Isotopic Feeding Experiments for the Explorations of Notoamides Biosynthesis. (A) The Isotopic Incorporation of $[^{13}C]_2$-$[^{15}N]$-Deoxybrevianamide E. (B) The Isotopic Incorporation of $[^{13}C]_2$-Notoamide E. (C) The Feeding Experiment Results of Isotopically Labeled Stephacidin A. (D) The Isotopic Incorporation of $[^{13}C]_2$-$[^{15}N]$-6-Hydroxydeoxybrevianamide E. (E) The Isotopic Incorporation of $[^{13}C]_2$-$[^{15}N]_2$-Notoamide S. (F) The Isotopic Feeding Experiment of $[^{13}C]_2$-Notoamide T in *A. amoenus*. (G) The Isotopic Incorporation of $[^{13}C]_2$-Notoamide T in *A. protuberus*

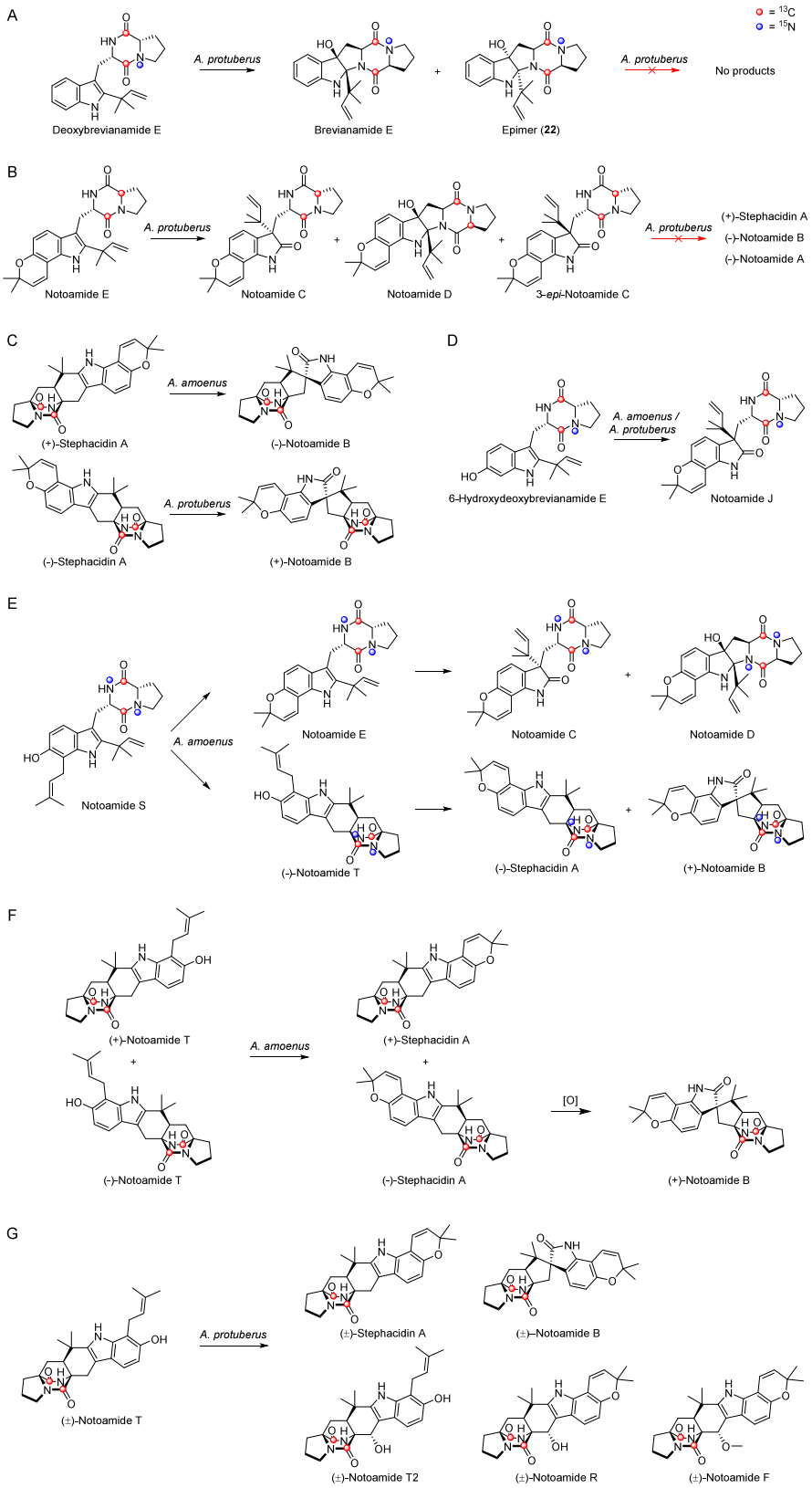

https://doi.org/10.1021/acs.chemrev.4c00250
Chem. Rev. XXXX, XXX, XXX−XXX

Scheme 13. Proposed Biosynthetic Origins of Stephacidins in *A. protuberus* (A) and *A. amoenus* (B)

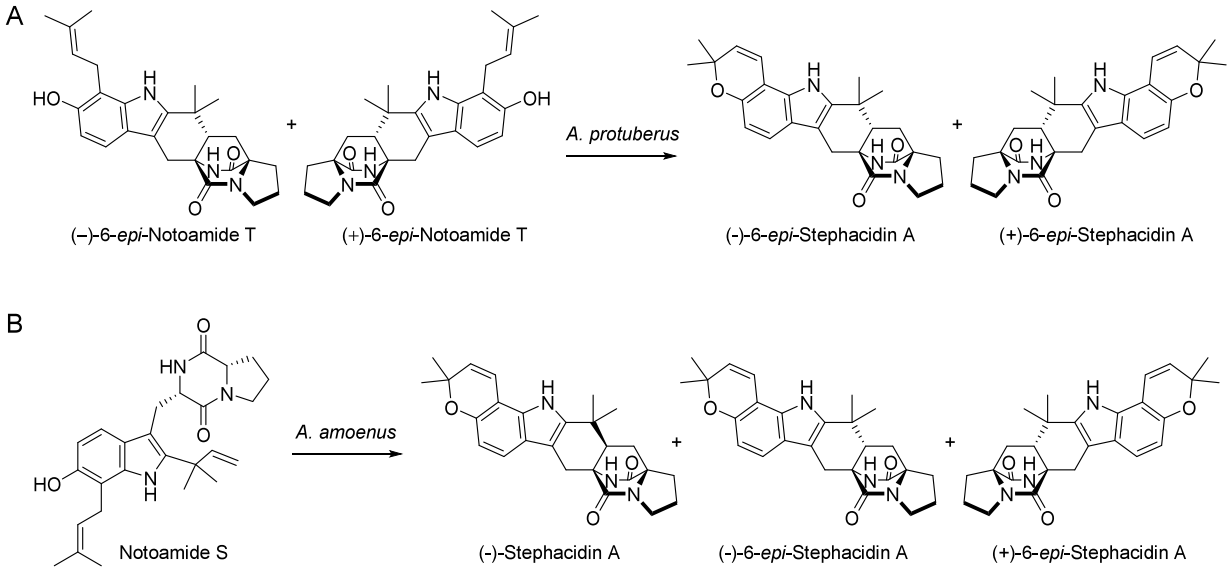

2,3-disubstituted indole would then yield the corresponding spiro-oxindoles, (−)- and (+)-notoamide B, respectively.

Stephacidin A was proposed as a key biosynthetic intermediate with a BCDO core in notoamide biosynthesis. Following an established biomimetic strategy,[45−47] the doubly ^{13}C-labeled racemic stephacidin A was synthesized and fed to *A. amoenus* and *A. protuberus*,[56] respectively. Product analysis revealed the enantiospecific incorporation of intact (+)-stephacidin A into (−)-notoamide B in *A. amoenus* and (−)-stephacidin A into (+)-notoamide B in *A. protuberus* (Scheme 12C). These results provided strong experimental evidence for the hypothesis that complementary face-selective oxidative enzymes (presumed to be flavoenzymes) likely exist in the two different *Aspergillus* strains.

As the immediate precursor of notoamide S, [^{13}C]$_2$-[^{15}N]-6-hydroxydeoxybrevianamide E, was also chemically synthesized according to the established synthetic route with isotopically labeled substrates.[57] Unexpectedly, its feeding studies with the terrestrial-derived *A. amoenus*[58] and marine-derived *A. protuberus*[49] showed that only the isotopically labeled notoamide J could be isolated (Scheme 12D).

Notoamide S was proposed to be the substrate for oxidative desaturation, which yields the key azadiene intermediate for the subsequent hypothetical [4+2] IMDA cyclization.[54,59] This compound was also considered a pivotal branching point in the notoamide biosynthetic pathway. To address this hypothesis, [^{13}C]$_2$-[^{15}N]$_2$-notoamide S was chemically synthesized using the strategy previously established by the Williams group.[58] Feeding the labeled notoamide S to the culture of *A. amoenus* showed that (−)-stephacidin A and (+)-notoamide B, as well as notoamide C and D, incorporated significant amounts of isotopes[60] (Scheme 12E). These results, together with the fact that notoamide S was identified as a minor metabolite of *A. amoenus*,[61] strongly supported that the construction of the BCDO ring system should occur prior to the formation of the pyran ring.

Notoamide T differs from stephacidin A in that its pyran ring remains unclosed. It was hypothesized to be derived from notoamide S through putative oxidation followed by a [4+2] IMDA reaction and was considered the direct precursor to stephacidin A.[54] In an effort to verify the biogenesis of stephacidin A and notoamide B, the total synthesis of notoamide T was achieved by Williams and co-workers.[62] Furthermore, racemic D,L-[^{13}C]$_2$-notoamide T was synthesized for the following precursor incorporation studies[62] (Scheme 12F). Complete consumption of racemic D,L-[^{13}C]$_2$-notoamide T was observed for *A. amoenus*, indicating that the construction of the pyran ring might be mediated by a promiscuous oxidase to accept both enantiomers of notoamide T. The isotopically labeled (+)-stephacidin A and (+)-notoamide B were subsequently isolated. (+)-Notoamide B was likely derived from the unisolated intermediate (−)-stephacidin A. Since (+)-stephacidin A is not an endogenous natural metabolite produced by *A. amoenus*, it was not incorporated into the biosynthetic pathway, thus being isolated from the feeding experiments, which supported the proposed enantiospecific pathway (Scheme 10E) in *A. amoenus*.

In the precursor incorporation study in *A. protuberus*, racemic [^{13}C]$_2$-notoamide T was also consumed and transformed into D,L-[^{13}C]$_2$-stephacidin A, D,L-[^{13}C]$_2$-notoamide B, D,L-[^{13}C]$_2$-notoamide F, D,L-[^{13}C]$_2$-notoamide R, and D,L-[^{13}C]$_2$-notoamide T2[62] (Scheme 12G). Further investigations revealed that, different from the selective D,L-[^{13}C]$_2$-notoamide T incorporation results in *A. amoenus* (Scheme 12F), all the isolated metabolites were racemic mixtures, suggesting that orthologous enzymes in *A. protuberus* might respectively recognize the two enantiomers of notoamide T and stephacidin A in the biosynthetic process to notoamide B. These results also implied that the feeding of racemic notoamide T might have activated the expression of some dormant tailoring enzymes to alter the metabolite profile of producing organism.

Moreover, one could speculate that 6-*epi*-stephacidin A should be derived from 6-*epi*-notoamide T. To verify this hypothesis, the Tsukamoto and Williams groups sought to detect 6-*epi*-stephacidin A in the culture of *A. protuberus* with the feeding of 6-*epi*-notoamide T.[63] Considering 6-*epi*-stephacidin A might be a short-lived precursor, time course studies of the metabolite profiles of *A. protuberus* were conducted. The results clearly indicated that 6-*epi*-stephacidin A was produced by the fungus in the early phase of growth and then rapidly converted to other downstream metabolites.

https://doi.org/10.1021/acs.chemrev.4c00250
Chem. Rev. XXXX, XXX, XXX−XXX

Scheme 14. Proposed Biogenesis of Versicolamide B

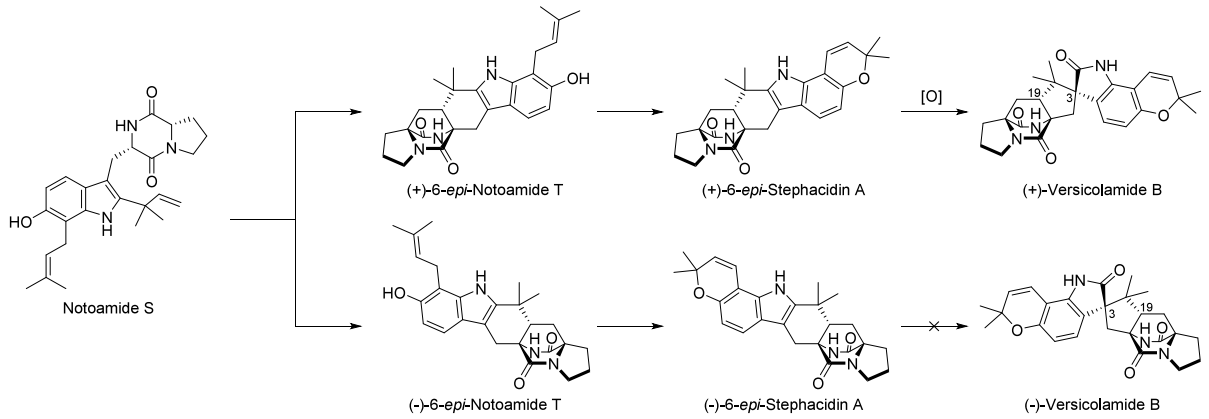

Scheme 15. Precursor Feeding Experiments Using the Isotopically Labeled Notoamide S (A) and 6-*epi*-Notoamide T (B)

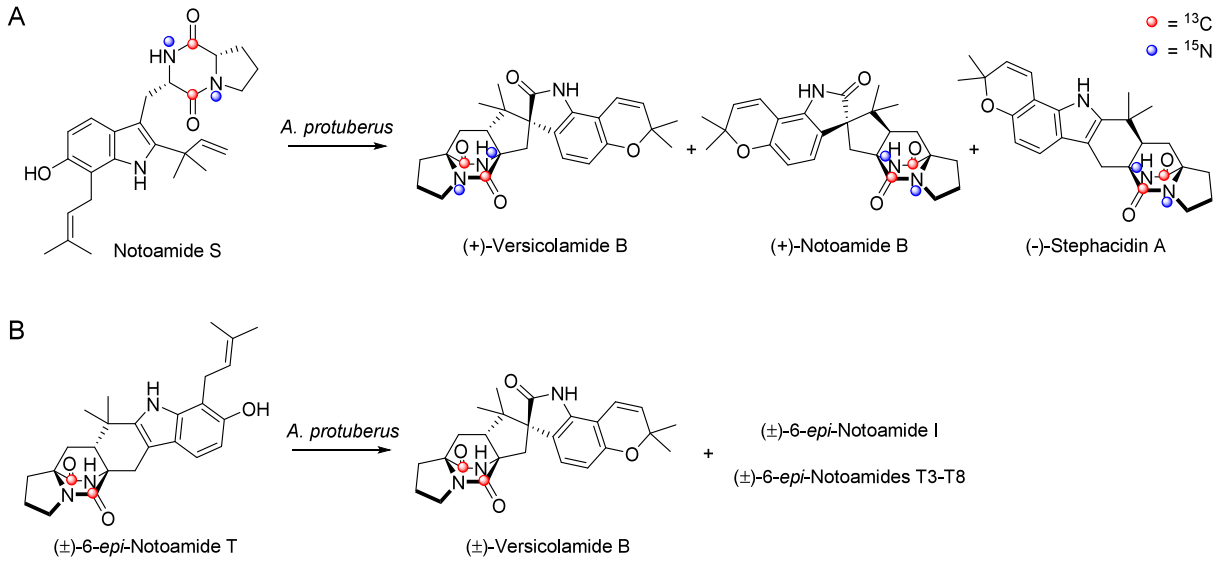

However, the precursor incorporation experiments using synthetic $[^{13}C]_2$-(±)-6-*epi*-notoamide T did not result in the detectable level of ^{13}C-labeled 6-*epi*-stephacidin A. Interestingly, the feeding of nonlabeled (±)-6-*epi*-notoamide T on minimal medium agar plates led to the accumulation of racemic 6-*epi*-stephacidin A (Scheme 13A). However, the possibility that the racemic 6-*epi*-stephacidin A was generated from an endogenous biosynthetic pathway of *A. protuberus* could not be excluded.

Besides the major metabolite (−)-stephacidin A, Tsukamoto and co-workers also isolated 6-*epi*-stephacidin A from *A. amoenus*.[61] Careful analysis by chiral HPLC showed that the isolated 6-*epi*-stephacidin A was actually an enantiomeric mixture enriched with the (−)-isomer. Meanwhile, notoamide S was also identified from the fermentation extract of *A. amoenus*. These results indicated that notoamide S was indeed a natural metabolite and could be converted into (−)-stephacidin A, (+)- and (−)-6-*epi*-stephacidin A (Scheme 13B).

3.1.3. Versicolamides. As the representative structure of versicolamide family members, versicolamide B was first isolated from the fungus *A. amoenus*.[37] The absolute configuration was determined to be an (+)-enantiomer. Versicolamide B and notoamide B have the same polycyclic structure with differences in the two stereogenic centers of C3 and C19. Considering that oxidation of the 2,3-indole moiety of (−)-stephacidin A to the corresponding spiro-oxindole generates (+)-notoamide B, it was proposed that similar face-selective oxidation of the presumed precursor 6-*epi*-stephacidin A would produce (+)-versicolamide B (Scheme 14). Consistent with this proposal, 6-*epi*-stephacidin A was later found to be an actual natural metabolite of *A. amoenus*.[61]

When the ^{13}C (C12 and C18) and ^{15}N (N13 and N19) quadruply labeled notoamide S was synthesized and fed to the cultures of *A. amoenus*[60] (Scheme 15A), (−)-versicolamide B, together with (+)-notoamide B and (−)-stephacidin A, were found to contain significantly incorporated ^{13}C and ^{15}N isotopes, indicating that notoamide S should be a common precursor for these metabolites.

The initially isolated versicolamide B from *A. protuberus* was assigned as a (−)-enantiomer.[38] Through careful reanalysis of the natural metabolite, it was revealed that the absolute configuration should be revised to the (+)-form.[63] Thus, both the marine-derived fungus *A. protuberus* and terrestrial-derived *A. amoenus* produce the same (+)-versicolamide B. Considering this fact and the previous report about the bioconversion of notoamide T into (+)-stephacidin A and (−)-notoamide B,[62] the Tsukamoto and Williams groups proposed that versicolamide B might be biosynthesized from 6-*epi*-notoamide T via 6-

https://doi.org/10.1021/acs.chemrev.4c00250
Chem. Rev. XXXX, XXX, XXX−XXX

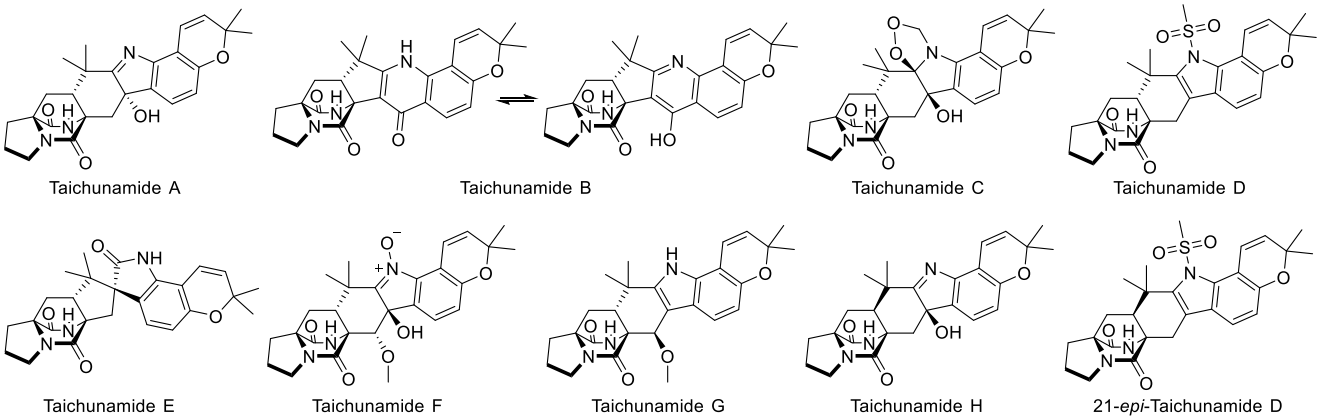

Figure 4. Structures of taichunamides.

Scheme 16. Proposed Biogenesis of Taichunamides

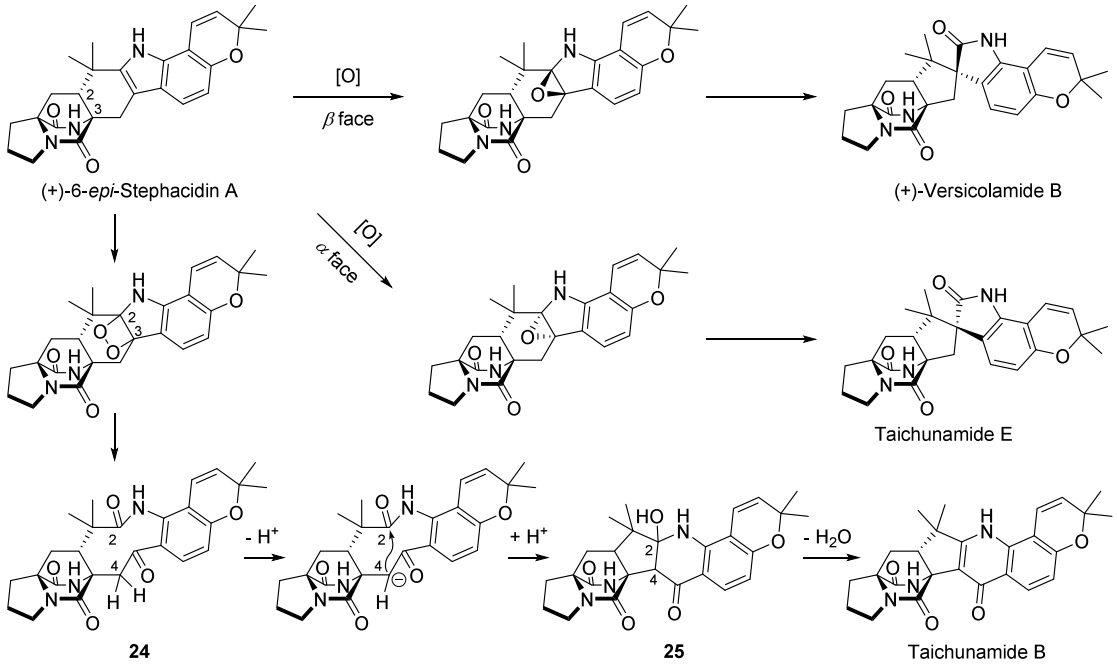

epi-stephacidin A[63] (Scheme 14). To test this hypothesis, the precursor feeding experiment of *A. protuberus* using synthetic $[^{13}C]_2$-(±)-6-*epi*-notoamide T was conducted (Scheme 15B). Interestingly, this precursor was converted to a racemic mixture of (±)-versicolamide B and seven new metabolites including (±)-6-*epi*-notoamides T3−T8 and (±)-6-*epi*-notoamide I (see Table 1 for structures).

To date, only (+)-versicolamide B has been isolated,[37,38,61,63−65] while (−)-versicolamide B has not been detected yet as a natural metabolite of any fungal species. From a biosynthetic point of view, the precursor of (+)-versicolamide B should be (+)-6-*epi*-stephacidin A, which could be isolated from the culture of *A. protuberus*. Interestingly, the isolated 6-*epi*-stephacidin A from *A. amoenus* was determined to be an enantiomeric mixture enriched with the (−)-isomer.[61] Based on these results, Tsukamoto and co-workers proposed that notoamide S could be converted into both (+)- and (−)-6-*epi*-stephacidin A by *A. amoenus* through (+)- and (−)-6-*epi*-notoamide T, respectively, but only (+)-6-*epi*-stephacidin A could be further transformed into (+)-versicolamide B (Scheme 14). The presence of (+)-versicolamide B suggested that this fungus might only contain the indole oxidase that is able to recognize (+)-6-*epi*-stephacidin A rather than (−)-6-*epi*-stephacidin A. Consequently, (−)-6-*epi*-stephacidin A became an end product without being converted to (−)-versicolamide B.

3.1.4. Taichunamides. Taichunamides A−G were isolated from the fungus *Aspergillus taichungensis* IBT 19404[65] (Figure 4 and Table 1). After comparative structural analysis of these new indole alkaloids from the corresponding structures discovered from the fungus *A. versicolor* HDN11-84 by Li and co-workers, the structure of taichunamide A was revised to a 3-hydroxyindolenine.[66] Taichunamide B was determined to exist as an equilibrium mixture of keto−enol tautomers, one of which contains a rare 4-pyridone ring. Taichunamide C features a unique endoperoxide bridge structure, while taichunamide D has a methylsulfonyl unit, which is the first reported isolation of a 1-methylsulfonylindole alkaloid from natural sources. Zhang and co-workers isolated another new component 21-*epi*-taichunamide D from cultures of the endophytic *A. versicolor* F210.[67]

https://doi.org/10.1021/acs.chemrev.4c00250
Chem. Rev. XXXX, XXX, XXX−XXX

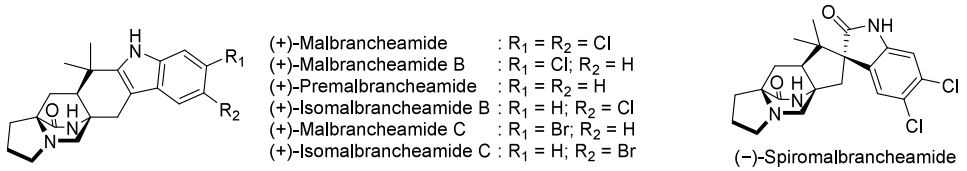

Figure 5. Structures of malbrancheamides.

Scheme 17. Initially Proposed Biosynthetic Pathway of Malbrancheamides

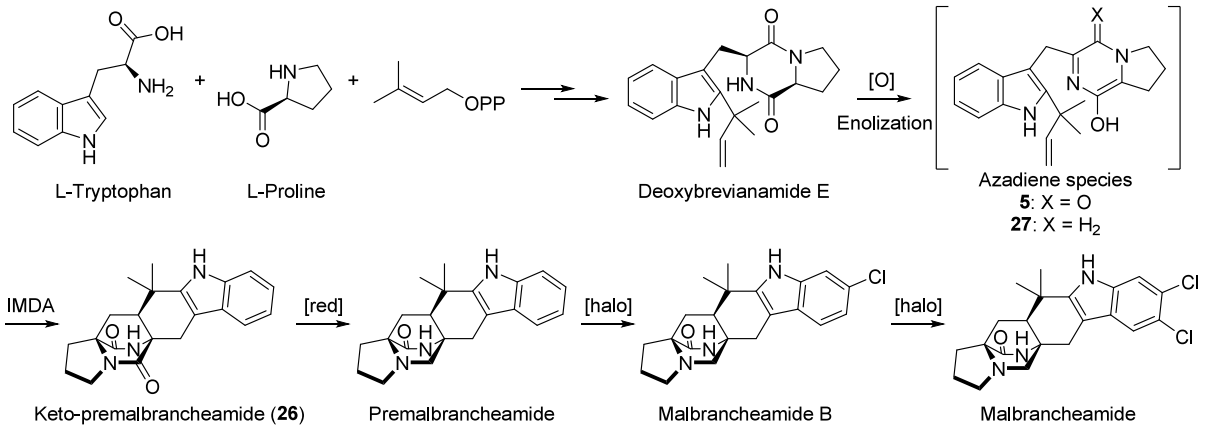

Biosynthetically,[65] (+)-6-*epi*-stephacidin A was proposed to be the key intermediate for taichunamides (Scheme 16), which is also the putative precursor for versicolamides. Specifically, β-face epoxidation followed by pinacol rearrangement would afford versicolamides B and C, while taichunamide E presumably arises from α-face epoxidation followed by pinacol rearrangement. The unique 4-pyridone unit in taichunamide B could be derived from (+)-6-*epi*-stephacidin A. The oxidative C−C bond cleavage at the indole 2,3-position would give product **24**. Afterward, cyclization between C2 and C4 generates intermediate **25**, which then undergoes dehydration to form a double bond, resulting in taichunamide B.

3.2. Monoketopiperazines

Structurally, the BCDO core structure of MKPs is different from that of DKPs in terms of the number of BCDO-tethered keto group(s) (Figure 2). This difference originates from distinct biosynthesis of the initial cyclic dipeptide precursors. Similar to the exploration of DKPs biogenesis, the early understandings of MKPs biosynthesis also relied on precursor feeding experiments and related chemical principles. In this section, we will discuss the studies on biogenesis of some representative MKP compounds.

3.2.1. Malbrancheamides. (+)-Malbrancheamide and (+)-malbrancheamide B were isolated from the cultures of the fungus *Malbranchea aurantiaca* RRC1813.[68,69] These two metabolites are the first members of the BCDO-containing alkaloids with a halogenated indole moiety (Figure 5). Later, the Williams group reported the isolation of the non-halogenated premalbrancheamide from the cultures of *M. aurantiaca*. Crews et al. also isolated two new chlorinated derivatives (−)-spiromalbramide and (+)-isomalbrancheamide B from another fungal strain *Malbranchea graminicola*, and two brominated analogues (+)-malbrancheamide C and (+)-isomalbrancheamide C in the cultures with added bromine salts.[70]

Based on the structures of isolated natural malbrancheamides, a putative biosynthetic pathway was proposed (Scheme 17).[71] Deoxybrevianamide E was again proposed to be an early precursor, oxidation of which could lead to the intermediate azadiene **5**. This azadiene would undergo an [4+2] IMDA reaction to give the cycloadduct keto-premalbrancheamide **26**, which is then reduced to premalbrancheamide. After sequential chlorinations, the monochlorinated malbrancheamide B and dichlorinated malbrancheamide are formed.

To test this biosynthetic hypothesis, the doubly ^{13}C-labeled premalbrancheamide and keto-premalbrancheamide **26** were synthesized using the method developed for the synthesis of stephacidin A.[37,47,71] In the precursor feeding experiment of *M. aurantiaca*,[71] the labeled premalbrancheamide was incorporated into malbrancheamide B, but not malbrancheamide (Scheme 18A). It was presumed that the kinetics of the second chlorination reaction might be much slower than those of the first one. By contrast, the feeding of doubly ^{13}C-labeled keto-premalbrancheamide **26** to *M. aurantiaca* labeled neither malbrancheamide nor malbrancheamide B (Scheme 18B).

Scheme 18. Isotopic Incorporation with ^{13}C-Labeled Premalbrancheamide (A) and Keto-premalbrancheamide (B)

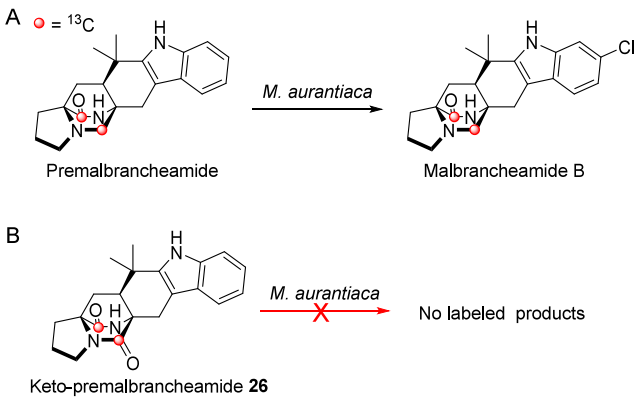

https://doi.org/10.1021/acs.chemrev.4c00250
Chem. Rev. XXXX, XXX, XXX−XXX

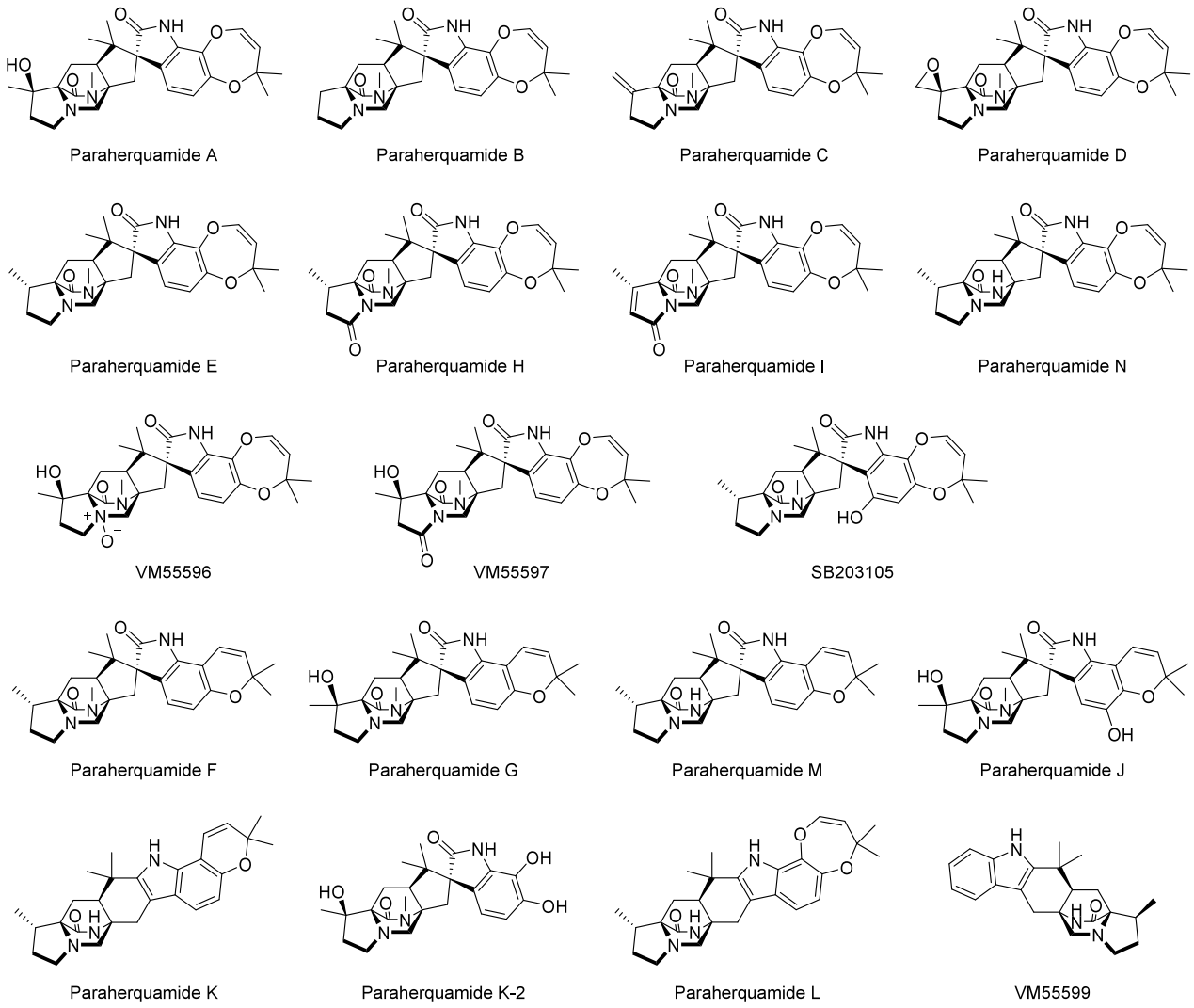

Figure 6. Structures of paraherquamide derivatives.

These results strongly suggested that the reduction of the tryptophan-derived amide carbonyl residue might precede the formation of the BCDO core. More importantly, these findings indicated an alternative pathway that the putative [4+2] IMDA reaction for malbrancheamides likely involves a key MKP azadiene intermediate **27** (Scheme 17), which could be the direct precursor of premalbrancheamide.

To validate the sequence of malbrancheamide biosynthesis, Williams and co-workers chemically synthesized premalbrancheamide through a biomimetic approach, however giving rise to both (+)- and (−)-enantiomers.[3] By contrast, the optically pure (+)-premalbrancheamide is formed by *Malbranchea* spp., suggesting that an enzyme-directed cyclization process might occur in the producing strains.

3.2.2. Paraherquamides. The first member of the paraherquamide family, paraherquamide A, which contains an unusual amino acid, *β*-methyl-*β*-hydroxyproline, was isolated in 1981 from the cultures of *Penicillium paraherquei* by Yamazaki and co-workers (Figure 6).[72] From then on, more family members, such as paraherquamides B−M, were isolated from various *Penicillium* spp. and *Aspergillus* spp.[73−82] Of note, many related natural products, such as VM55595, VM55596, VM55597, VM55599, SB203105, and SB200437, were also isolated from *Penicillium* sp. IMI332995[73,74] and *Aspergillus* sp. IMI337664.[82] Due to their structural complexity, intriguing biogenesis, and potent antiparasitic activity, paraherquamides have attracted great attention from both academia and industry.

In 1996, Williams and co-workers conducted feeding experiments on *Penicillium fellutanum* ATCC 20841 using [1-^{13}C]-L-tryptophan, [methyl-^{13}C]-L-methionine, and [1-^{13}C]-L-isoleucine to determine the primary metabolic building blocks for the MKP BCDO ring system of paraherquamide A (Scheme 19A).[83] ^{13}C NMR analysis of products showed that the three amino acids were indeed the building blocks of paraherquamide A. Interestingly, [methyl-^{13}C]-methionine was incorporated into the *N*-methyl position of the MKP ring, but not in the *β*-methylproline ring. Subsequent feeding of [1-^{13}C]-L-isoleucine, followed by isolation and ^{13}C NMR analysis of paraherquamide A, revealed efficient isotope incorporation into the MKP ring system. This finding clearly indicated that the methyl group of the unusual nonproteinogenic amino acid *β*-methylproline should originate from L-isoleucine.

To investigate the downstream pathway from *β*-methylproline to paraherquamide A, L-[1-^{13}C]-*β*-methylproline was chemically synthesized by means of a Hoffman−Loeffler−Freytag reaction sequence from [1-^{13}C]-L-isoleucine (Scheme 20).[84] The feeding experiment in growing cultures of *P.*

https://doi.org/10.1021/acs.chemrev.4c00250
Chem. Rev. XXXX, XXX, XXX−XXX

Scheme 19. Isotopic Feeding Experiments for Exploring Paraherquamides Biogenesis by *P. fellutanum*. (A) The Isotopic Incorporations of Three ^{13}C-Labeled Amino Acids. (B) The Isotopic Incorporations of Doubly ^{13}C-Labeled Building Blocks. (C) The Isotopic Incorporation of [$^{13}C_2$]-Acetate. (D) The Isotopic Incorporation of ^{13}C-Labeled L-Isoleucine and Two Possible Oxidation Mechanisms for β-Methylproline Biosynthesis. (E) The Isotopic Incorporation of ^{13}C-Labeled Preparaherquamide, VM55599, and Other Counterparts. (F) Isotopic Incorporation with ^{13}C-Labeled 7-Hydroxy-preparaherquamide

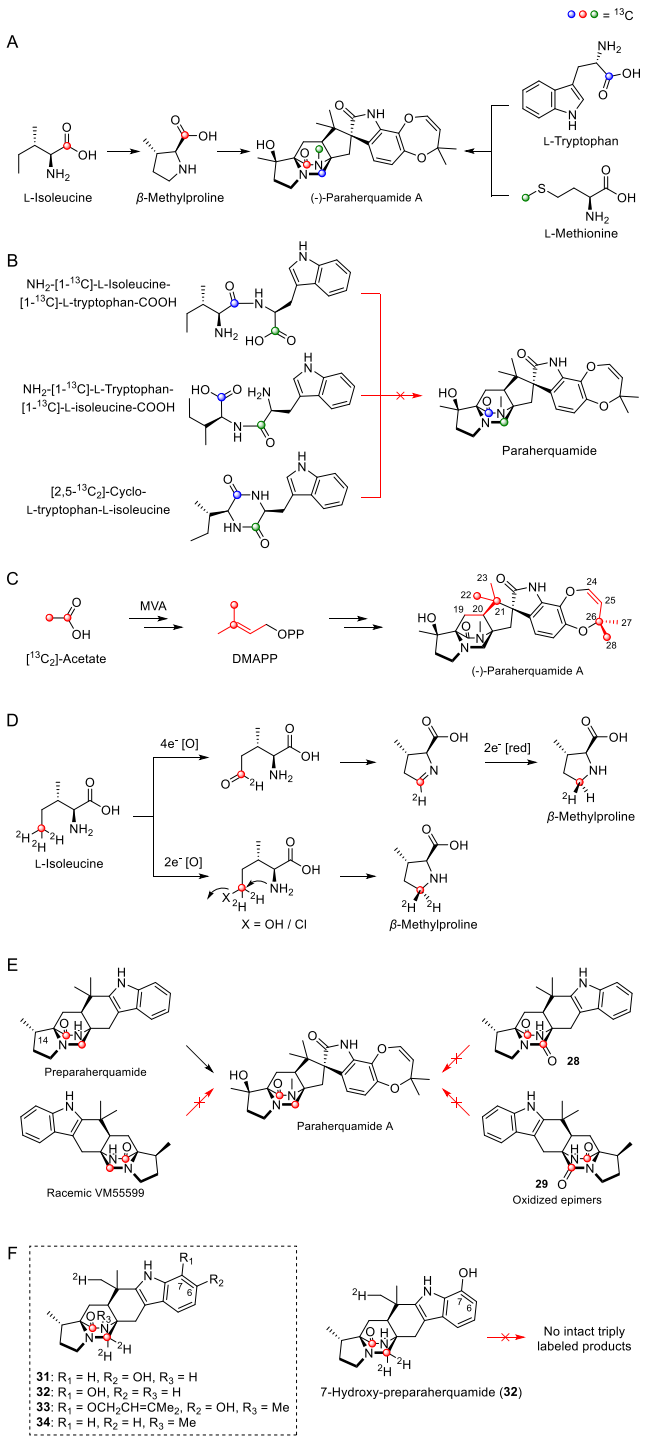

fellutanum with [1-^{13}C]-β-methylproline gave paraherquamide A with high isotope incorporation, indicating this amino acid is a direct biosynthetic precursor to paraherquamide A (Scheme 19A).

After determining the primary amino acid building blocks for paraherquamide A, the same group further explored the possible biosynthetic process of isoleucine/tryptophan conjugation.[83,84] The authors set out to determine at which point the formation of the β-methylproline group occurs. Specifically, doubly labeled NH_2-[1-^{13}C]-L-isoleucine-[1-^{13}C]-L-tryptophan-COOH, NH_2-[1-^{13}C]-L-tryptophan-[1-^{13}C]-L-isoleucine-COOH, and [2,5-$^{13}C_2$]-*cyclo*-L-tryptophan-L-isoleucine were synthesized and individually fed to *P. fellutanum* (Scheme 19B). However, NMR analysis of the isolated paraherquamide A did not provide compelling evidence for site-specific incorporation of both isotopic labels from these dipeptides. The mass spectra of the paraherquamide A isolated from these feeding experiments also did not show the expected isotopic patterns resulting from incorporation of the intact doubly labeled metabolites. The low levels of incorporation were considered to be likely due to hydrolysis of dipeptides and reincorporation of the singly labeled amino acids. Taken together, it was deduced that L-isoleucine should first be converted to β-methylproline and then undergo downstream biosynthetic steps to paraherquamide A.

To further explore how the oxidative cyclization of L-isoleucine to β-methylproline could occur, Stocking et al. proposed two putative pathways regarding 2 e$^-$ and 4 e$^-$ oxidation mechanisms (Scheme 19D).[85] Using chemically synthesized L-[5-^{13}C,5-$^2H_3$]-isoleucine, the feeding experiments with *P. fellutanum* were carried out. The isolation of monodeuterated β-methylproline instead of dideuterated β-methylproline indicated that the cyclization of L-isoleucine should undergo a 4 e$^-$ oxidation of the terminal methyl group, followed by a diastereoselective 2 e$^-$ reduction.

Paraherquamide A contains two isoprene units with one comprising the dioxepin ring and the other one incorporated in the BCDO ring system. In order to elucidate the origin of the two isoprene units, the feeding experiments were carried out for *P. fellutanum* with [$^{13}C_2$]-acetate and [$^{13}C_6$]-glucose.[25,86] It was confirmed that acetate is the precursor for both isoprene moieties, which should be constructed via the classical mevalonic acid pathway (Scheme 19C). The results of feeding experiments with [$^{13}C_2$]-acetate also demonstrated that the isoprene units in paraherquamide A were incorporated in a stereofacially distinct manner. The stereochemical integrity of DMAPP was maintained during the formation of the C−O bond in the dioxepin ring, whereas the stereochemical integrity of DMAPP for the BCDO core was broken at some biosynthetic stage. These observations suggested the putative reverse and normal prenyltransferases in paraherquamide A biosynthesis to exhibit distinct facial selectivities. The loss of the face-selective biosynthesis of the reverse isoprene unit was also observed in other BCDO alkaloids, such as brevianamide A.[25]

Reading and co-workers isolated the natural metabolite VM55599 from the paraherquamide-producing *Penicillium* strain IMI332995 and assigned the relative stereochemistry through extensive ^{1}H NMR NOE analysis.[73] This BCDO-containing species was originally postulated as a biosynthetic precursor for paraherquamide A (Scheme 19E) and other related indole alkaloids.[18] The isolation of VM55599 also suggested that construction of the BCDO ring probably

https://doi.org/10.1021/acs.chemrev.4c00250
Chem. Rev. XXXX, XXX, XXX−XXX

Scheme 20. Chemical Synthesis of L-[1-^{13}C]-β-Methylproline

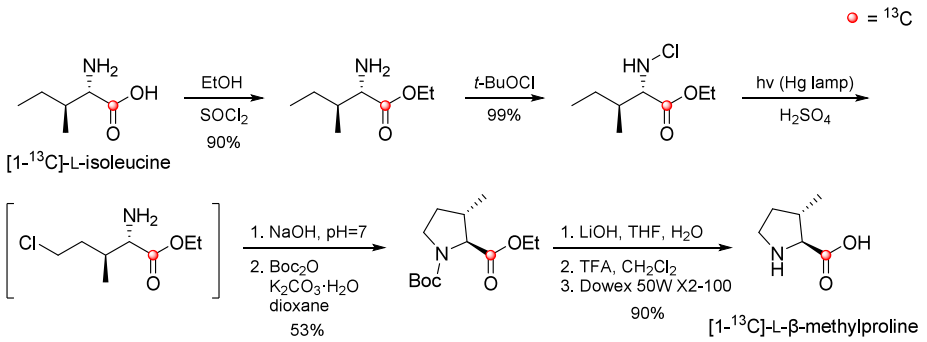

Scheme 21. Different Biosynthetic Proposals for Paraherquamides. (A) Unified Proposal for Biosynthesis of Paraherquamides and VM55599. (B) Proposed Biogenesis of Dioxepin Ring. (C) Two Alternative Biogenetic Sequences from Preparaherquamide

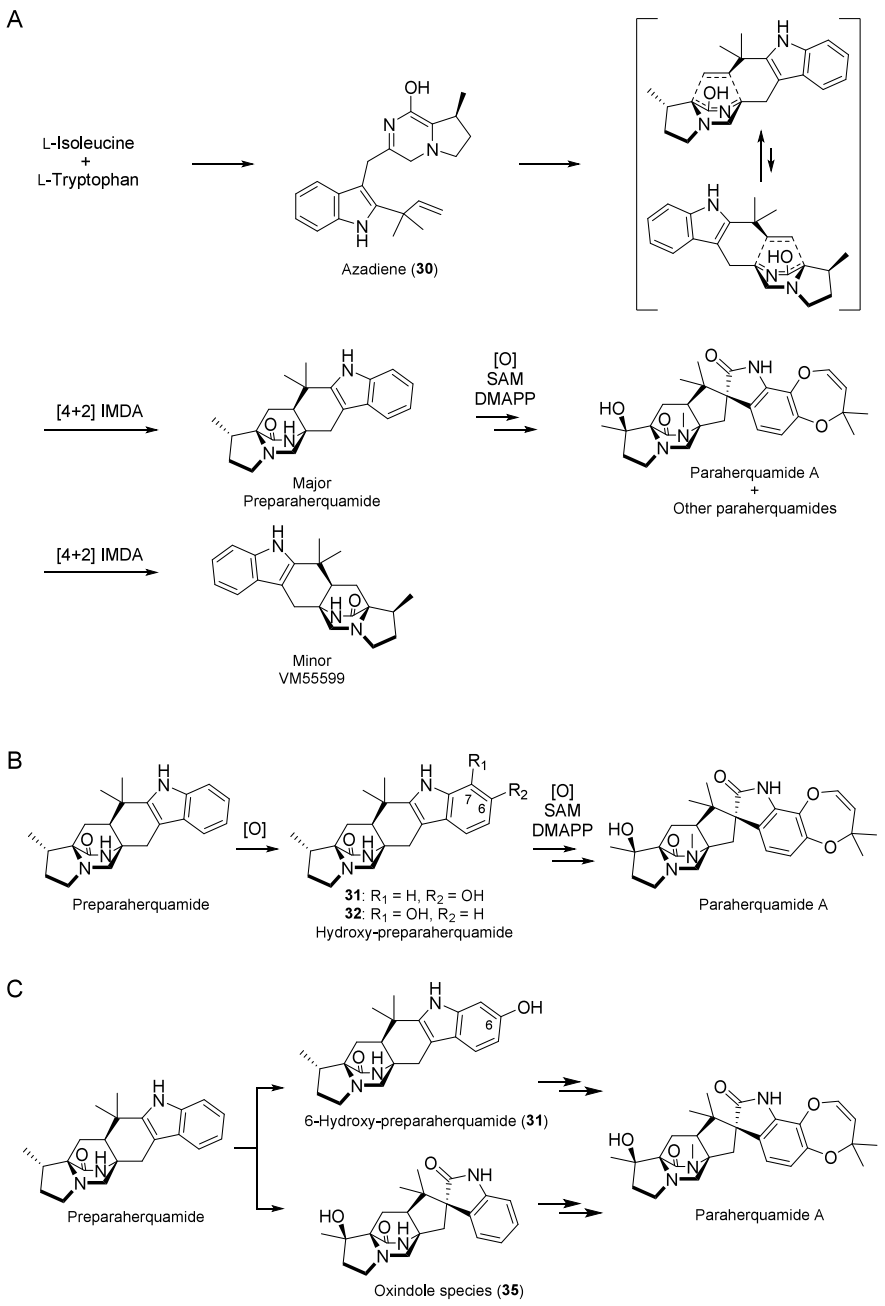

https://doi.org/10.1021/acs.chemrev.4c00250
Chem. Rev. XXXX, XXX, XXX−XXX

precedes the oxidative tailoring of the side chain of tryptophan. Nonetheless, it is worth noting that the determined stereochemistry of the methyl group of methylproline in VM55599 was found to be opposite to that in paraherquamide A.

Previous studies had shown that the stereochemistry of the methyl group of L-isoleucine was retained in the final product paraherquamide A.[83−85] This made Williams and co-workers speculate that L-isoleucine might be a common biosynthetic precursor for both paraherquamides and VM55599. If so, the absolute configuration of the BCDO ring system of VM55599 should be enantiomeric to that of paraherquamides. Experimental observations and speculations on VM55599 led to a unified proposal for biosynthesis of VM55599 and the paraherquamides (Scheme 21A).[22,23,87] Specifically, the biosynthetic precursors of paraherquamides and VM55599 arise as diastereomeric products of the [4+2] IMDA cycloaddition of a common azadiene **30** through two out of four possible diastereomeric transition states. The minor product of this kind of cycloaddition would culminate in VM55599, while the major product would be the proposed diastereomer preparaherquamide, which would lead to paraherquamide A.

To test this hypothesis, four racemic doubly ^{13}C-labeled cycloadducts were synthesized according to the previously established synthesis of racemic VM55599.[87,88] Feeding experiments were performed on *P. fellutanum* with all four potential precursors, followed by isolation and purification of paraherquamide A (Scheme 19E). Analysis of ^{13}C NMR and mass spectra showed that significant isotopic incorporation was observed in paraherquamide A when ^{13}C-labeled preparaherquamide was fed, while no incorporation was observed for racemic VM55599 and the other two oxidized counterparts **28** and **29**. These results provided additional circumstantial evidence that VM55599 should not be the precursor of paraherquamide A, but probably a minor shunt metabolite. The significant incorporation of this C-14 epimer (Scheme 19E) also indicated that the formation of the BCDO moiety should occur prior to the oxidation on the tryptophyl moiety. Moreover, oxidations of the indole ring to form both the catechol-derived dioxepin and spirooxindole, as well as the dioxepin-derived isoprenylation and *S*-adenosylmethionine-involved *N*-methylation, should occur after the formation of preparaherquamide.

Next, Williams and co-workers chemically synthesized (−)-VM55599 through an enantiospecific biomimetic strategy starting from a chiral, nonracemic compound of known absolute configuration.[89] Analyses including optical rotation and CD measurement and comparison of retention times on chiral HPLC confirmed that the synthesized product was identical in all respects to natural VM55599 produced by *Penicillium* spp. IMI332995. These results not only confirmed the absolute stereochemistry of VM55599 but also supported the biosynthetic route proposed for VM55599 and paraherquamides (Scheme 21A).

The incorporation of preparaherquamide into paraherquamide A indicated that preparaherquamide should be a genuine metabolite of paraherquamide-producing fungi. In order to confirm this, Williams and co-workers carefully examined the cultures of *P. fellutanum* and *A. japonicus* by comprehensive LC-MS analysis.[77] As expected, preparaherquamide was detected in the cultures of both fungi, which further validated the putative biosynthetic pathway of paraherquamide A. With respect to the downstream biosynthetic route from preparaherquamide, it was proposed that the intermediate might be oxidized to the hypothetical intermediate 6/7-hydroxy-preparaherquamide **31** or **32**,[90] which could suffer prenylation and cyclization to form the dioxepin ring, giving rise to the final product paraherquamide A (Scheme 21B).

Based on the above hypothesis, the Williams group further attempted to explore the exact sequence of hydroxylations and prenylation in forming the unique dioxepin moiety of paraherquamide A and the dihydropyran system of paraherquamides F and G. The authors proposed four possible hexacyclic biosynthetic intermediates (**31**−**34**) and initiated studies on chemical synthesis of the ^{2}H- and/or ^{13}C-labeled intermediates (Scheme 19F).[90] Among the four compounds, preparative synthesis of D_3-7-hydroxy-preparaherquamide **32** was achieved first.[90] The feeding experiment with this compound was performed on *P. fellutanum* followed by isolation and purification of paraherquamide A. No isotopic incorporation was observed for the intact triply labeled intermediate **32** within the detection limit of ^{2}H NMR spectroscopy, indicating that the C-6 hydroxylation of the indole ring likely precedes the C-7 hydroxylation (Schemes 19F and 21C). However, it is also possible that the oxidative transformation of preparaherquamide to the oxindole species **35** precedes the hydroxylation at either C-6 or C-7 (Scheme 21C).

4. ELUCIDATION OF BIOSYNTHETIC PATHWAYS AND FUNCTIONAL AND MECHANISTIC STUDIES OF BIOSYNTHETIC ENZYMES

Breakthroughs in the biosynthesis of BCDO alkaloids have only begun to emerge in the past decade, mainly owing to the recent technical advances in genome sequencing and editing. Strikingly, these biosynthetic systems have evolved multiple strategies for controlling the diastereo- and enantioselective outcomes by recruiting a variety of enzyme classes. These findings highlight the power of nature to deploy diversified biocatalytic strategies for creating structurally convergent but diastereo-/enantio-divergent BCDO indole alkaloids.

4.1. Diketopiperazines

With the advent of the genomic era, DKP biosynthesis has been extensively studied in terms of biosynthetic gene clusters (BGCs) and related enzymatic functions and mechanisms. The family-founding member brevianamide A is also the first DKP BCDO-containing alkaloid with a fully resolved biosynthetic pathway, in which the spontaneous IMDA process was clearly demonstrated. In this section, we will review the current understandings on biogenesis of the BCDO-containing DKP alkaloids, including brevianamides, notoamides, and others.

4.1.1. Brevianamides. For half a century since the first isolation of brevianamide A, despite great efforts on deciphering its biogenesis, the enzymatic details of its biosynthesis have long remained elusive. We recently cracked this black box through genomics, gene disruption, heterologous expression, precursor incorporation experiments, *in vitro* biochemical analysis, structural biology, and quantum mechanical calculations.[2]

Using the nonribosomal peptide synthetase (NRPS) gene *notE*[54] in notoamide biosynthetic gene cluster as a probe, genome mining of the whole genome of the brevianamides A/B producing *Penicillium brevicompactum* NRRL 864 located the homologous NRPS gene *bvnA* that is putatively responsible for assembling the *cyclo*-dipeptide brevianamide F. Subsequently, a

https://doi.org/10.1021/acs.chemrev.4c00250
Chem. Rev. XXXX, XXX, XXX−XXX

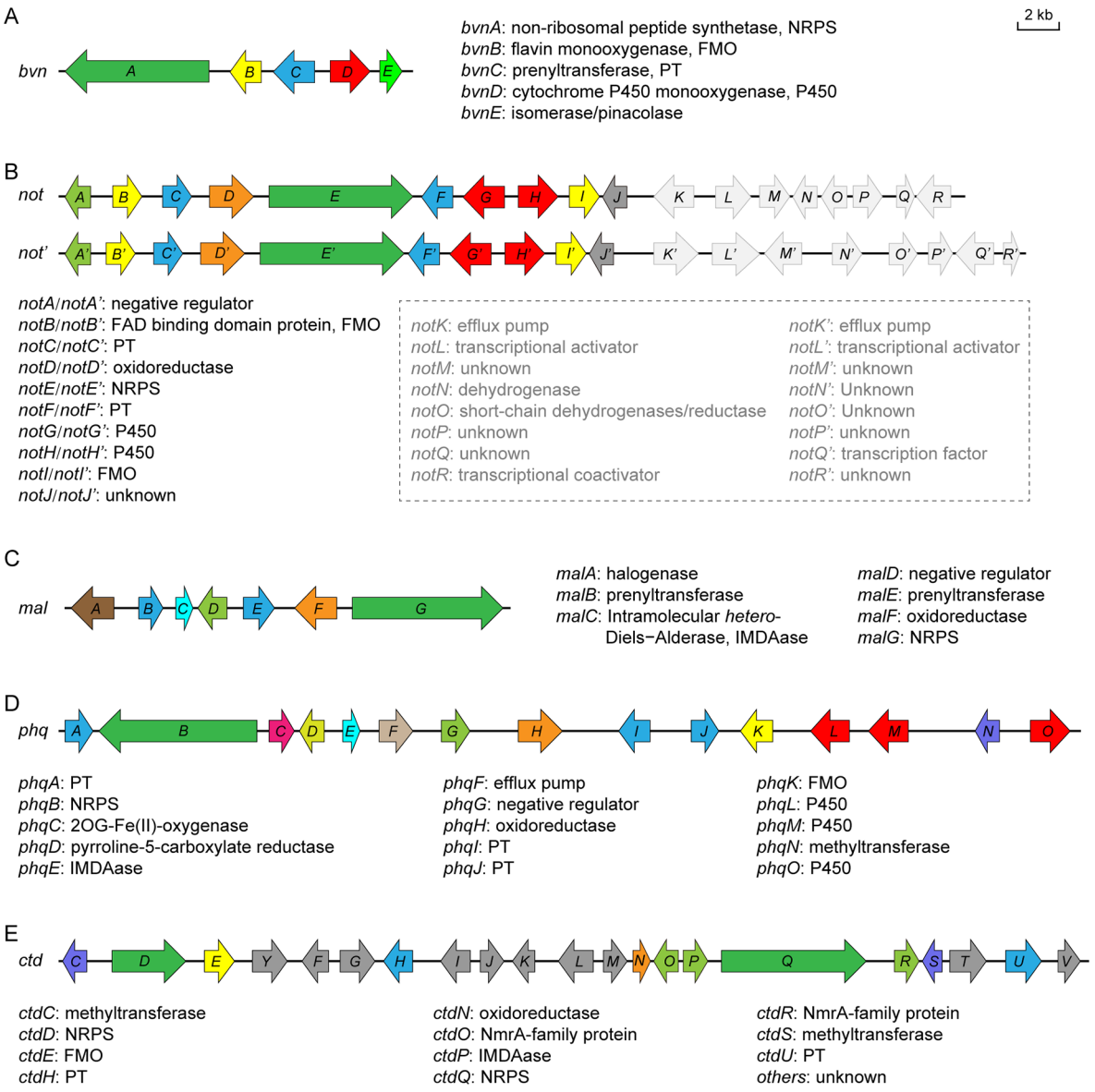

Figure 7. Biosynthetic gene clusters of brevianamides (A), notoamides (B), malbrancheamides (C), paraherquamides (D), and 21*R*-citrinadin A (E).

gene cluster (*bvn*) containing five genes including *bvnA* (NRPS), *bvnB* (flavin monooxygenase, FMO), *bvnC* (prenyltransferase, PT), *bvnD* (cytochrome P450 monooxygenase, P450), and *bvnE* (isomerase/pinacolase) was revealed (Figure 7A).

As predicted, the bimodular NRPS BvnA was confirmed to be a brevianamide F synthase through the heterologous expression of *bvnA* in *Aspergillus oryzae* M-2-3 (Scheme 22), functionally identical to its homologues FtmA in fumitremorgin biosynthesis[91] and NotE in notoamide biogenesis.[54] The results of *bvnC* gene knockout in *P. brevicompactum*, heterologous expression of *bvnC* in *A. oryzae*, and *in vitro* enzymatic reaction clearly demonstrated the reverse prenyltransferase functionality of BvnC, which is responsible for generating the key intermediate deoxybrevianamide E from brevianamide F with a cosubstrate dimethylallyl pyrophosphate (DMAPP). Then, FMO BvnB was characterized to catalyze a β-face epoxidation followed by ring-opening of the indole epoxide intermediate, giving rise to the unstable intermediate 3-hydroxyindolenine **36**. Brevianamide E was confirmed to be a rearranged shunt product resulting from the initial 2,3-indole epoxidation of deoxybrevianamide E (probably via the intermediate 3-hydroxyindolenine **36**). Without downstream gene products, BvnB could efficiently convert deoxybrevianamide E into brevianamide E through an energetically favored N−C ring closure, which was considered to follow a similar mechanism previously established for the formation of notoamide D by the homologous FMO NotB.[60]

Afterward, in the presence of P450 BvnD, 3-hydroxyindolenine **36** is likely hydroxylated by BvnD and then undergoes spontaneous dehydration/tautomerization to yield the key azadiene intermediate **37**, which is required for [4+2] IMDA cyclization (Scheme 22). Subsequent semipinacol rearrangement catalyzed by the cofactor-independent isomerase/pinacolase BvnE mediates the formation of the 3-oxo indoxyl azadiene species **14**, which is spontaneously cyclized to brevianamides A and B via a nonenzymatic process. This is consistent with the Lawrence proposal as described above.[26]

https://doi.org/10.1021/acs.chemrev.4c00250
Chem. Rev. XXXX, XXX, XXX−XXX

Scheme 22. Elucidated Biosynthetic Pathway of Brevianamides[a]

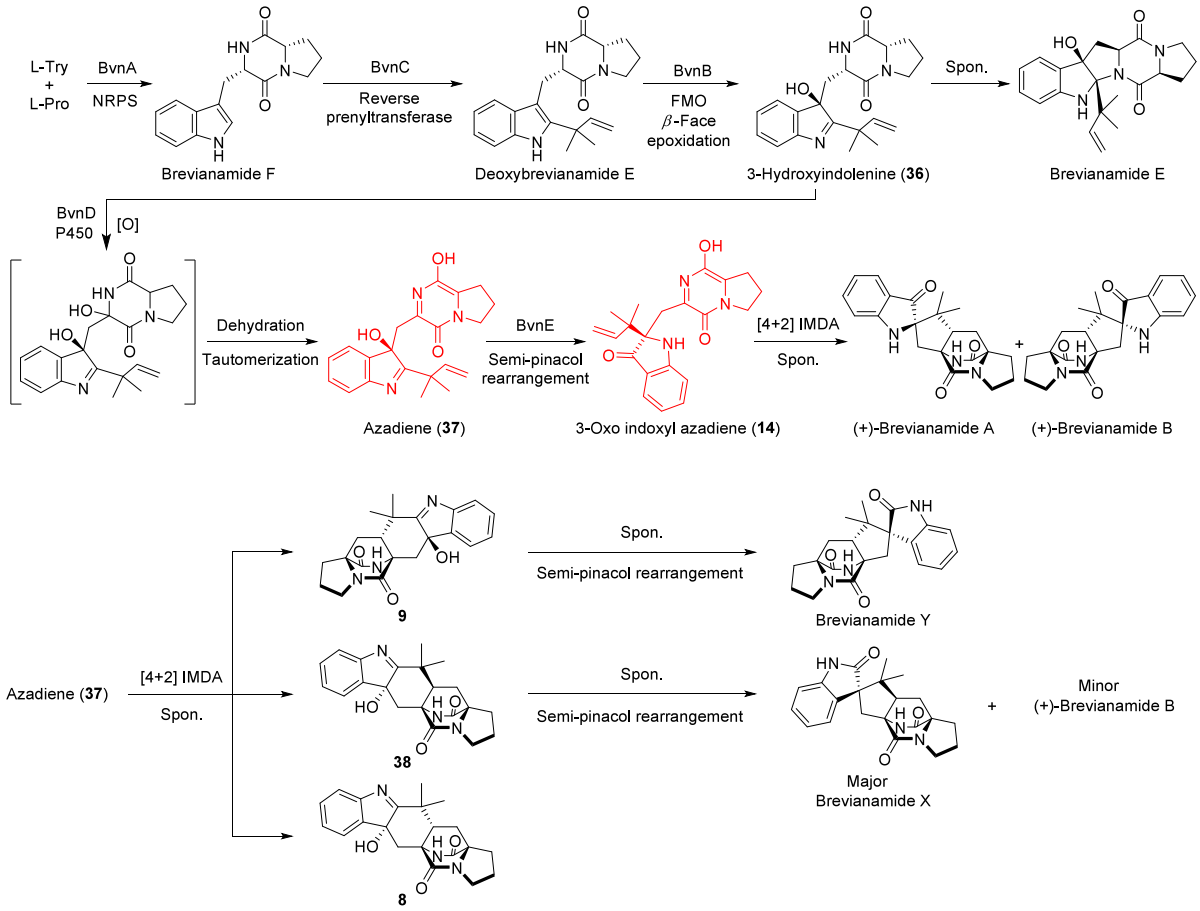

[a]Putative key intermediates are highlighted in red.

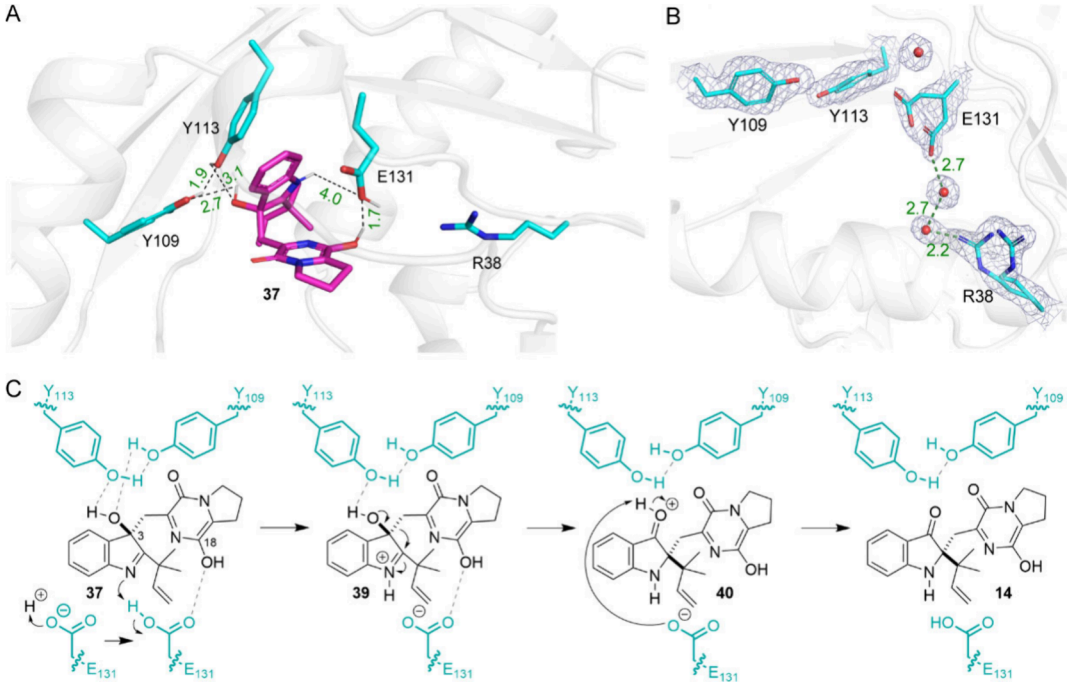

Figure 8. Proposed catalytic mechanism of BvnE. (A) The docked BvnE-**37** complex with the key residues (in cyan). (B) The key interactions between Arg38 and Glu131. (C) The proposed isomerization mechanism.

https://doi.org/10.1021/acs.chemrev.4c00250
Chem. Rev. XXXX, XXX, XXX−XXX

Scheme 23. Biosynthetic Pathways of Notoamides. (A) The Latest Proposed Pathway. (B) The Possible Pathway Involving Notoamide TI. (C) Brevianamide A-like Route[a]

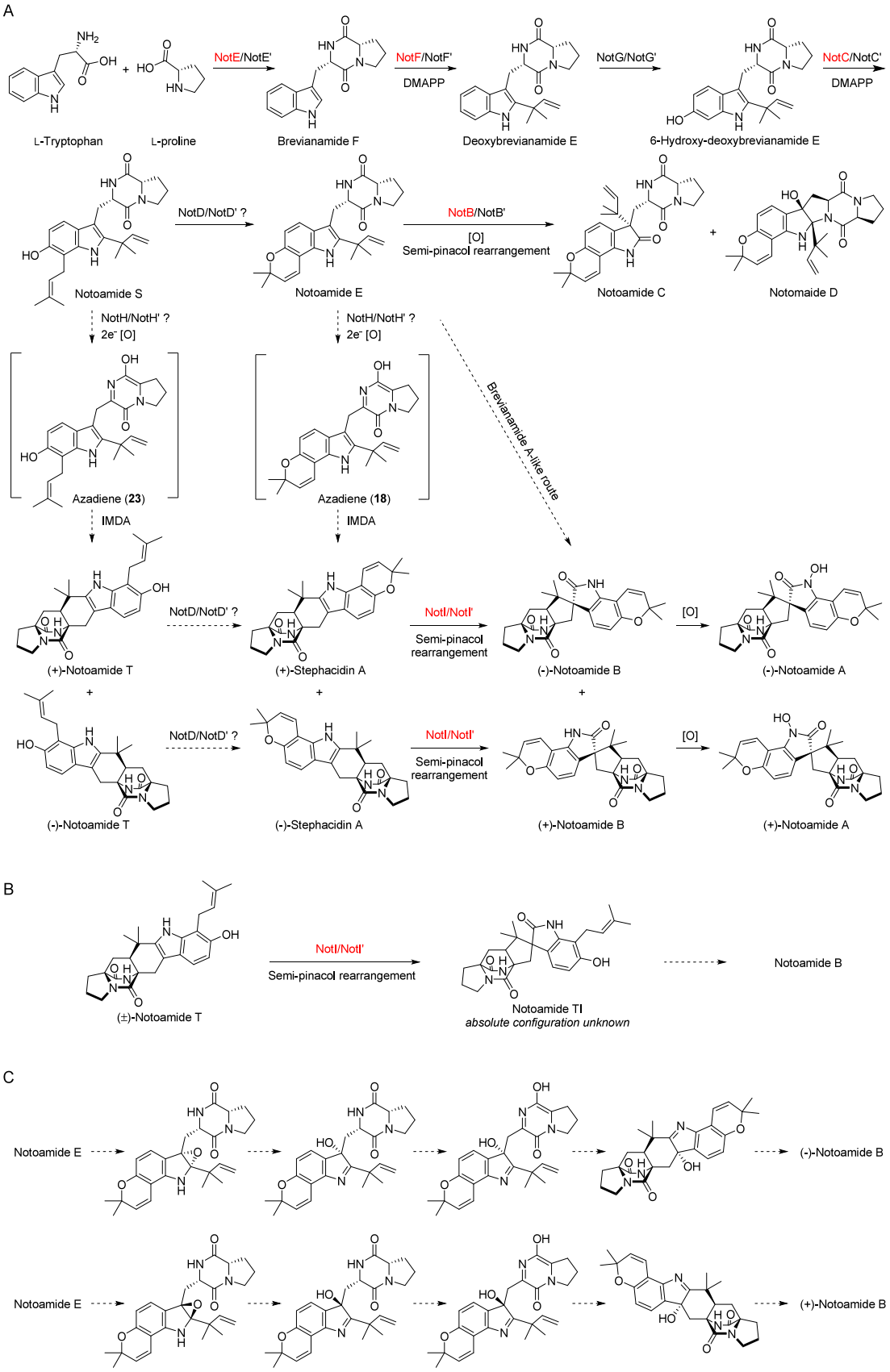

[a]The functionally characterized enzymes are shown in red.

https://doi.org/10.1021/acs.chemrev.4c00250
Chem. Rev. XXXX, XXX, XXX−XXX

Interestingly, brevianamides X and Y were produced by the *bvnE* knockout mutant. We reasoned that the azadiene intermediate **37** could spontaneously undergo three different [4+2] IMDA cyclization routes to generate three new and chemically confirmed 3-hydroxyindolenine derivatives (**8**, **9** and **38**). Due to instability, two of them collapsed to brevianamides X (with a minority of brevianamide B) and Y. Of note, the quantum chemical calculation results supported the experimentally observed product distribution. Essentially, the isomerase/pinacolase BvnE was demonstrated to be a central enzyme for controlling the stereochemistry and hence product profile in brevianamide biosynthesis.

The catalytic mechanism of BvnE was investigated through X-ray crystal structure analysis and molecular docking (Figure 8). BvnE is a symmetric homodimer, the catalytic cavity of which shows a hydrophobic interior with several polar residues, which are considered to be involved in acid/base catalysis. Site-directed mutagenesis of Arg38, Tyr109, Tyr113 and Glu131 residues caused severely attenuated activity. Docking analysis showed that the reverse prenyl group of the substrate **37** packed into a hydrophobic pocket. Tyr109 and Tyr113 interact with the 3-OH group, while Glu131 is positioned to interact with the indole nitrogen and C-18 oxygen. The semipinacol rearrangement likely initiates from the proton transfer mediated by Glu131, followed by hydrogen bond-assisted activation through Tyr109/Try113 via intermediates **39** and **40**. During this process, Glu131 also provides charge stabilization of the intermediate **39**. The hydrogen bonding network among Arg38, Glu131 and two ordered water molecules suggests that this residue may assist in regeneration of the carboxylate form of E131 via proton transfer.

4.1.2. Notoamides and Stephacidins. The first biosynthetic gene cluster of notoamides (*not*) was reported by Sherman and co-workers.[54] Using *ftmA*[91] that encodes a brevianamide F synthase of the fumitremogin biosynthetic pathway as a probe, the bimodular NRPS gene *notE*, presumably responsible for the biosynthesis of brevianamide F (Scheme 23A), was identified through whole genome mining of the marine-derived (−)-notoamides A/B, producing strain *A. protuberus*. The *not* gene cluster was found to contain 18 open reading frames (Figure 7B). Among the *not* encoding enzymes, the two predicted aromatic prenyltransferases NotC and NotF were functionally characterized.[54] *In vitro* enzymatic reactions showed that NotF is the deoxybrevianamide E synthase with reverse prenyltransferase functionality, and NotC catalyzes a normal prenylation reaction of 6-hydroxy-deoxybrevianamide E to afford notoamide S (Scheme 23A). Later, a large and solvent-exposed active site of NotF was revealed after solving the crystal structure in complex with the native substrate and prenyl donor mimic dimethylallyl *S*-thiolodiphosphate (DMSPP). Of note, NotF showed a broad substrate scope to accept sterically and electronically differentiated tryptophanyl DKPs.[92]

The Sherman laboratory also sequenced the genome of the terrestrial-derived *A. amoenus* that produces (+)-notoamides A/B and identified another notoamide biosynthetic gene cluster (*not′*) (Figure 7B), which contains nine genes (*notA′-J′*) that display high amino acid sequence similarity (>70%), with the corresponding proteins encoded by the *not* gene cluster in *A. protuberus*.[5] Of note, the sequence similarity decreases drastically and the cluster architecture differs after *notK*/*notK′*, strongly suggesting the *not*/*not′* gene clusters probably end at the genes *notJ*/*notJ′*.

Based on the confirmed functions of the two prenyltransferases NotF and NotC, and the predicted enzyme activities of the remaining gene products, the putative notoamide biosynthetic pathway was initially proposed[54] (Scheme 10D) and lately updated[93] (Scheme 23A). Brevianamide F is produced from L-Trp and L-Pro by NRPS NotE and subsequently reverse prenylated by NotF to produce deoxybrevianamide E. Cytochrome P450 monooxygenase (P450) NotG likely catalyzes the hydroxylation on the indole ring. Then NotC is responsible for normal prenylation to produce the key intermediate notoamide S. Notoamide E is generated by an oxidative ring closure to afford the pyran moiety by oxidase NotD, which is further oxidatively converted into notoamide C and D by flavin monooxygenase (FMO) NotB. The step from notoamide E to stephacidin A is still uncertain because the ^{13}C-labeled stephacidin A was not observed in the above-mentioned [^{13}C]$_2$-notoamide E feeding experiment (Scheme 12B).[39,53] Subsequently, oxidation and tautomerization of the proposed precursor notoamide S (presumably mediated by P450 NotH) would yield the key achiral azadiene species **23**, which undergoes the [4+2] IMDA reaction enzymatically or nonenzymatically to generate notoamide T, followed by the pyran ring formation (presumably mediated by oxidase NotD) to give stephacidin A. Then stephacidin A is regiospecifically hydroxylated, followed by pinacol rearrangement to produce notoamide B. The final *N*-hydroxylation gives rise to notoamide A.

Following functional investigation of the two prenyltransferases NotC and NotF, the FAD-dependent monooxygenase NotB was also characterized *in vitro*.[60] This FMO was determined to catalyze the indole 2,3-epoxidation of notoamide E, leading to the two end products notoamides C (through pinacol-like rearrangement) and D (Scheme 23A). The conversion from stephacidin A to notoamide B was proposed to undergo the 2,3-epoxidation followed by pinacol-type rearrangement, which was predicted to be catalyzed by the second FMO NotI/NotI′,[5] which was biochemically confirmed.[93] Both (+)- and (−)-stephacidin A could be accepted by either NotI or NotI′ *in vitro* and converted to (−)- and (+)-notoamide B (Scheme 23A), respectively. Comparatively, both NotI and NotI′ prefer (−)-stephacidin A to (+)-stephacidin A. These results clearly indicated that NotI/NotI′ are not responsible for controlling the enantiodivergence in notoamides biosynthesis.

Interestingly, NotI/NotI′ demonstrated a wide substrate scope by showing varied oxidative activities toward brevianamide F, deoxybrevianamide E, 6-hydroxy-deoxybrevianamide E, notoamide S, notoamide E, (+)-notoamide T, and (−)-notoamide T.[93] For some substrates, multiple products could be detected, suggesting either a loss of stereocontrol for collapse of the epoxide or the generation of alternative oxidized products. Racemic notoamide T could be converted by NotI into a new compound notoamide TI, whose absolute configuration was not determined (Scheme 23B). The production of this compound suggested that there might be another possible pathway leading to notoamide B through (+)/(−)-notoamide T. However, it is still questionable whether notoamide TI is a natural metabolite because it has not been isolated in any of the notoamide-producing strains so far.

With previous knowledge on notoamide biosynthesis, Fraley et al. summarized the biosynthetic pathway of notoamides A/B (Scheme 23A).[93] Considering the similarity and homology of

https://doi.org/10.1021/acs.chemrev.4c00250
Chem. Rev. XXXX, XXX, XXX−XXX

related structures and enzymes between notoamides and brevianamides (Scheme 22 and Figure 7A and B), another possible biosynthetic route of notoamide B was also proposed (Scheme 23A and C, brevinamide A-like route). In this route, the formation of notoamide B does not go through the intermediate notoamide T; instead, it is generated from notoamide E through "brevinamide A-like" oxidation, IMDA and rearrangement.

Despite these elucidated enzymatic steps, there remain a number of unsolved problems in the notoamide biosynthetic pathway. For example, it is still uncertain whether notoamide S or E (or both) is the real precursor for the [4+2] IMDA reaction and which enzyme is the determining factor for the alternative stereo-outcome of (+)- and (−)-notoamides A/B. Moreover, another possibility still cannot be ruled out that notoamide B might be derived from notoamide E via a brevianamide-like mechanism (i.e., sequential FMO-mediated epoxidation, P450-catalyzed C−N bond desaturation, and spontaneous IMDA).[2]

4.1.3. Versicolamide B. Versicolamide B is a diastereomer of notoamide B, both of which share a common polycyclic structure and can be produced by the same fungus. Thus, it is reasonable to speculate that the two natural metabolites originate from the same biosynthetic gene cluster (*not*/*not*′). Consistent with previous proposals,[61,63] the Sherman and Williams groups reported the biochemical functions of the late-stage FMOs NotI/NotI′ in (+)/(−)-notoamide biosynthetic gene clusters from *A. protuberus*/*A. amoenus*. These two FMOs were able to catalyze the semipinacol rearrangement to generate the spiro-oxindole moiety present in many of the BCDO indole alkaloids (Scheme 24).[93] Both NotI and NotI′

Scheme 24. Activities of NotI/NotI′ toward (+)/(−)-6-*epi*-Stephacidin A

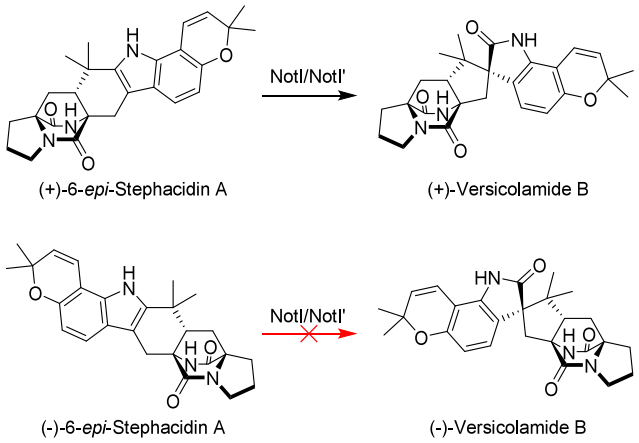

were able to catalyze the reaction of (+)-6-*epi*-stephacidin A to (+)-versicolamide B, but no reaction was observed for (−)-6-*epi*-stephacidin A. These *in vitro* results are compatible with the product patterns observed in *A. protuberus* and *A. amoenus*,[61,63] which both produced (+)-versicolamide B while *A. amoenus* accumulated (−)-6-*epi*-stephacidin A as terminal product.

4.1.4. Taichunamides. Taichunamides, notoamides and versicolamides were reported to be natural metabolites of *A. taichungensis* (Figure 9).[65] Comparing the structural profiles of the three kinds of family members of BCDO fungal indole alkaloids reveals the distinct yet subtle stereochemical diversity. Considering the similar gene organization of the two notoamide biosynthetic gene clusters (*not*/*not*′ of *A. protuberus*/*A. amoenus*, Figure 9) and their high sequence homology,[5] it is reasonable to hypothesize that the difference in product patterns ((+)-stephacidin A, (+)-6-*epi*-stephacidin A, (−)-notoamide B, (+)-versicolamide B vs (−)-stephacidin A, (+)-6-*epi*-stephacidin A, (+)-notoamide B, (+)-versicolamide B, (−)-6-*epi*-stephacidin A) between the two strains[61,63] is likely due to the stereoselectivity of the involved enzymes. Thus, we surmise that a similar gene cluster might be responsible for biogenesis of taichunamides and other related BCDO indole alkaloids in *A. taichungensis*, which contains the enzymes responsible for both enantio- and diastereodivergent biosynthetic processes.

4.2. Monoketopiperazines

Similar to DKPs, MKPs have also been extensively studied with regard to their biosynthetic genes and key enzymatic mechanisms. The mechanisms related to the IMDA cycloaddition during the biosynthesis of paraherquamides and malbrancheamides were elucidated earlier than those of DKPs. Unlike the representative DKP alkaloid brevianamide A, the BCDO structure of MKPs is assembled by different DAases instead of a spontaneous process. In this section, we will summarize the progress on the DAases and other related enzymes involved in MKP biosynthesis.

4.2.1. Malbrancheamides. By genome mining of *M. aurantiaca* RRC1813A, the Sherman and Williams groups identified the seven-gene containing malbrancheamide biosynthetic gene cluster (*mal*) (Figure 7C).[5] The genes of the *mal* cluster show higher sequence similarity to those of the MKP paraherquamide biosynthetic gene cluster than those of DKP clusters (*bvn* and *not*/*not*′). Unlike the DKP NRPSs (BvnA and NotE/NotE′), which have a *C*-terminal condensation domain, the MKP NRPS MalG harbors a reductase domain at its carboxy terminus. The reductase domain was proposed to be responsible for reductive offloading resulting in the MKP moiety. MalA was predicted to be a flavin-dependent halogenase, which is consistent with the presence of chlorine atoms in the malbrancheamide structures.

According to the bioinformatically predicted functions of *mal*-encoded proteins, a biosynthetic pathway was proposed (Scheme 25A). The NRPS MalG (A-T-C-A-T-R: A, adenylation domain; T, thiolation/peptidyl carrier protein (PCP) domain; C, condensation domain; R, reductase domain) was proposed to catalyze the condensation of L-tryptophan and L-proline with reduction of the keto group (by R domain) to give the intermediate cyclic dipeptide (**41**). Then **41** is prenylated by one of the two prenyltransferases (MalE or MalB), generating the key precursor azadiene **27**, which undergoes the [4+2] IMDA reaction to give premalbrancheamide. Subsequently, the halogenase MalA presumably catalyzes a halogenation reaction to afford the natural product malbrancheamide B, which could be further chlorinated to the final product malbrancheamide.

In order to elucidate the halogenation process during malbrancheamide biosynthesis, Sherman and co-workers heterologously expressed the predicted halogenases MalA and MalA′ from *M. aurantiaca* and *M. graminicola*, respectively, and characterized their biochemical function and catalytic mechanism *in vitro* (Scheme 26).[94] The purified MalA was found to catalyze the iterative chlorination of the natural precursor premalbrancheamide at both the C8 and C9 positions, giving malbrancheamide B and isomalbrancheamide

https://doi.org/10.1021/acs.chemrev.4c00250
Chem. Rev. XXXX, XXX, XXX−XXX

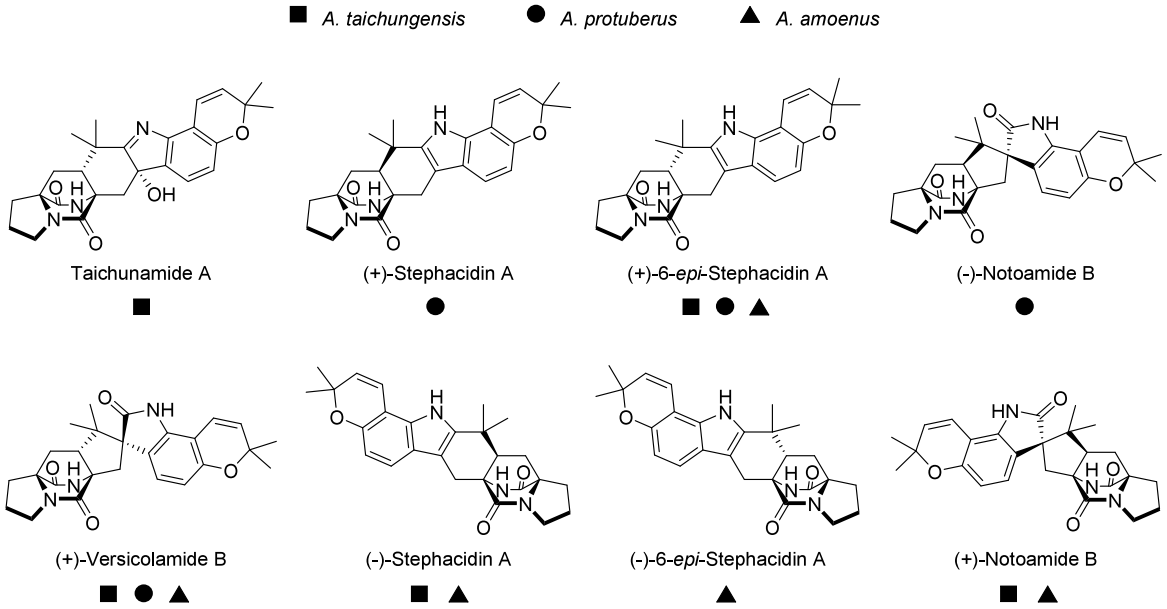

Figure 9. Major BCDO indole alkaloids produced by several *Aspergillus* strains as indicated by different symbols.

B, respectively, both of which could be further chlorinated to malbrancheamide. Interestingly, the monochlorinated products, malbrancheamide B and isomalbrancheamide B, could also be brominated to the novel indole alkaloids malbrancheamide D and isomalbrancheamide D, respectively. It was also determined that the activity of MalA′ is essentially identical to that of MalA.

To elucidate the unique halogenation mechanism of MalA/MalA′, the cocrystal structures of MalA′ in complex with premalbrancheamide, malbrancheamide B, and isomalbrancheamide B were determined, demonstrating the ternary complexes with FAD, chloride ion, and each of the three substrates.[94] The roles of amino acid residues in the active site were analyzed through site-directed mutagenesis, and Lys108 was determined to be necessary for halogenation activity (Figure 10). Glu494 is important for substrate binding by forming a hydrogen bond with the proton of the N−H of indole. Molecular dynamics simulation analysis and DFT calculations revealed that the enzyme represents a new class of zinc-binding flavin-dependent halogenases and provided new insights into a unique reaction mechanism (Scheme 26B). Briefly, an active Lys108-chloramine intermediate was proposed to be formed, which interacts with C9 or C8 to enable an electrophilic aromatic substitution, thus generating a Wheland intermediate (**42** and **43**) before the final deprotonation step. The deprotonation could be affected by a water molecule acting as a base or in the case of C8 by Ser129.

The first step of malbrancheamide biosynthesis was proposed to be the condensation of L-proline and L-tryptophan by the bimodular NRPS MalG (A-T-C-A-T-R), producing L-Pro-L-Trp aldehyde intermediate **44** through reductive release (Scheme 25B). To verify this hypothesis, the excised A1-T1, C, T2 and R domains of MalG, the full-length of which could not be produced in soluble form, were separately expressed and purified.[3] *In vitro* enzymatic reactions revealed that the NRPS MalG (in term of separate domains) product rapidly cyclized and dehydrated to the proposed dipeptide intermediate **45**, which was spontaneously oxidized to a zwitterion product **46**. Thus, the MalG terminal R domain catalyzes an NADPH-dependent two-electron reductive release to produce the key aldehyde intermediate **44**.

Next, MalE catalyzed the reverse prenyltransfer reaction to produce the prenylated zwitterion intermediate **47**, whereas the other prenyltransferase MalB in *mal* cluster displayed similar but modest activity, suggesting that *malB* might be a redundant gene.[3] In contrast to zwitterion product **46**, the synthetic dipeptide **45** could be rapidly prenylated by MalE, strongly suggesting that it is the native substrate for this prenyltransferase. A one-pot reaction with MalG, MalE and MalC produced (+)-premalbrancheamide, confirming that MalC functions as an intramolecular [4+2] DAase. Further reactions of the synthetic prenylated substrates (**47** and **48**) with MalC confirmed that the prenylated zwitterion **47** should be the native substrate for MalC. Therefore, MalC possesses the ability to mediate both NADPH-dependent reduction (giving the key azadiene **27**) and the diastereo- and enantio-controlled cycloaddition reactions. Moreover, when the involving enzymes MalG, MalE, MalC and MalA were coincubated with the starting substrates and necessary cofactors, the final product (+)-malbrancheamide could be produced in a one-pot manner, indicating a complete biosynthetic pathway for this MKP compound (Scheme 25B).

Further structural analysis together with site-directed mutagenesis and molecular dynamics simulations confirmed that the bifunctional reductases/DAases MalC (and PhqE, the MalC homologue in the paraherquamide pathway, see below) catalyzes the diastereo- and enantioselective cyclization in the construction of the MKP skeleton (Figure 11). MalC and PhqE were annotated as short-chain dehydrogenases. However, structural analysis revealed that they do not contain the conserved YXXXK motif that is required for catalysis in canonical short-chain dehydrogenases. Moreover, close interaction of the substrate with the NADP(H) cofactor was observed in PhqE substrate (**47**) and product (premalbrancheamide) complexes. And the bound prenylated zwitterion substrate **47** demonstrated preorganization toward the biological (+)-*syn* product.

https://doi.org/10.1021/acs.chemrev.4c00250
Chem. Rev. XXXX, XXX, XXX−XXX

Scheme 25. Initial Proposal from 2012 (A) and 2019 Revision (B) for the Biosynthetic Pathway of Malbrancheamides

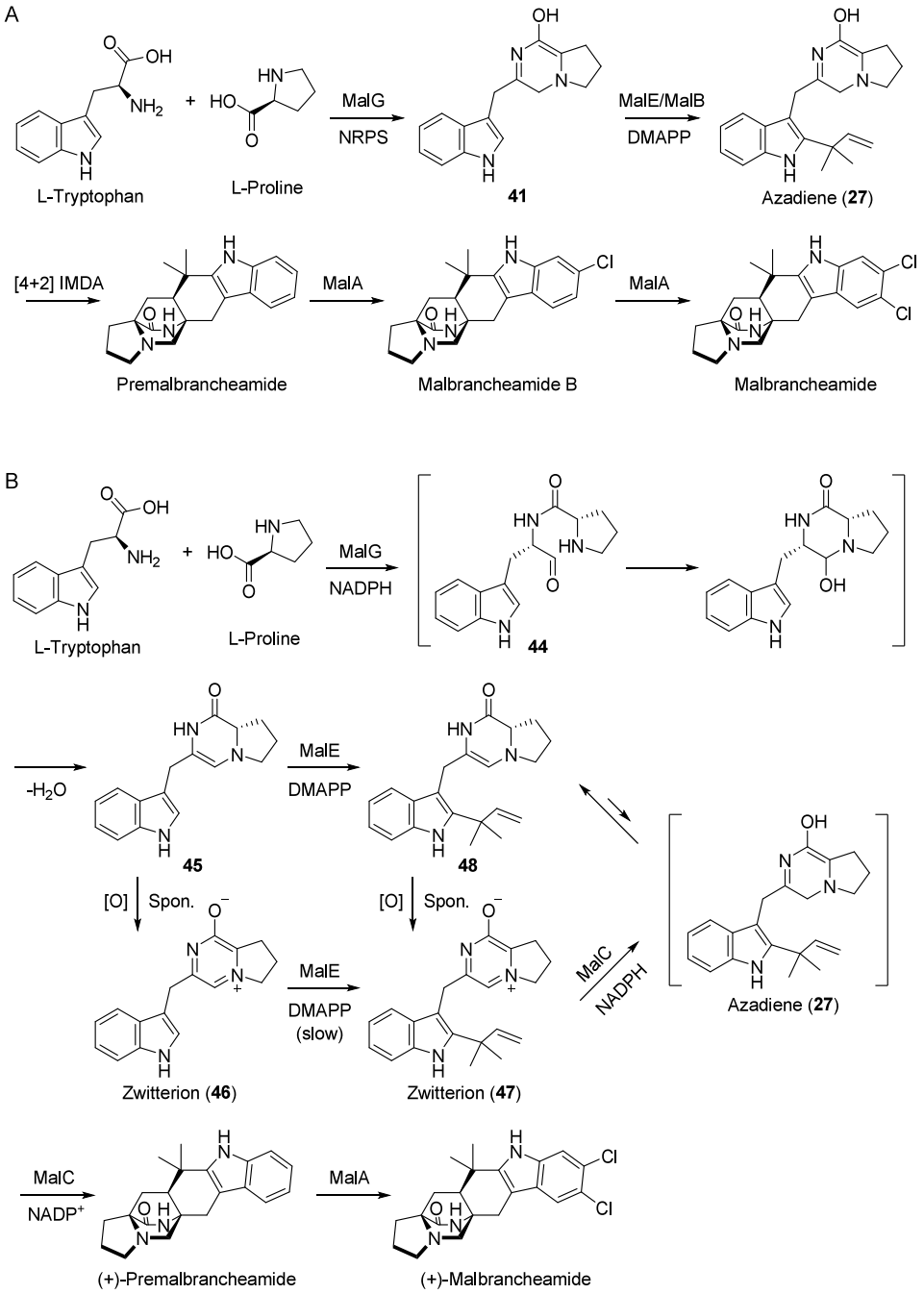

4.2.2. Paraherquamides. The gene cluster responsible for biosynthesis of paraherquamides was identified through genome mining of *P. fellutanum* in 2012[5] and contains 15 genes (Figure 7D). The bimodular NRPS gene *phqB* encodes a reductase (R) domain located at the *C* terminus, different from the condensation (C) domain of *bvnA* in the brevianamide gene cluster and *notE* in the notoamide gene cluster. The reductase domain was proposed to account for the presence of the MKP core structure in paraherquamides.

Based on the predicted functions of *phq*-encoded proteins, a plausible biosynthetic pathway of paraherquamide A was proposed (Scheme 27A).[5] Putatively, L-isoleucine is initially hydroxylated by an unknown enzyme. The short chain dehydrogenase PhqE, later characterized to have another function (see below), was proposed to oxidize the terminally hydroxylated L-isoleucine to the corresponding aldehyde **49**. Next, the aldehyde undergoes spontaneous cyclization and dehydration to yield 4-methyl pyrolline-5-carboxylic acid (**50**). The pyrroline-5-carboxylate reductase PhqD presumably reduces the intermediate **50** to β-methyl proline. Works by Walsh[95] and Tang[96] on the echinocandin and UCS1025A system indicated another possibility that the 2-oxoglutarate (2OG)-Fe(II)-oxygenase PhqC is likely responsible for the oxidation of isoleucine to generate β-methyl-proline. The PhqC homologues EcdK and UcsF iteratively oxygenate L-isoleucine *en route* to 4(*R*)-methyl-L-proline and β-methyl proline, respectively, in an α-ketoglutarate and oxygen-dependent manner. The bimodular paraherquamide NRPS

https://doi.org/10.1021/acs.chemrev.4c00250
Chem. Rev. XXXX, XXX, XXX−XXX

Scheme 26. Biochemical Function (A) and Catalytic Mechanism (B) of MalA

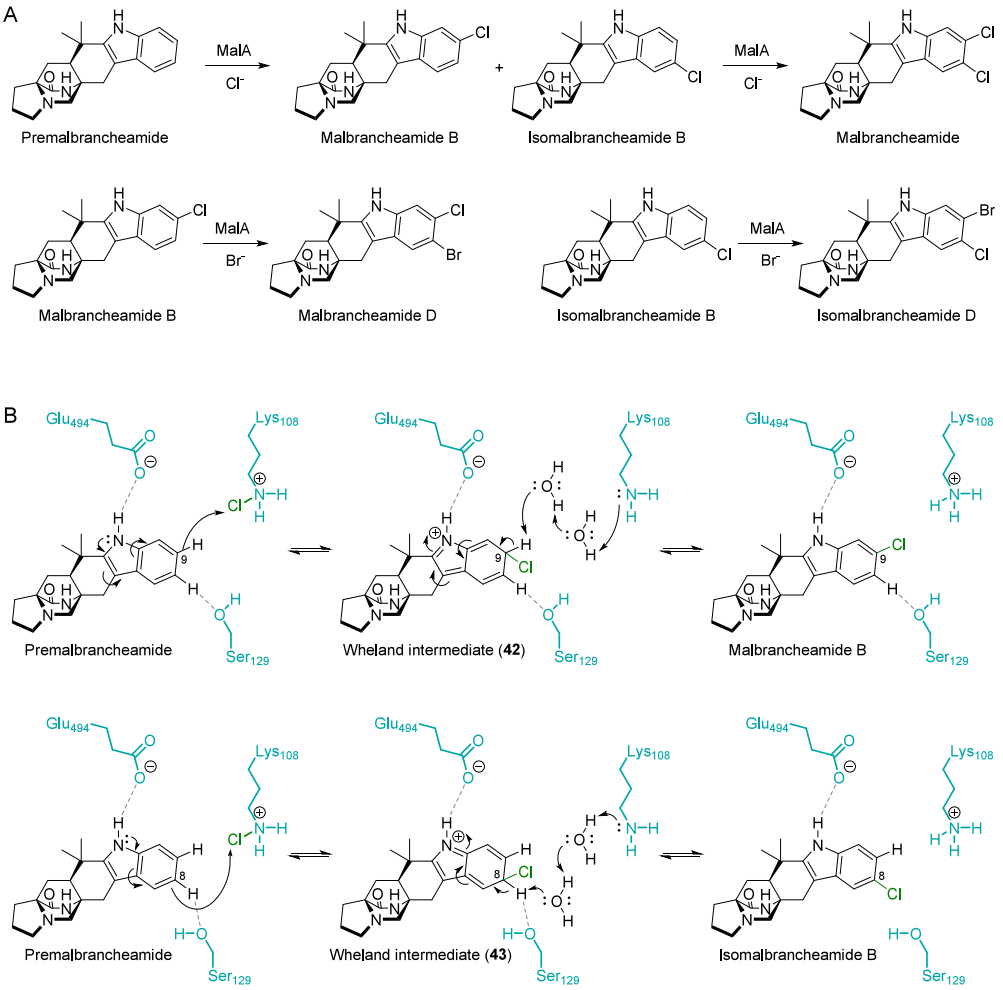

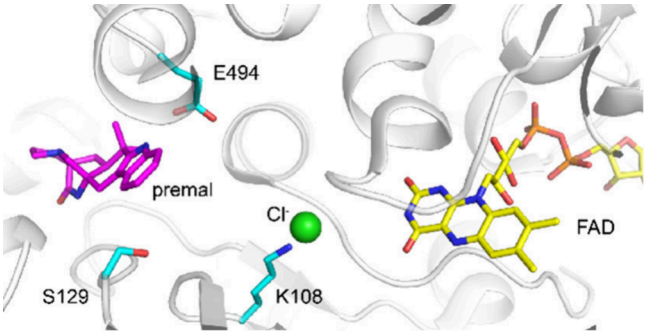

Figure 10. Active site of substrate-bound MalA. Conserved Lys108 and a bound chloride ion are adjacent to the substrate binding pocket.

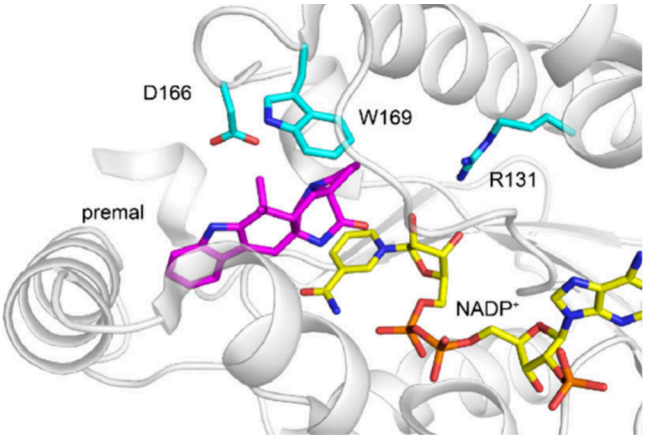

Figure 11. Active site of product-bound PhqE. Premalbrancheamide interacts with the NADP$^+$ cofactor and the essential Trp169.

PhqB (A-T-C-A-T-R), containing a *C*-terminal NAD(P)-dependent reductase domain, might utilize NADPH to reduce the thioester bond of the T domain-tethered linear dipeptide. This reduction would lead to spontaneous cleavage of the C−S bond, releasing the aldehyde intermediate **51**. The aldehyde then undergoes spontaneous dehydration and double bond rearrangement (tautomerization), giving the key azadiene precursor **52**. The reverse prenyltransferase (proposed to be PhqJ) then introduces the reverse prenyl group and mediates the subsequent [4+2] IMDA reaction to form the earliest BCDO-containing intermediate preparaherquamide. The formation of the pyran ring (in paraherquamides F and G) was believed to be comediated by prenyltransferase PhqA, P450 PhqL, and oxidoreductase PhqH or P450 PhqM. The FMO PhqK (a homologue of NotI) and methyltransferase PhqN are likely responsible for generation of the *spiro*-oxindole and the *N*-methylation, respectively. The third P450 monooxygenase PhqO probably catalyzes the C14 hydroxylation. The initial speculation suggested that the oxygenase PhqC might participate in the ring expansion process, forming the 7-

https://doi.org/10.1021/acs.chemrev.4c00250
Chem. Rev. XXXX, XXX, XXX−XXX

Scheme 27. Proposed Paraherquamide Biosynthetic Pathways. (A) The Biosynthetic Pathway of Paraherquamide A Proposed in 2012. (B) Alternative Biosynthetic Pathway of Paraherquamide A Proposed in 2018. (C) A 2019 Update to the Proposed Biosynthetic Pathway of Preparaherquamide

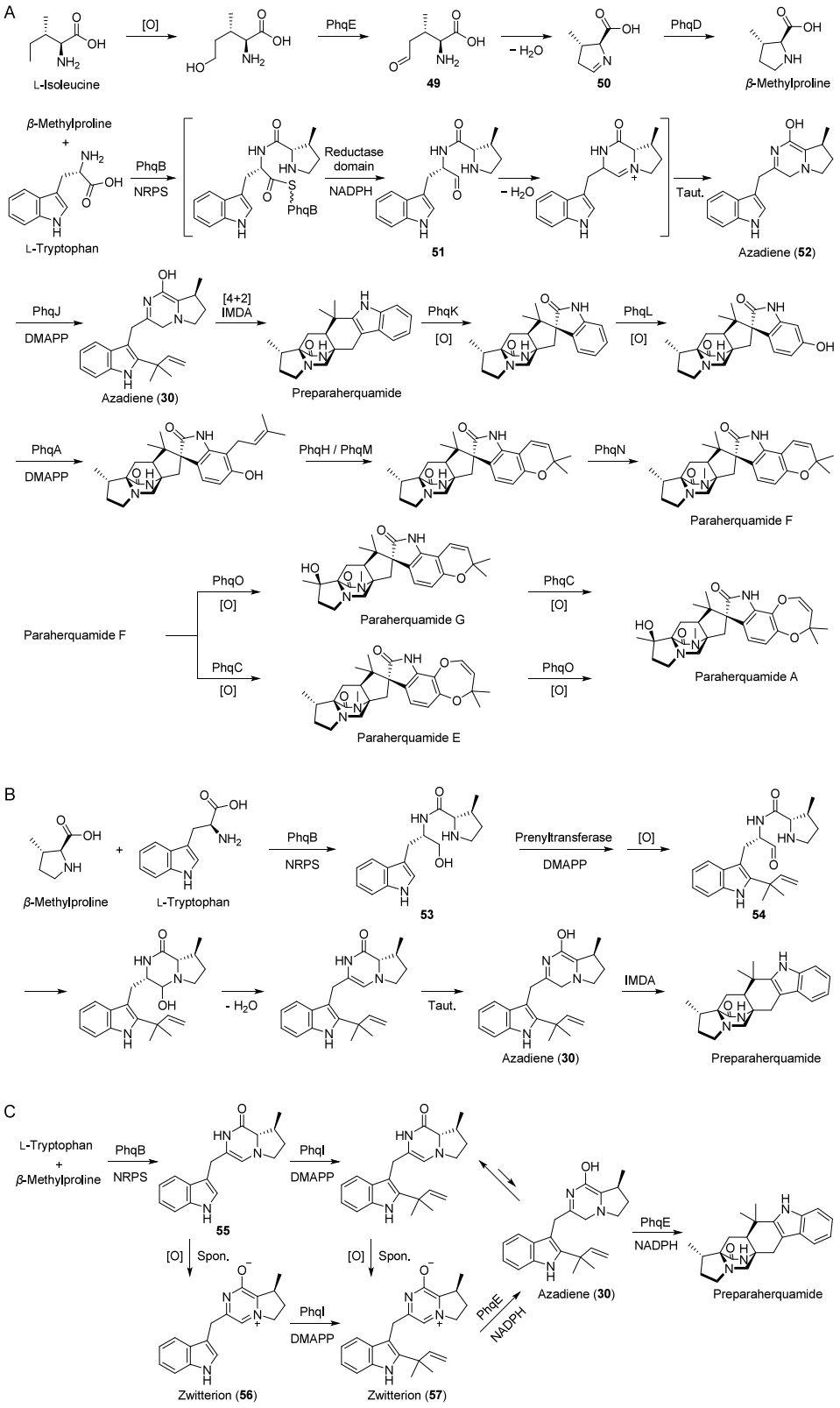

membered dioxepin ring in paraherquamide A.[5] However, the aforementioned biosynthetic study of β-methyl-proline[95,96] seemed to exclude this possibility, suggesting that PhqC is more likely involved in isoleucine oxidation rather than in the ring expansion. Given that the oxidative ring closure to form the pyran moiety is probably catalyzed by the NotD

https://doi.org/10.1021/acs.chemrev.4c00250
Chem. Rev. XXXX, XXX, XXX−XXX

Scheme 28. Functional Characterization of PhqK and the Revised Paraherquamide Biosynthetic Pathway

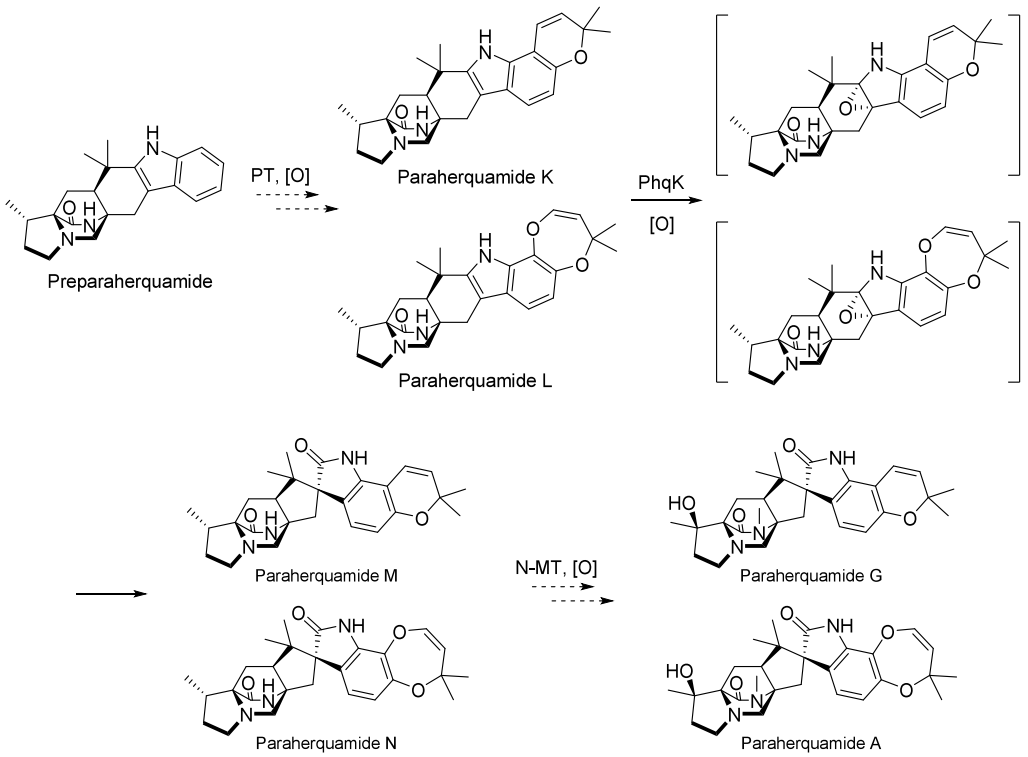

homologue PhqH, the remaining P450 enzyme PhqM is most likely responsible for the ring expansion. Despite these reasonable functional predictions, the order of the proposed biosynthetic steps needs to be established by detailed genetic and biochemical studies.

Interestingly, Williams and co-workers also raised an alternative biogenetic hypothesis for the key prenylated azadiene **30** (Scheme 27B).[97] The NRPS PhqB conducts reductive release of the dipeptide via a four-electron process, giving rise to an amino alcohol species **53**, which is then reverse-prenylated and oxidized to afford a key amino-aldehyde intermediate **54**. Following spontaneous cyclization, dehydration and tautomerization, the azadiene intermediate **30** is formed for the IMDA cycloaddition, leading to preparaherquamide.

After elucidation of the malbrancheamide biosynthetic pathway,[3] the biogenesis of preparaherquamide was also revised (Scheme 27C). The NRPS PhqB (MalG homologue) likely catalyzes the reductive condensation of β-methylproline and L-tryptophan to give the first MKP precursor compound **55**, followed by spontaneous oxidation to a zwitterion compound **56**. A reverse prenyltransferase (presumably PhqI) then catalyzes the prenylation of the zwitterion **56** (yielding **57**). Subsequently, the dehydrogenase PhqE (MalC homologue) mediates the NADPH-dependent reduction to furnish the key intermediate azadiene **30** and catalyzes the [4+2] IMDA cyclization to generate preparaherquamide. Notably, the culture extraction of the paraherquamide-producing strain *P. simplicissimum* with *phqE* knockout confirmed the existence of the proposed zwitterion intermediate **57**.[3]

After assembly of preparaherquamide, the spirocycle formation in paraherquamides was identified to be catalyzed by the FAD-dependent monooxygenase (FMO) PhqK (Scheme 28).[81] Two new paraherquamide derivatives (i.e., paraherquamides K and L) were accumulated by the *phqK*-knockout strain of *P. simplicissimum*, indicating that these two compounds might be the substrates of PhqK. Subsequent *in vitro* enzymatic reactions of paraherquamides K and L with PhqK confirmed their conversions into the spirocyclized products paraherquamides M and N, respectively. On the basis of these findings, a revised biosynthetic scheme (Scheme 28) for the production of paraherquamides A and G was proposed, in which spirocyclization occurs after formation of the pyran and dioxepin moieties.

Despite great efforts on elucidation of the whole paraherquamide biosynthetic pathway, there remain a number of uncharacterized biosynthetic steps, such as the formation of the pyran and dioxepin rings, *N*-methylation, and hydroxylation of β-methylproline.

4.2.3. Citrinadins. During the investigation of 21*R*-citrinadin A biosynthesis, several BCDO-containing compounds, including (+)-precitrinadin A and chrysogenamide A, were identified from the wild-type strain or gene-knockout mutants of *Penicillium citrinum* ATCC 9849 (Figure 12).[4,98] One of these compounds, citrinadin-4, is the only natural MKP indole alkaloid with an [*R*,*S*,*R*] configuration (Figure 2) discovered to date.

Liu et al. reported the biosynthetic gene cluster (Figure 7E) of 21*R*-citrinadin A in 2021 and biochemically characterized the functions of four proteins, including NRPS CtdQ, prenyltransferase CtdU, FMO CtdE, and DAase CtdP.[4,98] Based on the gene knockout analysis, CtdQ was confirmed to be responsible for initial synthesis of the dipeptide precursor **58**, and CtdU was deduced to catalyze the normal prenylation at the C7 position (Scheme 29A).[98]

CtdE was characterized to be an oxygenase/semipinacolase, which can catalyze oxidative semipinacol rearrangements on

https://doi.org/10.1021/acs.chemrev.4c00250
Chem. Rev. XXXX, XXX, XXX−XXX

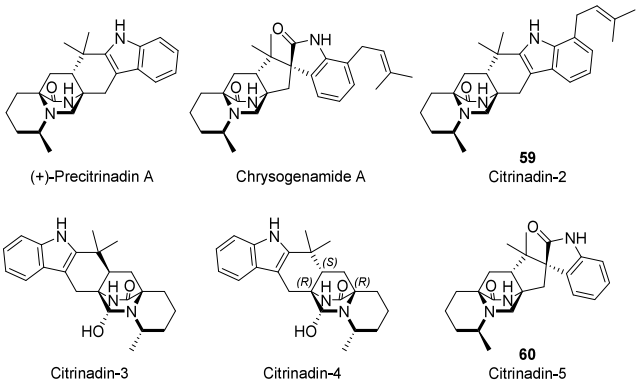

Figure 12. Structures of citrinadin-related natural products.

(+)-precitrinadin A and its prenylated derivative **59**, yielding corresponding spirooxindole products (**60** and chrysogenamide A) (Scheme 29A and B).[98] Unlike the previously characterized FMO PhqK[81] in paraherquamides biosynthesis, which catalyzes the formation of the 3*R*-spirooxindole, CtdE specifies the 3*S*-spirooxindole construction. The crystal structures of CtdE with the substrate and cofactor, site-directed mutagenesis, and computational studies together illustrated the catalytic mechanism for the plausible *β*-face epoxidation followed by a regioselective semipinacol rearrangement of the epoxide intermediate, thus forming the 3*S*-spirooxindole (Scheme 29B and Figure 13A).

Recently, the Gao and Sherman laboratories reported the discovery and characterization of CtdP as the member of a new class of bifunctional oxidoreductase/DAase, which catalyzes the inherently disfavored cycloaddition to form the BCDO core with a strict *α-anti*-selectivity in the biosynthetic step of generating the IMDA product (+)-precitrinadin A.[4] Based on the crystal structure of CtdP in complex with the cofactor $NADP^+$ and product, mutagenesis analysis, and quantum chemical calculations, a detailed unique redox mechanism of CtdP catalysis was proposed (Scheme 29C). Briefly, the substrate **61** is first bound to the active pocket of CtdP, preorganized into an *α-anti* conformation, and subsequently oxidized by cofactor $NADP^+$ to generate the oxidized intermediate **62** with an active iminium diene, which is likely stabilized by the 2′-OH of NADPH and residue Tyr280 (Figure 13B). The active dienyl iminium then undergoes a highly stereoselective IMDA cycloaddition to form an iminium adduct **63**, and a reductive rescue by NADPH generates the final *α-anti*-cycloadduct precitrinadin.

5. TOTAL SYNTHESIS

During the course of overcoming the daunting synthetic challenges associated with total syntheses of the BCDO-containing indole alkaloids, various synthetic approaches and elegant strategies/methodologies to manage the diastereo- and enantioselectivity have been developed. To construct the BCDO skeleton, intramolecular SN2′ cyclizations, biologically inspired Diels–Alder reactions, radical involved cyclizations, cationic involved cascade reactions, and other strategies have been explored. Of note, the majority of the biomimetic synthetic approaches share a common chemical logic of IMDA to assemble the core structures. Importantly, all these synthetic efforts have significantly advanced the understanding of biosynthesis, especially before the genomic era.

5.1. Total Synthesis of Brevianamides

In 1988, Williams and co-workers accomplished the first enantioselective total synthesis of brevianamide B using the stereocontrolled intramolecular S_N2' cyclization strategy (Scheme 30).[13,18,99] The 18-step total synthesis began with the known enantiomerically pure proline derivative **64**. Nucleophilic addition of the lactone with *p*-methoxybenzylaminolithium reagent **65** gave the protected chiral proline amide **66**, which was further converted to the DKP **67** via acylation and alkylation. Ozonolysis followed by Wittig olefination and reduction provided the homologated *E*-allylic alcohol **70**, which was protected to afford the silyl ether and further transformed to the intermediate **71** as a mixture of 4:1 diastereomers via carbomethoxylation. The mixture was directly used for the diastereoselective Kametani condensation to yield the intermediate **73**. This intermediate was converted into the allylic chloride **74** via four straightforward steps, including hydrolysis/decarboxylation of methyl formate, Boc protection of indole, deprotection of the TBS group, and chlorination of the resulting alcohol. With the key precursor **74** in hand, the subsequent intramolecular S_N2' cyclization was performed to build up the crucial C10-stereogenic center under the previously established conditions using a model substrate (NaH, DMF, r.t.).[100] The authors found that, when the reaction was performed in hot benzene with 18-crown-6 as additive, the cyclization products **75a**/**75b** were produced at a 1:3.85 ratio in a 56% combined yield. Finally, the S_N2' cyclization in a 1:3–4.9 ratio with NaH (10 equiv) and 18-crown-6 (5.0 equiv) in warm THF gave a 64–77% combined yield of **75**. After deprotection and olefin/cation cyclization, the resulting hexacyclic indole **76** was oxidized, producing the stereospecific hydroxyl indolenine **77**, which was treated with NaOMe to form the indoxyl **78** via pinacol rearrangement. The *p*-methoxylbenzyl group was finally removed with the use of *t*-BuLi and O_2 to give the final product, brevianamide B, in a 40% yield. This very first synthesis of brevianamide B not only demonstrated an efficient strategy of the intramolecular S_N2' cyclization to build the BCDO skeleton but also provided direct evidence for the structure originally proposed by Birch.[7]

In 1998, the same group developed the total synthesis of racemic brevianamide B in 12 steps[22,23] (Scheme 31). Essentially, a biomimetic IMDA reaction was first used as the key step to construct the BCDO skeleton of brevianamide B, starting from a known substrate *epi*-deoxybrevianamide E (**79**), which was converted to the lactim ether **80** with the combined utility of Me_3OBF_4 and $NaHCO_3$ in CH_2Cl_2. Next, the oxidation of **80** with DDQ yielded the IMDA precursor **81**. Upon the treatment of **81** with aq. KOH to form **82**, the labile azadiene underwent the biomimetic IMDA reaction to produce the BCDO core of brevianamide B with a 2:1 ratio of two diastereomers (**83**/**84**) in a 60% combined yield. The minor diastereomer **84** with the right stereochemistry was further transformed to the final racemic brevianamide B via sequential reactions of oxidation, pinacol rearrangement, and deprotection of the lactim ether. This is the first application of the biomimetic IMDA strategy to build a BCDO skeleton, although the diastereoselectivity did not favor the desired diastereomer.

During the explorations of brevianamides synthesis, more total synthetic approaches were reported. In 2006, Adams et al. developed the third generation of the bioinspired IMDA strategy to synthesize brevianamide B.[24] As shown in Scheme 32, the synthesis started from the readily available **86**, which

https://doi.org/10.1021/acs.chemrev.4c00250
Chem. Rev. XXXX, XXX, XXX–XXX

Scheme 29. Biosynthesis of 21*R*-Citrinadin A. (A) The Partially Characterized Biosynthetic Pathway. (B) The Catalytic Mechanism of Oxygenase/Semipinacolase CtdE. (C) The Catalytic Mechanism of DAase CtdP

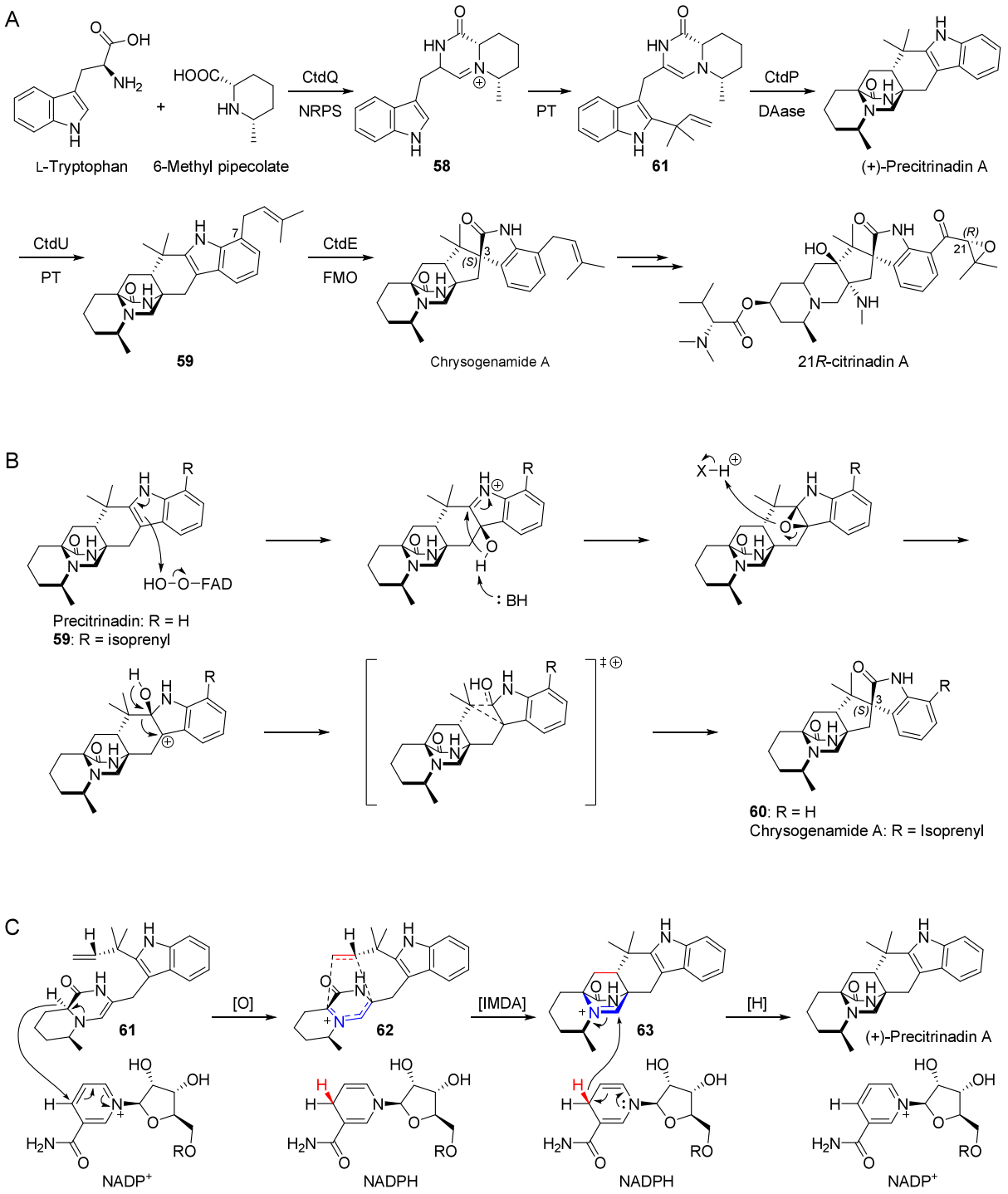

underwent the conjugate addition to afford the ester **88** in a 76% yield. Hydrolysis of the ester with LiOH in THF/EtOH/H_2O gave rise to the acid **89**, followed by amide coupling with L-prolinamide **90** to produce the intermediate **91** in a 77% yield, which was deprotected under oxidative conditions using NCS and $AgNO_3$ to afford a mixture of DKP **93** and the acyclic amide **92**. Treatment of the mixture with 3 equiv of $AlCl_3$ under reflux yielded the desired IMDA product **94**. The IMDA product containing a BCDO moiety was further converted into the corresponding hydrazone and then to the intermediate **7** in the presence of $ZnCl_2$ via the Fischer indole reaction. The 2,3-disubstituted indole **7** was oxidized to afford the 3-hydroxyindolenine, and then the pinacol rearrangement generated the final racemic brevianamide B under basic conditions. In this concise synthetic route, brevianamide B was synthesized in 9 steps from a known ketone via the IMDA and Fisher indole reactions as the key steps.

The unprotected DKP **95** was originally proposed in 1970 as the putative biosynthetic intermediate for the construction of the BCDO skeleton in nature. In 2007, the Williams group

https://doi.org/10.1021/acs.chemrev.4c00250
Chem. Rev. XXXX, XXX, XXX−XXX

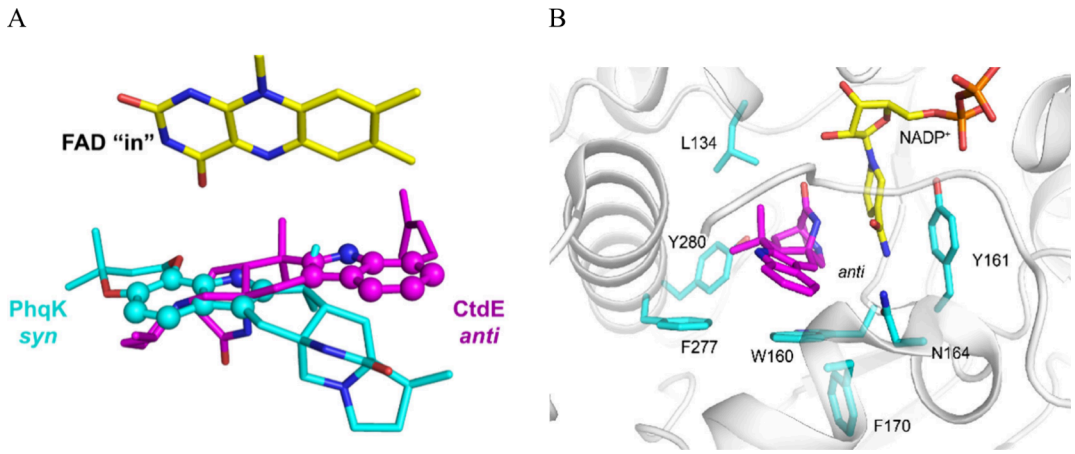

Figure 13. Structural analysis of PhqK, CtdE and CtdP. (A) Superposition of substrate bound PhqK and CtdE complexes. The respective *syn* and *anti* substrates bound in opposing orientations in accordance with their differing facial selectivity. (B) Active site of product-bound CtdP. Amino acid residues that were shown to be essential for *anti* selectivity are shown as cyan sticks.

Scheme 30. First Total Synthesis of Brevianamide B

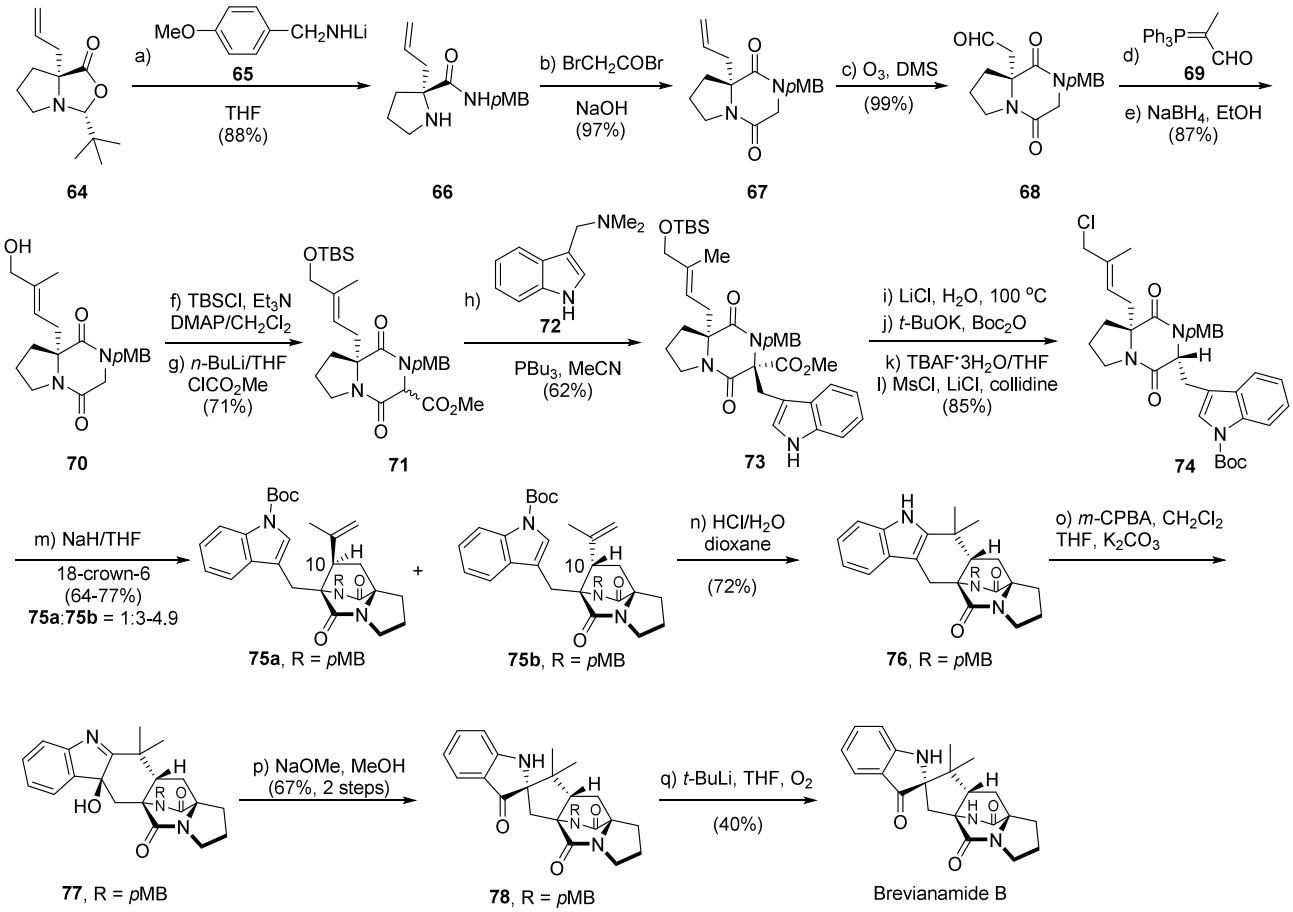

reported for the first time that it could be used as a starting material for the biomimetic total synthesis of (−)-brevianamide B via the classical Mitsunobu conditions (Bu_3P, DEAD) based IMDA cycloaddition, thus avoiding the utility of a protecting group on the lactam.[45,101] In this regard, the total synthesis of brevianamide B was completed in 14 steps. (Scheme 33)

Simpkins et al. also accomplished the synthesis of brevianamide B by starting from a prenylated proline derivative prepared with the Seebach "self-reproduction of chirality" method. Next, a cationic cascade sequence was adopted as the key step to form the late-stage bridged DKP intermediates.[102] As shown in Scheme 34, the synthetic intermediate **97** was coupled with indole-3-pyruvic acid **98** to afford the closed hydroxy-DKP **99**, which further underwent the key cationic cascade sequence mediated by TMSOTf to form the desired BCDO skeleton **100**/**101** (4:1 dr). After purification, the minor C-6 epimer **101** was oxidized to form intermediate **102**,

https://doi.org/10.1021/acs.chemrev.4c00250
Chem. Rev. XXXX, XXX, XXX−XXX

Scheme 31. Biomimetic Synthesis of Racemic Brevianamide B via the [4+2] IMDA Strategy

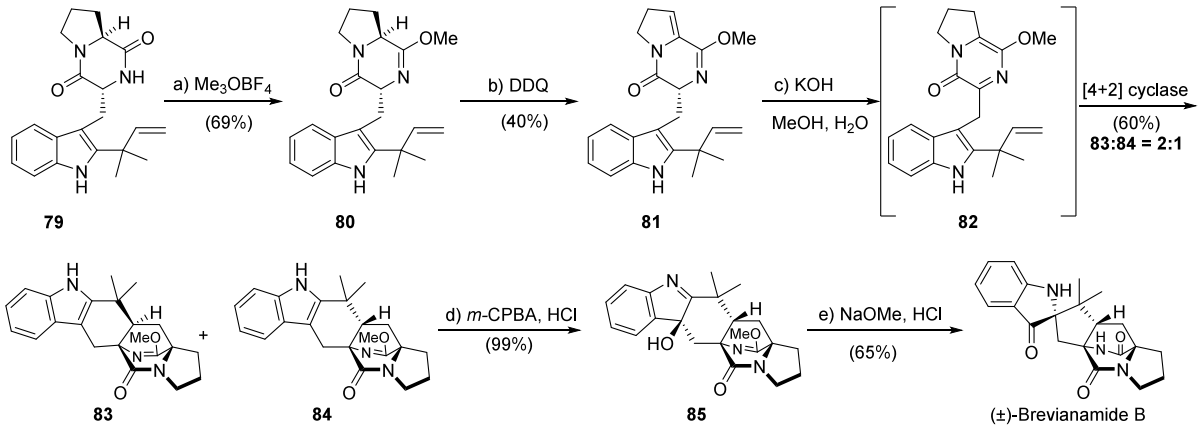

Scheme 32. Synthesis of Brevianamide B Based on the IMDA/Fischer Indole Strategy

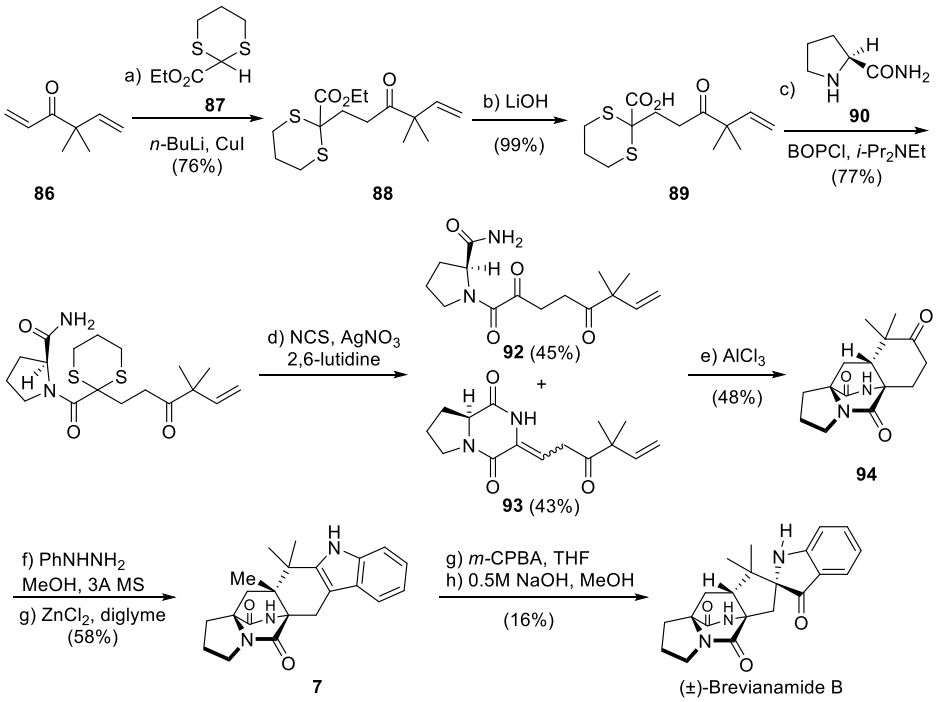

Scheme 33. Modified IMDA Cycloaddition under the Mitsunobu Condition

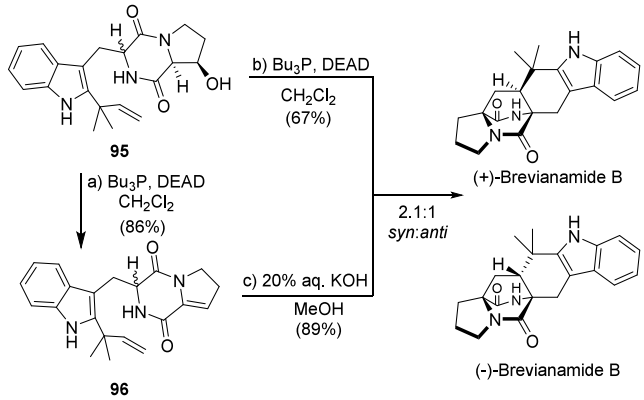

which underwent the semi-pinacol rearrangement to give the spiro-indoxyl **103**. The following deprotection and oxidation achieved the final production of *ent*-brevianamide B.

Scheerer and co-workers reported two other formal syntheses of brevianamide B.[103,104] In their process, the BCDO core structure was built by an early stage IMDA reaction. The straightforward cycloaddition of prazinone **105** with electron-deficient dienophile maleic anhydride **109** at room temperature produced the corresponding cycloadducts **110**/**111** in a moderate yield with high diastereoselectivity (1:8), which could be further transformed into the known intermediate **7** to realize the production of brevianamide B[45,99] (Scheme 35).

Despite five decades of research efforts, brevianamide A remained an elusive target for chemical synthesis due to several unsolved issues of reactivity and selectivity. All attempts to synthesize brevianamide A ended up with the formation of brevianamide B or other undesired isomers. Until recently, Lawrence and co-workers speculated a modified biosynthetic

https://doi.org/10.1021/acs.chemrev.4c00250
Chem. Rev. XXXX, XXX, XXX−XXX

Scheme 34. Synthesis of *ent*-Brevianamide B

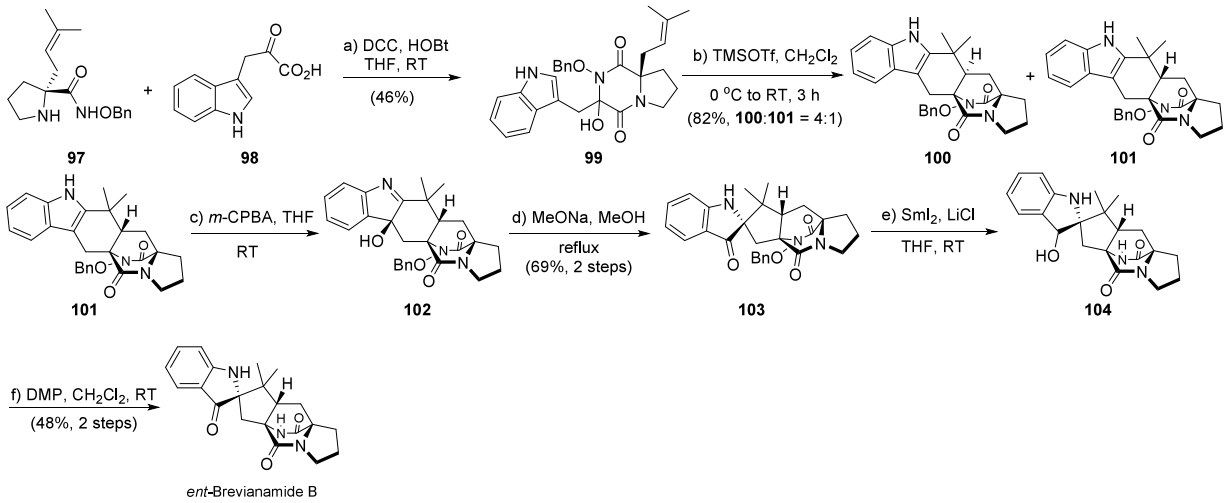

Scheme 35. Early Stage IMDA Reactions for the Formal Syntheses of Brevianamide B

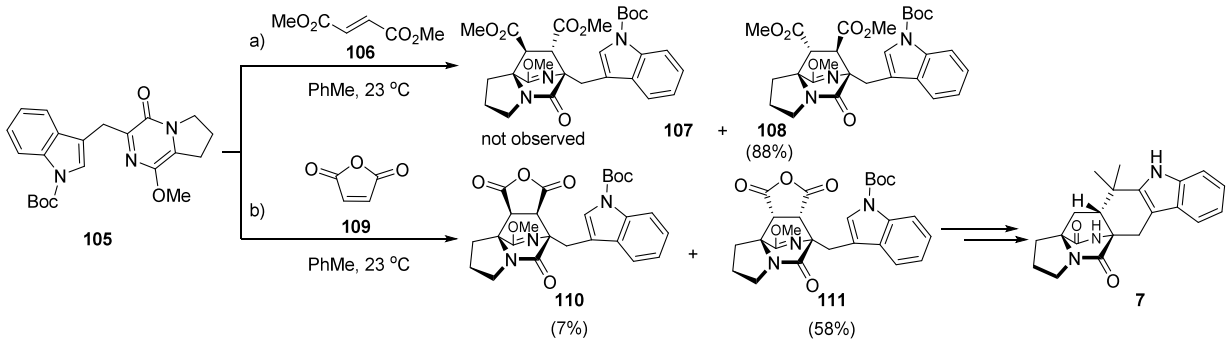

pathway of brevianamide A and finally achieved the chemical synthesis of the topologically complex bridged-*spiro*-fused structure.[26] As shown in Scheme 36, the concise total synthesis of brevianamide A followed a bioinspired cascade from (−)-dehydrobrevianamide E to brevianamide A. Starting from L-tryptophan methyl ester **112**, phthaloyl protection of this commercially available reagent gave the ester **114**, which was transformed to the intermediate **116** using B-prenyl-9-borabicyclo[3.3.1]nonane **115** with *t*-BuOCl and Et_3N in THF. Then, hydrolysis of the methyl ester with LiOH in H_2O/THF was conducted; meanwhile, the phthaloyl group was opened to form the unwanted diacid **117**. Many hydrolysis conditions to remove the methyl ester group were screened, and the Krapcho-type demethylation with the use of LiCl in DMF was found to form the desired lithium carboxylate **118**, which was transformed to the acyl chloride under standard conditions, forming the *N*-acyl enamine **120** in one-pot operation with dehydroproline **119**. The deprotection of the phthaloyl using hydrazine, methylamine, and ethylene diamine produced the unwanted byproducts. However, the use of ammonia, a less nucleophilic reagent in methanol, smoothly deprotected the phthaloyl group and the resulted primary amine could undergo the spontaneous cyclization to produce (+)-dehydrodeoxy-brevianamide E in a 49% yield for 3 steps, avoiding the protecting group transformations. Thus, the synthesis of (+)-dehydrodeoxy-brevianamide E was realized in five steps with a 34% overall yield. It is worth mentioning that only two chromatographic purification steps were required, providing the most convenient total synthesis of (+)-dehydrodeoxy-brevianamide E compared with the previous report (12 steps, 8% overall yield).[45]

With the efficient synthesis of (+)-dehydrodeoxy-brevianamide E as the key synthetic intermediate, the chemical oxidation to form dehydrobrevianamide E was further investigated by screening of a variety of chemical oxidants including peroxyl acids, dioxiranes, singlet oxygen and so on. Upon optimization of the oxidative conditions, it was revealed that the slow addition of 1 equiv of *m*-CPBA to dehydrodeoxybrevianamide E in $CHCl_3$ at room temperature could produce the corresponding diastereomers dehydrobrevianamide E/**121**) in a 57% overall yield (dr 63:37). The intermediate dehydrobrevianamide E was converted into natural (+)-brevianamide A in a moderate yield after being treated with LiOH in water for 30 min, together with (+)-brevianamide B as a minor product. Putatively, **121** could similarly result from a late-staged IMDA reaction, giving rise to the unnatural (−)-brevianamides A and B upon the same treatment.

Thus, the Lawrence group came up with the first and efficient biomimetic total synthesis of natural (+)-brevianamide A in 7 steps, together with (+)-brevianamide B and the unnatural (−)-*ent*-brevianamides A and B as minor products. The key steps included the 1,2-shift to construct the indoxyl skeleton via the transient 3-hydroxyindolenine species, and the tautomerization/IMDA reaction sequence, demonstrating the advantages in the efficiency of divergent total synthesis of brevianamides.

https://doi.org/10.1021/acs.chemrev.4c00250
Chem. Rev. XXXX, XXX, XXX−XXX

Scheme 36. Lawrence Total Synthesis of Brevianamides A and B

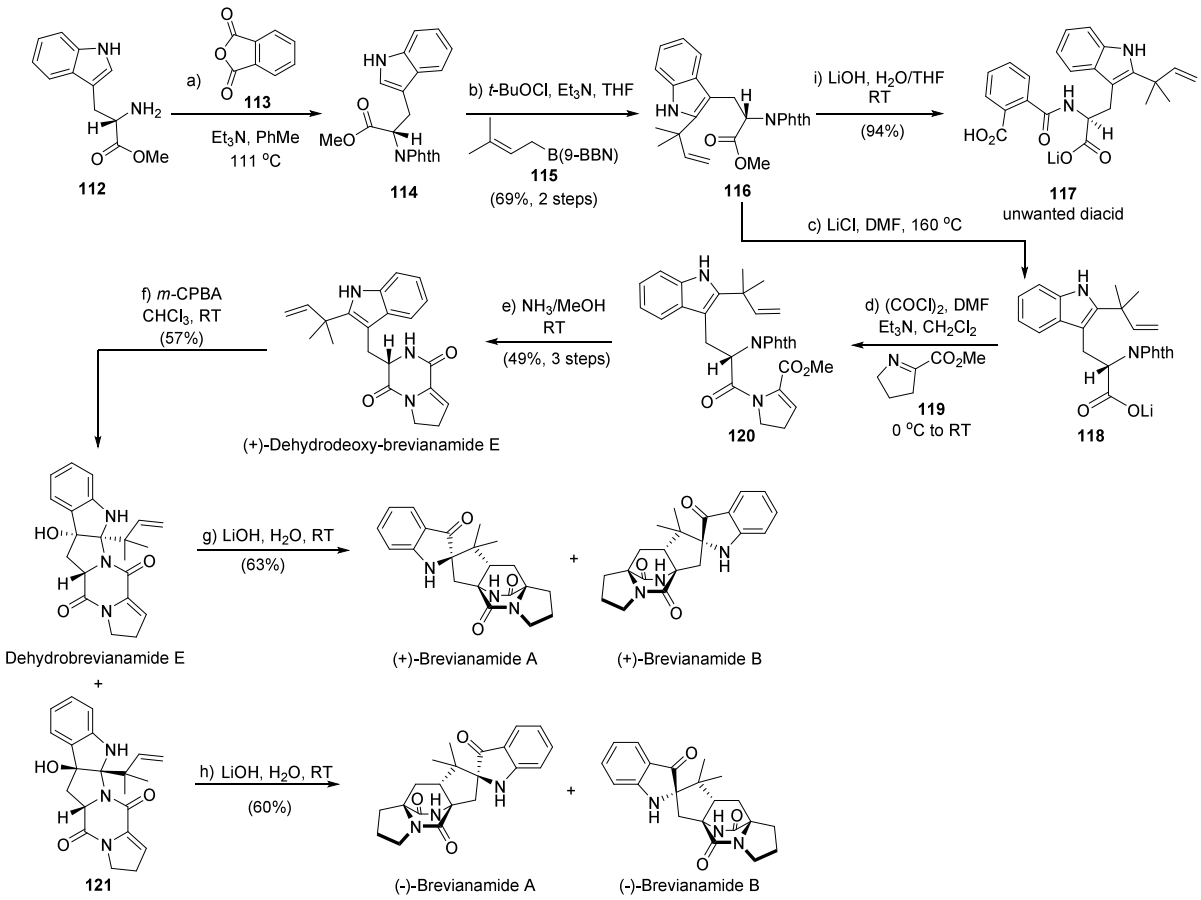

During the synthesis of (+)-brevianamide B, Williams and co-workers found that the indole **7** could be oxidized by oxaziridine **122** and the resulting intermediate could undergo the rearrangement to form oxindole, which was later identified as the natural product brevianamide Y in 2017 (Scheme 37A).[45,101,105] In 2015, Qin et al. reported the total synthesis of the unnatural (−)-enantiomer of brevianamide Y, which was named as depyranoversicolamide B. As shown in Scheme 37B, the intermediate **123**, synthesized in 16 steps, was oxidized to afford *ent*-brevianamide Y in two steps.[106] In 2020, based on their biosynthetic knowledge, Williams, Sherman, Li and co-workers completed the synthesis of brevianamide Y in 12 steps (Scheme 37C).[2] In 2022, Lawrence and co-workers also successfully demonstrated the feasibility of these IMDA transformations through chemical approaches and established the biomimetic chemical synthesis of brevianamides Z, Y, and X (Scheme 37D).[31] They found that the intermediate (+)-dehydrodeoxy-brevianamide E could be converted into brevianamides Y and Z in two chemical steps. When treated with NCS (*N*-chlorosuccinimide) and aqueous TFA in methanol, dehydrodeoxybrevianamide E was transformed to oxindoles **16** and **124** in good yields as separable mixtures (d.r. 69:31). Then the major diastereoisomer oxindole **16** underwent the Sammes-type Diels−Alder reaction to afford the natural product brevianamide Y and another diastereoisomer named as brevianamide Z, while the minor diastereoisomer oxindole **124** would be transformed to *ent*-brevianamide Y and *ent*-brevianamide Z. Of note, brevianamide Z therein was a predicted natural product by Lawrence and co-workers that had yet to be isolated. Another natural product called brevianamide Z was isolated later in 2022 by Liu and co-workers,[34] which is a different compound not discussed in this review. Furthermore, (+)-dehydrodeoxy-brevianamide E could be used for efficient production of the BCDO skeleton in a moderate yield with two diastereoisomers (d.r. 57:43 of **125** and **7**). The major diastereomer **125** was converted to (+)-brevianamide X in a 50% yield over two steps.

In 2021, Smith et al. established a useful methodology to construct the 2,2-disubstituted indoxyl skeleton.[107] A readily available 2-substituted indole was converted into 2,2-disubstituted indoxyls through nucleophile cross-coupling with a 2-alkoxyindoxyl species in the presence of *p*-TsOH as catalyst. Based on this methodology and inspired by the Lawrence work,[26] another concise total synthesis of brevianamide A in 7 steps without the 1,2-shift was established. As shown in Scheme 38, this synthesis was initiated with the protected amino acid **127**, which was transformed into the enamide **129** by coupling with the imine **119** under the Ghosez's condition. Then palladium catalyst **131** and CuI catalyzed Sonogashira coupling of **129** and 2-iodoaniline (**130**), producing the 2-alkyny aniline **132**, which was further converted to the indole **134** in the presence of JohnphosAu(MeCN)SbF_6 (**133**). The oxidation with MoOPH (**135**) produced the desired 2-ethyoxylindoxyl intermediate, which further underwent the key nucleophile coupling reaction with a prenyl coupling partner **136** to afford the indoxyl **137** as a mixture of two diastereomers (d.r. 1.2:1). Finally, the use of the Lawrence condition delivered (+)-brevianamide A. Overall, the total synthesis of brevianamide A was achieved in 7 steps with a 6% overall yield.

https://doi.org/10.1021/acs.chemrev.4c00250
Chem. Rev. XXXX, XXX, XXX−XXX

Scheme 37. Approaches for Synthesis of Brevianamides X, Y and Z

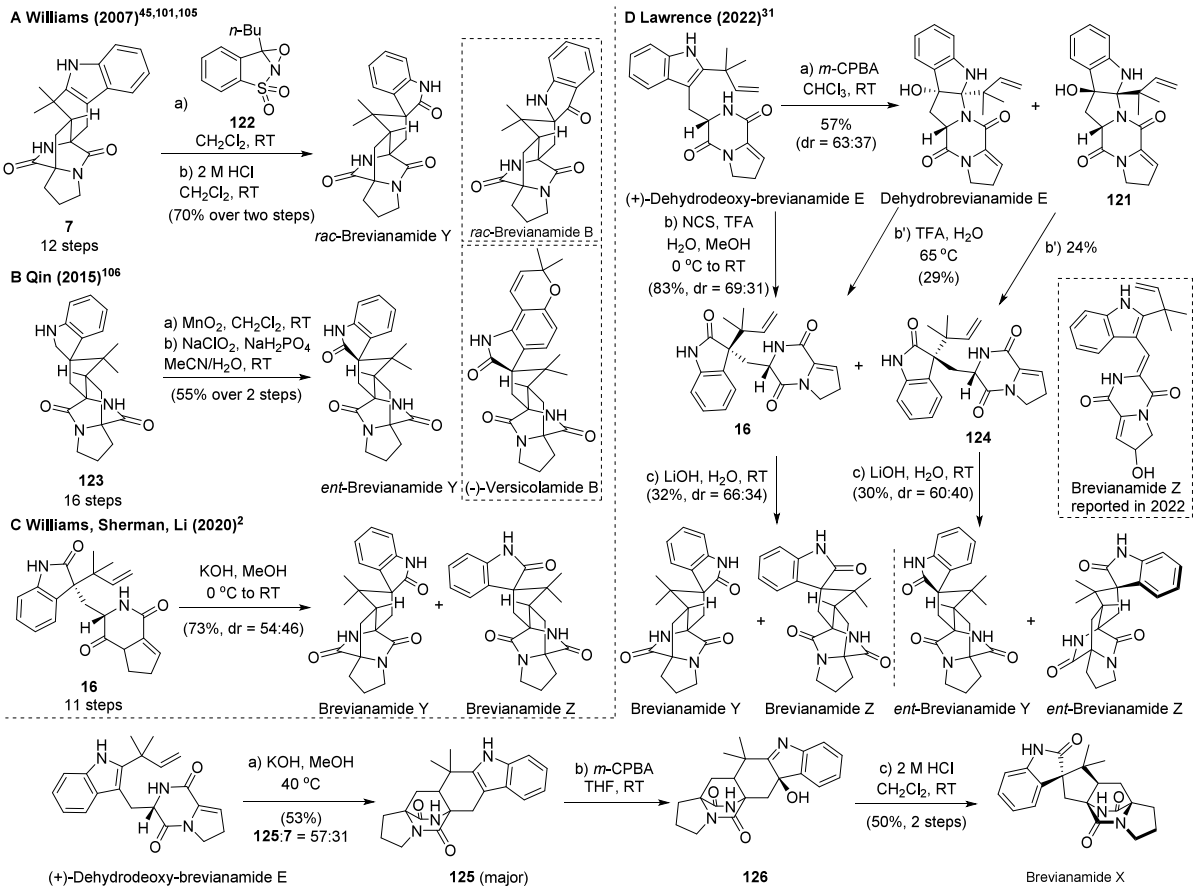

Scheme 38. Smith's Total Synthesis of Brevianamide A

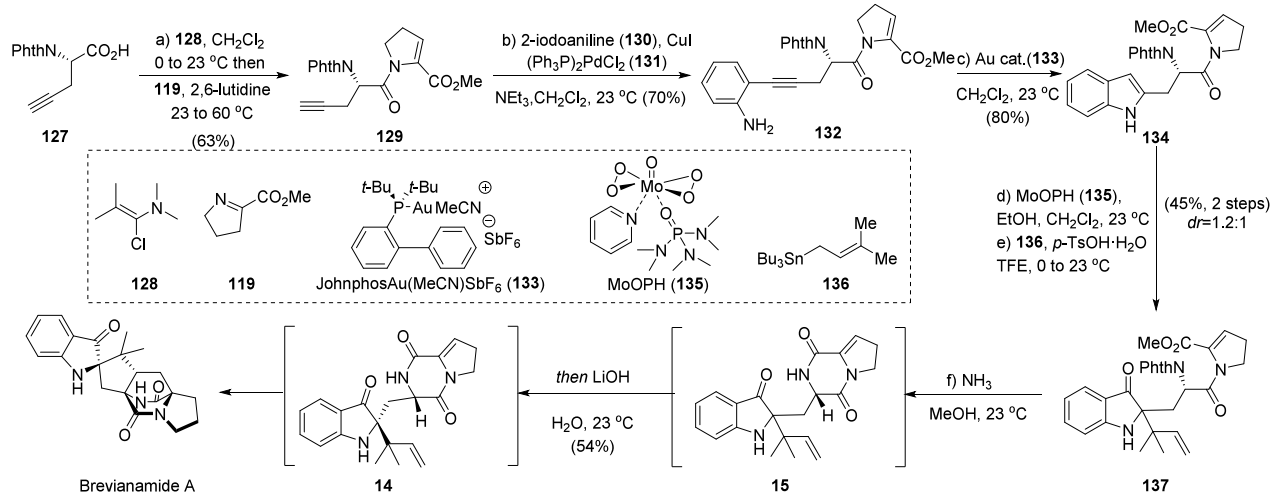

In 2022, Gagosz and co-workers reported other concise approaches to realize the total synthesis of (±)-brevianamide A using a readily available starting material **138** (Scheme 39).[108] Essentially, a gold(I)-catalyzed cascade transformation was developed as the key step to quickly build the pseudo-indoxyl core of brevianamide A with two adjacent quaternary centers, giving rise to the shortest total synthesis of (±)-brevianamide A to date.

5.2. Notoamides, Stephacidins and Avrainvillamide

In 2005, Baran and co-workers reported the first total synthesis of stephacidin A from commercially available L-proline and pyroglutamate in 15 steps (Scheme 40).[109] In the work, an oxidative enolate coupling reaction was adopted as the key step to construct the BCDO skeleton. The protected amino acid **144**[109] was coupled with the proline derivative **145** to form **146.** Then deprotection of the Cbz carbamate afforded the DKP **147**, which was further protected with MOM-Cl to produce the precursor **148** of the oxidative enolate coupling.

https://doi.org/10.1021/acs.chemrev.4c00250
Chem. Rev. XXXX, XXX, XXX−XXX

Scheme 39. Gagosz's Approach toward the Total Synthesis of (±)-Brevianamide A

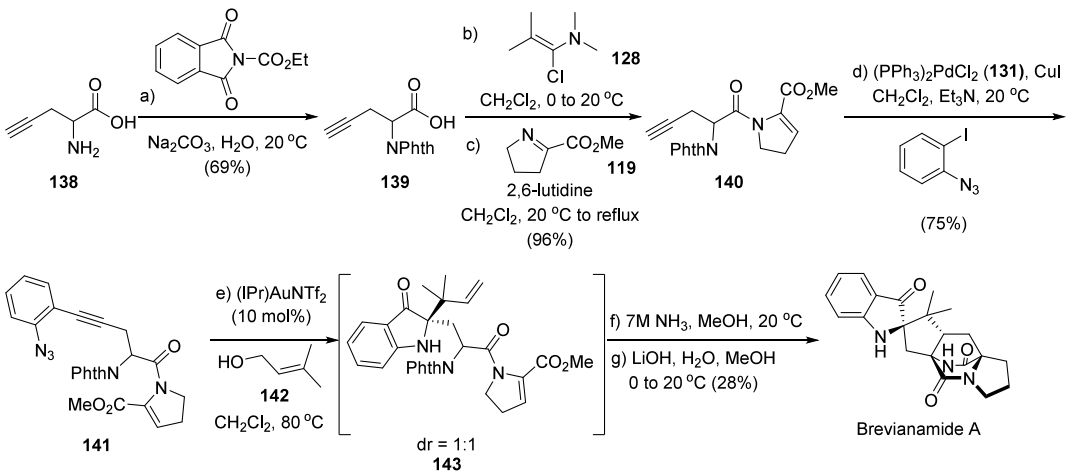

Scheme 40. Baran's First Total Synthesis of (+)-Stephacidin A

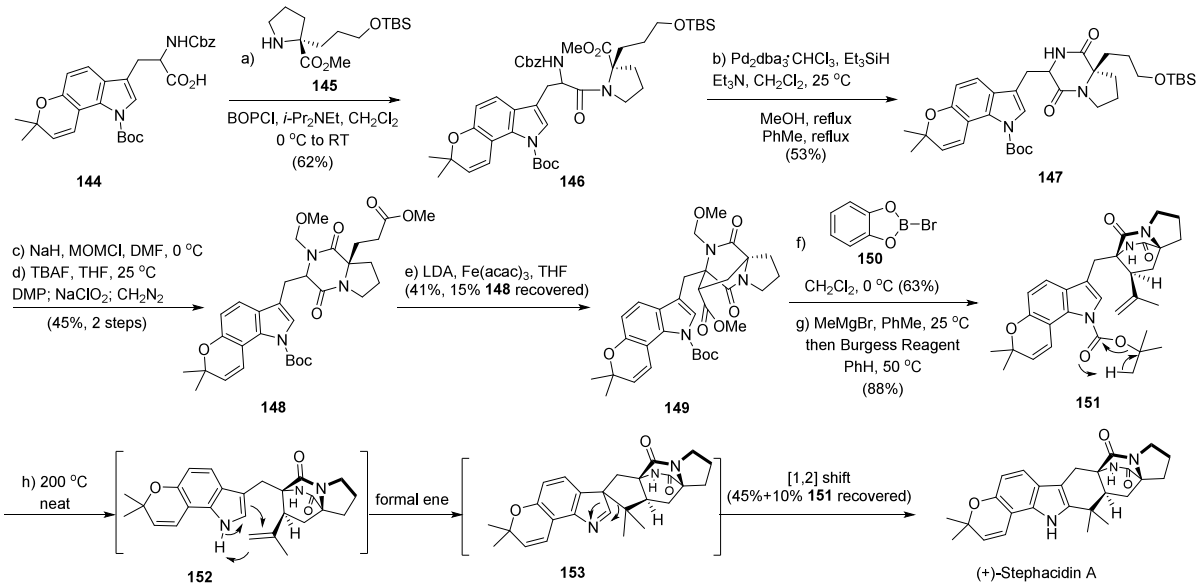

Scheme 41. Baran's Second Total Synthesis of (−)-Stephacidin A

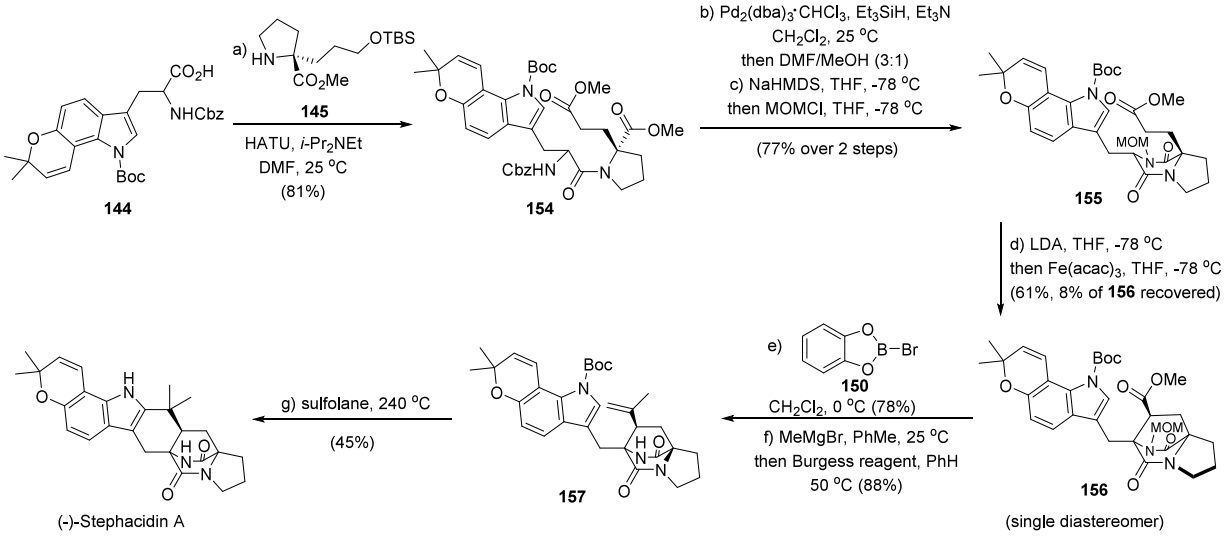

https://doi.org/10.1021/acs.chemrev.4c00250
Chem. Rev. XXXX, XXX, XXX−XXX

Scheme 42. Transformation from Stephacidin A to Avrainvillamide and (−)-Stephacidin B

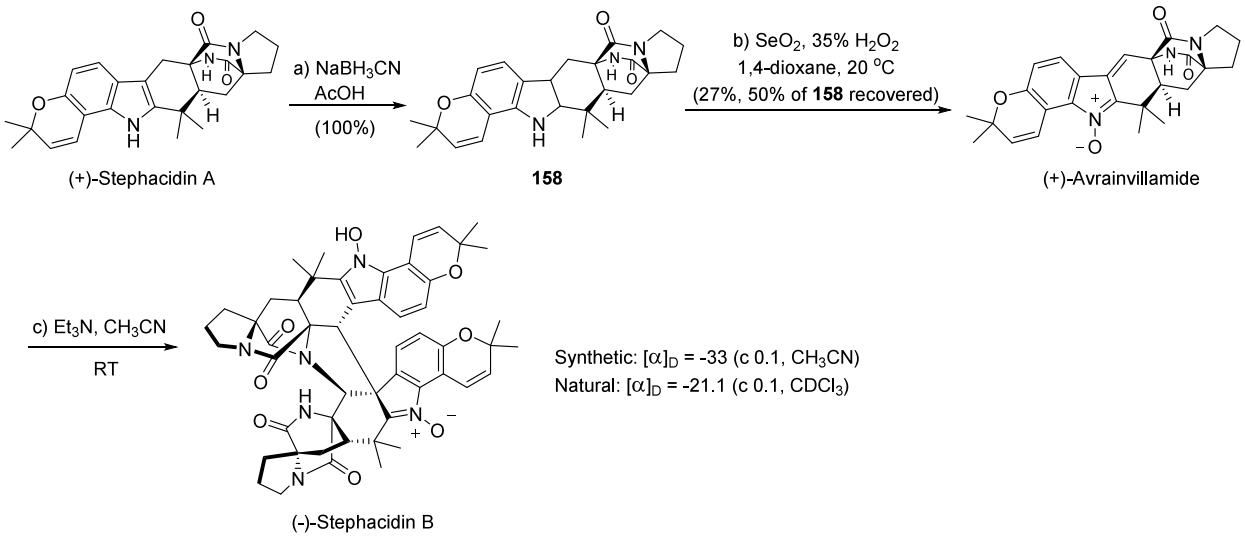

Scheme 43. Myers Total Synthesis of (−)-Avrainvillamide and (+)-Stephacidin B

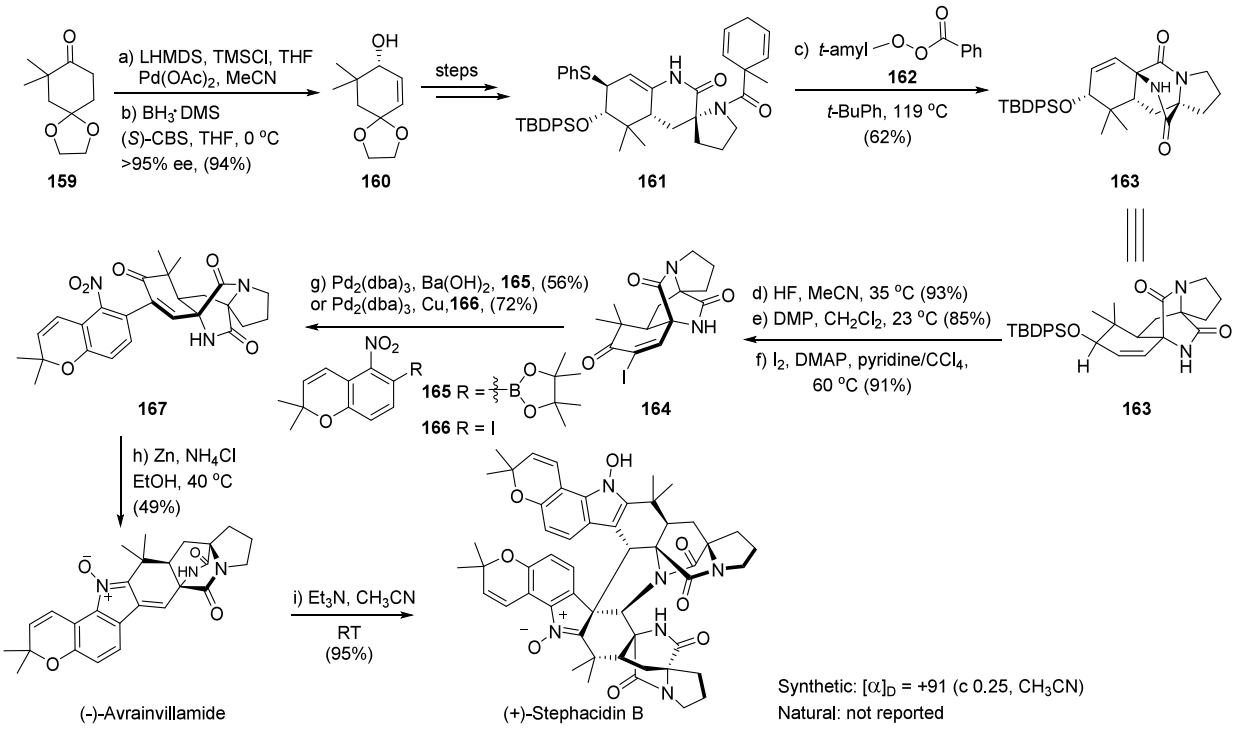

Next, a series of oxidative reagents were screened and $Fe(acac)_3$ was found to be the best choice. Thus, the combined utility of $Fe(acac)_3$ and LDA realized the coupling product **149**. The MOM-protecting group was deprotected and then the disubstituted alkene **151** was generated via sequential transformations, which underwent the deprotection of the Boc group and sequential cyclization to complete the total synthesis of stephacidin A.

Later in the same year, the same group further developed an improved synthesis of (−)-stephacidin A.[110] As illustrated in Scheme 41, the proline derivative **145** was used as one of the starting materials, which underwent the peptide coupling with **144** to afford **154**. Then deprotection of the Cbz-group generated the lactam, which was protected with the MOM-protecting group to afford the enolate coupling precursor **155**. In this regard, the yield of this straightforward enolate coupling reaction was enhanced, achieving the construction of the BCDO core. Of note, the thermal annulation became more reproducible by using sulfolane at 240 °C. In sum, both (+)-stephacidin A and (−)-stephacidin A could be synthesized in 7 steps with a 12% overall yield from readily available starting materials.

On the basis of the total synthesis of stephacidin A, Baran and co-workers further developed a two-step sequence from stephacidin A toward the synthesis of (+)-avrainvillamide. Upon the treatment with $NaBH_3(CN)$, the indole pyrrole ring of (+)-stephacidin A was reduced to the saturated intermediate **158**. However, only a trace amount of avrainvillamide could be

https://doi.org/10.1021/acs.chemrev.4c00250
Chem. Rev. XXXX, XXX, XXX−XXX

Scheme 44. Intramolecular S_N2' Cyclization Approach toward Stephacidins and Avrainvillamide

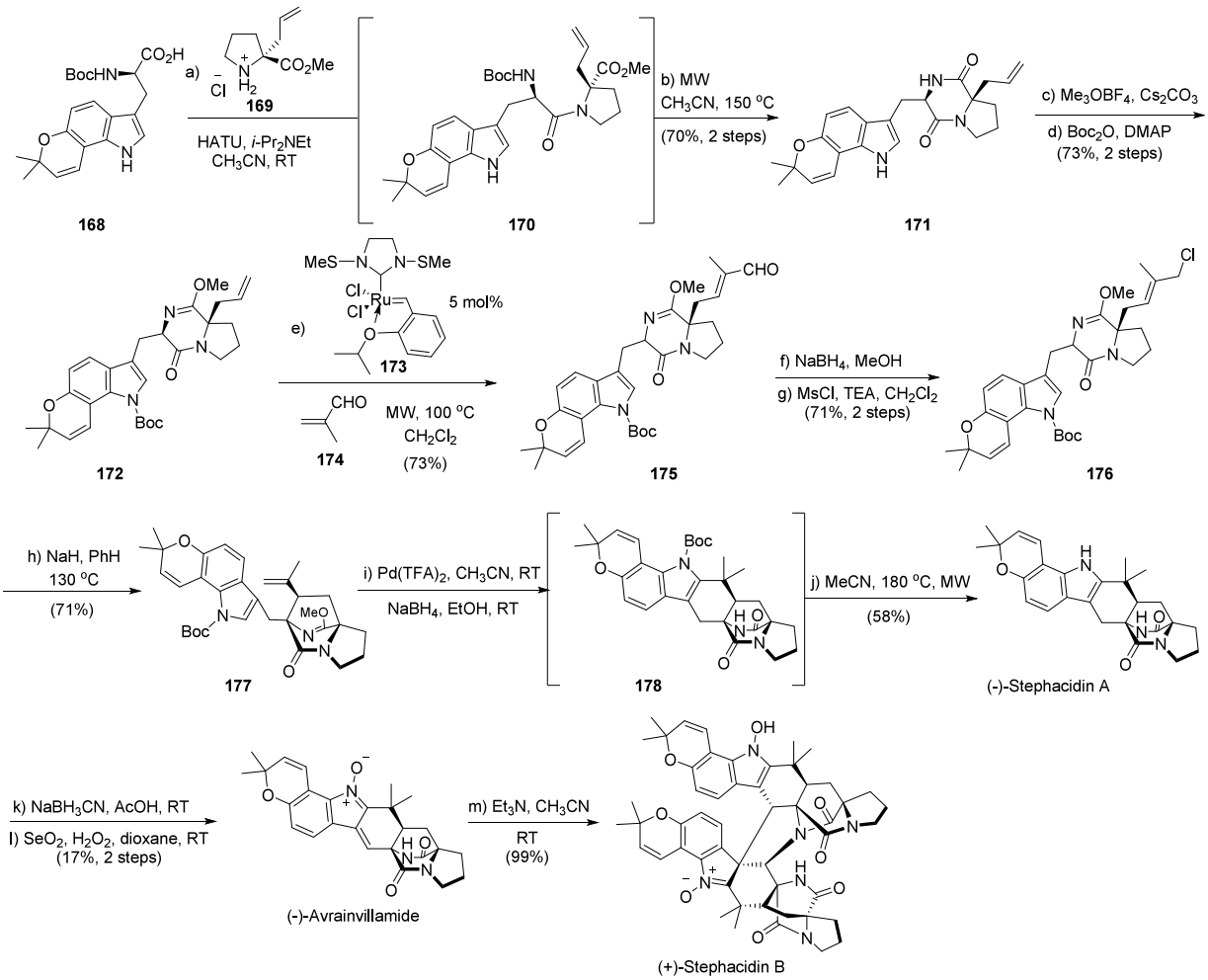

detected under Somei conditions. After intense screening of different oxidative systems, the authors found that SeO_2/H_2O_2 induced the transformation from **158** to (+)-avrainvillamide in a 27% yield (Scheme 42),[111] which was then dimerized to form (−)-stephacidin B.

Meanwhile, the Myers group reported an enantioselective total synthesis of (−)-avrainvillamide and (+)-stephacidin B (Scheme 43).[112] The total synthesis started from the readily available achiral cyclohexanone derivative **159**.[113] Saegusa oxidation of **159** led to the corresponding α,β-unsaturated skeleton, which was enantioselectively reduced to the chiral alcohol intermediate **160** with (*S*)-CBS catalyst and BH_3·DMS. Then the chiral substrate **160** was transformed to the radical cyclization precusor **161** via a series of straightforward chemical steps. Heating of **161** in *tert*-butyl benzene with *tert*-amyl peroxylbenzoate **162** at 119 °C under O_2-free atmosphere produced the bridged diketopiperazine core and formed the tetracyclic product **163**. This key transformation involved the generation of an aminoacyl radical intermediate, which attacked the enamide C−C double bond to form the full-substituted carbocenter and finally the phenylthiyl radical. After establishment of the BCDO skeleton, deprotection of the TBDPS group of **163** with HF and subsequent oxidation of the resulting alcohol yielded an enone, which was further transformed to the (*R*)-iodoenone intermediate **164**. Then a Suzuki reaction with **165** or Ullmann-like coupling with **166** afforded the intermediate **167**. Reduction of the nitroarene **167** with activated zinc powder produced the heptacyclic unsaturated nitrone, which was converted into stephacidin B when treated with triethylamine at room temperature. Finally, the heptacyclic unsaturated nitrone was confirmed as the natural product (−)-avrainvillamide.

In 2007, the Williams group reported the total synthesis of stephacidin A, avrainvillamide and stephacidin B using an intramolecular S_N2' cyclization strategy.[46] As shown in Scheme 44, this total synthesis began with the protected tryptophan derivative **168**. Upon coupling with ally proline **169**, microwave-enabled Boc-deprotection, and sequential amide formation, the intermediate **171** was produced. Afterward, a two-step functional group protection gave the Boc-carbamate **172**, which underwent the cross-metathesis with **174** in the presence of Hoveyda−Grubbs second-generation catalyst **173** to form the aldehyde **175** in an excellent yield. Then, the aldehyde was reduced and converted to the allylic chloride **176**, which was subject to the intramolecular S_N2' cyclization to build the BCDO core generating **177**. In this key step, a "closed" transition state driven by contact ion pair was proposed to explain the high *syn*-diastereoselectivity during the intramolecular S_N2' cyclization. Subsequently, the palladium-mediated cyclization of **177** afforded heptacycle **178** and removal of the Boc-group produced the final natural product (−)-stephacidin A. The concise and efficient total synthesis of

https://doi.org/10.1021/acs.chemrev.4c00250
Chem. Rev. XXXX, XXX, XXX−XXX

Scheme 45. Concise Biomimetic Synthesis of Stephacidin A

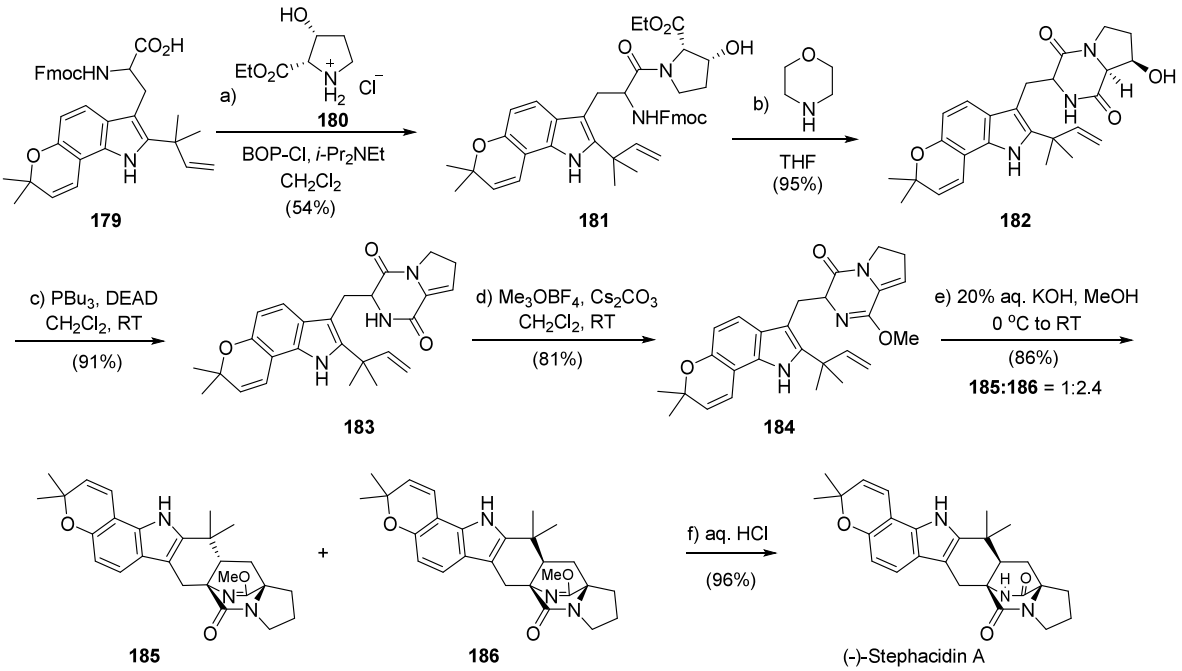

Scheme 46. Concise Total Synthesis of Stephacidin A from an Unprotected DKP

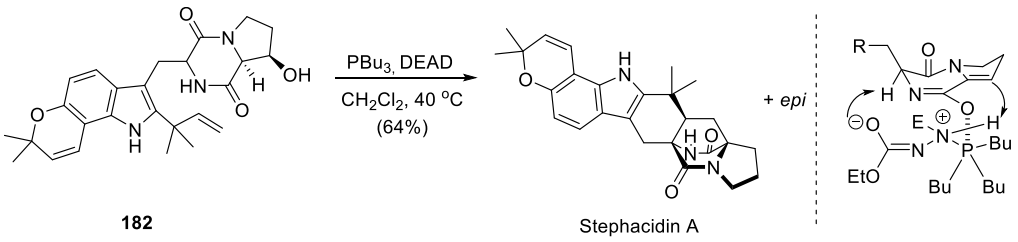

Scheme 47. Chemical Synthesis of Notoamide B from Stephacidin A.

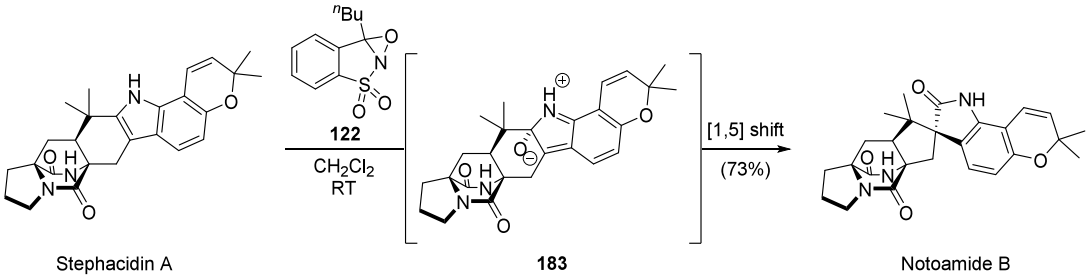

(−)-stephacidin A was realized in merely 17 chemical steps from commercially available substrates with a 6% overall yield. Following the reported methods, the synthetic (−)-stephacidin A was further chemically converted to avrainvillamide and stephacidin B in 2 and 3 steps, respectively. The cross-metathesis reaction to introduce the allylic chloride and the intramolecular S_N2' cyclization were the key steps to achieve this concise total syntheses.

In the same year, Williams and co-workers achieved an even more concise total synthesis of stephacidin A using the biomimetic Diels−Alder cycloaddition strategy (Scheme 45).[47] Specifically, the prenylated tryptophan **179**, synthesized via 11 chemical steps from 6-hydroxylindole, underwent the amide coupling reaction with the chiral proline derivative **180** to form the peptide **181**. Deprotection of the Fmoc group, followed by amide formation, yielded **182**, which was transformed to the enamide **183** via the Mitsunobu dehydration. The lactam was protected to form the lactim ether **184**, which underwent the IMDA reaction to produce the cycloadduct as two diastereomers **185** and **186**. The major isomer **186** was deprotected under acidic conditions to afford stephacidin A in 17 chemical steps with a 5.4% overall yield.

Meanwhile, Greshock and Williams developed another concise total synthesis of stephacidin A.[45] They found that the unprotected DKP intermediate **182** could be transformed to stephacidin A via dehydration, tautomerization, and Diels−Alder reactions after treatment with excess amount of PBu_3 and DEAD. In this work, the zwitterionic complex was proposed to act as proton chaperone during the PBu_3 and DEAD comediated IMDA reaction (Scheme 46).

https://doi.org/10.1021/acs.chemrev.4c00250
Chem. Rev. XXXX, XXX, XXX−XXX

Scheme 48. Simpkins' Synthesis of Stephacidin A and Notoamide B

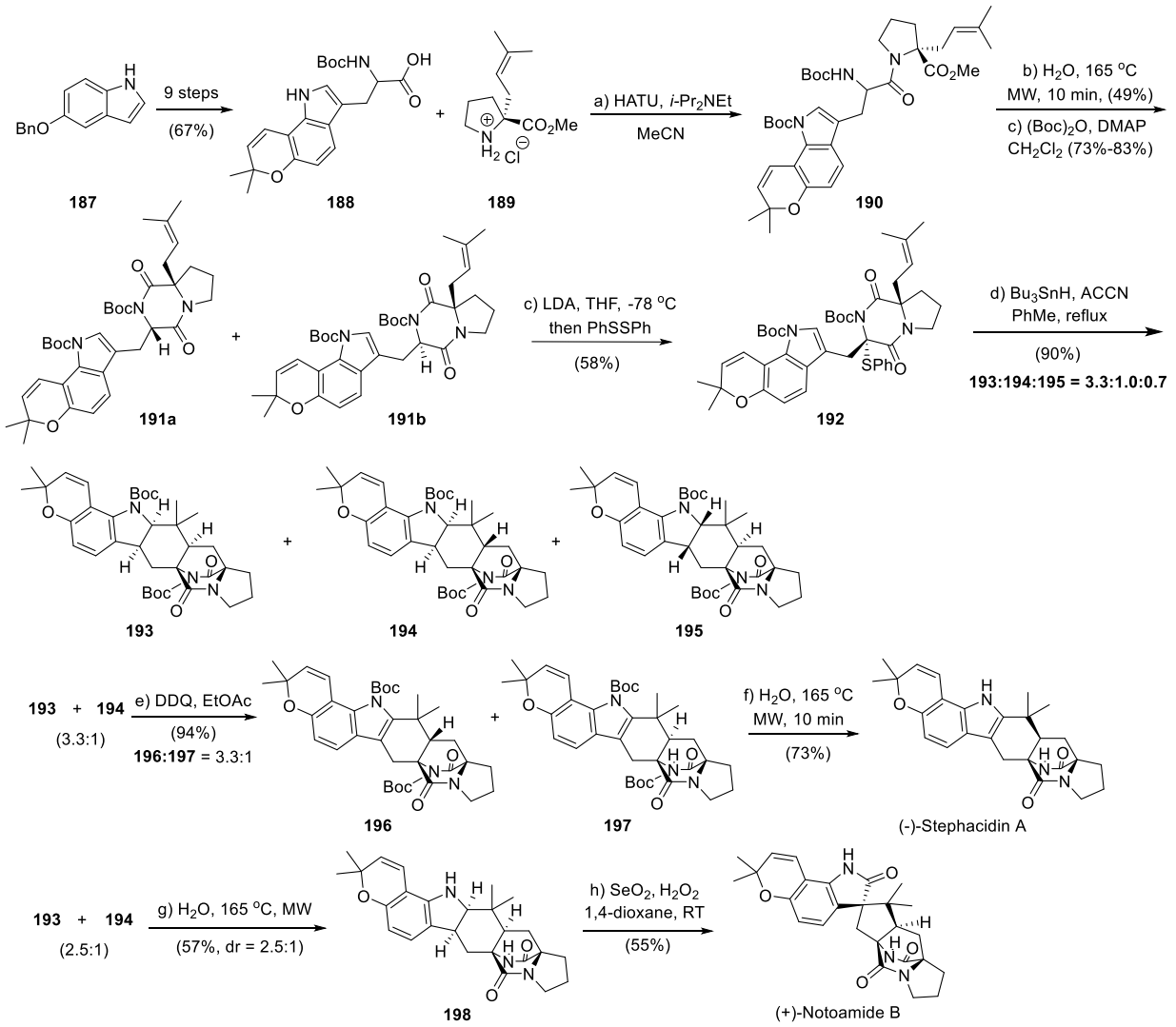

Scheme 49. Transformation from Stephacidin A to Notoamide T

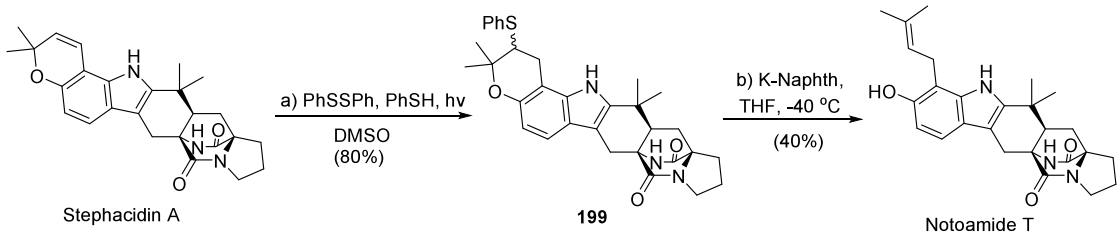

Later, the same group found that an excess amount of oxaziridine **122** in CH_2Cl_2 could induce the oxidative pinacol rearrangement to produce notoamide B as the only product in a 73% yield (Scheme 47). The high selectivity was explained as the epoxidation possibly occurring from the α face of the 2,3-disubstituted intermediate, which is less sterically hindered. Then the diastereoselective [1,5] sigmatropic shift from the α face would produce notoamide B as the single diastereomer.[46,47]

In 2013, Simpkins and co-workers developed a cascade radical cyclization strategy to construct the core of the polycyclic indoline structure to achieve the total synthesis of stephacidin A[114] (Scheme 48). The known intermediate **188** underwent amide coupling with a proline derivative **189** to form intermediate **190**, and then intramolecular amination formed the substituted DKP core with two diastereomers **191a**/**191b**. After protection with a Boc group, the mixture of two diastereomers **191a**/**191b** was transformed to the sulfenylated DKP **192** as a single diastereoisomer in a moderate yield, which further went through the radical cascade cyclization to construct the polycyclic indoline core **193**/**194**/**195** (with a ratio of 3.3:1:0.7). Column purification yielded pure **195** and a mixture of **193**/**194**, which was subsequently oxidized with DDQ to produce indoles **196**/**197**. These indoles were then separated from each other using silica chromatography. Removal of the Boc group gave the final

https://doi.org/10.1021/acs.chemrev.4c00250
Chem. Rev. XXXX, XXX, XXX−XXX

Scheme 50. Concise Total Synthesis of Notoamide T and 6-*epi*-Notoamide T

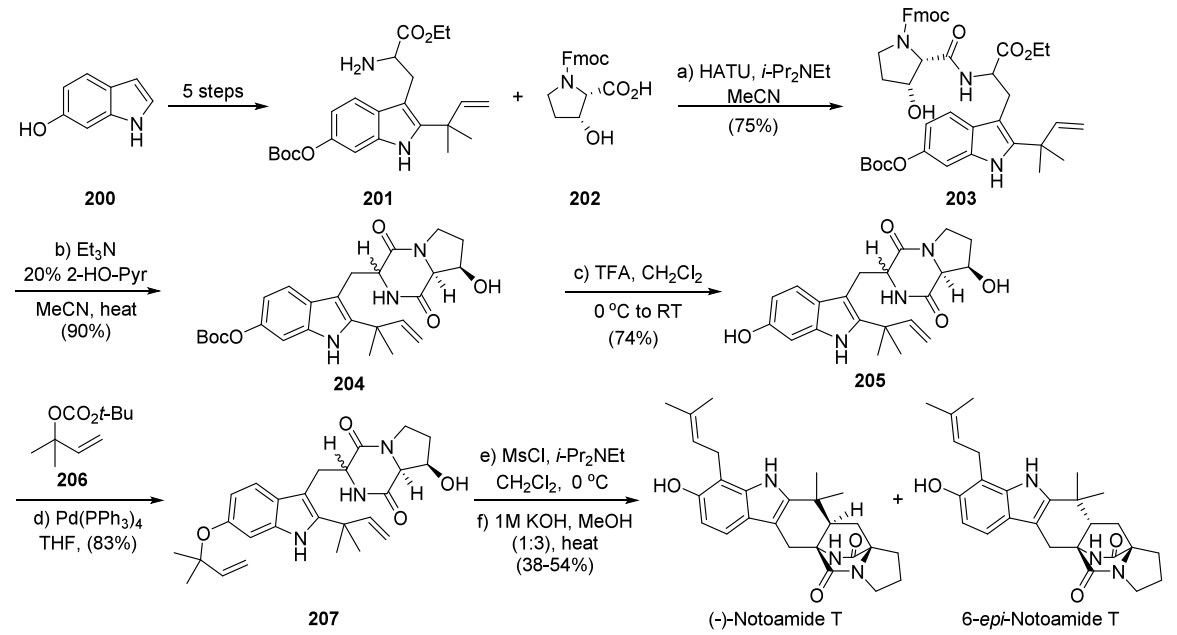

Scheme 51. Sarpong's Total Synthesis of (+)-Stephacidin A, (+)-Notoamide I and Other Related Natural Products

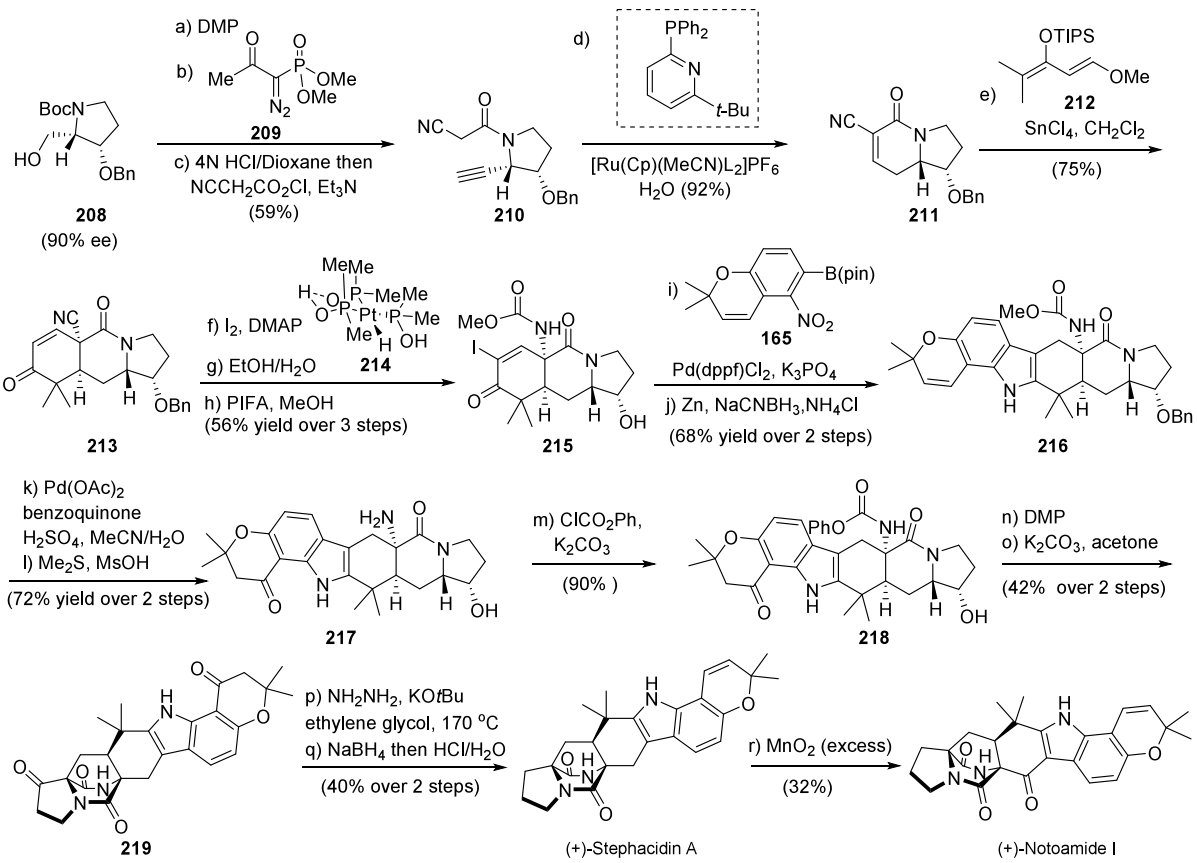

product (−)-stephacidin A. The authors further found that, after deprotection of the Boc group from the mixture of **193**/**194** (2.5:1) in microwave conditions, the intermediate **198** could be isolated and subjected to the oxidative system with a catalytic amount of SeO_2 and excess H_2O_2 to yield (+)-notoamide B, probably through the *in situ* generated (−)-stephacidin A (Scheme 48).

Williams and co-workers also established the total synthesis of notoamide T (Scheme 49).[58] Their initial work showed that stephacidin A could be transformed into notoamide T by treatment with PhSSPh and PhSH in DMSO in the presence of light for 48 h. The corresponding sulfide **199** could be formed in an 80% yield, which was further subject to the reductive

https://doi.org/10.1021/acs.chemrev.4c00250
Chem. Rev. XXXX, XXX, XXX−XXX

Scheme 52. Total Synthesis of Notoamides F, I, R and Sclerotiamide

condition with potassium naphthalide in THF at −40 °C, and the desired notoamide T was obtained in a moderate yield.

Nonetheless, an efficient and shorter synthetic route toward notoamide T from commercially available starting material was still desirable. Thus, the same group came up with the total synthesis of notoamide T from 6-hydroxy-indole **200** as starting material,[62] which was transformed to the tryptophan derivative **201** in 5 steps. Then it was coupled with proline derivative **202** to afford peptide **203** in a good yield, which was further converted to the corresponding lactam **204** after deprotection of the Fmoc group. Next, deprotection of the Boc group, followed by a palladium catalyzed allylic alkylation of the resulted phenol **205**, introduced the side chain of notoamide T. The alcohol of intermediate **207** was transformed to its mesylate, which was treated with KOH under reflux in MeOH, producing the final products notoamide T and 6-*epi*-notoamide T as a separable mixture (1.3:1). In the final step, the cascade reactions occurred in one operation, including elimination, tautomerization, IMDA reaction, and Claisen rearrangement, making this route very concise and efficient (Scheme 50).

In 2015, Sarpong and co-workers developed an efficient method to construct a divergent intermediate **217** to achieve the total synthesis of (+)-stephacidin A, (+)-notoamide I, and other related natural products.[115] As shown in Scheme 51, the reported enantioenriched alcohol **208** was oxidized and underwent the alkynylative homologation to afford the terminal alkyne, whose Boc-group was deprotected, followed by acylation to form alkyne **210**. Then a formal cycloisomerization occurred to afford the bicycle **211**, which underwent the Diels−Alder reaction with diene **212** in the presence of $SnCl_4$, giving rise to enone **213**. Iodination, hydration of nitrile group, and then Hoffmann rearrangement provided carbamate **215**, which further underwent a Suzuki cross-coupling reaction followed by reductive cyclization to form indole hexacycle **216**. Wacker oxidation and sequential treatment with dimethyl sulfide (Me_2S) and methanesulfonic acid yielded the common intermediate **217**. Chemoselective *N*-acylation reaction gave the phenyl carbamate **218**. Oxidation of the secondary alcohol and then treatment of the ketone with K_2CO_3 produced the BCDO **219** via the Dieckmann condensation of the *in situ* formed isocyanate/enolate, which was the key step in this total synthesis. Then, selective removal of the ketone moiety on the pyrrolidine ring followed by the reduction/elimination sequence afforded the final product of (+)-stephacidin A. With the synthetic (+)-stephacidin A in

https://doi.org/10.1021/acs.chemrev.4c00250
Chem. Rev. XXXX, XXX, XXX−XXX

Scheme 53. Concise Total Synthesis of Stephacidin A

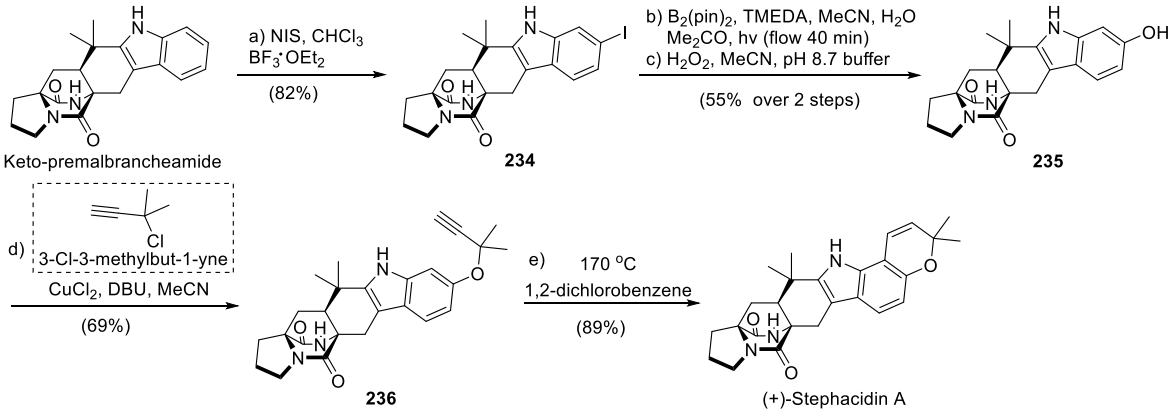

Scheme 54. Concise Synthesis of Multiple Natural Products from (+)-Stephacidin A

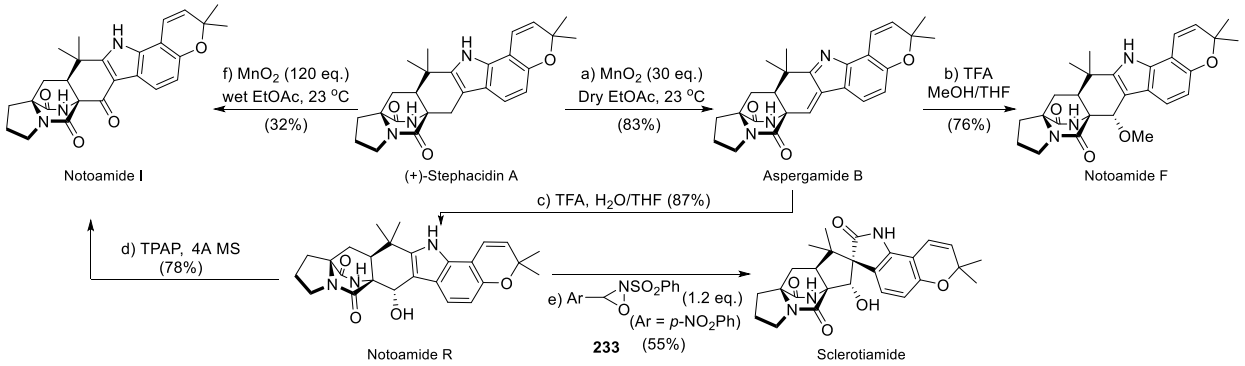

hand, another natural product (+)-notoamide I was readily synthesized by treatment with MnO_2 in EtOAc. Furthermore, following the reported procedure,[47,110] the formal syntheses of (−)-notoamide B, (+)-avrainvillamide, and (−)-stephacidin B could also be realized.

In 2015, Li and co-workers reported another strategy for the enantioselective total synthesis of natural alkaloids (+)-notoamide F, I and R in 10−12 synthetic steps from readily available substrates (Scheme 52).[116] In this synthetic work, the construction of the BCDO core was realized using an oxidative aza-Prins cyclization reaction, which is a quite different strategy compared to the previous IMDA reaction, radical cyclization and so on. Furthermore, a radical isomerization catalyzed by a cobalt complex was used as another key transformation to build the cyclohexenyl ring.

The total synthesis started from the readily available starting material **220**. Prenylation, followed by Boc protection, afforded intermediate **221** in a good yield, which was coupled with dimethyl 2-aminomalonate to produce the amide **222** in almost quantitative yield. Deprotection of the Boc group and subsequent lactamation provided the aza-Prins cyclization precursor **223**. When treated with 3 equiv of $FeCl_3$ in MeCN/CH_2Cl_2 at room temperature, the corresponding BCDO **225** could be isolated in a 67% yield as the only stereoisomer. The ketone **227** was formed in a moderate yield when treating **225** with 3-iodoindole **226** in the presence of Grignard reagent, which underwent the isomerization reaction to form the cyclohexenyl ring. After that, debenzylation followed by propargylation afforded ether **232** in a good yield, which underwent the Claisen rearrangement to finish the total synthesis of notoamide I in 10 steps with a 7.3% overall yield. Stereoselective reduction of notoamide I with DIBAL-H afforded notoamide R. Notoamide F could be isolated when notoamide R was treated with AcOH/MeOH. Treatment of notoamide R with oxaziridine **233** could induce the stereoselective pinacol rearrangement to give sclerotiamide in a 55% yield. (Scheme 52)

In 2017, Sarpong and co-workers found that (+)-stephacidin A could be synthesized from the known intermediate keto-premalbrancheamide A, which underwent the selective iodination at the C6 position, giving **234**.[117] Then photo-mediated borylation and the following oxidation of the resulting boronic ester produced the corresponding phenol **235**. Thus, stephacidin A could be readily synthesized by the late-stage construction of the chromene ring following the previous Williams' report.[118] The synthesis of stephacidin A was accomplished in 11 steps with a 4.7% overall yield from D-proline. Notably, 300 mg of stephacidin A was prepared following this synthetic strategy, demonstrating its scalability (Scheme 53).

Based on the efficient synthesis of stephacidin A, Sarpong and co-workers showed that it could be used to prepare a series of related natural products such as notoamides I, R, and F via the selective functionalization under different conditions. As shown in Scheme 54, the group found that the treatment of stephacidin A with excess amount of MnO_2 in dry EtOAc produced aspergamide B, which could accept the nucleophilic addition by H_2O or MeOH in the presence of TFA to afford notoamide R or F in good yields. Notoamide R could be further oxidized to notoamide I or sclerotiamide.

https://doi.org/10.1021/acs.chemrev.4c00250
Chem. Rev. XXXX, XXX, XXX−XXX

Scheme 55. Biomimetic Total Synthesis of Versicolamide B and Notoamide B

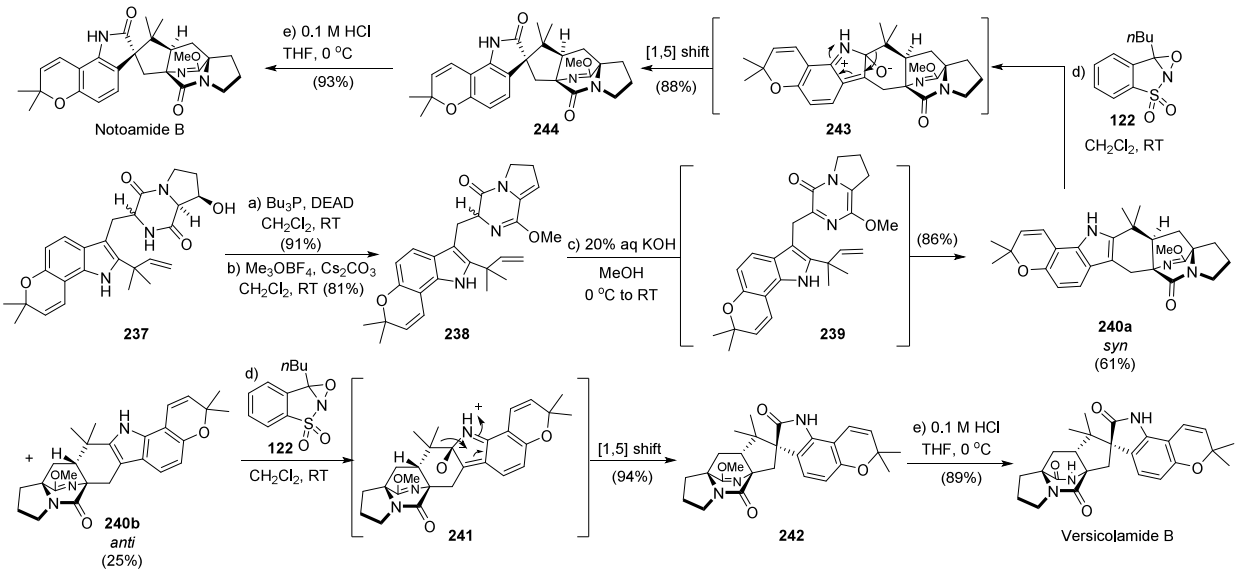

Scheme 56. Concise Total Synthesis of Versicolamide B

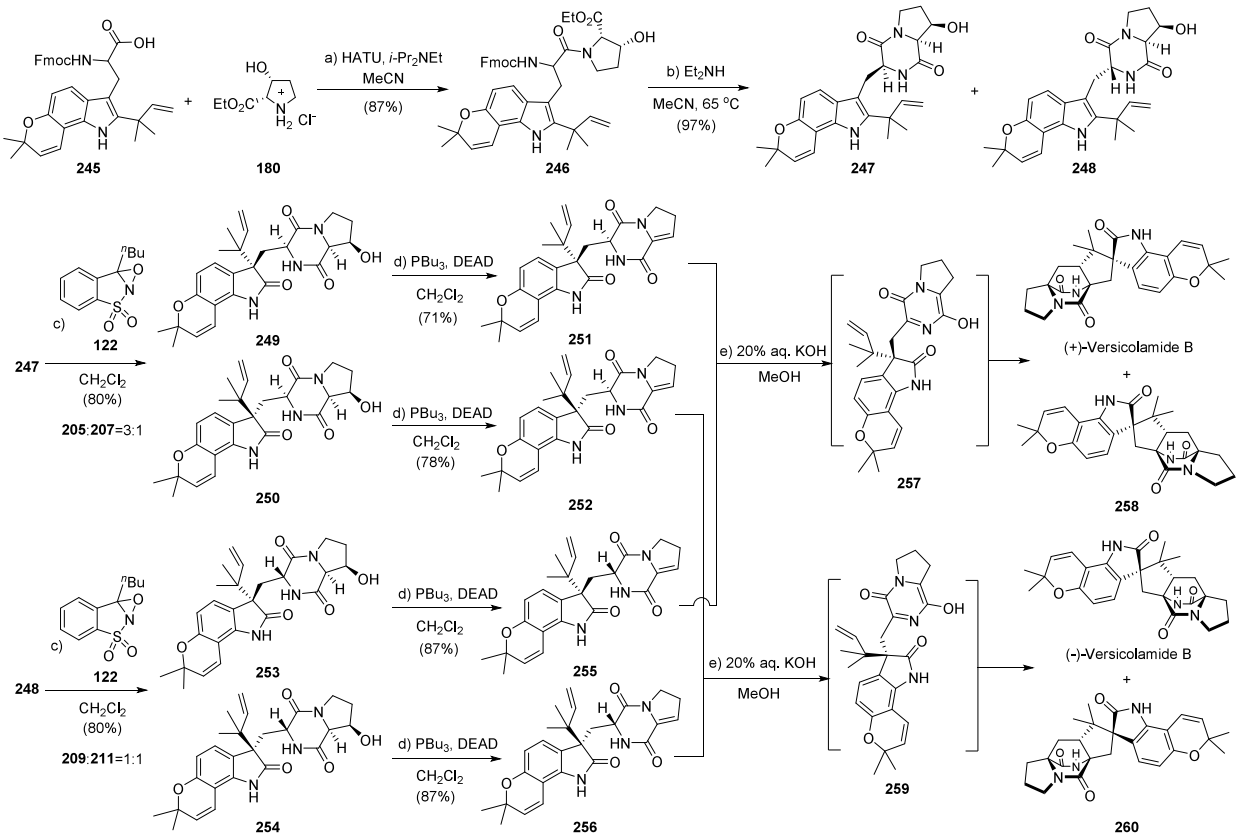

5.3. Versicolamides

In 2008, Williams and co-workers reported the biomimetic total synthesis of versicolamide B (Scheme 55), which well supported the proposed biosynthetic pathway (Scheme 14).[37] The total synthesis started with the known alcohol (**237**) through a Mitsunobu type elimination in the presence of PBu_3 and DEAD to afford the enamide intermediate, which was transformed to the lactim ether **238** using Me_3OBF_4 and Cs_2CO_3. The lactim ether **238** tautomerized to the azadiene **239** and then underwent the key IMDA cycloaddition to afford intermediates **240a** and **240b** at 2.4:1 dr with 20% aqueous KOH in MeOH. The minor diastereoisomer **240b** could produce the corresponding spiro-oxindoles **242** as a single diastereomer by treatment with excess oxaziridine **122** in CH_2Cl_2. Finally, the lactim ether of **242** was removed with diluted aq. HCl (0.1 M, 3 equiv) in THF (0 °C, 5 min) to provide versicolamide B. Overall, the total synthesis of versicolamide B was finished in 18 steps with a 1.8% overall yield. Following the same procedure, the major diaster-

https://doi.org/10.1021/acs.chemrev.4c00250
Chem. Rev. XXXX, XXX, XXX−XXX

Scheme 57. Biomimetic Synthesis of (−)-Depyranoversicolamide B

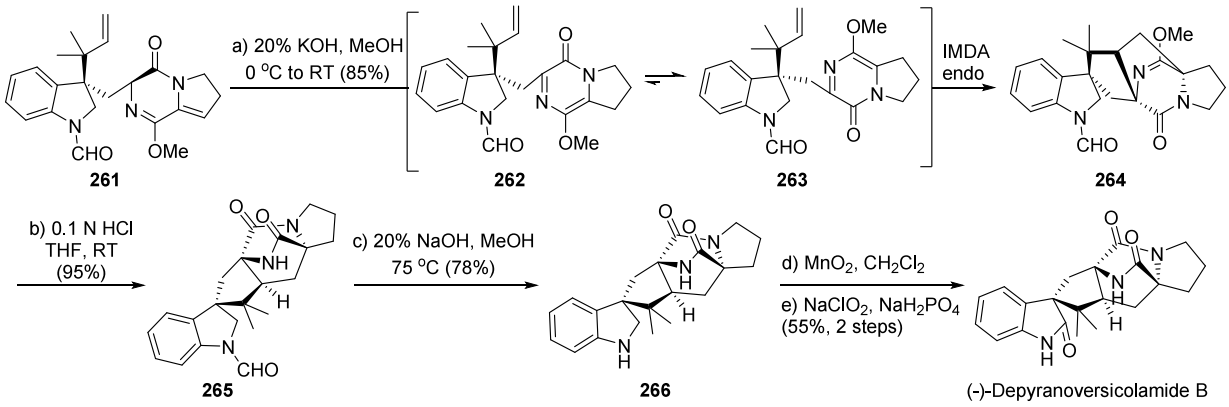

Scheme 58. Synthesis of Malbrancheamides

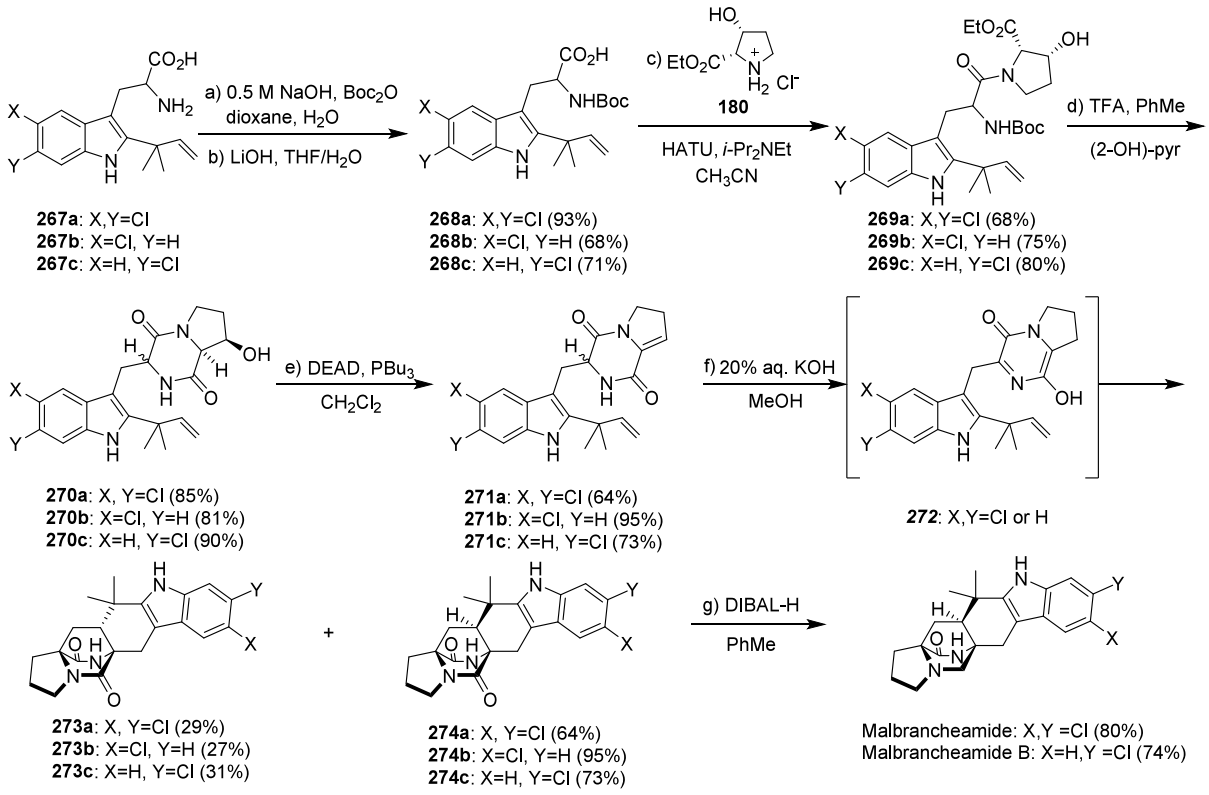

eoisomer **240a** could be transformed to the natural product notoamide B sequentially via **243** and **244**.[37]

Then Williams and co-workers further developed the asymmetric total synthesis of (+)- and (−)-versicolamide B via the bioinspired IMDA reaction as the key step[119] (Scheme 56). The total synthesis began with the reported amino acid derivative **245**. Coupling of **245** with the chiral proline derivative **180** afforded amide **246** as a mixture of diastereomers, which were deprotected and cyclized to form two diastereomers **247** and **248**. The following oxidation led to the formation of oxindoles **249**/**250** (3:1) and **253**/**254** (1:1), which were subsequently dehydrated to form **251**/**252** and **255**/**256**, respectively. The four diastereomers were tautomerized individually under basic conditions and underwent the IMDA reaction smoothly to produce (+)-, (−)-versicolamide B and their diastereomers.

In 2015, Qin and co-workers reported the total synthesis of (−)-depyranoversicolamide B,[108] which is an unnatural product that contains the common BCDO skeleton but lacks the pyran motif.[106] Tautomerization of the intermediate **261** under Willams' condition (20% KOH in MeOH at 0 °C to room temperature) formed two reversible transition states **262**/**263** and then underwent the stereoselective *endo*-Diels–Alder cycloaddition to afford *anti*-adduct **264** as the sole product in an 85% yield. This intermediate was further converted to (−)-depyranoversicolamide B via hydrolysis, deformylation and oxidation. The bioinspired IMDA reaction was the key step to construct the BCDO core of (−)-depyranoversicolamide B as shown in Scheme 57.

5.4. Malbrancheamides

In order to elucidate the exact structure of malbrancheamide B, Williams and co-workers synthesized malbrancheamide and

https://doi.org/10.1021/acs.chemrev.4c00250
Chem. Rev. XXXX, XXX, XXX−XXX

Scheme 59. Domino Reaction Sequence for the Synthesis of (±)-Malbrancheamide B

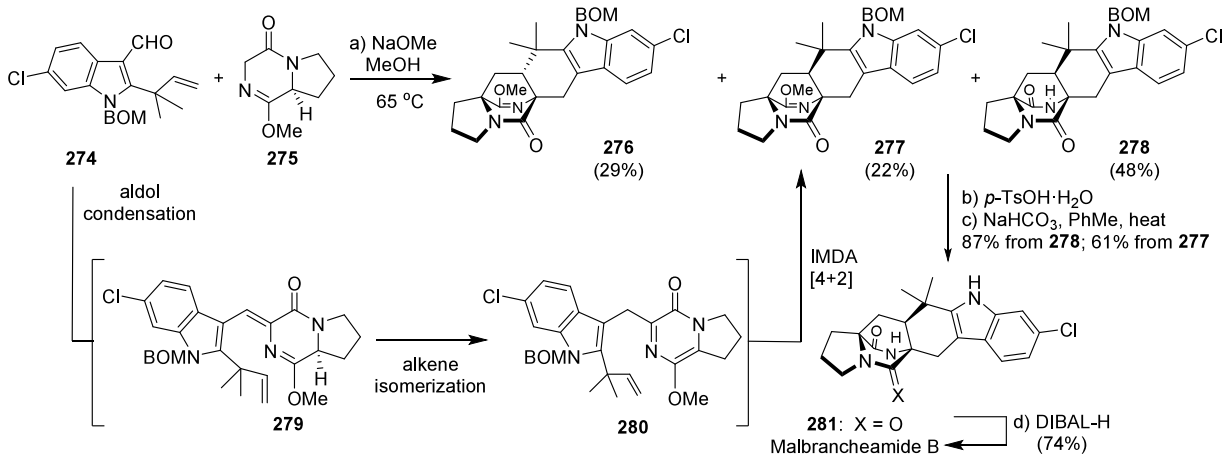

Scheme 60. Asymmetric Synthesis of (+)-Malbrancheamide B

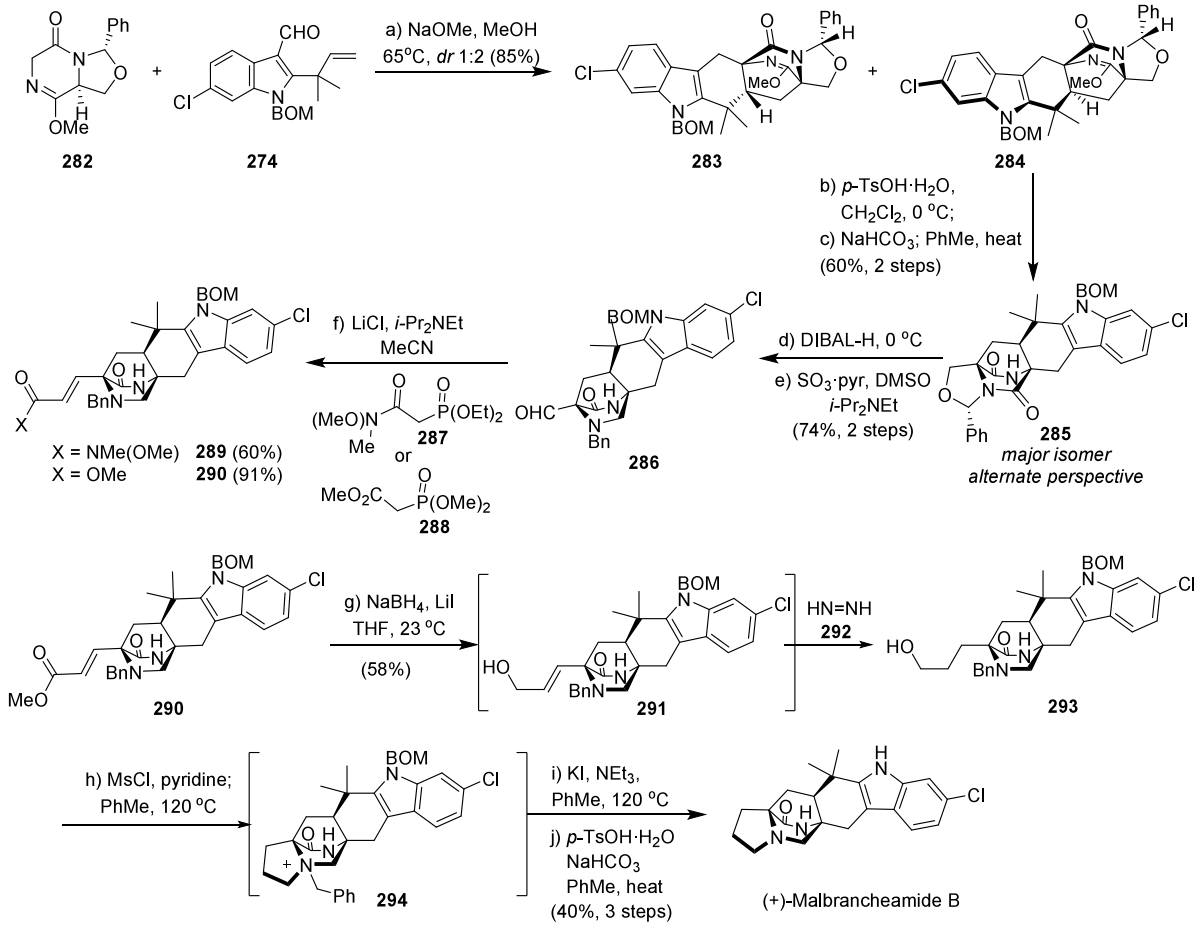

malbrancheamide B in 12 steps with 5.3% and 8.2% overall yields, respectively,[120] in which the biomimetic IMDA reaction was adopted as the key step to build the BCDO skeleton. As shown in Scheme 58, the Mitsunobu dehydration product **271** was treated with aq. KOH in MeOH for isomerization to form the required azadiene **272**. The azadiene realized the IMDA cycloaddition to afford the cycloadducts **273**/**274** with a ∼1:2 ratio (*anti*:*syn*) in a good combined yield. Then, **274a** and **274c** were selectively reduced with DIBAL-H to afford malbrancheamide and malbrancheamide B, respectively. Comparison of the NMR spectra of chemically synthesized C-5-chlorinated and C-6-chlorinated regioisomers to those of natural malbrancheamide B confirmed that the natural product contains a 6-chloroindole ring.

In 2013, Scheerer and co-workers reported a formal total synthesis of (±)-malbrancheamide B in 7 steps (Scheme 59).[121] The total synthesis started from indole carboxaldehyde **274**, which was synthesized from 6-chloroindole in 4 steps by following the reported procedure.[120] The indole carboxaldehyde underwent a domino chemistry with DKP **275** (prepared

https://doi.org/10.1021/acs.chemrev.4c00250
Chem. Rev. XXXX, XXX, XXX−XXX

Scheme 61. Concise Total Synthesis of Malbrancheamides

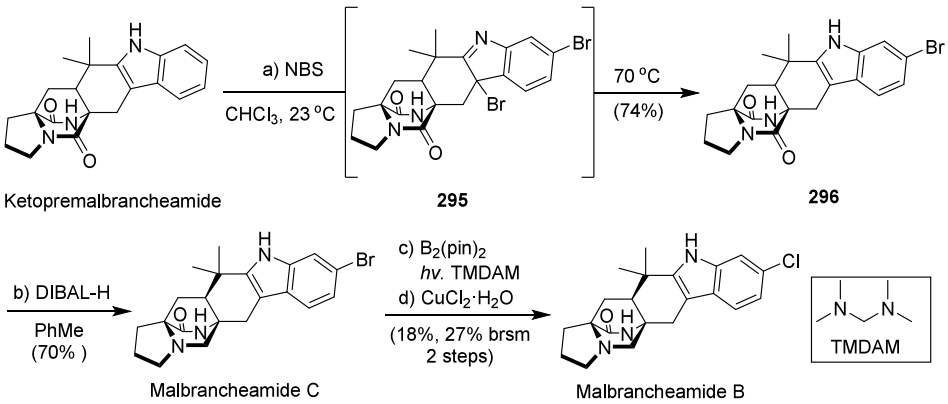

Scheme 62. Synthesis of Intermediates toward Paraherquamides

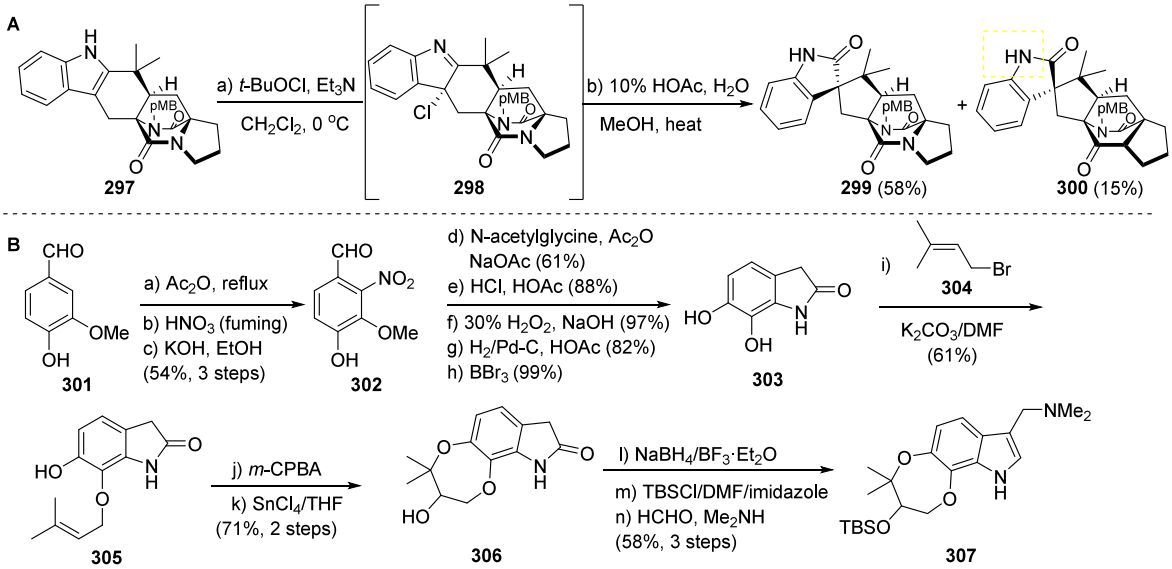

from proline methyl ester via 3 steps) to produce the corresponding BCDO skeleton **276**/**277**/**278** in an excellent combined yield in the presence of NaOMe in MeOH at 65 °C. In this domino chemistry, the cascade sequence could occur efficiently via DKP enolization. Then addition to the aldehyde of **274** afforded the aldol condensation intermediate **279**, which was isomerized to form the desired reactive endocyclic azadiene **280** followed by IMDA reaction under basic conditions to produce **276**/**277**. Meanwhile, the DKP **278** could be formed from the selective hydrolysis of **277**. Thus, the domino sequence could efficiently couple the two starting materials and rapidly enhance the molecular complexity with a high yield. Hydrolysis with *p*-TsOH in CH_2Cl_2 at room temperature readily resulted in deprotection and imine cleavage of **277**/**278** to afford the lactam **281**, which was the intermediate of Williams' synthesis[120] of (±)-malbrancheamide B. Overall, this total synthesis was completed in 10 steps (the longest linear sequence consisted of 7 steps).

Encouraged by this racemic approach, the same group further developed an asymmetric method for the total synthesis of (+)-malbrancheamide B (Scheme 60).[121] The diastereoselective domino sequence between readily available **282** and indole carboxaldehyde **274** delivered the cycloadducts **283** and **284** in a high combined yield with 2:1 dr. The process showed that the stereochemistry of the aminal intermediate could be controlled by the chirality of the azadiene. The mixture of **283** and **284** was hydrolyzed with TsOH·H_2O, followed by basification to DKP **285**, which was selectively reduced with DIBAL-H, and the resulting primary alcohol was oxidized by SO_3·pyr and DIPEA in DMSO to form aldehyde **286**. The aldehyde was subject to Horner–Wadsworth–Emmons olefination to deliver the chain extension skeleton **289**/**290**. The ester **290** was reduced to afford the mixture of alcohols **291** and **293**. After purification, the ally alcohol **291** was reduced with diimide **292** generated *in situ* from the thermal decomposition of $TsNHNH_2$ in EtOH to form **293**. The primary alcohol was transformed to the mesylate and then underwent intramolecular *N*-alkylation to form the salt **294** when heated at 120 °C in toluene. The quaternized amine was heated in the presence of KI and Et_3N, generating the malbrancheamide ring skeleton. The NBOM group was hydrolyzed under mild acidic conditions to produce the final product (+)-malbrancheamide B. Thus, the asymmetric synthesis of (+)-malbrancheamide B was realized in 13 steps,[121] during which the aldol condensation, alkene isomerization, and IMDA cycloaddition were the key transformations. This cascade reaction sequence provided an efficient enantioselective route for construction of the BCDO indole alkaloids.

https://doi.org/10.1021/acs.chemrev.4c00250
Chem. Rev. XXXX, XXX, XXX−XXX

Scheme 63. Concise Total Synthesis of (+)-Paraherquamide B

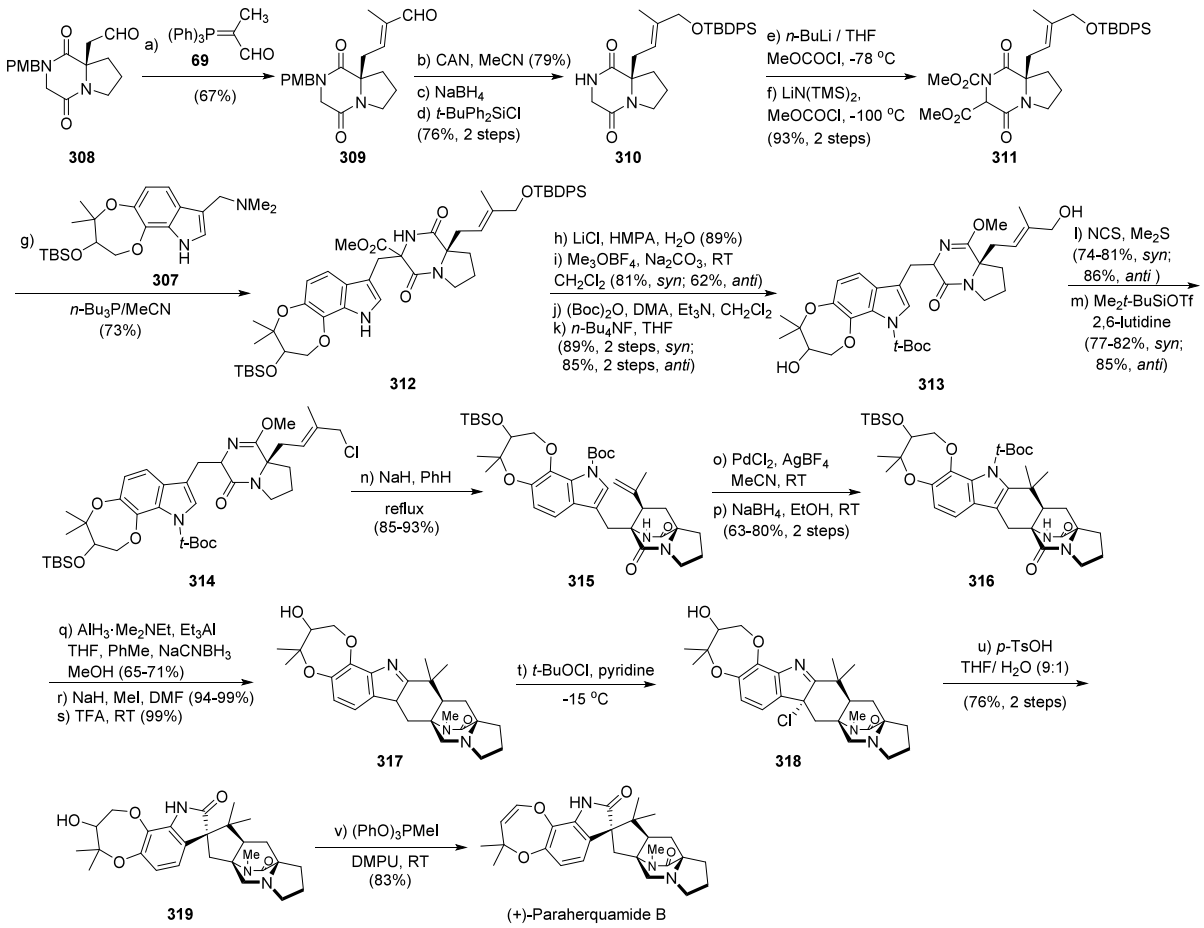

In 2017, Sarpong and co-workers reported another efficient construction of malbrancheamides B and C via the selective functionalization of the C6 position of the known intermediate ketopremalbrancheamide (Scheme 61), which was selectively brominated to form the intermediate **295** and then heated at 70 °C to yield the intermediate **296**. Subsequent chemoselective reduction of **296** yielded malbrancheamide C. Then malbrancheamide C was transformed to the corresponding boronic ester with a photoirradiation strategy, which was further chlorinated to form malbrancheamide B.[117]

5.5. Preparaherquamides

In 1989, Williams et al. reported the first synthetic model for paraherquamides (Scheme 62A).[122] They found that a hexacylic indole **297** could become 3-chloroindolenines with two diastereomers (4:1 ratio, **298** as the major isomer) when treated with *tert*-butyl hypochlorite. The major isomer **298** was further rearranged to form spiro-oxindoles as a 3.86:1 mixture of diastereomers **299**/**300**, while the major isomer (**299**) had the correct relative stereochemistry with the paraherquamide-type natural products. Vanillin (**301**) was transformed to 2-nitro vanillin **302** via a three-step sequence including acetylation, nitration and hydrolysis, which was further converted to a known catechol **303** in five steps. Then, selective prenylation provided the desired **305** as the major product, which was epoxidized followed by ring-opening to afford oxindole **306**. The oxindole was further converted to the gramine derivative **307** in a three-step sequence (Scheme 62B).

Based on the previous work about the biomimetic total synthesis of brevianamides, the authors established the first total synthesis of (+)-paraherquamide B from the starting material **308**[123] (Scheme 63). In this synthesis, Somei/Kametani reaction, stereoselective S_N2' reaction, palladium catalyzed indole cyclization, chemoselective amide reduction, and an oxidative pinacol rearrangement were used as the key steps to realize the indole-oxindole formation.

As shown in Scheme 63, the *para*-methoxylbenzyl protecting group of enal **309** was removed with CAN to afford an amide intermediate, and the resulting aldehyde was reduced with $NaBH_4$ to form an alcohol and then protected to give **310**. The intermediate **310** was further converted to the desired imidocarbamate **311** as a mixture of diastereomers via a one-pot process with methyl chloroformate. The imidocarbamate **311** and gramine derivative **307** could form the desired coupling intermediate **312** when refluxed with *n*-Bu_3P in MeCN. Indole **312** underwent decarbomethoxylation at 100 °C with LiCl in HMPA to afford diastereomers that could be readily separated by chromatography. After treatment with Me_3OBF_4 and Na_2CO_3 in CH_2Cl_2, the diastereomers were transformed to the corresponding lactim ethers and then to the diols **313** with the use of $(Boc)_2O$ and *n*-Bu_4NF. Following Corey's protocol, the sensitive allylic chlorides were synthesized with NCS and Me_2S, and the secondary alcohol was protected with TBS-triflate to afford the key S_N2 cyclization precursor **314**. The treatment of diastereomers of **314** with an excess amount of NaH in hot benzene produced the stereoselective intramolecular S_N2' cyclization product, afford-

https://doi.org/10.1021/acs.chemrev.4c00250
Chem. Rev. XXXX, XXX, XXX−XXX

Scheme 64. An Ion-Pair Driven Model toward the Synthesis of (+)-Paraherquamide A

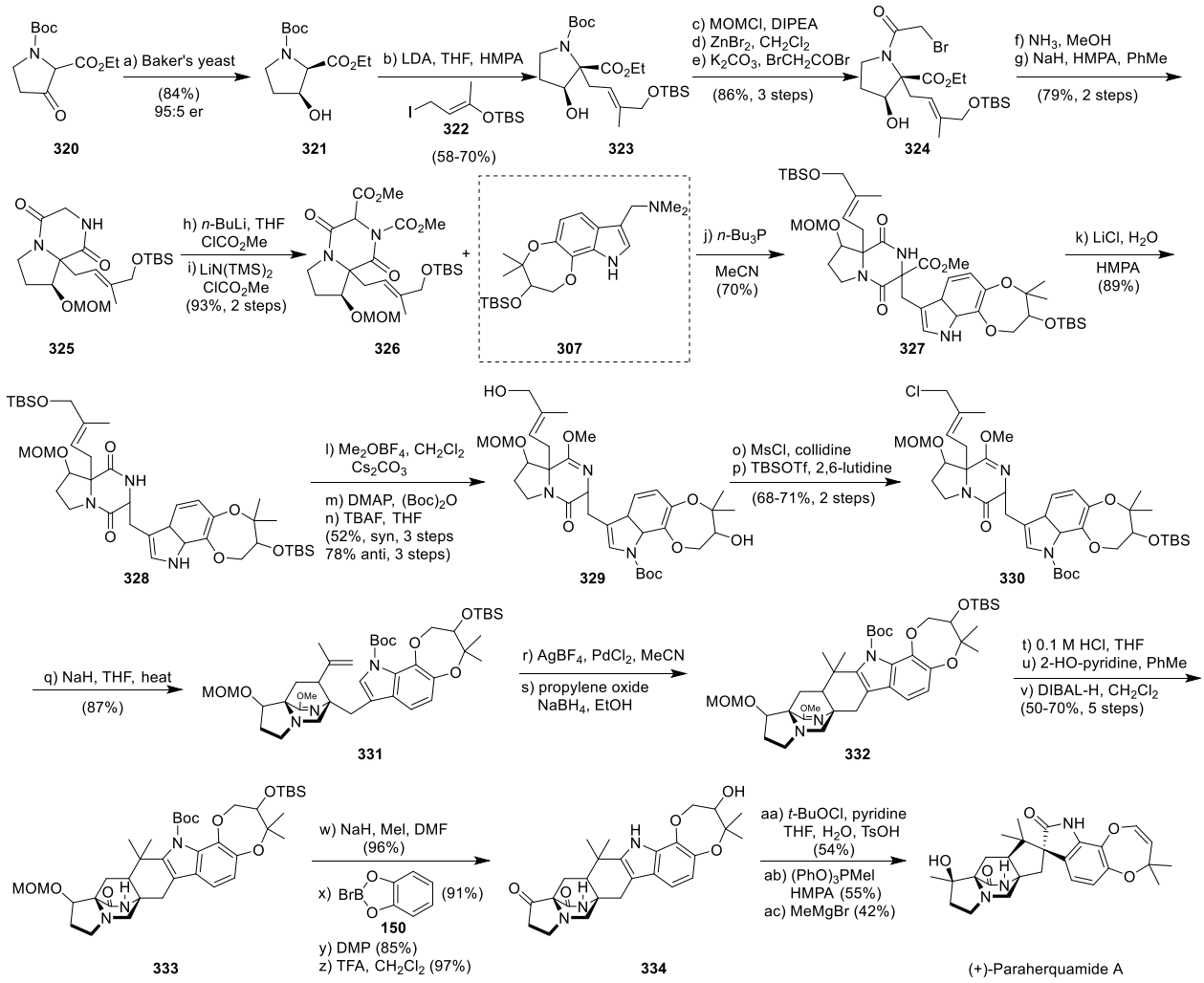

ing the BCDO core of (+)-paraherquamide B. With the core motif of the (+)-paraherquamide B in hand, the heptacycle **316** was generated under the Trost's condition, together with the loss of the lactim ether. Selective reduction of the tertiary amide **316** with alumina reagent and $NaCNBH_3$ afforded tertiary amine. *N*-methylation of the tertiary amine followed by removal of the protecting groups under acidic conditions produced the indole **317** in a combined 59% yield over 3 steps. After that, the oxidative spiro-oxidation was realized by chlorination of **317** with *t*-BuOCl and pyridine; then hydration induced the rearrangement to form the spiro-oxindole **319**. Finally, (+)-paraherquamide B was produced via elimination of the alcohol using MTPI in DMPU with an 83% yield.

Paraherquamide A, containing the special *β*-hydroxy-*β*-methyl proline skeleton, is more challenging to be synthesized compared to paraherquamide B. Williams and co-workers came up with an ion-pair driven *syn*-selective S_N2' cyclization as a general procedure to construct the *α*-alkylated-*β*-hydroxyproline skeleton (Scheme 64). In this total synthesis,[124] the racemic *β*-keto ester **320** prepared in three steps from glycine ethyl ester was used as the starting material, which was reduced to the optically active *β*-hydroxyester **321** (ca. 95:5 er) using Baker's yeast. The selective carbon-alkylation rather than *O*-alkylation with allyl iodide **322** produced the desired *α*-alkylated product **323** in a moderate to good yield. The second alcohol was protected with MOM-Cl followed by removal of the Boc group and then acylation of the resulting secondary amine under basic conditions, giving rise to the bromoacetamide **324** in an 86% yield over three steps. The *in situ* generated glycinamide derivative via the treatment of **324** with ammonia in methanol underwent cyclization to afford the bicyclic skeleton **325** in a 79% yield in the presence of NaH in toluene/HMPA. Compound **325** was subject to the one-pot double carbomethoxylation process to provide **326** in a high yield. Afterward, the Somei−Kametani coupling reaction with gramine derivative **307** produced the tryptophan intermediate **327** in the presence of n-Bu_3P as two diastereomers (3:1 ratio), which further underwent decarbomethoxylation to afford **328** as two separable diastereomers with LiCl in aq. HMPA at 105 °C. The secondary amide was protected as methyl lactim ether after treatment with Meerwein's reagent. Protection of the indole with Boc group and the silyl ether was deprotected to form the corresponding diol **329**, which was transformed to the allilic chloride by mesylation in the presence of collidine. The remaining secondary alcohol was protected with TBSOTf to afford the key intermediate **330**, which was the precursor of the intramolecular S_N2' cyclization. After treatment with NaH in hot THF, the cyclized product **331** could be isolated in a good yield with the desired conformation. The intramolecular S_N2'

https://doi.org/10.1021/acs.chemrev.4c00250
Chem. Rev. XXXX, XXX, XXX−XXX

Scheme 65. Concise Total Synthesis of Preparaherquamide and (+)-VM55599

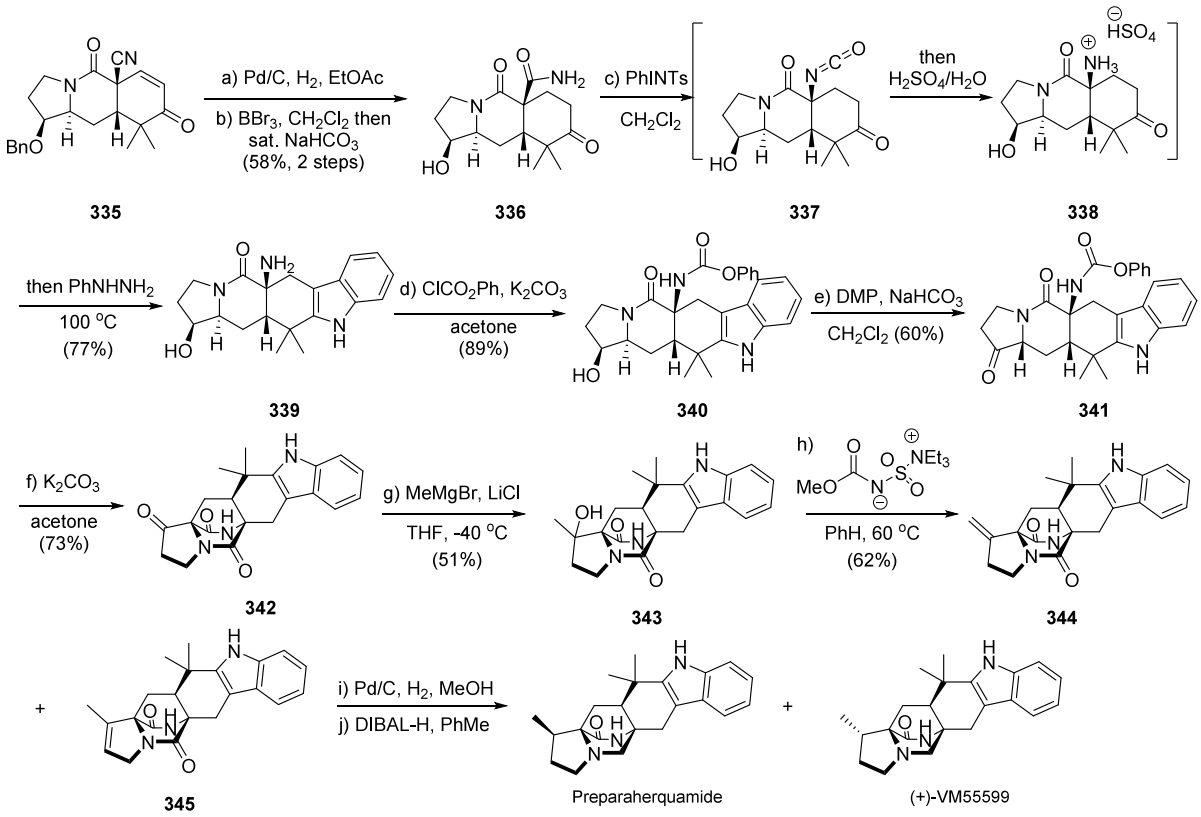

cyclization process was driven by the ion-pair via the "closed" transition state with high *syn* selectivity, as discussed above. When treated with an excess amount of $PdCl_2$ and $AgBF_4$ in MeCN with propylene oxide to absorb acid, the seven-membered ring was formed, which was further reduced to afford the corresponding 2,3-disubstituted indole **332** by $NaBH_4$ in EtOH. It is worth mentioning that the propylene oxide was essential to buffer the reaction system, as the MOM ether would be cleaved without the propylene oxide. The lactim ether **332** was deprotected under acidic conditions, and then the resulting ring-opened intermediate was recyclized under basic conditions, giving rise to the heptacyclic piperazinedione, which was reduced with DIBAL to form **333**. Methylation of the secondary amide and deprotection of the MOM-protecting groups yielded the secondary alcohol, which was oxidized to form a ketone intermediate. Subsequently, the *N*-Boc and TBS-protecting groups were removed in one step upon treatment with TFA to provide the intermediate **334**. By treating **334** with *t*-BuOCl in pyridine, 3-chloroindolenine, the precursor of the pinacol-type rearrangement, was formed and then transformed to the corresponding spiro-oxindole skeleton with a 54% yield under acidic conditions. After that, the dioxepin ring was formed via the dehydration of the alcohol with $(PhO)_3PMeI$ in DMPU to afford 14-oxoparaherquamide B. Following the reported procedure,[125] the stereoselective 1,2-addition of the methyl group with MeMgBr gave the final product (−)-paraherquamide A in a 42% yield.

In 2020, Sarpong and co-workers developed an efficient route toward the synthesis of preparaherquamide and (+)-VM55599.[126] Obtained from enone **335** via a two-step sequence, amide **336** then underwent the Hoffmann rearrangement in the presence of PhINTs, and the *in situ* generated isocyanate **337** was further converted to ammonium intermediate **338** when treated with aq. H_2SO_4. Next, the Fischer indolization afforded pentacyclic indole **339** in one-pot from **338**. The primary amine was transformed to the phenyl carbamate **340**. Then, the secondary alcohol of **340** was oxidized to form the cyclization precursor **341**, which was treated with K_2CO_3 to afford the BCDO core of **342**, via the Dieckmann cyclization of the *in situ* generated enolate and isocyanate group. Overall, the BCDO skeleton was built in 5 steps from the known intermediate **335**, presenting a concise approach to a series of related natural products. The desired tertiary alcohol **343** was formed with the combined utility of MeMgBr and LiCl and then dehydrated with the Burgess reagent to afford a mixture of alkenes with two regioisomers **344**/**345** in a 71% yield (1:2 ratio). These two isomers were further hydrogenated followed by chemoselective reduction with DIBAL-H, giving preparaherquamide and (+)-VM55599 in 25% and 27% yields, respectively (Scheme 65).[126]

5.6. VM55599

As shown in Scheme 66, Williams and co-workers reported the total synthesis of VM55599.[88] This total synthesis started from benzophenone imine **346**, condensation of which with the gramine derivative **10** gave the tryptophan derivative **347** in a good yield in the presence of n-Bu_3P in MeCN. The amino ethyl ester **348** was obtained after cleavage of the benzophenone imine. Boc protection and ester hydrolysis formed acid **349**, which was coupled with racemic proline derivative **351** to produce the desired peptide **352**. The Boc group was deprotected with TFA, and the resulting amino ethyl ester underwent cyclization to form the corresponding piperazinedione **353**, which was treated with $SOCl_2$ in pyridine

https://doi.org/10.1021/acs.chemrev.4c00250
Chem. Rev. XXXX, XXX, XXX−XXX

Scheme 66. Total Synthesis of VM55599 from Benzophenone Imine

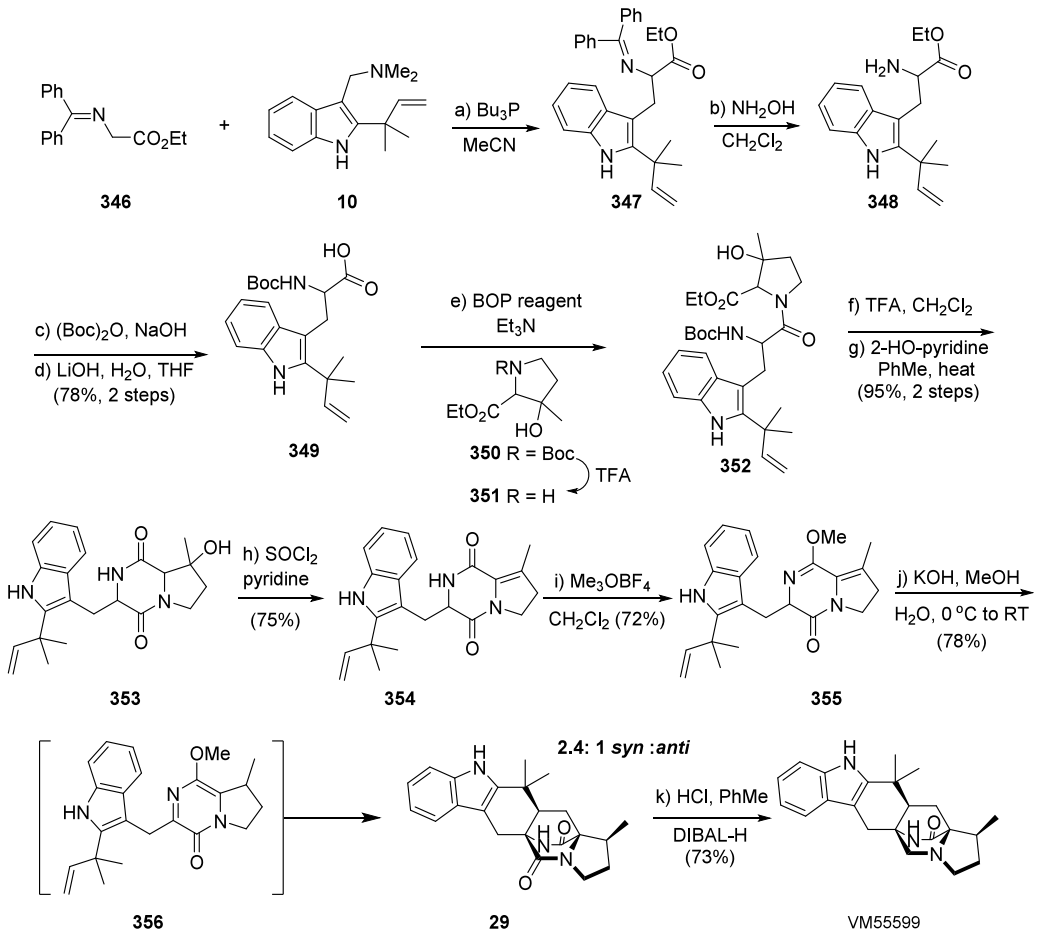

to generate the unsaturated substance **354**. Then, the lactam was protected to afford azadiene **355**, which underwent the tautomerization/IMDA reaction to form the cycloadducts in a 78% yield in the presence of KOH in MeOH. Upon structural analysis, the cycloadduct was confirmed to have the desired skeleton, which was treated with diluted HCl aqueous to cleave the lactim ether to give the amide. The following selective reduction with excess DIBAL-H produced the final product VM55599.

In 2002, Williams and co-workers reported the asymmetric total synthesis of (−)-VM55599 (Scheme 67), which used L-isoleucine **357** as the starting material to build the α-methylproline ring.[89] Compound **357** was transformed to the chiral methylproline derivative **358** via the Hoffmann−Loeffler−Freytag sequence in 5 steps with a 47% overall yield, which was hydrolyzed, and the resultant acid **359** was coupled with glycine methyl ester **360** to form the corresponding dipeptide **361** in a high yield. Then deprotection of the Boc group and heating gave the DKP **362** with an excellent yield in 3 steps, which was further protected to form its *N*-methylthiomethyl (MTM) derivative. The MTM protected substrate **364** could be easily purified by chromatography, which underwent the Aldol reaction with aldehyde **365** to form the intermediate **366** with a mixture of diastereomers. Removal of the MTM protecting group and elimination produced the sole compound **367**, which was further treated with AcCl at ambient temperature for 14 days to generate the corresponding cycloadducts **370** (35% yield), **28** (15% yield), and **29** (10% yield) as separable products. It was proposed that when AcCl was added, *O*-acyl lactim A would be formed and then isomerized to yield azadiene B, which then underwent the IMDA reaction to afford the cycloadducts. Finally, selective reduction of **29** with an excess amount of DIBAL-H gave the final natural product (−)-VM55599.

5.7. Marcfortine

In 2007, Trost and co-workers reported the total synthesis of the natural product marcfortine B, using the Pd-catalyzed trimethylenemethane [3+2]-cycloaddition strategy (TMM reaction) developed in their previous study.[127] The synthesis started from the known substrate **371**, which was converted to the TMM-acceptor **372** via a 2-step sequence. The TMM cycloaddition occurred smoothly between **372** and TMM donor **373**, producing a spirocyclic acid in the presence of palladium catalyst, which was converted to the methyl ester **374**. Further epoxidation and elimination of **374** gave the allylic alcohol **375**. Then the free alcohol **375** was equipped with the Ms-leaving group and coupled with piperdine **376** to afford intermediate **377**, upon which the Boc group was removed and a straightforward aza-Michael addition gave the cyclized skeleton **378** in quantitative yield with high selectivity. After reprotection of the amine with a PMB group, the ester was reduced to the primary alcohol, which was further transformed to xanthanate ester **379**. A stoichiometric amount of AIBN and 20 mol % Bu_3SnH induced the radical cyclization to form the BCDO core. Meanwhile, the radical species could

https://doi.org/10.1021/acs.chemrev.4c00250
Chem. Rev. XXXX, XXX, XXX−XXX

Scheme 67. Total Synthesis of VM55599 from L-Isoleucine

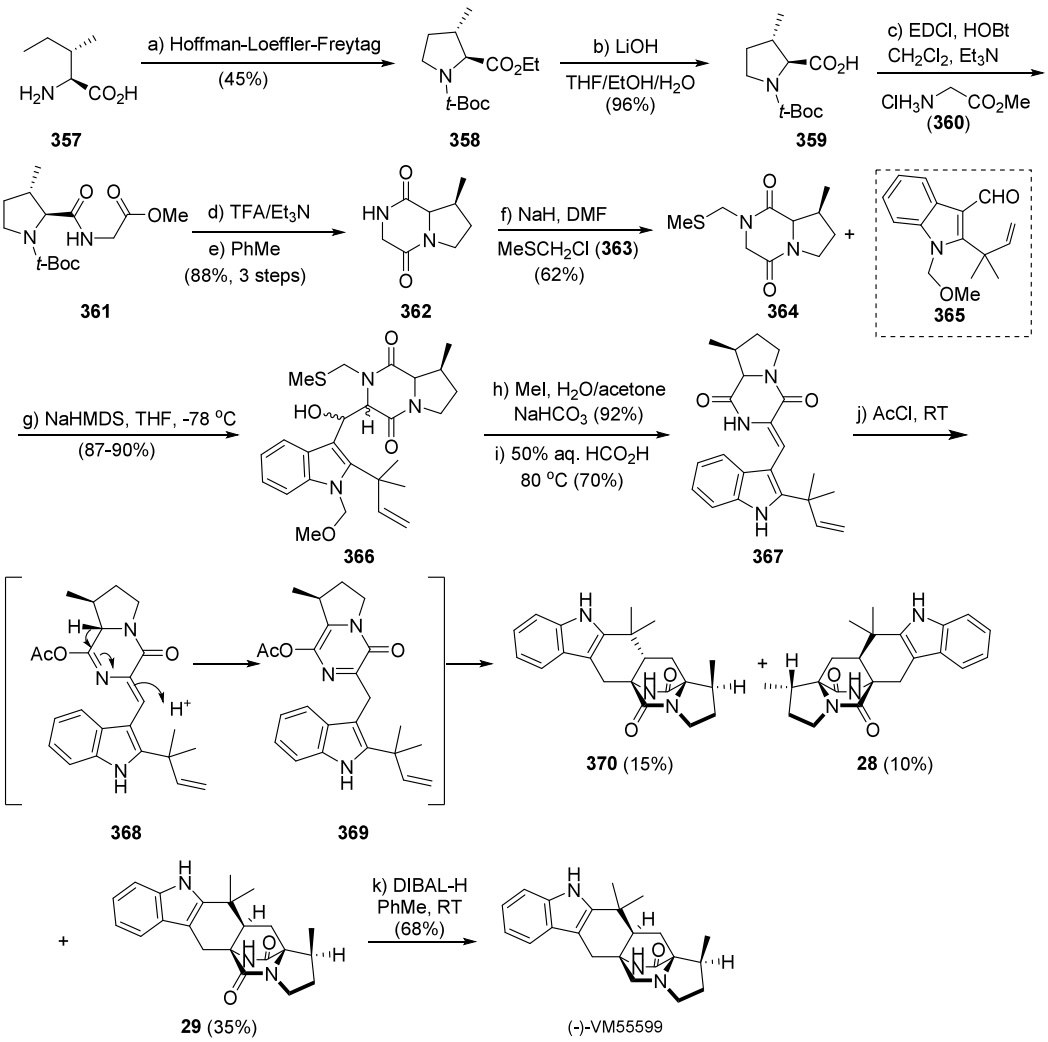

further react with AIBN to form the *N* radical species to afford the unsaturated intermediate **380**, which was reduced to the target skeleton **381**. Removal of the PMB and methyl groups formed the hexacycle **382**, and the stereochemistry was confirmed by the X-ray crystal structure. Following the known procedure, the final product marcfortine B was achieved. Pd-catalyzed TMM cycloaddition, aza-Michael addition, and radical cyclization were the key steps to construct the central motif of this natural product (Scheme 68).

In 2013, the same group reported the asymmetric total synthesis of (−)-marcfortine C using enantioselective Pd-catalyzed TMM cycloaddition.[127−129] As shown in Scheme 69, the starting material 6-benzyloxyindole **383**, protected with the Boc group, was transformed to **384** via Cu-catalyzed propargylation after deprotection of the Bn-group, which was further converted to the chromene **385** via Claisen rearrangement in the presence of $PtCl_4$. Then **385** was transformed into the oxindole **386** in 2 steps. Removal of the Boc group, transformation to the acetone adduct **387**, and protection by a MOM group formed the TMM acceptor **388**, which underwent the enantioselective palladium catalyzed TMM [3+2] cyclization with a chiral phosphine ligand **390**. Subsequently, the terminal olefin was oxidized to the primary alcohol **392** with the Davis oxaziridine **391**, which was further transformed to the radical cyclization precursor **394** in 3 steps. The primary carboxamide **394** underwent the aza-Michael addition to form **395** in the presence of *t*-BuOLi, which was further converted to an aldehyde and reduced to form the primary alcohol **396**. Next, **396** was converted to the radical precursor **397**, which went through the radical cyclization with *n*-Bu_3SnH, AIBN, in the presence of BSA to afford the BCDO skeleton **398** in a moderate yield. Compound **398** was further transformed to the final product marcfortine C via the chemoselective reduction of the olefin and deprotection of the MOM group. Taken together, the enantioselective total synthesis of marcfortine C was achieved in 19 steps with a 2.6% overall yield.

5.8. Asperversiamides

Very Recently, Banwell, Lan and co-workers developed the total syntheses of asperversiamides.[130] Based on the reported biosynthetic proposals by Birch, Williams and others,[1,8,31,97] asperversiamide G, synthesized from commercially available 4-bromo-3-methoxyaniline via 15 chemical steps, was transformed to asperversiamides D and E via [1,5]-H shift and subsequent IMDA reactions (Scheme 70). With treatment of AcCl at 22 °C for 5 days and hydrolytic workup, asperversiamides D and E were obtained as a separable mixture in 32% and 17% yields, respectively. During this process, the heterodiene **403** was formed via the [1,5]-H shift

https://doi.org/10.1021/acs.chemrev.4c00250
Chem. Rev. XXXX, XXX, XXX−XXX

Scheme 68. Total Synthesis of Marcfortine B

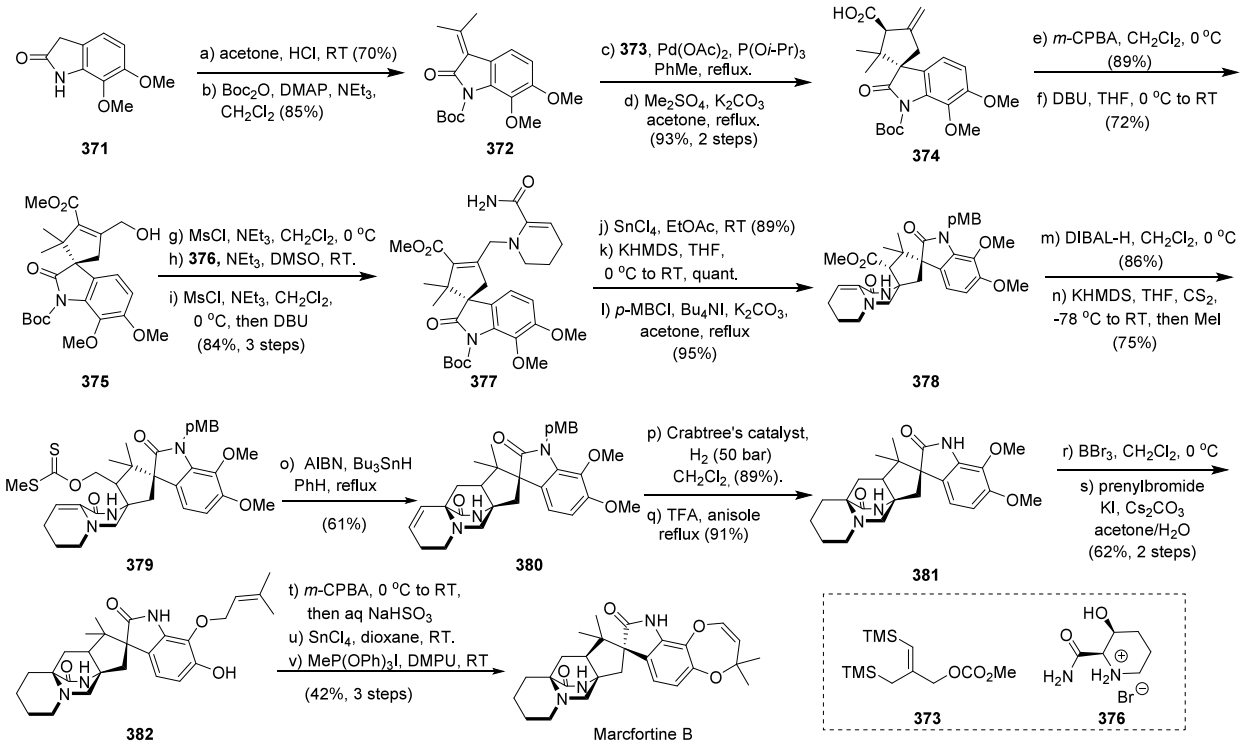

from the *in situ* formed intermediate **402** and then underwent an IMDA reaction through a *syn* transition state to afford asperversiamide D upon hydrolysis. Asperversiamide E was also prepared from this procedure by a less favored *anti* transition state. After that, more efficient approaches were developed to realize the transformations as follows: the Aldol condensation of BOM protected intermediate **400** with diketopiperazine **275** using NaOMe under reflux and the subsequent acidic workup produced IMDA adduct intermediates **404** and **405**, which were then transformed to (±)-asperversiamide D and (±)-asperversiamide E upon deprotection of the BOM group. After careful screening of the oxidizing agents, when using *m*-chloroperbenzoic acid (*m*-CPBA), asperversiamides A (51%) and B (23%) were generated as separable mixtures, while the spiro-fused oxindole (±)-C8a′-*epi*-asperversiamide C was produced from (±)-asperversiamide D via [1,5]-H shift.

6. BIOLOGICAL ACTIVITIES

With the unique core structures and diversified stereochemistry and tailoring modifications, the fungal BCDO indole alkaloids exhibit a wide spectrum of biological and pharmaceutical activities, including but not limited to insecticidal, anticancer, antimicrobial, cytotoxicity, anti-inflammatory, antiparasitic, and calmodulin-inhibiting effects (Table 1).

Brevianamides A and D were identified as potent antifeedants against the larvae of two lepidopterous pests, *Spodoptera frugiperda* and *Heliothis virescens*.[131,132] Brevianamide A showed a marked dose−response relationship and retained activity at 100 ppm. Brevianamide D displayed a less antifeedant activity than brevianamide A, being active at 1,000 ppm against *S. frugiperda*. Nonetheless, brevianamide D was more effective than brevianamide A on reducing pupal weight.

Notoamides A−C showed moderate cytotoxicity against HeLa and L1210 cells, with notoamide D having the best IC_{50} value.[35] Notoamide B displayed potential anti-inflammatory activities by inhibiting production of the pro-inflammatory cytokines TNF-α and IL-1β[133] and was able to inhibit the colony formation of 22Rv1 prostate cancer cells at a concentration of 100 μM.[134] (−)-Enantiomers of notoamides A and B, and 6-*epi*-notoamide T inhibited the receptor activator of nuclear factor-κB (NF-κB) ligand (RANKL)-induced osteoclastogenic differentiation of murine RAW264 cells more strongly than their corresponding (+)-enantiomers.[135] Besides the insecticidal activity against first instar larvae of the cotton bollworm, notoamide D also showed activities toward human and plant bacterial pathogens, and seven widespread pathogenic fungi.[136] Notoamide G demonstrated great antitumor activities against a panel of hepatocellular carcinoma (HCC) cell lines and was considered as a potent lead for further development of an antitumor agent.[137] Specifically, notoamide G inhibited the viability of HepG2 and Huh-7 cells via both apoptosis and autophagy pathways. Further investigation revealed that notoamide G promoted P38 and JNK phosphorylation. Notoamide H showed antifungal activity with an MIC value of 25 μg/mL against *Rhizoctonia solani*.[138] By measuring the inhibitory effects on *Propionibacterium acnes*-induced THP-1 cells, notoamides H and R displayed moderate anti-inflammatory activities with IC_{50} values of 46.2 and 34.3 μM, respectively. Moreover, notoamide I showed weak cytotoxicity against HeLa cells, with an IC_{50} value of 21 μg/mL.[36]

Both stephacidins A and B exhibited *in vitro* cytotoxicity against a number of human tumor cell lines.[44] Stephacidin A and 6-*epi*-stephacidin A showed inhibitory activities against RANKL-induced osteoclastogenic differentiation of murine RAW264 cells, with (−)-enantiomers being more active than their corresponding (+)-enantiomers.[135] Stephacidin A also

https://doi.org/10.1021/acs.chemrev.4c00250
Chem. Rev. XXXX, XXX, XXX−XXX

Scheme 69. Enantioselective Total Synthesis of Marcfortine C

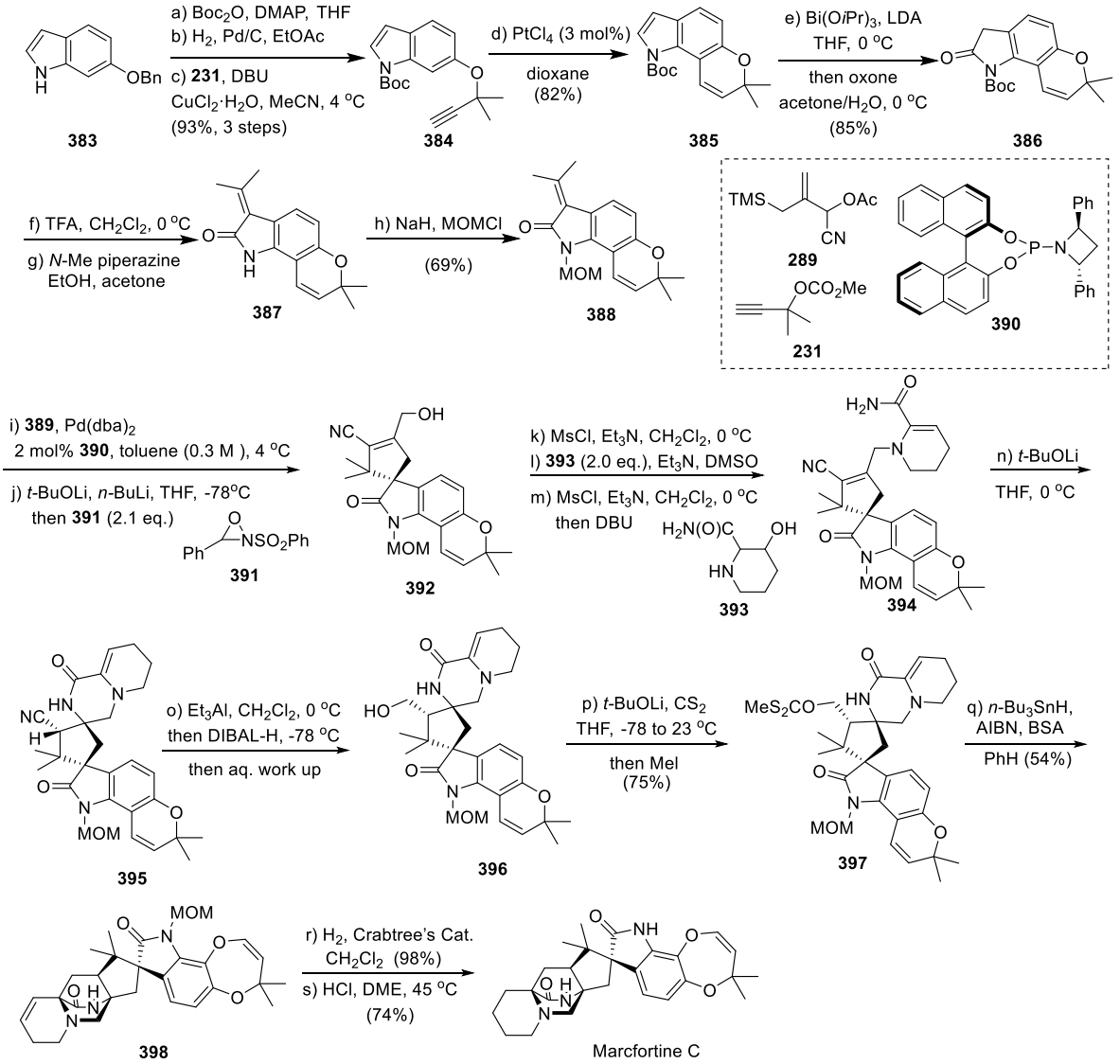

Scheme 70. Total Syntheses of Asperversiamides Using IMDA Strategy

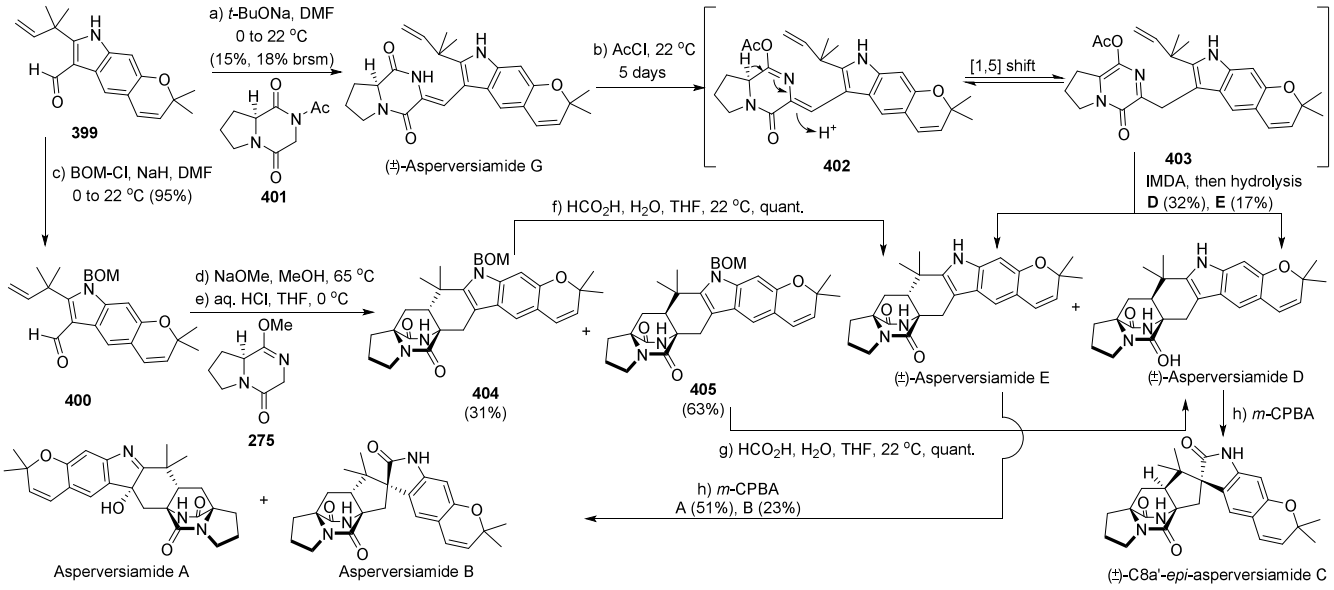

https://doi.org/10.1021/acs.chemrev.4c00250
Chem. Rev. XXXX, XXX, XXX−XXX

displayed potential anti-inflammatory activities, showing 46.5% and 32.6% inhibition ratios for cytokines IL-1β and TNF-α, respectively, at the concentration of 20 μM.[133] As to the activity against pathogenic bacteria, stephacidin A displayed good selectivity toward *Staphylococcus epidermidis*.[139] It was also reported that stephacidin A showed antibacterial activity and respiratory inhibitor activity, being able to inhibit the respiratory chain with an IC_{50} value of 35 μM.[140] Stephacidin B demonstrated more potent and selective antitumor activities, especially against the prostate testosterone-dependent LNCaP cells.[44]

The *in vitro* anti-inflammatory activity of taichunamide D was investigated by using LPS-stimulated murine macrophage RAW 264.7 cells, showing significant inhibition of cytokines IL-1β at the concentration of 20 μM.[133] Taichunamide H exhibited a moderate activity against *Pseudomonas aeruginosa* with an MIC value of 0.8 μM.[136,141]

Malbrancheamide is a calmodulin (CaM) antagonist, inhibiting the activity of CaM-dependent phosphodiesterase (PDE1) in a concentration-dependent manner with an IC_{50} of 3.65 μM[68,142−144] and could cause moderate inhibition of radicle growth of *Amaranthus hypochondriacus* with an IC_{50} of 0.37 μM.[68] *In vitro* assays showed that malbrancheamide exhibited inhibitory activity toward yeast α-glucosidase (αGHY) with an IC_{50} value of 458.7 μM, and the activity was corroborated *in vivo* using a sucrose tolerance test in normoglucemic mice.[145] Malbrancheamide also showed moderate inhibitory activity against the protein tyrosine phosphatase 1B (PTP-1B) with an IC_{50} value of 14.5 μM.[145] The interactions of malbrancheamide, malbrancheamide B, and isomalbrancheamide B with CaM were analyzed using enzymatic, fluorescent, spectroscopic, nuclear magnetic resonance (NMR), and molecular modeling approaches.[144] The enzymatic and fluorescent experiments showed that all three alkaloids were classical CaM inhibitors. The results also revealed that malbrancheamide, malbrancheamide B and isomalbrancheamide B induced a significant vasorelaxant activity in an endothelium-intact model in rat aorta rings and a lesser effect in an endothelium-denuded model.[146] Docking analysis indicated that the endothelium-independent relaxation could be mediated by its CaM inhibitory properties through an interference with myosin light chain phosphorylation and positive modulation of eNOS.

Paraherquamides exhibit a broad spectrum of anthelmintic and insecticidal activities (even toward some drug-resistant strains of nematodes).[73,74,147,148] The bioactivity of paraherquamide A was tested against immature *Trichostrongylus colubriformis* in gerbils,[148] *Hemonchus contortus* larvae *in vitro*, adult *T. colubriformis* infections,[74] and the common gastrointestinal nematode species of sheep,[149] and it showed great effectiveness. However, when paraherquamide A was examined for the common gastrointestinal nematodes of dogs, it produced unexpected and severe toxicosis at doses far below those that were safe in the ruminants.[150,151] Paraherquamides A, B, and E and other paraherquamide-related compounds VM55596 and VM55597 exhibited insecticidal activity against the hemipteran *Oncopeltus fasciatus* Dallas, and the most potent compound was paraherquamide E with an LD_{50} of 0.089 μg/nymph.[78] The oral activity of paraherquamide E against adult *T. colubriformis* infections in gerbils was determined, showing significant effectiveness in reduction of faecal egg count.[82] Paraherquamide E was also evaluated against the human liver cancer cell line Bel-7402, giving the IC_{50} value of 1.9 μM.[80] Additionally, paraherquamides F and G exhibited anthelmintic activities against *Hemonchus contortus* larvae *in vitro* and adult *T. colubriformis* infections in gerbils.[74]

It is worth noting that, based on the bioactivity and toxicity of paraherquamide A, the 2-deoxy-derivitive of paraherquamide A, namely 2-desoxoparaherquamide (later named Derquantel by Pfizer), was chemically synthesized from paraherquamide A and determined to display better anthelmintic activity and maintain a safe level of toxicity.[152] Mechanism exploration revealed that 2-desoxoparaherquamide blocked nicotinic stimulation of cells expressing α3 ganglionic (IC_{50} = 6 μM) and muscle-type (IC_{50} = 3 μM) receptors, suggesting that the anthelmintic action of this compound is acting as an antagonist of nicotinic acetylcholine receptor (nAChRs) to block cholinergic neuromuscular transmission.[152] The combination of Derquantel and the macrocyclic lactone abamectin has an excellent broad-spectrum efficacy against several parasitic nematodes in sheep. Therefore, Derquantel in a formulated combination with abamectin has been released and marketed as an anthelmintic medicine under the trade name STARTECT.[153,154]

7. CONCLUDING REMARKS

Progress toward understanding a growing number of BCDO alkaloid metabolic systems and characterization of biosynthetic enzyme functions has enabled their expanded application in the synthesis of unnatural derivatives. For example, Kelly et al. pursued a data science-driven protein engineering analysis of the reverse prenyltransferase NotF from the notoamide biosynthetic pathway and developed a one-pot cascade reaction using NotF and FMO BvnB from the brevianamide biosynthetic pathway. This approach provided an efficient route to the 3-hydroxypyrroloindoline scaffold from readily accessible diketopiperazine building blocks, culminating in the first biocatalytic synthesis of (−)-eurotiumin A.[92] We anticipate further interactions between chemical and biological syntheses, driven by BCDO genetic and biocatalytic building blocks to explore diverse combinatorial biosynthesis and chemoenzymatic synthesis approaches for structural diversification. An expanded BCDO alkaloid library will contribute to more extensive bioactivity evaluations and future development of therapeutic agents.

Among the four representative BCDO alkaloids, the biosynthetic pathways of DKPs brevianamide A/B and MKP malbrancheamide have been fully elucidated. However, several important questions remain for the construction of DKP notoamide A and MKP paraherquamide A. The uncharacterized biosynthetic steps include: 1) the intramolecular [4+2] IMDA cyclization to assemble the BCDO core in notoamide A; 2) the cyclization of the dimethylpyran ring in notoamide A; 3) the biosynthetic route to stephacidin A during assembly of notoamide A; and 4) expansion of the pyran moiety to the 7-membered dioxepin ring in paraherquamide A. Moreover, *N*-methylation and hydroxylation of the prolyl group to complete the paraherquamide A pathway remain to be established. Further bioinformatics, genetic and biochemical analyses of uncharacterized enzymes are required for complete elucidation of these biosynthetic systems. Another outstanding question relates to the formation of antipodal metabolites of notoamide A and stephacidin A, which are produced by different fungal species. Have these microorganisms convergently evolved strain-specific biosynthetic enzymes for production of enantiomeric BCDO alkaloids, or have mutations accumulated from

https://doi.org/10.1021/acs.chemrev.4c00250
Chem. Rev. XXXX, XXX, XXX−XXX

an early common progenitor? Future experimental and mechanistic characterization of the presumed enantioselective enzymes will enlighten our understanding of this fascinating question.

This review sought to summarize the research history from the viewpoints of both biological and synthetic chemists and proposed select future prospects to provide inspiration for the long-sought biogenesis of fungal indole alkaloids that comprise BCDO metabolites. We anticipate that remaining mysteries of unknown biosyntheses will be fully resolved in the not too distant future. This report, supplemented with our previous work that focused on biosynthesis[5,59,97,221−227] and chemical synthesis,[59,97,226,227] provides detailed insights by systematically reviewing the advances of the endlessly fascinating fungal BCDO indole alkaloids.

AUTHOR INFORMATION

Corresponding Authors

David H. Sherman − *Life Sciences Institute, University of Michigan, Ann Arbor, Michigan 48109, United States; Departments of Medicinal Chemistry, Chemistry and Microbiology & Immunology, University of Michigan, Ann Arbor, Michigan 48109, United States;* orcid.org/0000-0001-8334-3647; Email: davidhs@umich.edu

Shengying Li − *State Key Laboratory of Microbial Technology, Shandong University, Qingdao, Shandong 266237, China; Laboratory for Marine Biology and Biotechnology, Qingdao Marine Science and Technology Center, Qingdao, Shandong 266237, China;* orcid.org/0000-0002-5244-870X; Email: lishengying@sdu.edu.cn

Authors

Lei Du − *State Key Laboratory of Microbial Technology, Shandong University, Qingdao, Shandong 266237, China;* orcid.org/0000-0003-2245-7100

Longyang Dian − *State Key Laboratory of Microbial Technology, Shandong University, Qingdao, Shandong 266237, China*

Sean A. Newmister − *Life Sciences Institute, University of Michigan, Ann Arbor, Michigan 48109, United States*

Yuwei Xia − *State Key Laboratory of Microbial Technology, Shandong University, Qingdao, Shandong 266237, China; Key Laboratory of Marine Drugs, Ministry of Education of China, School of Medicine and Pharmacy, Ocean University of China, Qingdao, Shandong 266003, China*

Guanzhong Luo − *State Key Laboratory of Microbial Technology, Shandong University, Qingdao, Shandong 266237, China*

Complete contact information is available at: https://pubs.acs.org/10.1021/acs.chemrev.4c00250

Author Contributions

[†]Lei Du and Longyang Dian contributed equally to this work.

Notes

The authors declare no competing financial interest.

Biographies

Lei Du is a professor at the State Key Laboratory of Microbial Technology, Shandong University. He obtained his Bachelor's and Master's degrees from Tianjin University. He earned his doctoral degree in 2018 and subsequently pursued postdoctoral research under the mentorship of Prof. Shengying Li at the University of Chinese Academy of Sciences. He began his independent research career at Shandong University as a full professor in 2020. His current research focuses on the biosynthesis of microbial natural products.

Longyang Dian is a professor at the State Key Laboratory of Microbial Technology, Shandong University. He received his Ph.D. degree in 2015 from Tianjin University with Profs. Kang Zhao and Yunfei Du. After working as a senior researcher in Technion-Israel Institute of Technology with Prof. Ilan Marek (2015−2018) and a postdoctoral research fellow with Prof. David A. Leigh in University of Manchester (2018−2019), he started his independent research career in Shandong University as a full professor in 2020. His current research interests include novel organic reaction development and application in the synthesis and late-stage functionalization of natural products.

Sean A. Newmister is a research scientist at the Life Sciences Institute, University of Michigan. He earned his Bachelor's degree in 2007 at The Ohio State University and his Ph.D. in 2012 with Prof. Ivan Rayment at the University of Wisconsin—Madison. His current research focuses on enzymology and structural biology of indole alkaloid, polyketide and additional natural product biosynthetic pathways.

Yuwei Xia obtained her Ph.D. in 2024 from School of Medicine and Pharmacy, Ocean University of China, with Prof. Weiming Zhu. Her doctoral research has been focused on the biosynthesis of novel natural products and the identification of novel enzymes. Presently, she serves as a biosystem scientist at LifeFoundry with an emphasis on synthetic biology applications.

Guanzhong Luo was a postgraduate student at the State Key Laboratory of Microbial Technology, Shandong University, focusing on organic chemistry.

David H. Sherman is the Hans W. Vahlteich Professor of Medicinal Chemistry at the University of Michigan College of Pharmacy, and Research Professor in the Life Sciences Institute. He received his B.A. in Chemistry at UC Santa Cruz (Phil Crews), received his Ph.D. at Columbia University (Gilbert Stork), and conducted postdoctoral research at the John Innes Institute (David Hopwood). He began his academic career at the University of Minnesota and has been at the University of Michigan since 2003, focusing on the characterization of natural product biosynthetic pathways from bacteria and fungi. Sherman currently serves as faculty lead of the UM Natural Products Biosciences Initiative, which includes efforts in natural products drug discovery from pure culture microbes, plants, complex microbiomes and animals using diverse chemical biology and engineering methods. He received the 2024 Norman R. Farnsworth Research Achievement Award from the American Society of Pharmacognosy.

Shengying Li is a distinguished professor of Shandong University. He earned his Bachelor's degree in Biology (2000) and Master's degree in Microbiology (2003) with Professor Zhonghui Zheng at School of Life Sciences, Xiamen University. He received his Ph.D. degree in Medicinal Chemistry (2009) from the University of Michigan with Professor David H. Sherman. He then carried out his postdoctoral research on microbial natural product biosynthesis in the same laboratory at Life Sciences Institute, the University of Michigan. In 2012, he became a full professor at Qingdao Institute of Bioenergy and Bioprocess Technology, Chinese Academy of Sciences. Since 2018, he has served as the principal investigator of the Enzyme Engineering Group at the State Key Laboratory of Microbial Technology, Shandong University. His research interests include natural product biosynthesis, cytochrome P450 enzymology, enzyme engineering, and synthetic biology.

ACKNOWLEDGMENTS

We wish to dedicate this review article to the pioneer in this field as well as our long-time collaborator, friend, and colleague Robert M. Williams, a prodigious and uniquely insightful organic chemist, who passed away on May 13, 2020. Among many others, Bob made remarkable contributions to the biomimetic synthesis of bicyclo[2.2.2]diazaoctane indole alkaloids based on proposed biosynthetic routes of assembly. This work was supported by National Key Research and Development Program of China (2021YFA0911500), National Natural Science Foundation of China (22237004, 32370032, 32170088, 22101153, 32025001), Shandong Provincial Natural Science Foundation (ZR2020ZD23, ZR2019ZD20, 2021QB004), Taishan Young Scholars (tsqn202103019, tsqn202312032), the Overseas Excellent Young Scientists Fund Program of Shandong Province (2022HWYQ003), and the Natural Science Foundation of Jiangsu Province (BK20210106). We are also grateful to NIH grant R35 GM118101 and the Hans W. Vahlteich Professorship (to D.H.S.).

REFERENCES

(1) Porter, A. E. A.; Sammes, P. G. A Diels-Alder reaction of possible biosynthetic importance. *J. Chem. Soc. D* **1970**, *17*, 1103.

(2) Ye, Y.; Du, L.; Zhang, X.; Newmister, S. A.; McCauley, M.; Alegre-Requena, J. V.; Zhang, W.; Mu, S.; Minami, A.; Fraley, A. E.; Adrover-Castellano, M. L.; Carney, N. A.; Shende, V. V.; Qi, F.; Oikawa, H.; Kato, H.; Tsukamoto, S.; Paton, R. S.; Williams, R. M.; Sherman, D. H.; Li, S. Fungal-derived brevianamide assembly by a stereoselective semipinacolase. *Nat. Catal.* **2020**, *3*, 497−506.

(3) Dan, Q.; Newmister, S. A.; Klas, K. R.; Fraley, A. E.; McAfoos, T. J.; Somoza, A. D.; Sunderhaus, J. D.; Ye, Y.; Shende, V. V.; Yu, F.; Sanders, J. N.; Brown, W. C.; Le, Z.; Paton, R. S.; Houk, K. N.; Smith, J. L.; Sherman, D. H.; Williams, R. M. Fungal indole alkaloid biogenesis through evolution of a bifunctional reductase/Diels-Alderase. *Nat. Chem.* **2019**, *11*, 972−980.

(4) Liu, Z.; Rivera, S.; Newmister, S. A.; Sanders, J. N.; Nie, Q.; Liu, S.; Zhao, F.; Ferrara, J. D.; Shih, H.-W.; Patil, S.; Xu, W.; Miller, M. D.; Phillips, G. N.; Houk, K. N.; Sherman, D. H.; Gao, X. An NmrA-like enzyme-catalysed redox-mediated Diels-Alder cycloaddition with *anti*-selectivity. *Nat. Chem.* **2023**, *15*, 526−534.

(5) Li, S.; Srinivasan, K.; Tran, H.; Yu, F.; Finefield, J. M.; Sunderhaus, J. D.; McAfoos, T. J.; Tsukamoto, S.; Williams, R. M.; Sherman, D. H. Comparative analysis of the biosynthetic systems for fungal bicyclo[2.2.2]diazaoctane indole alkaloids: the (+)/(−)-notoamide, paraherquamide and malbrancheamide pathways. *MedChemComm* **2012**, *3*, 987−996.

(6) Baldas, J.; Birch, A. J.; Russell, R. A. Studies in relation to biosynthesis. Part XLVI. Incorporation of *cyclo*-L-tryptophyl-L-proline into brevianamide A. *J. Chem. Soc., Perkin Trans. 1* **1974**, *1*, 50−52.

(7) Birch, A. J.; Russell, R. A. Studies in relation to biosynthesis—XLIV: Structural elucidations of brevianamides-B, -C, -D and -F. *Tetrahedron* **1972**, *28*, 2999−3008.

(8) Birch, A. J.; Wright, J. J. Studies in relation to biosynthesis—XLII: The structural elucidation and some aspects of the biosynthesis of the brevianamides-A and -E. *Tetrahedron* **1970**, *26*, 2329−2344.

(9) Birch, A. J.; Wright, J. J. The brevianamides: a new class of fungal alkaloid. *J. Chem. Soc. D* **1969**, *12*, 644−645.

(10) Wilson, B. J.; Yang, D. T. C.; Harris, T. M. Production, isolation, and preliminary toxicity studies of brevianamide A from cultures of *Penicillium viridicatum*. *Appl. Microbiol.* **1973**, *26*, 633−635.

(11) Robbers, J. E.; Straus, J. W. Isolation of brevianamide A from *Penicillium ochraceum*. *Lloydia* **1975**, *38*, 355−356.

(12) Coetzer, J. The structure and absolute configuration of 5-bromobrevianamide A. *Acta Crystallogr.* **1974**, *B30*, 2254−2256.

(13) Williams, R. M.; Glinka, T.; Kwast, E. Facial selectivity of the intramolecular SN2' cyclization: stereocontrolled total synthesis of brevianamide B. *J. Am. Chem. Soc.* **1988**, *110*, 5927−5929.

(14) Williams, R. M.; Kwast, E.; Coffman, H.; Glinka, T. Remarkable, enantio-divergent biogenesis of brevianamide A and B. *J. Am. Chem. Soc.* **1989**, *111*, 3064−3065.

(15) Dunkerton, L. V.; Chen, H.; McKillican, B. P. Synthetic approaches to brevianamides A and B I. Preparation of 4-p-methoxybenzyl-5-(1'-carbomethoxy-2'-[1'',1''-dimethylallyl-2',3'dihydroindole]methylidene)-1,2-L-pyrrolidinopiperazine-3,6-dione via an Ireland ester enolate Claisen rearrangement. *Tetrahedron Lett.* **1988**, *29*, 2539−2542.

(16) Birch, A. J.; English, R. J.; Massy-Westropp, R. A.; Smith, H. Studies in relation to biosynthesis. Part XV. Origin of terpenoid structures in mycelianamide and mycophenolic acid. *J. Chem. Soc.* **1958**, 369−375.

(17) Steyn, P. S. Austamide, a new toxic metabolite from *Aspergillus ustus*. *Tetrahedron Lett.* **1971**, *12*, 3331−3334.

(18) Williams, R. M.; Glinka, T.; Kwast, E.; Coffman, H.; Stille, J. K. Asymmetric, stereocontrolled total synthesis of (−)-brevianamide B. *J. Am. Chem. Soc.* **1990**, *112*, 808−821.

(19) Sanz-Cervera, J. F.; Glinka, T.; Williams, R. M. Biosynthesis of brevianamides A and B: in search of the biosynthetic Diels-Alder construction. *Tetrahedron* **1993**, *49*, 8471−8482.

(20) Sanz-Cervera, J. F.; Glinka, T.; Williams, R. M. Biosynthesis of the brevianamides: quest for a biosynthetic Diels-Alder cyclization. *J. Am. Chem. Soc.* **1993**, *115*, 347−348.

(21) Domingo, L. R.; Sanz-Cervera, J. F.; Williams, R. M.; Picher, M. T.; Marco, J. A. Biosynthesis of the brevianamides. An *ab Initio* study of the biosynthetic intramolecular Diels-Alder cycloaddition. *J. Org. Chem.* **1997**, *62*, 1662−1667.

(22) Williams, R. M.; Sanz-Cervera, J. F.; Sancenon, F.; Marco, J. A.; Halligan, K. M. Biomimetic Diels-Alder cyclizations for the construction of the brevianamide, paraherquamide, sclerotamide, asperparaline and VM55599 ring systems. *Bioorg. Med. Chem.* **1998**, *6*, 1233−1241.

(23) Williams, R. M.; Sanz-Cervera, J. F.; Sancenon, F.; Marco, J. A.; Halligan, K. Biomimetic Diels-Alder cyclizations for the construction of the brevianamide, paraherquamide, sclerotiamide, and VM55599 ring systems. *J. Am. Chem. Soc.* **1998**, *120*, 1090−1091.

(24) Adams, L. A.; Valente, M. W. N.; Williams, R. M. A concise synthesis of *d*, *l*-brevianamide B via a biomimetically-inspired IMDA construction. *Tetrahedron* **2006**, *62*, 5195−5200.

(25) Stocking, E. M.; Williams, R. M.; Sanz-Cervera, J. F. Reverse prenyl transferases exhibit poor facial discrimination in the biosynthesis of paraherquamide A, brevianamide A, and austamide. *J. Am. Chem. Soc.* **2000**, *122*, 9089−9098.

(26) Godfrey, R. C.; Green, N. J.; Nichol, G. S.; Lawrence, A. L. Total synthesis of brevianamide A. *Nat. Chem.* **2020**, *12*, 615−619.

(27) Steyn, P. S. The structures of five diketopiperazines from *Aspergillus ustus*. *Tetrahedron* **1973**, *29*, 107−120.

(28) Scott, P. M.; Kennedy, B. P. C.; Harwig, J.; Chen, Y.-K. Formation of diketopiperazines by *Penicillium italicum* isolated from oranges. *Appl. Microbiol.***1974**, *28*, 892−894.

(29) Kaur, A.; Raja, H. A.; Deep, G.; Agarwal, R.; Oberlies, N. H. Pannorin B, a new naphthopyrone from an endophytic fungal isolate of *Penicillium* sp. *Magnetic Reson. Chemistry***2016**, *54*, 164−167.

(30) Bird, B. A.; Remaley, A. T.; Campbell, I. M. Brevianamides A and B are formed only after conidiation has begun in solid cultures of *Penicillium brevicompactum*. *Appl. Environ. Microbiol.* **1981**, *42*, 521−525.

(31) Godfrey, R. C.; Jones, H. E.; Green, N. J.; Lawrence, A. L. Unified total synthesis of the brevianamide alkaloids enabled by chemical investigations into their biosynthesis. *Chem. Sci.* **2022**, *13*, 1313−1322.

(32) Liu, W.; Wang, L.; Wang, B.; Xu, Y.; Zhu, G.; Lan, M.; Zhu, W.; Sun, K. Diketopiperazine and diphenylether derivatives from marine algae-derived *Aspergillus versicolor* OUCMDZ-2738 by epigenetic activation. *Mar. Drugs* **2019**, *17*, 6.

https://doi.org/10.1021/acs.chemrev.4c00250
Chem. Rev. XXXX, XXX, XXX−XXX

(33) Wakefield, J.; Hassan, H. M.; Jaspars, M.; Ebel, R.; Rateb, M. E. Dual induction of new microbial secondary metabolites by fungal bacterial co-cultivation. *Front. Microbiol.* **2017**, *8*, 1284.
(34) Li, L.; Chang, Q.-H.; Zhang, S.-S.; Yang, K.; Chen, F.-L.; Zhu, H.-J.; Cao, F.; Liu, Y.-F. (±)-Brevianamides Z and Z1, new diketopiperazine alkaloids from the marine-derived fungus *Aspergillus versicolor*. *J. Mol. Struct.* **2022**, *1261*, 132904.
(35) Kato, H.; Yoshida, T.; Tokue, T.; Nojiri, Y.; Hirota, H.; Ohta, T.; Williams, R. M.; Tsukamoto, S. Notoamides A-D: prenylated indole alkaloids isolated from a marine-derived fungus, *Aspergillus* sp. *Angew. Chem., Int. Ed. Engl.* **2007**, *46*, 2254−2256.
(36) Tsukamoto, S.; Kato, H.; Samizo, M.; Nojiri, Y.; Onuki, H.; Hirota, H.; Ohta, T. Notoamides F-K, prenylated indole alkaloids isolated from a marine-derived *Aspergillus sp*. *J. Nat. Prod.* **2008**, *71*, 2064−2067.
(37) Greshock, T. J.; Grubbs, A. W.; Jiao, P.; Wicklow, D. T.; Gloer, J. B.; Williams, R. M. Isolation, structure elucidation, and biomimetic total synthesis of versicolamide B, and the isolation of antipodal (−)-stephacidin A and (+)-notoamide B from Aspergillus versicolor NRRL 35600. *Angew. Chem., Int. Ed.* **2008**, *47*, 3573−3577.
(38) Tsukamoto, S.; Kawabata, T.; Kato, H.; Greshock, T. J.; Hirota, H.; Ohta, T.; Williams, R. M. Isolation of antipodal (−)-versicolamide B and notoamides L-N from a marine-derived *Aspergillus sp*. *Org. Lett.* **2009**, *11*, 1297−1300.
(39) Tsukamoto, S.; Kato, H.; Greshock, T. J.; Hirota, H.; Ohta, T.; Williams, R. M. Isolation of notoamide E, a key precursor in the biosynthesis of prenylated indole alkaloids in a marine-derived fungus, *Aspergillus* sp. *J. Am. Chem. Soc.* **2009**, *131*, 3834−3835.
(40) Tsukamoto, S.; Umaoka, H.; Yoshikawa, K.; Ikeda, T.; Hirota, H. Notoamide O, a structurally unprecedented prenylated indole alkaloid, and notoamides P-R from a marine-derived fungus, *Aspergillus sp*. *J. Nat. Prod.* **2010**, *73*, 1438−1440.
(41) Tsukamoto, S.; Umaoka, H.; Yoshikawa, K.; Ikeda, T.; Hirota, H. Correction to notoamide O, a structurally unprecedented prenylated indole alkaloid, and notoamides P-R from a marine-derived fungus, *Aspergillus* sp. *J. Nat. Prod.* **2013**, *76*, 1232.
(42) Tsukamoto, S.; Kato, H.; Samizo, M.; Nojiri, Y.; Ohnuki, H.; Hirota, H.; Ohta, T. Correction to notoamides F-K, prenylated indole alkaloids isolated from a marine-derived *Aspergillus sp*. *J. Nat. Prod.* **2013**, *76*, 1233.
(43) Tsukamoto, S.; Kato, H.; Greshock, T. J.; Hirota, H.; Ohta, T.; Williams, R. M. Correction to Isolation of notoamide E, a key precursor in the biosynthesis of prenylated indole alkaloids in a marine-derived fungus, *Aspergillus* sp. *J. Am. Chem. Soc.* **2013**, *135*, 10878.
(44) Qian-Cutrone, J.; Huang, S.; Shu, Y. Z.; Vyas, D.; Fairchild, C.; Menendez, A.; Krampitz, K.; Dalterio, R.; Klohr, S. E.; Gao, Q. Stephacidin A and B: two structurally novel, selective inhibitors of the testosterone-dependent prostate LNCaP cells. *J. Am. Chem. Soc.* **2002**, *124*, 14556−14557.
(45) Greshock, T. J.; Williams, R. M. Improved biomimetic total synthesis of D,L-stephacidin A. *Org. Lett.* **2007**, *9*, 4255−4258.
(46) Artman, G. D., III; Grubbs, A. W.; Williams, R. M. Concise, asymmetric, stereocontrolled total synthesis of stephacidins A, B and notoamide B. *J. Am. Chem. Soc.* **2007**, *129*, 6336−6342.
(47) Greshock, T. J.; Grubbs, A. W.; Tsukamoto, S.; Williams, R. M. A concise, biomimetic total synthesis of stephacidin A and notoamide B. *Angew. Chem., Int. Ed.* **2007**, *46*, 2262−2265.
(48) Grubbs, A. W.; Artman, G. D.; Tsukamoto, S.; Williams, R. M. A concise total synthesis of the notoamides C and D. *Angew. Chem., Int. Ed.* **2007**, *46*, 2257−2261.
(49) Kato, H.; Nakamura, Y.; Finefield, J. M.; Umaoka, H.; Nakahara, T.; Williams, R. M.; Tsukamoto, S. Study on the biosynthesis of the notoamides: pinacol-type rearrangement of the isoprenyl unit in deoxybrevianamide E and 6-hydroxydeoxybrevianamide E. *Tetrahedron Lett.* **2011**, *52*, 6923−6926.
(50) Kato, H.; Nakamura, Y.; Finefield, J. M.; Umaoka, H.; Nakahara, T.; Williams, R. M.; Tsukamoto, S. Corrigendum to "Study on the biosynthesis of the notoamides: pinacol-type rearrangement of the isoprenyl unit in deoxybrevianamide E and 6-hydroxydeoxybrevianamide E" [Tetrahedron Lett. 52 (2011) 6923−6926]. *Tetrahedron Lett.* **2014**, *55*, 559−560.
(51) Kametani, T.; Kanaya, N.; Ihara, M. Studies on the syntheses of heterocyclic compounds. Part 876. The chiral total synthesis of brevianamide E and deoxybrevianamide E. *J. Chem. Soc., Perkin Trans. 1* **1981**, 959−963.
(52) Somei, M.; Karasawa, Y.; Kaneko, C. Selective monoalkylation of carbon nucleophiles with gramine. *Heterocycles* **1981**, *16*, 941−949.
(53) Finefield, J. M.; Greshock, T. J.; Sherman, D. H.; Tsukamoto, S.; Williams, R. M. Notoamide E: biosynthetic incorporation into notoamides C and D in cultures of *Aspergillus versicolor* NRRL 35600. *Tetrahedron Lett.* **2011**, *52*, 1987−1989.
(54) Ding, Y.; Wet, J. R.; Cavalcoli, J.; Li, S.; Greshock, T. J.; Miller, K. A.; Finefield, J. M.; Sunderhaus, J. D.; McAfoos, T. J.; Tsukamoto, S.; Williams, R. M.; Sherman, D. H. Genome-based characterization of two prenylation steps in the assembly of the stephacidin and notoamide anticancer agents in a marine-derived *Aspergillus* sp. *J. Am. Chem. Soc.* **2010**, *132*, 12733−12740.
(55) Williams, R. M.; McAfoos, T. J.; Li, S.; Tsukamoto, S.; Sherman, D. H. Studies on the biosynthesis of the stephacidins and notoamides. Total synthesis of notoamide S. *Heterocycles* **2010**, *82*, 461−472.
(56) Finefield, J. M.; Kato, H.; Greshock, T. J.; Sherman, D. H.; Tsukamoto, S.; Williams, R. M. Biosynthetic studies of the notoamides: isotopic synthesis of stephacidin A and incorporation into notoamide B and sclerotiamide. *Org. Lett.* **2011**, *13*, 3802−3805.
(57) Finefield, J. M.; Williams, R. M. Synthesis of notoamide J: a potentially pivotal intermediate in the biosynthesis of several prenylated indole alkaloids. *J. Org. Chem.* **2010**, *75*, 2785−2789.
(58) Finefield, J. M.; Sherman, D. H.; Tsukamoto, S.; Williams, R. M. Studies on the biosynthesis of the notoamides: synthesis of an isotopomer of 6-hydroxydeoxybrevianamide E and biosynthetic incorporation into notoamide J. *J. Org. Chem.* **2011**, *76*, 5954−5958.
(59) Sunderhaus, J. D.; Sherman, D. H.; Williams, R. M. Studies on the biosynthesis of the stephacidin and notoamide natural products: a stereochemical and genetic conundrum. *Isr. J. Chem.* **2011**, *51*, 442−452.
(60) Li, S.; Finefield, J. M.; Sunderhaus, J. D.; McAfoos, T. J.; Williams, R. M.; Sherman, D. H. Biochemical characterization of NotB as an FAD-dependent oxidase in the biosynthesis of notoamide indole alkaloids. *J. Am. Chem. Soc.* **2012**, *134*, 788−791.
(61) Kato, H.; Nakahara, T.; Sugimoto, K.; Matsuo, K.; Kagiyama, I.; Frisvad, J. C.; Sherman, D. H.; Williams, R. M.; Tsukamoto, S. Isolation of notoamide S and enantiomeric 6-*epi*-stephacidin A from the fungus *Aspergillus amoenus*: biogenetic implications. *Org. Lett.* **2015**, *17*, 700−703.
(62) Sunderhaus, J. D.; McAfoos, T. J.; Finefield, J. M.; Kato, H.; Li, S.; Tsukamoto, S.; Sherman, D. H.; Williams, R. M. Synthesis and bioconversions of notoamide T: a biosynthetic precursor to stephacidin A and notoamide B. *Org. Lett.* **2013**, *15*, 22−25.
(63) Kato, H.; Nakahara, T.; Yamaguchi, M.; Kagiyama, I.; Finefield, J. M.; Sunderhaus, J. D.; Sherman, D. H.; Williams, R. M.; Tsukamoto, S. Bioconversion of 6-*epi*-notoamide T produces metabolites of unprecedented structures in a marine-derived *Aspergillus sp*. *Tetrahedron Lett.* **2015**, *56*, 247−251.
(64) Zhang, D.; Yi, W.; Ge, H.; Zhang, Z.; Wu, B. A new antimicrobial indoloditerpene from a marine-sourced fungus *Aspergillus versicolor* ZZ761. *Nat. Prod. Res.* **2021**, *35*, 3114−3119.
(65) Kagiyama, I.; Kato, H.; Nehira, T.; Frisvad, J. C.; Sherman, D. H.; Williams, R. M.; Tsukamoto, S. Taichunamides: prenylated indole alkaloids from *Aspergillus taichungensis* (IBT 19404). *Angew. Chem., Int. Ed. Engl.* **2016**, *55*, 1128−1132.
(66) Li, F.; Zhang, Z.; Zhang, G.; Che, Q.; Zhu, T.; Gu, Q.; Li, D. Determination of taichunamide H and structural revision of taichunamide A. *Org. Lett.* **2018**, *20*, 1138−1141.
(67) Li, H.; Xu, Q.; Sun, W.; Zhang, R.; Wang, J.; Lai, Y.; Hu, Z.; Zhang, Y. 21-*Epi*-taichunamide D and (±)-versicaline A, three

unusual alkaloids from the endophytic *Aspergillus versicolor* F210. *Tetrahedron Lett.* **2020**, *61*, 152219.
(68) Martinez-Luis, S.; Rodriguez, R.; Acevedo, L.; Gonzalez, M. C.; Lira-Rocha, A.; Mata, R. Malbrancheamide, a new calmodulin inhibitor from the fungus *Malbranchea aurantiaca*. *Tetrahedron* **2006**, *62*, 1817−1822.
(69) Figueroa, M.; Del Carmen Gonzalez, M.; Mata, R. Malbrancheamide B, a novel compound from the fungus *Malbranchea aurantiaca*. *Nat. Prod. Res.* **2008**, *22*, 709−714.
(70) Watts, K. R.; Loveridge, S. T.; Tenney, K.; Media, J.; Valeriote, F. A.; Crews, P. Utilizing DART mass spectrometry to pinpoint halogenated metabolites from a marine invertebrate-derived fungus. *J. Org. Chem.* **2011**, *76*, 6201−6208.
(71) Ding, Y.; Greshock, T. J.; Miller, K. A.; Sherman, D. H.; Williams, R. M. Premalbrancheamide: synthesis, isotopic labeling, biosynthetic incorporation, and detection in cultures of *Malbranchea aurantiaca*. *Org. Lett.* **2008**, *10*, 4863−4866.
(72) Yamazaki, M.; Okuyama, E.; Kobayashi, M.; Inoue, H. The structure of paraherquamide, a toxic metabolite from *Penicillium paraherquei*. *Tetrahedron Lett.* **1981**, *22*, 135−136.
(73) Blanchflower, S. E.; Banks, R. M.; Everett, J. R.; Reading, C. Further novel metabolites of the paraherquamide family. *J. Antibiot.* **1993**, *46*, 1355−1363.
(74) Blanchflower, S. E.; Banks, R. M.; Everett, J. R.; Manger, B. R.; Reading, C. New paraherquamide antibiotics with anthelmintic activity. *J. Antibiot.* **1991**, *44*, 492−497.
(75) Ondeyka, J. G.; Goegelman, R. T.; Schaeffer, J. M.; Kelemen, L.; Zitano, L. Novel antinematodal and antiparasitic agents from *Penicillium Charlesii*. I. Fermentation, isolation and biological-activity. *J. Antibiot.* **1990**, *43*, 1375−1379.
(76) Liesch, J. M.; Wichmann, C. F. Novel antinematodal and antiparasitic agents from *Penicillium charlesii*. II. Structure determination of paraherquamide-B, C, D, E, F, and G. *J. Antibiot.* **1990**, *43*, 1380−1386.
(77) Ding, Y.; Gruschow, S.; Greshock, T. J.; Finefield, J. M.; Sherman, D. H.; Williams, R. M. Detection of VM55599 and preparaherquamide from *Aspergillus japonicus* and *Penicillium fellutanum*: biosynthetic implications. *J. Nat. Prod.* **2008**, *71*, 1574−1578.
(78) López-Gresa, M. P.; González, M. C.; Ciavatta, L.; Ayala, I.; Moya, P.; Primo, J. Insecticidal activity of paraherquamides, including paraherquamide H and paraherquamide I, two new alkaloids isolated from *Penicillium cluniae*. *J. Agric. Food Chem.* **2006**, *54*, 2921−2925.
(79) Zheng, Y.-Y.; Shen, N.-X.; Liang, Z.-Y.; Shen, L.; Chen, M.; Wang, C.-Y. Paraherquamide J, a new prenylated indole alkaloid from the marine-derived fungus *Penicillium janthinellum* HK1−6. *Nat. Prod. Res.* **2020**, *34*, 378−384.
(80) Wu, J.; Wang, F.; He, L.-M.; Zhou, S.-Y.; Wang, S.-B.; Jia, J.; Hong, K.; Cai, Y.-S. Aculeaquamide A, cytotoxic paraherquamide from the marine fungus *Aspergillus aculeatinus* WHUF0198. *Nat. Prod. Res.* **2022**, *36*, 4382−4387.
(81) Fraley, A. E.; Caddell Haatveit, K.; Ye, Y.; Kelly, S. P.; Newmister, S. A.; Yu, F.; Williams, R. M.; Smith, J. L.; Houk, K. N.; Sherman, D. H. Molecular basis for spirocycle formation in the paraherquamide biosynthetic pathway. *J. Am. Chem. Soc.* **2020**, *142*, 2244−2252.
(82) Banks, R. M.; Blanchflower, S. E.; Everett, J. R.; Manger, B. R.; Reading, C. Novel anthelmintic metabolites from an *Aspergillus* species; the aspergillimides. *J. Antibiot.* **1997**, *50*, 840−846.
(83) Stocking, E. M.; Sanz-Cervera, J. F.; Williams, R. M.; Unkefer, C. J. Studies on the biosynthesis of paraherquamide A. Origin of the β-methylproline ring. *J. Am. Chem. Soc.* **1996**, *118*, 7008−7009.
(84) Stocking, E. M.; Sanz-Cervera, J. F.; Unkefer, C. J.; Williams, R. M. Studies on the biosynthesis of paraherquamide. Construction of the amino acid framework. *Tetrahedron* **2001**, *57*, 5303−5320.
(85) Stocking, E. M.; Martinez, R. A.; Silks, L. A.; Sanz-Cervera, J. F.; Williams, R. M. Studies on the biosynthesis of paraherquamide: Concerning the mechanism of the oxidative cyclization of L-Isoleucine to β-Methylproline. *J. Am. Chem. Soc.* **2001**, *123*, 3391−3392.
(86) Stocking, E. M.; Sanz-Cervera, J. F.; Williams, R. M. Reverse versus normal prenyl transferases in paraherquamide biosynthesis exhibit distinct facial selectivities. *Angew. Chem., Int. Ed.* **1999**, *38*, 786−789.
(87) Stocking, E. M.; Sanz-Cervera, J. F.; Williams, R. M. Studies on the biosynthesis of paraherquamide: Synthesis and incorporation of a hexacyclic indole derivative as an advanced metabolite. *Angew. Chem., Int. Ed.* **2001**, *40*, 1296−1298.
(88) Stocking, E. M.; Sanz-Cervera, J. F.; Williams, R. M. Total synthesis of VM55599. Utilization of an intramolecular Diels-Alder cycloaddition of potential biogenetic relevance. *J. Am. Chem. Soc.* **2000**, *122*, 1675−1683.
(89) Sanz-Cervera, J. F.; Williams, R. M. Asymmetric total synthesis of (−)-VM55599: establishment of the absolute stereochemistry and biogenetic implications. *J. Am. Chem. Soc.* **2002**, *124*, 2556−2559.
(90) Sommer, K.; Williams, R. M. Studies on paraherquamide biosynthesis: synthesis of deuterium-labeled 7-hydroxy-pre-paraherquamide, a putative precursor of paraherquamides A, E, and F. *Tetrahedron* **2009**, *65*, 3246−3260.
(91) Maiya, S.; Grundmann, A.; Li, S. M.; Turner, G. The fumitremorgin gene cluster of *Aspergillus fumigatus*: identification of a gene encoding brevianamide F synthetase. *ChemBioChem.* **2006**, *7*, 1062−1069.
(92) Kelly, S. P.; Shende, V. V.; Flynn, A. R.; Dan, Q.; Ye, Y.; Smith, J. L.; Tsukamoto, S.; Sigman, M. S.; Sherman, D. H. Data science-driven analysis of substrate-permissive diketopiperazine reverse prenyltransferase NotF: applications in protein engineering and cascade biocatalytic synthesis of (−)-eurotiumin A. *J. Am. Chem. Soc.* **2022**, *144*, 19326−19336.
(93) Fraley, A. E.; Tran, H. T.; Kelly, S. P.; Newmister, S. A.; Tripathi, A.; Kato, H.; Tsukamoto, S.; Du, L.; Li, S.; Williams, R. M.; Sherman, D. H. Flavin-dependent monooxygenases NotI and NotI' mediate spiro-oxindole formation in biosynthesis of the notoamides. *ChemBioChem.* **2020**, *21*, 2449−2454.
(94) Fraley, A. E.; Garcia-Borras, M.; Tripathi, A.; Khare, D.; Mercado-Marin, E. V.; Tran, H.; Dan, Q.; Webb, G. P.; Watts, K. R.; Crews, P.; Sarpong, R.; Williams, R. M.; Smith, J. L.; Houk, K. N.; Sherman, D. H. Function and structure of MalA/MalA', iterative halogenases for late-stage C-H functionalization of indole alkaloids. *J. Am. Chem. Soc.* **2017**, *139*, 12060−12068.
(95) Jiang, W.; Cacho, R. A.; Chiou, G.; Garg, N. K.; Tang, Y.; Walsh, C. T. EcdGHK are three tailoring iron oxygenases for amino acid building blocks of the echinocandin scaffold. *J. Am. Chem. Soc.* **2013**, *135*, 4457−4466.
(96) Li, L.; Tang, M. C.; Tang, S.; Gao, S.; Soliman, S.; Hang, L.; Xu, W.; Ye, T.; Watanabe, K.; Tang, Y. Genome mining and assembly-line biosynthesis of the UCS1025A pyrrolizidinone family of fungal alkaloids. *J. Am. Chem. Soc.* **2018**, *140*, 2067−2071.
(97) Klas, K. R.; Kato, H.; Frisvad, J. C.; Yu, F.; Newmister, S. A.; Fraley, A. E.; Sherman, D. H.; Tsukamoto, S.; Williams, R. M. Structural and stereochemical diversity in prenylated indole alkaloids containing the bicyclo[2.2.2]diazaoctane ring system from marine and terrestrial fungi. *Nat. Prod. Rep.* **2018**, *35*, 532−558.
(98) Liu, Z.; Zhao, F.; Zhao, B.; Yang, J.; Ferrara, J.; Sankaran, B.; Venkataram Prasad, B. V.; Kundu, B. B.; Phillips, G. N.; Gao, Y.; Hu, L.; Zhu, T.; Gao, X. Structural basis of the stereoselective formation of the spirooxindole ring in the biosynthesis of citrinadins. *Nat. Commun.* **2021**, *12*, 4158.
(99) Williams, R. M.; Kwast, E. Carbanion-mediated oxidative deprotection of non-enolizable benzylated amides. *Tetrahedron Lett.* **1989**, *30*, 451−454.
(100) Williams, R. M.; Glinka, T. Promising cyclization reactions to construct the ring systems of brevianamides A,B. *Tetrahedron Lett.* **1986**, *27*, 3581−3584.
(101) Greshock, T. J.; Williams, R. M. Improved biomimetic total synthesis of D,L-stephacidin A. *Org. Lett.* **2012**, *14*, 6377−6378.
(102) Frebault, F. C.; Simpkins, N. S. A cationic cyclisation route to prenylated indole alkaloids: synthesis of malbrancheamide B and

brevianamide B, and progress towards stephacidin A. *Tetrahedron* **2010**, *66*, 6585−6596.
(103) Robins, J. G.; Kim, K. J.; Chinn, A. J.; Woo, J. S.; Scheerer, J. R. Intermolecular Diels-Alder cycloaddition for the construction of bicyclo[2.2.2]diazaoctane structures: Formal synthesis of brevianamide B and premalbrancheamide. *J. Org. Chem.* **2016**, *81*, 2293−2301.
(104) Perkins, J. C.; Wang, X.; Pike, R. D.; Scheerer, J. R. Further investigation of the intermolecular Diels-Alder cycloaddition for the synthesis of bicyclo[2.2.2]diazaoctane alkaloids. *J. Org. Chem.* **2017**, *82*, 13656−13662.
(105) Xu, X.; Zhang, X.; Nong, X.; Wang, J.; Qi, S. Brevianamides and mycophenolic acid derivatives from the deep-sea-derived fungus *Penicillium brevicompactum* DFFSCS025. *Mar. Drugs* **2017**, *15*, 43.
(106) Qin, W.-F.; Xiao, T.; Zhang, D.; Deng, L.-F.; Wang, Y.; Qin, Y. Total synthesis of (−)-depyranoversicolamide B. *Chem. Commun.* **2015**, *51*, 16143−16146.
(107) Xu, F.; Smith, M. W. A general approach to 2,2-disubstituted indoxyls: total synthesis of brevianamide A and trigonoliimine C. *Chem. Sci.* **2021**, *12*, 13756−13763.
(108) Mansour, A.; Gagosz, F. Expedited total synthesis of (±)-brevianamide A via the strategic use of gold(I) catalysis. *Org. Lett.* **2022**, *24*, 7200−7204.
(109) Baran, P. S.; Guerrero, C. A.; Ambhaikar, N. B.; Hafensteiner, B. D. Short, enantioselective total synthesis of stephacidin A. *Angew. Chem., Int. Ed.* **2005**, *44*, 606−609.
(110) Baran, P. S.; Guerrero, C. A.; Hafensteiner, B. D.; Ambhaikar, N. B. Total synthesis of avrainvillamide (CJ-17,665) and stephacidin B. *Angew. Chem., Int. Ed.* **2005**, *44*, 3892−3895.
(111) Baran, P. S.; Hafensteiner, B. D.; Ambhaikar, N. B.; Guerrero, C. A.; Gallagher, J. D. Enantioselective total synthesis of avrainvillamide and the stephacidins. *J. Am. Chem. Soc.* **2006**, *128*, 8678−8693.
(112) Herzon, S. B.; Myers, A. G. Enantioselective synthesis of stephacidin B. *J. Am. Chem. Soc.* **2005**, *127*, 5342−5344.
(113) Nelson, L. A. K.; Shaw, A. C.; Abrams, S. R. Synthesis of (+)-, (−)- and (±)-7′-hydroxyabscisic acid. *Tetrahedron* **1991**, *47*, 3259−3270.
(114) Simpkins, N. S.; Pavlakos, I.; Weller, M. D.; Male, L. The cascade radical cyclisation approach to prenylated alkaloids: synthesis of stephacidin A and notoamide B. *Org. Biomol. Chem.* **2013**, *11*, 4957−4970.
(115) Mercado-Marin, E. V.; Sarpong, R. Unified approach to prenylated indole alkaloids: total syntheses of (−)-17-hydroxycitrinalin B, (+)-stephacidin A, and (+)-notoamide I. *Chem. Sci.* **2015**, *6*, 5048−5052.
(116) Zhang, B.; Zheng, W.; Wang, X.; Sun, D.; Li, C. Total synthesis of notoamides F, I, and R and sclerotiamide. *Angew. Chem., Int. Ed.* **2016**, *55*, 10435−10438.
(117) Mukai, K.; de Sant'Ana, D. P.; Hirooka, Y.; Mercado-Marin, E. V.; Stephens, D. E.; Kou, K. G. M.; Richter, S. C.; Kelley, N.; Sarpong, R. Bioinspired chemical synthesis of monomeric and dimeric stephacidin A congeners. *Nat. Chem.* **2018**, *10*, 38−44.
(118) Cox, R. J.; Williams, R. M. Synthetic studies towards paraherquamide F: synthesis of the 1,7-dihydropyrano[2,3-*g*]indole ring system. *Tetrahedron Lett.* **2002**, *43*, 2149−2152.
(119) Miller, K. A.; Tsukamoto, S.; Williams, R. M. Asymmetric total syntheses of (+)- and (−)-versicolamide B and biosynthetic implications. *Nat. Chem.* **2009**, *1*, 63−68.
(120) Miller, K. A.; Welch, T. R.; Greshock, T. J.; Ding, Y.; Sherman, D. H.; Williams, R. M. Biomimetic total synthesis of malbrancheamide and malbrancheamide B. *J. Org. Chem.* **2008**, *73*, 3116−3119.
(121) Laws, S. W.; Scheerer, J. R. Enantioselective synthesis of (+)-malbrancheamide B. *J. Org. Chem.* **2013**, *78*, 2422−2429.
(122) Williams, R. M.; Glinka, T.; Kwast, E. Synthetic studies on paraherquamide: regioselectivity of indole oxidation. *Tetrahedron Lett.* **1989**, *30*, 5575−5578.
(123) Cushing, T. D.; Sanz-Cervera, J. F.; Williams, R. M. Stereocontrolled total synthesis of (+)-paraherquamide B. *J. Am. Chem. Soc.* **1993**, *115*, 9323−9324.
(124) Williams, R. M.; Cao, J.; Tsujishima, H. Asymmetric, stereocontrolled total synthesis of paraherquamide A. *Angew. Chem., Int. Ed.* **2000**, *39*, 2540−2544.
(125) Lee, B. H.; Clothier, M. F. Conversion of marcfortine A to paraherquamide A *via* paraherquamide B. The first formal synthesis of paraherquamide A. *J. Org. Chem.* **1997**, *62*, 1795−1798.
(126) Roque, J. B.; Mercado-Marin, E. V.; Richter, S. C.; Pereira de Sant'Ana, D.; Mukai, K.; Ye, Y.; Sarpong, R. A unified strategy to reverse-prenylated indole alkaloids: total syntheses of preparaherquamide, premalbrancheamide, and (+)-VM-55599. *Chem. Sci.* **2020**, *11*, 5929−5934.
(127) Trost, B. M.; Cramer, N.; Bernsmann, H. Concise total synthesis of (±)-marcfortine B. *J. Am. Chem. Soc.* **2007**, *129*, 3086−3087.
(128) Trost, B. M.; Bringley, D. A.; Zhang, T.; Cramer, N. Rapid access to spirocyclic oxindole alkaloids: application of the asymmetric palladium-catalyzed [3 + 2] trimethylenemethane cycloaddition. *J. Am. Chem. Soc.* **2013**, *135*, 16720−16735.
(129) Trost, B. M.; Mata, G. Forging odd-membered rings: palladium-catalyzed asymmetric cycloadditions of trimethylenemethane. *Acc. Chem. Res.* **2020**, *53*, 1293−1305.
(130) Xu, Z.; Liang, X.-T.; Lan, P.; Banwell, M. G. Total syntheses of certain asperversiamides, linearly-fused and prenylated indole alkaloids. *Org. Chem. Front.* **2024**, *11*, 2433−2441.
(131) Paterson, R. R. M.; Simmonds, M. J. S.; Kemmelmeier, C.; Blaney, W. M. Effects of brevianamide A, its photolysis product brevianamide D, and ochratoxin A from two *Penicillium* strains on the insect pests *Spodoptera frugiperda* and *Heliothis virescens*. *Mycol. Res.* **1990**, *94*, 538−542.
(132) Wright, V. F.; Vesonder, R. F.; Ciegler, A. In *Microbial and viral pesticides*; Kurstak, E., Ed.; Dekker: New York, 1982.
(133) Wen, H.; Liu, X.; Zhang, Q.; Deng, Y.; Zang, Y.; Wang, J.; Liu, J.; Zhou, Q.; Hu, L.; Zhu, H.; Chen, C.; Zhang, Y. Three new indole diketopiperazine alkaloids from *Aspergillus ochraceus*. *Chem. Biodivers.* **2018**, *15*, No. e1700550.
(134) Afiyatullov, S. S.; Zhuravleva, O. I.; Antonov, A. S.; Berdyshev, D. V.; Pivkin, M. V.; Denisenko, V. A.; Popov, R. S.; Gerasimenko, A. V.; von Amsberg, G.; Dyshlovoy, S. A.; Leshchenko, E. V.; Yurchenko, A. N. Prenylated indole alkaloids from co-culture of marine-derived fungi *Aspergillus sulphureus* and *Isaria felina*. *J. Antibiot.* **2018**, *71*, 846−853.
(135) Kato, H.; Kai, A.; Kawabata, T.; Sunderhaus, J. D.; McAfoos, T. J.; Finefield, J. M.; Sugimoto, Y.; Williams, R. M.; Tsukamoto, S. Enantioselective inhibitory abilities of enantiomers of notoamides against RANKL-induced formation of multinuclear osteoclasts. *Bioorg. Med. Chem. Lett.* **2017**, *27*, 4975−4978.
(136) Zhang, P.; Yuan, X.-L.; Du, Y.-M.; Zhang, H.-B.; Shen, G.-M.; Zhang, Z.-F.; Liang, Y.-J.; Zhao, D.-L.; Xu, K. Angularly prenylated indole alkaloids with antimicrobial and insecticidal activities from an endophytic fungus *Fusarium sambucinum* TE-6L. *J. Agric. Food Chem.* **2019**, *67*, 11994−12001.
(137) Hu, L.; Zhang, T.; Liu, D.; Guan, G.; Huang, J.; Proksch, P.; Chen, X.; Lin, W. Notoamide-type alkaloid induced apoptosis and autophagy *via* a P38/JNK signaling pathway in hepatocellular carcinoma cells. *RSC Adv.* **2019**, *9*, 19855−19868.
(138) Yang, J.; Gong, L.; Guo, M.; Jiang, Y.; Ding, Y.; Wang, Z.; Xin, X.; An, F. Bioactive indole diketopiperazine alkaloids from the marine endophytic fungus *Aspergillus sp*. YJ191021. *Mar. Drugs* **2021**, *19*, 157.
(139) Chen, M.; Shao, C.-L.; Fu, X.-M.; Xu, R.-F.; Zheng, J.-J.; Zhao, D.-L.; She, Z.-G.; Wang, C.-Y. Bioactive indole alkaloids and phenyl ether derivatives from a marine-derived *Aspergillus* sp. Fungus. *J. Nat. Prod.* **2013**, *76*, 547−553.
(140) Lopez-Gresa, M. P.; Gonzalez, M. C.; Primo, J.; Moya, P.; Romero, V.; Estornell, E. Circumdatin H, a new inhibitor of mitochondrial NADH oxidase, from *Aspergillus ochraceus*. *J. Antibiot.* **2005**, *58*, 416−419.
(141) Chang, Y.-W.; Yuan, C.-M.; Zhang, J.; Liu, S.; Cao, P.; Hua, H.-M.; Di, Y.-T.; Hao, X.-J. Speramides A-B, two new prenylated

https://doi.org/10.1021/acs.chemrev.4c00250
Chem. Rev. XXXX, XXX, XXX−XXX

indole alkaloids from the freshwater-derived fungus *Aspergillus ochraceus* KM007. *Tetrahedron Lett.* **2016**, *57*, 4952−4955.
(142) Miller, K. A.; Figueroa, M.; Valente, M. W. N.; Greshock, T. J.; Mata, R.; Williams, R. M. Calmodulin inhibitory activity of the malbrancheamides and various analogs. *Bioorg. Med. Chem. Lett.* **2008**, *18*, 6479−6481.
(143) Gonzalez-Andrade, M.; Figueroa, M.; Rodriguez-Sotres, R.; Mata, R.; Sosa-Peinado, A. An alternative assay to discover potential calmodulin inhibitors using a human fluorophore-labeled CaM protein. *Anal. Biochem.* **2009**, *387*, 64−70.
(144) Figueroa, M.; Gonzalez-Andrade, M.; Sosa-Peinado, A.; Madariaga-Mazon, A.; Del Rio-Portilla, F.; Gonzalez, M. D. C.; Mata, R. Fluorescence, circular dichroism, NMR, and docking studies of the interaction of the alkaloid malbrancheamide with calmodulin. *J. Enzyme Inhib. Med. Chem.* **2011**, *26*, 378−385.
(145) Rangel-Grimaldo, M.; Macias-Rubalcava, M. L.; Gonzalez-Andrade, M.; Raja, H.; Figueroa, M.; Mata, R. α-Glucosidase and protein tyrosine phosphatase 1B inhibitors from *Malbranchea circinata*. *J. Nat. Prod.* **2020**, *83*, 675−683.
(146) Madariaga-Mazon, A.; Hernandez-Abreu, O.; Estrada-Soto, S.; Mata, R. Insights on the vasorelaxant mode of action of malbrancheamide. *J. Pharm. Pharmacol.* **2015**, *67*, 551−558.
(147) Lee, B. H.; Taylor, R. N.; Whaley, H. A.; Nelson, S. J.; Marshall, V. P. Marcfortine/paraherquamide derivatives useful as antiparasitic agents. US005776936, 1993.
(148) Ostlind, D. A.; Mickle, W. G.; Ewanciw, D. V.; Andriuli, F. J.; Campbell, W. C.; Hernandez, S.; Mochales, S.; Munguira, E. Efficacy of paraherquamide against immature Trichostrongylus colubriformis in the gerbil (*Meriones unguiculatus*). *Res. Vet. Sci.* **1990**, *48*, 260−261.
(149) Shoop, W. L.; Egerton, J. R.; Eary, C. H.; Suhayda, D. Anthelmintic activity of paraherquamide in sheep. *J. Parasitol.* **1990**, *76*, 349−351.
(150) Shoop, W. L.; Eary, C. H.; Michael, B. F.; Haines, H. W.; Seward, R. L. Anthelmintic activity of paraherquamide in dogs. *Vet. Parasitol.* **1991**, *40*, 339−341.
(151) Shoop, W. L.; Haines, H. W.; Eary, C. H.; Michael, B. F. Acute toxicity of paraherquamide and its potential as an anthelmintic. *Am. J. Vet. Res.* **1992**, *53*, 2032−2034.
(152) Lee, B. H.; Clothier, M. F.; Dutton, F. E.; Nelson, S. J.; Johnson, S. S.; Thompson, D. P.; Geary, T. G.; Whaley, H. D.; Haber, C. L.; Marshall, V. P.; Kornis, G. I.; McNally, P. L.; Ciadella, J. I.; Martin, D. G.; Bowman, J. W.; Baker, C. A.; Coscarelli, E. M.; Alexander-Bowman, S. J.; Davis, J. P.; Zinser, E. W.; Wiley, V.; Lipton, M. F.; Mauragis, M. A. Marcfortine and paraherquamide class of anthelmintics: discovery of PNU-141962. *Curr. Top. Med. Chem.* **2002**, *2*, 779−793.
(153) Kaminsky, R.; Bapst, B.; Stein, P. A.; Strehlau, G. A.; Allan, B. A.; Hosking, B. C.; Rolfe, P. F.; Sager, H. Differences in efficacy of monepantel, derquantel and abamectin against multi-resistant nematodes of sheep. *Parasitol. Res.* **2011**, *109*, 19−23.
(154) Little, P. R.; Hodge, A.; Watson, T. G.; Seed, J. A.; Maeder, S. J. Field efficacy and safety of an oral formulation of the novel combination anthelmintic, derquantel-abamectin, in sheep in New Zealand. *N. Z. Vet. J.* **2010**, *58*, 121−129.
(155) Vinale, F.; Salvatore, M. M.; Nicoletti, R.; Staropoli, A.; Manganiello, G.; Venneri, T.; Borrelli, F.; Della Greca, M.; Salvatore, F.; Andolfi, A. Identification of the main metabolites of a marine-derived strain of *Penicillium brevicompactum* using LC and GC MS techniques. *Metabolites* **2020**, *10*, 55.
(156) Russell, R.; Paterson, M.; Kemmelmeier, C. Gradient high-performance liquid chromatography using alkylphenone retention indices of insectidical extracts of *Penicillium* strains. *J. Chromatogr.* **1989**, *483*, 153−168.
(157) Chen, L.; Zhu, T.; Zhu, G.; Liu, Y.; Wang, C.; Piyachaturawat, P.; Chairoungdua, A.; Zhu, W. Bioactive natural products from the marine-derived *Penicillium brevicompactum* OUCMDZ-4920. *Youji Huaxue* **2017**, *37*, 2752−2762.
(158) Bringmann, G.; Lang, G.; Steffens, S.; Schaumann, K. Petrosifungins A and B, novel cyclodepsipeptides from a sponge-derived strain of *Penicillium brevicompactum*. *J. Nat. Prod.* **2004**, *67*, 311−315.
(159) Fischer, G.; Muller, T.; Schwalbe, R.; Ostrowski, R.; Dott, W. Species-specific profiles of mycotoxins produced in cultures and associated with conidia of airborne fungi derived from biowaste. *Int. J. Hyg. Environ. Health* **2000**, *203*, 105−116.
(160) Frisvad, J. C. High-performance liquid chromatographic determination of profiles of mycotoxins and other secondary metabolites. *J. Chromatogr.* **1987**, *392*, 333−347.
(161) Bultinck, P.; Cherblanc, F. L.; Fuchter, M. J.; Herrebout, W. A.; Lo, Y.-P.; Rzepa, H. S.; Siligardi, G.; Weimar, M. Chiroptical studies on brevianamide B: vibrational and electronic circular dichroism confronted. *J. Org. Chem.* **2015**, *80*, 3359−3367.
(162) Paterson, R. R. M.; Hawksworth, D. L. Detection of secondary metabolites in dried cultures of *Penicillium* preserved in herbaria. *Trans. Br. Mycol. Soc.* **1985**, *85*, 95−100.
(163) Malysheva, S. V.; Polizzi, V.; Moretti, A.; van Peteghem, C.; Kimpe, N.; van Bocxlaer, J.; Di Mavungu, J. D.; Saeger, S. Untargeted screening of secondary metabolites in fungal cultures and samples from mouldy indoor environments by time-of-flight mass spectrometry. *World Mycotoxin Journal* **2014**, *7*, 35−44.
(164) Vesely, D.; Vesela, D.; Jelinek, R. Nineteen mycotoxins tested on chicken embryos. *Toxicol. Lett.* **1982**, *13*, 247−251.
(165) Miller, J. D.; McMullin, D. R. Fungal secondary metabolites as harmful indoor air contaminants: 10 years on. *Appl. Microbiol. Biotechnol.* **2014**, *98*, 9953−9966.
(166) Mueller, H. M.; Boley, A. Studies on the refrigerated storage of wheat (Triticum aestivum). 2. Ergosterol, xanthomegnin, violmellein and brevianamide A after inoculation with *Penicillium viridicatum*. *Zentralbl. Mikrobiol.* **1993**, *148*, 419−431.
(167) Smedsgaard, J.; Frisvad, J. C. Using direct electrospray mass spectrometry in taxonomy and secondary metabolite profiling of crude fungal extracts. *J. Microbiol. Methods* **1996**, *25*, 5−17.
(168) Hallas-Moeller, M.; Nielsen, K. F.; Frisvad, J. C. Secondary metabolite production by cereal-associated penicillia during cultivation on cereal grains. *Appl. Microbiol. Biotechnol.* **2018**, *102*, 8477−8491.
(169) Jansen, C. M.; Dose, K. Simultaneous isolation of xanthomegnin, viomellein, rubrosulphin, viopurpurin, and brevianamide A by preparative HPLC. *Mycotoxin Res.* **1985**, *1*, 11−18.
(170) Zain, M. E.; El-Sheikh, H. H.; Soliman, H. G.; Khalil, A. M. Effect of certain chemical compounds on secondary metabolites of *Penicillium janthinellum* and *P. duclauxii*. *J. Saudi Chem. Soc.* **2011**, *15*, 239−246.
(171) Paterson, R. R. M. Standardized one- and two-dimensional thin-layer chromatographic methods for the identification of secondary metabolites in *Penicillium* and other fungi. *J. Chromatogr.* **1986**, *368*, 249−264.
(172) Wang, F.; Sarotti, A. M.; Jiang, G.; Huguet-Tapia, J. C.; Zheng, S.-L.; Wu, X.; Li, C.; Ding, Y.; Cao, S. Waikikiamides A-C: complex diketopiperazine dimer and diketopiperazine-polyketide hybrids from a Hawaiian marine fungal strain *Aspergillus sp*. FM242. *Org. Lett.* **2020**, *22*, 4408−4412.
(173) Gao, S.; Tian, W. J.; Liao, Z. J.; Wang, G. H.; Zeng, D. Q.; Liu, X. Z.; Wang, X. Y.; Zhou, H.; Chen, H. F.; Lin, T. Chemical constituents from endophytic fungus *Annulohypoxylon cf. stygium* in leaves of *Anoectochilus roxburghii*. *Chem. Biodivers.* **2020**, *17*, No. e2000424.
(174) Sugimoto, K.; Sadahiro, Y.; Kagiyama, I.; Kato, H.; Sherman, D. H.; Williams, R. M.; Tsukamoto, S. Isolation of amoenamide A and five antipodal prenylated alkaloids from *Aspergillus amoenus* NRRL 35600. *Tetrahedron Lett.* **2017**, *58*, 2797−2800.
(175) Cui, C.-M.; Li, X.-M.; Li, C.-S.; Sun, H.-F.; Gao, S.-S.; Wang, B.-G. Benzodiazepine alkaloids from marine-derived endophytic fungus *Aspergillus ochraceus*. *Helv. Chim. Acta* **2009**, *92*, 1366−1370.
(176) Wang, X.; You, J.; King, J. B.; Powell, D. R.; Cichewicz, R. H. Waikialoid A suppresses hyphal morphogenesis and inhibits biofilm development in pathogenic Candida albicans. *J. Nat. Prod.* **2012**, *75*, 707−715.

https://doi.org/10.1021/acs.chemrev.4c00250
Chem. Rev. XXXX, XXX, XXX−XXX

(177) Cai, S.; Luan, Y.; Kong, X.; Zhu, T.; Gu, Q.; Li, D. Isolation and photoinduced conversion of 6-*epi*-stephacidins from *Aspergillus taichungensis*. *Org. Lett.* **2013**, *15*, 2168−2171.
(178) Wang, B.; Park, E. M.; King, J. B.; Mattes, A. O.; Nimmo, S. L.; Clendinen, C.; Edison, A. S.; Anklin, C.; Cichewicz, R. H. Transferring fungi to a deuterium-enriched medium results in assorted, conditional changes in secondary metabolite production. *J. Nat. Prod.* **2015**, *78*, 1415−1421.
(179) Frank, M.; Özkaya, F. C.; Müller, W. E. G.; Hamacher, A.; Kassack, M. U.; Lin, W.; Liu, Z.; Proksch, P. Cryptic secondary metabolites from the sponge-associated fungus *Aspergillus ochraceus*. *Mar. Drugs* **2019**, *17*, 99.
(180) Liu, L.; Wang, L.; Bao, L.; Ren, J.; Bahadur Basnet, B.; Liu, R.; He, L.; Han, J.; Yin, W.-B.; Liu, H. Versicoamides F-H, prenylated indole alkaloids from *Aspergillus tennesseensis*. *Org. Lett.* **2017**, *19*, 942−945.
(181) von Nussbaum, F. Stephacidin B—A new stage of complexity within prenylated indole alkaloids from fungi. *Angew. Chem., Int. Ed.* **2003**, *42*, 3068−3071.
(182) Mikkola, R.; Andersson, M. A.; Hautaniemi, M.; Salkinoja-Salonen, M. S. Toxic indole alkaloids avrainvillamide and stephacidin B produced by a biocide tolerant indoor mold *Aspergillus westerdijkiae*. *Toxicon* **2015**, *99*, 58−67.
(183) Wulff, J. E.; Herzon, S. B.; Siegrist, R.; Myers, A. G. Evidence for the rapid conversion of stephacidin B into the electrophilic monomer avrainvillamide in cell culture. *J. Am. Chem. Soc.* **2007**, *129*, 4898−4899.
(184) Whyte, A. C.; Gloer, J. B.; Wicklow, D. T.; Dowd, P. F. Sclerotiamide: a new member of the paraherquamide class with potent antiinsectan activity from the sclerotia of *Aspergillus sclerotiorum*. *J. Nat. Prod.* **1996**, *59*, 1093−1095.
(185) Lavey, N. P.; Coker, J. A.; Ruben, E. A.; Duerfeldt, A. S. Sclerotiamide: the first non-peptide-based natural product activator of bacterial caseinolytic protease P. *J. Nat. Prod.* **2016**, *79*, 1193−1197.
(186) Peng, J.; Zhang, X.-Y.; Tu, Z.-C.; Xu, X.-Y.; Qi, S.-H. Alkaloids from the deep-sea-derived fungus *Aspergillus westerdijkiae* DFFSCS013. *J. Nat. Prod.* **2013**, *76*, 983−987.
(187) Zhang, X.-Y.; Xu, X.-Y.; Peng, J.; Ma, C.-F.; Nong, X.-H.; Bao, J.; Zhang, G.-Z.; Qi, S.-H. Antifouling potentials of eight deep-sea-derived fungi from the South China Sea. *J. Ind. Microbiol. Biotechnol.* **2014**, *41*, 741−748.
(188) Guo, X.; Meng, Q.; Liu, J.; Wu, J.; Jia, H.; Liu, D.; Gu, Y.; Liu, J.; Huang, J.; Fan, A.; Lin, W. Sclerotiamides C-H, notoamides from a marine gorgonian-derived fungus with cytotoxic activities. *J. Nat. Prod.* **2022**, *85*, 1067−1078.
(189) Kai, A.; Kato, H.; Sherman, D. H.; Williams, R. M.; Tsukamoto, S. Isolation of a new indoxyl alkaloid, amoenamide B, from *Aspergillus amoenus* NRRL 35600: biosynthetic implications and correction of the structure of Speramide B. *Tetrahedron Lett.* **2018**, *59*, 4236−4240.
(190) Andresen, V.; Erikstein, B. S.; Mukherjee, H.; Sulen, A.; Popa, M.; Soernes, S.; Reikvam, H.; Chan, K.-P.; Hovland, R.; McCormack, E.; Bruserud, O.; Myers, A. G.; Gjertsen, B. T. Anti-proliferative activity of the NPM1 interacting natural product avrainvillamide in acute myeloid leukemia. *Cell Death Dis.* **2016**, *7*, No. e2497.
(191) Sugie, Y.; Hirai, H.; Inagaki, T.; Ishiguro, M.; Kim, Y.-J.; Kojima, Y.; Sakakibara, T.; Sakemi, S.; Sugiura, A.; Suzuki, Y.; Brennan, L.; Duignan, J.; Huang, L. H.; Sutcliffe, J.; Kojima, N. A new antibiotic CJ-17,665 from *Aspergillus ochraceus*. *J. Antibiot.* **2001**, *54*, 911−916.
(192) Fenical, W.; Jensen, P. R.; Cheng, X. C. Avrainvillamide, a cytotoxic marine natural product, and derivatives thereof. US006066635, 2000.
(193) Wulff, J. E.; Siegrist, R.; Myers, A. G. The natural product avrainvillamide binds to the oncoprotein nucleophosmin. *J. Am. Chem. Soc.* **2007**, *129*, 14444−14451.
(194) Grubbs, A. W.; Artman, G. D.; Williams, R. M. Concise syntheses of the 1,7-dihydropyrano[2,3-*g*]indole ring system of the stephacidins, aspergamides and norgeamides. *Tetrahedron Lett.* **2005**, *46*, 9013−9016.
(195) Li, H.; Sun, W.; Deng, M.; Zhou, Q.; Wang, J.; Liu, J.; Chen, C.; Qi, C.; Luo, Z.; Xue, Y.; Zhu, H.; Zhang, Y. Asperversiamides, linearly fused prenylated indole alkaloids from the marine-derived fungus *Aspergillus versicolor*. *J. Org. Chem.* **2018**, *83*, 8483−8492.
(196) Zhang, P.; Li, X.-M.; Wang, J.-N.; Li, X.; Wang, B.-G. Prenylated indole alkaloids from the marine-derived fungus *Paecilomyces variotii*. *Chin. Chem. Lett.* **2015**, *26*, 313−316.
(197) Zhao, D.-L.; Huo, X.-Y.; Li, P.-P.; Yuan, X.-L.; Li, S.-Y.; Du, L.; Huang, L.-J.; Zhang, P. Asperinamide A, an anti-inflammatory prenylated indole alkaloid possessing an unprecedented bicyclo[2.2.2]diazaoctane fused with substituted piperidine scaffold from *Aspergillus* sp. TE-65L. *Tetrahedron* **2023**, *149*, 133744.
(198) Chen, Y.; Wang, S.-P.; Xu, L.-C.; Liang, C.; Liu, G.-D.; Ji, X.; Luo, W.-H.; Liu, S.; Zhang, Z.-X.; Cao, G.-Y. Aspertaichamide a, a novel cytotoxic prenylated indole alkaloid possessing a bicyclo[2.2.2]-diazaoctane framework from a marine algal-derived endophytic fungus *Aspergillus taichungensis* 299. *Fitoterapia* **2024**, *172*, 105763.
(199) Wu, C.-J.; Li, C.-W.; Gao, H.; Huang, X.-J.; Cui, C.-B. Penicimutamides D-E: two new prenylated indole alkaloids from a mutant of the marine-derived *Penicillium purpurogenum* G59. *RSC Adv.* **2017**, *7*, 24718−24722.
(200) Sherman, D. H.; Fraley, A. E.; Tripathi, A. Variant flavin-dependent halogenase from *Malbranchea* and their use for halogenation of malbrancheamides. 2020. US 20200048617 USA.
(201) Nishikori, S.; Takemoto, K.; Kamisuki, S.; Nakajima, S.; Kuramochi, K.; Tsukuda, S.; Iwamoto, M.; Katayama, Y.; Suzuki, T.; Kobayashi, S.; Watashi, K.; Sugawara, F. Anti-hepatitis C virus natural product from a fungus, *Penicillium herquei*. *J. Nat. Prod.* **2016**, *79*, 442−446.
(202) Zinser, E. W.; Wolf, M. L.; Alexander-Bowman, S. J.; Thomas, E. M.; Davis, J. P.; Groppi, V. E.; Lee, B. H.; Thompson, D. P.; Geary, T. G. Anthelmintic paraherquamides are cholinergic antagonists in gastrointestinal nematodes and mammals. *J. Vet. Pharmacol. Ther.* **2002**, *25*, 241−250.
(203) Antia, B. S.; Aree, T.; Kasettrathat, C.; Wiyakrutta, S.; Ekpa, O. D.; Ekpe, U. J.; Mahidol, C.; Ruchirawat, S.; Kittakoop, P. Itaconic acid derivatives and diketopiperazine from the marine-derived fungus *Aspergillus aculeatus* CRI322−03. *Phytochemistry* **2011**, *72*, 816−820.
(204) Hayashi, H.; Nishimoto, Y.; Nozaki, H. Asperparaline A, a new paralytic alkaloid from *Aspergillus japonicus* JV-23. *Tetrahedron Lett.* **1997**, *38*, 5655−5658.
(205) Hayashi, H.; Nishimoto, Y.; Akiyama, K.; Nozaki, H. New paralytic alkaloids, asperparalines A, B and C, from *Aspergillus japonicus* JV-23. *Biosci. Biotechnol. Biochem.* **2000**, *64*, 111−115.
(206) Mercado-Marin, E. V.; Garcia-Reynaga, P.; Romminger, S.; Pimenta, E. F.; Romney, D. K.; Lodewyk, M. W.; Williams, D. E.; Andersen, R. J.; Miller, S. J.; Tantillo, D. J.; Berlinck, R. G. S.; Sarpong, R. Total synthesis and isolation of citrinalin and cyclopiamine congeners. *Nature* **2014**, *509*, 318−324.
(207) Lee, C.; Sohn, J. H.; Jang, J.-H.; Ahn, J. S.; Oh, H.; Baltrusaitis, J.; Hwang, I. H.; Gloer, J. B. Cycloexpansamines A and B: spiroindolinone alkaloids from a marine isolate of *Penicillium sp.* (SF-5292). *J. Antibiot.* **2015**, *68*, 715−718.
(208) Zhang, P.; Li, X.-M.; Liu, H.; Li, X.; Wang, B.-G. Two new alkaloids from *Penicillium oxalicum* EN-201, an endophytic fungus derived from the marine mangrove plant *Rhizophora stylosa*. *Phytochemistry Letters* **2015**, *13*, 160−164.
(209) Hu, X.-L.; Bian, X.-Q.; Wu, X.; Li, J.-Y.; Hua, H.-M.; Pei, Y.-H.; Han, A.-H.; Bai, J. Penioxalamine A, a novel prenylated spiro-oxindole alkaloid from *Penicillium oxalicum* TW01−1. *Tetrahedron Lett.* **2014**, *55*, 3864−3867.
(210) Sumarah, M. W.; Miller, J. D.; Blackwell, B. A. Isolation and metabolite production by *Penicillium roqueforti*, *P. paneum* and *P. crustosum* isolated in Canada. *Mycopathologia* **2005**, *159*, 571−577.
(211) Rasmussen, R. R.; Rasmussen, P. H.; Larsen, T. O.; Bladt, T. T.; Binderup, M. L. In *vitro* cytotoxicity of fungi spoiling maize silage. *Food Chem. Toxicol.* **2011**, *49*, 31−44.

https://doi.org/10.1021/acs.chemrev.4c00250
Chem. Rev. XXXX, XXX, XXX−XXX

(212) Polonsky, J.; Merrien, M. A.; Prange, T.; Pascard, C.; Moreau, S. Isolation and structure (*X*-ray analysis) of marcfortine A, a new alkaloid from *Penicillium roqueforti*. *J. Chem. Soc., Chem. Commun.* **1980**, 601−602.
(213) Prange, T.; Billion, M. A.; Vuilhorgne, M.; Pascard, C.; Polonsky, J.; Moreau, S. Structures of marcfortine B and C (*X*-ray analysis), alkaloids from *Penicillium roqueforti*. *Tetrahedron Lett.* **1981**, *22*, 1977−1980.
(214) Mioso, R.; Toledo Marante, F. J.; Herrera Bravo de Laguna, I. *Penicillium roqueforti*: a multifunctional cell factory of high value-added molecules. *J. Appl. Microbiol.* **2015**, *118*, 781−791.
(215) Capon, R. J.; Skene, C.; Stewart, M.; Ford, J.; O'Hair, R. A. J.; Williams, L.; Lacey, E.; Gill, J. H.; Heiland, K.; Friedel, T. Aspergillicins A-E: five novel depsipeptides from the marine-derived fungus *Aspergillus carneus*. *Org. Biomol. Chem.* **2003**, *1*, 1856−1862.
(216) Lin, Z.; Wen, J.; Zhu, T.; Fang, Y.; Gu, Q.; Zhu, W. Chrysogenamide A from an endophytic fungus associated with *Cistanche deserticola* and its neuroprotective effect on SH-SY5Y cells. *J. Antibiot.* **2008**, *61*, 81−85.
(217) Costa, J. H.; Wassano, C. I.; Angolini, C. F. F.; Scherlach, K.; Hertweck, C.; Pacheco Fill, T. Antifungal potential of secondary metabolites involved in the interaction between citrus pathogens. *Sci. Rep.* **2019**, *9*, 18647.
(218) Yang, B.; Dong, J.; Lin, X.; Zhou, X.; Zhang, Y.; Liu, Y. New prenylated indole alkaloids from fungus *Penicillium sp*. derived of mangrove soil sample. *Tetrahedron* **2014**, *70*, 3859−3863.
(219) Yang, B.; Tao, H.; Lin, X.; Wang, J.; Liao, S.; Dong, J.; Zhou, X.; Liu, Y. Prenylated indole alkaloids and chromone derivatives from the fungus *Penicillium sp*. SCSIO041218. *Tetrahedron* **2018**, *74*, 77−82.
(220) Kwon, J.; Seo, Y. H.; Lee, J.-E.; Seo, E.-K.; Li, S.; Guo, Y.; Hong, S.-B.; Park, S.-Y.; Lee, D. Spiroindole alkaloids and spiroditerpenoids from *Aspergillus duricaulis* and their potential neuroprotective effects. *J. Nat. Prod.* **2015**, *78*, 2572−2579.
(221) Fraley, A. E.; Sherman, D. H. Enzyme evolution in fungal indole alkaloid biosynthesis. *FEBS J.* **2020**, *287*, 1381−1402.
(222) Fraley, A. E.; Sherman, D. H. Halogenase engineering and its utility in medicinal chemistry. *Bioorg. Med. Chem. Lett.* **2018**, *28*, 1992−1999.
(223) Klas, K.; Tsukamoto, S.; Sherman, D. H.; Williams, R. M. Natural Diels-Alderases: elusive and irresistable. *J. Org. Chem.* **2015**, *80*, 11672−11685.
(224) Finefield, J. M.; Sherman, D. H.; Kreitman, M.; Williams, R. M. Enantiomeric natural products: occurrence and biogenesis. *Angew. Chem., Int. Ed. Engl.* **2012**, *51*, 4802−4836.
(225) Finefield, J. M.; Frisvad, J. C.; Sherman, D. H.; Williams, R. M. Fungal origins of the bicyclo[2.2.2]diazaoctane ring system of prenylated indole alkaloids. *J. Nat. Prod.* **2012**, *75*, 812−833.
(226) Stocking, E. M.; Williams, R. M. Chemistry and biology of biosynthetic Diels-Alder reactions. *Angew. Chem., Int. Ed.* **2003**, *42*, 3078−3115.
(227) Williams, R. M.; Cox, R. J. Paraherquamides, brevianamides, and asperparalines: laboratory synthesis and biosynthesis. An interim report. *Acc. Chem. Res.* **2003**, *36*, 127−139.

https://doi.org/10.1021/acs.chemrev.4c00250
Chem. Rev. XXXX, XXX, XXX−XXX